



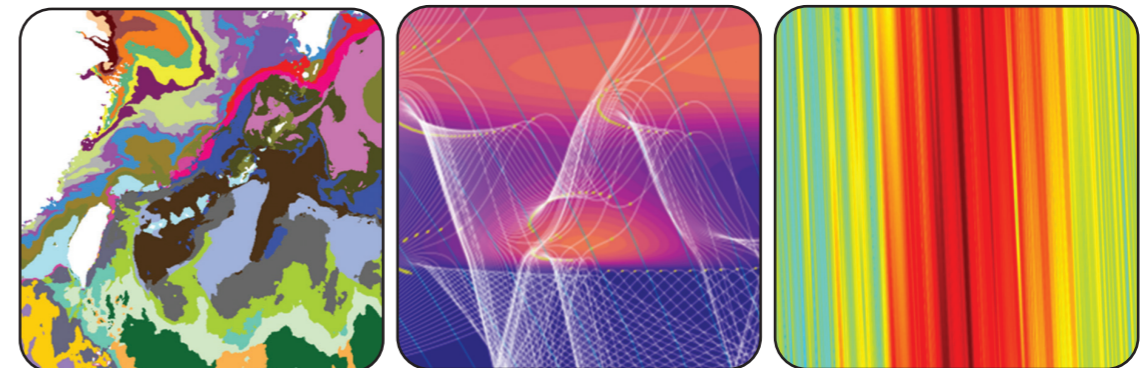
FY19 NRL DoD High Performance Computing Modernization Program Annual Reports

EDITED BY
BONNIE J. ASSAD

PREPARED BY
PORTIA A. SHINGLER AND BETH A. HOWELL

*Center for Computational Science
Information Technology Division*

October 1, 2021



REVIEWED AND APPROVED
NRL/PU/5594--21-664
RN: 21-1231-2482
October 2021

Stanley Chincheck
Superintendent, Information Technology Division

REPORT DOCUMENTATION PAGE

*Form Approved
OMB No. 0704-0188*

The public reporting burden for this collection of information is estimated to average 1 hour per response, including the time for reviewing instructions, searching existing data sources, gathering and maintaining the data needed, and completing and reviewing the collection of information. Send comments regarding this burden estimate or any other aspect of this collection of information, including suggestions for reducing the burden, to the Department of Defense, Executive Service Directorate (0704-0188). Respondents should be aware that notwithstanding any other provision of law, no person shall be subject to any penalty for failing to comply with a collection of information if it does not display a currently valid OMB control number.

PLEASE DO NOT RETURN YOUR FORM TO THE ABOVE ORGANIZATION.

| | | |
|---|--------------------------------------|--|
| 1. REPORT DATE (DD-MM-YYYY) 01 October 2021 | 2. REPORT TYPE Publication | 3. DATES COVERED (From - To) 01 October 2018 - 30 September 2019 |
|---|--------------------------------------|--|

| | |
|--|-----------------------------------|
| 4. TITLE AND SUBTITLE FY19 NRL DoD High Performance Computing Modernization Program Annual Reports | 5a. CONTRACT NUMBER |
| | 5b. GRANT NUMBER |
| | 5c. PROGRAM ELEMENT NUMBER |

| | |
|---|-----------------------------|
| 6. AUTHOR(S) Bonnie Assad, NRL Code 5594 Portia A. Shingler, NRL Code 5594 Beth A. Howell, Contractor, Peraton, Inc., Code 5590 | 5d. PROJECT NUMBER |
| | 5e. TASK NUMBER |
| | 5f. WORK UNIT NUMBER |

| | |
|---|--|
| 7. PERFORMING ORGANIZATION NAME(S) AND ADDRESS(ES) Naval Research Laboratory 4555 Overlook Avenue, SW Washington, DC 20375-5320 | 8. PERFORMING ORGANIZATION REPORT NUMBER NRL/5590/PU--2021/1 |
|---|--|

| | |
|---|--|
| 9. SPONSORING/MONITORING AGENCY NAME(S) AND ADDRESS(ES) Office of Naval Research 875 N. Randolph Street Arlington, VA 22217 | 10. SPONSOR/MONITOR'S ACRONYM(S) ONR |
| | 11. SPONSOR/MONITOR'S REPORT NUMBER(S) |

12. DISTRIBUTION/AVAILABILITY STATEMENT
Distribution A: Approved for public release; distribution unlimited.

13. SUPPLEMENTARY NOTES

14. ABSTRACT
These reports summarize the accomplishments of the NRL Principal Investigators who received computer allocations on the DoD High Performance Computing Modernization Program Shared Resource Center.

15. SUBJECT TERMS
Biomechanics Network encryption device Constitutive modeling Hyperelastic Viscoelastic
Constrained optimization Parameter estimation Model calibration Computational modeling

| | | | | | | |
|--|--------------------|---------------------|-----------------------------------|----------------------------|--|--|
| 16. SECURITY CLASSIFICATION OF: | | | 17. LIMITATION OF ABSTRACT | 18. NUMBER OF PAGES | 19a. NAME OF RESPONSIBLE PERSON | |
| a. REPORT | b. ABSTRACT | c. THIS PAGE | | | Bonnie Assad | |
| U | U | U | UU | 182 | 19b. TELEPHONE NUMBER (Include area code) 202-767-2046 | |

Introduction

This book is a compilation of reports on all the work accomplished by NRL scientists and engineers and their collaborators using the DoD High Performance Computing Modernization Program's (HPCMP) resources for fiscal year 2019. The reports encompass work performed by researchers at all three NRL sites: Washington, D.C.; Stennis Space Center, Mississippi; and Monterey, California.

These reports are categorized according to the primary Computational Technology Area (CTA) as specified by the HPCMP, and include resources at the DOD Supercomputing Resource Centers (DSRC) as well as the Affiliated Resource Centers (ARC). This volume includes three indices for ease of reference. These are an author index, a site index, and an NRL hierarchical index of reports from the Branches and Divisions in the Laboratory.

THIS PAGE INTENTIONALLY LEFT BLANK

Table of Contents

Computational Structural Mechanics (CSM)

Geometric, Constitutive and Loading Complexities in Structural Materials2

S.A. Wimmer¹, R.N. Saunders¹, A. Arcari², D.J. Hasler³, and J.G. Michopoulos¹

¹Naval Research Laboratory, Washington, DC

²Excet, Inc., Springfield, VA

³Naval Operational Support Center, Green Bay, WI

Computational Analysis of Warfighter Brain Injury and Protective Equipment.....4

X.G. Tan and R.N. Saunders

Naval Research Laboratory, Washington, DC

Stochastic Methods for Uncertainty Quantification in Computational Mechanics6

K. Teferra and R.N. Saunders

Naval Research Laboratory, Washington, DC

Computational Fluid Dynamics (CFD)

Advanced Computational Models that Exploit Emerging Computer

Architectures10

K. Obenschain and G. Patnaik

Naval Research Laboratory, Washington DC

Simulations of Laser-plasma Interactions and the Radiation Hydrodynamics

of High-velocity Laser-accelerated Matter12

J.W. Bates, A.J. Schmitt and K. Obenschain

Naval Research Laboratory, Washington, DC

Dynamics of Compressible Turbulent Flames and the Deflagration-to-Detonation

Transition.....14

V.N. Gamezo¹, and A.Y. Poludnenko^{2,3}

¹Naval Research Laboratory, Washington, DC

²Texas A&M University, College Station, TX

³University of Connecticut, Storrs, CT

Advanced Two-Phase CFD Model16

T.D. Holman

Naval Research Laboratory, Washington, DC

| | |
|---|-----------|
| The Impact of Foam and Aerosol Dynamics on Fire, Explosion Safety, and Suppression (Mechanisms of Water Mist Suppression of a Burning Solid Surface) | 18 |
| X. Zhuang ¹ and R. Ananth ² | |
| ¹ <i>ASEE Postdoctoral Fellow, Naval Research Laboratory, Washington, DC</i> | |
| ² <i>Naval Research Laboratory, Washington DC</i> | |
| High-Temperature and Rarefied Gas Dynamics in Hypersonic Flows | 20 |
| J.R. Maxwell, E.W. Hyde, and R.E. Rogers | |
| <i>Naval Research Laboratory, Washington, DC</i> | |
| Direct Numerical Simulation of Fluid-Sediment Wave Bottom Boundary Layer..... | 22 |
| A. Penko, S.P. Bateman, J.A. Simeonov, and J. Calantoni | |
| <i>Naval Research Laboratory, Stennis Space Center, MS</i> | |
| Bathymetry Prediction System | 24 |
| A. Penko ¹ , J. Veeramony ¹ , M. Palmsten ¹ , S. Harrison ¹ , K. Edwards ¹ , S. Trimble ² , and W. Lee ² | |
| ¹ <i>Naval Research Laboratory, Stennis Space Center, MS</i> | |
| ² <i>National Research Council Postdoctoral Fellow</i> | |
| Predicting Fluid-Structure Interaction for Military Applications | 26 |
| D.R. Mott, A.D. Kercher, R.F. Johnson, A. Corrigan, and D.A. Kessler | |
| <i>Naval Research Laboratory, Washington, DC</i> | |
| Multidimensional Chemically Reacting Fluid Dynamics with Application to Flameless Combustors | 28 |
| R.F. Johnson | |
| <i>Naval Research Laboratory, Washington, DC</i> | |
| Applications of FEFLO Incompressible Flow Solver | 30 |
| R. Ramamurti | |
| <i>Naval Research Laboratory, Washington, DC</i> | |
| Numerical Simulations of Turbulence Impact on Optical Signal Transmission and Near-Surface Turbulence | 32 |
| S. Matt, W. Hou, and A. Perez | |
| <i>Naval Research Laboratory, Stennis Space Center, MS</i> | |
| Detonations with Multi-Phase Flows for Propulsion..... | 34 |
| D.A. Schwer | |
| <i>Naval Research Laboratory, Washington, DC</i> | |
| Numerical Investigation of Advanced Military Aircraft Noise Reduction Concepts..... | 36 |
| J. Liu, A. Corrigan, R.F. Johnson and R. Ramamurti | |
| <i>Naval Research Laboratory, Washington, DC</i> | |

| | |
|--|-----------|
| Investigation of Jet Noise Reduction Optimization | 38 |
| J. Liu | |
| <i>Naval Research Laboratory, Washington, DC</i> | |
| Numerical Simulations of Noise Generated by Non-Circular Advanced Military Aircraft Nozzles..... | 40 |
| K. Viswanath and R. Ramamurti | |
| <i>Naval Research Laboratory, Washington, DC</i> | |
| Hypersonic Reactive Flow Modeling..... | 42 |
| G. Goodwin | |
| <i>Naval Research Laboratory, Washington, DC</i> | |
| Simulations of the Ionosphere and Magnetosphere..... | 44 |
| J. Krall ¹ and J.D. Huba ² | |
| ¹ <i>Naval Research Laboratory, Washington, DC</i> | |
| ² <i>Syntek Technologies, Fairfax, VA</i> | |
| Electron Scattering Cross Sections for Plasma Response Models..... | 46 |
| P.E. Adamson, S.B. Swaneekamp, and A.S. Richardson | |
| <i>Naval Research Laboratory, Washington, DC</i> | |
| Radiation Field Characteristics and Interaction in High Energy Density Z-Pinch Plasmas..... | 48 |
| Y. Chong | |
| <i>Naval Research Laboratory, Washington, DC</i> | |
| <u>Computational Biology, Chemistry, and Materials Science (CCM)</u> | |
| Ab initio Molecular Dynamics Simulations of High-energy-density Molecular Crystals | 52 |
| I.V. Schweigert | |
| <i>Naval Research Laboratory, Washington, DC</i> | |
| First-Principles Simulations of Condensed-Phase Decomposition of Energetic Materials | 54 |
| I.V. Schweigert | |
| <i>Naval Research Laboratory, Washington, DC</i> | |
| Quantum-Chemical Simulation of Surface-Science Experiments..... | 56 |
| V.M. Bermudez | |
| <i>Naval Research Laboratory, Washington, DC</i> | |
| Improved Calculation of Solid-Phase Heats of Formation Using Intermolecular Interactions Observed in Crystal Structures | 58 |
| I.D. Giles and G.H. Imler | |
| <i>Naval Research Laboratory, Washington, DC</i> | |

| | |
|---|-----------|
| Synthetic Biology for Military Environments | 60 |
| W.J. Hervey and G.J. Vora | |
| <i>Naval Research Laboratory, Washington, DC</i> | |
| Marine Biofilm Metaproteomics | 62 |
| W.J. Hervey and G.J. Vora | |
| <i>Naval Research Laboratory, Washington, DC</i> | |
| Preventing Corrosion by Controlling Cathodic Reaction Kinetics | 64 |
| S.A. Policastro, C.M. Hangarter and R.M. Anderson | |
| <i>Naval Research Laboratory, Washington, DC</i> | |
| Surfaces and Interfaces in Oxides and Semiconductors | 66 |
| C.S. Hellberg | |
| <i>Naval Research Laboratory, Washington, DC</i> | |
| High-Throughput Search for New Magnetic Materials and Noncollinear Magnetism | 68 |
| I. Mazin ¹ and J. Glasbrenner ² | |
| ¹ <i>Naval Research Laboratory, Washington, DC</i> | |
| ² <i>George Mason University, Fairfax, VA</i> | |
| Materials for Energy Storage and Generation..... | 70 |
| M. Johannes | |
| <i>Naval Research Laboratory, Washington, DC</i> | |
| Multiple Length and Time Scale Simulations of Material Properties | 72 |
| N. Bernstein | |
| <i>Naval Research Laboratory, Washington, DC</i> | |
| Calculation of Materials Properties via Density Functional Theory and Its Extensions | 74 |
| J.L. Lyons | |
| <i>Naval Research Laboratory, Washington, DC</i> | |
| IR Absorption Spectra for Nerve Agent-Sorbent Binding Using Density Functional Theory..... | 76 |
| S. Lambrakos, A. Shabaev, and Y. Kim | |
| <i>Naval Research Laboratory, Washington, DC</i> | |
| Numerical Studies of Semiconductor Nanostructures..... | 78 |
| T.L. Reinecke ¹ and S. Mukhopdhyay ² | |
| ¹ <i>Naval Research Laboratory, Washington, DC</i> | |
| ² <i>National Research Council Postdoctoral Program, Washington, DC</i> | |

Computational Electromagnetics and Acoustics (CEA)

Flowfield and Transport Models for Navy Applications82

W.G. Szymczak, A.J. Romano and S. Dey
Naval Research Laboratory, Washington, DC

Small Slope Approximation (SSA) Rough-Surface Back-Scattering Analysis84

J. Alatishe
Naval Research Laboratory, Washington, DC

Diffusive Wave Spectroscopy of Underwater Sound.....86

D. Photiadis and N. Valdivia
Naval Research Laboratory, Washington, DC

Intense Laser Physics and Advanced Radiation Sources.....88

D.F. Gordon¹, J. Penano¹, L. Johnson¹, J. Issacs¹, D. Kaganov¹, B. Hafizi¹, and A. Davidson²

¹*Naval Research Laboratory, Washington, DC*

²*National Research Council Postdoctoral Program, Washington, DC*

Low Grazing Angle Radar Backscatter90

J.V. Toporkov, J.D. Ouellette, and M.A. Sletten
Naval Research Laboratory, Washington, DC

Structural-Acoustic Response of Stifened Elastic Cylindrical Shell92

S. Dey¹, E.L. Mestreau², R.M. Aubry², M. Williamschen², and D. Williams²

¹*Naval Research Laboratory, Washington, DC*

²*KeyW Corporation, Hanover, MD*

Acoustic Parameter Variability over an Ocean Reanalysis (AVORA).....94

J.P. Fabre
Naval Research Laboratory, Stennis Space Center, MS

Computer-Aided Design of Vacuum Electronic Devices.....96

G. Stantchev¹, S. Cooke¹, J. Petillo², A. Jensen², and S. Ovtchinnikov²

¹*Naval Research Laboratory, Washington, DC*

²*Leidos, Billerica, MA*

Multidimensional Particle-in-Cell Modeling of Ultrashort Pulse Laser with Solid Targets98

G.M. Petrov
Naval Research Laboratory, Washington, DC

Climate Weather Ocean Modeling (CWO)

Coastal Mesoscale Modeling – COMAMPS-TC Intensity Prediction102

J.D. Doyle

Naval Research Laboratory, Monterey, CA

Coastal Mesoscale Modeling104

P.A. Reinecke

Naval Research Laboratory, Monterey, CA

Data Assimilation Studies Project106

W.F. Campbell and B. Ruston

Naval Research Laboratory, Monterey, CA

Coupled Ocean-Wave-Air-Ice Prediction System.....108

R. Allard¹, T. Campbell¹, J. Crout², E. Douglass¹, D. Hebert¹, T. Jensen¹, and T. Smith¹

¹*Naval Research Laboratory, Stennis Space Center, MS*

²*Perspecta, Stennis Space Center, MS*

Variational Data Assimilation110

S. Smith¹, C. Amerault², C. Barron¹, S. Boggs³, T. Campbell¹, M. Carrier¹, N. Cheshire³, J. D’Addezio^{1,4}, J. Dastugue¹, C. DeHaan⁵, S. deRada¹, E. Douglass¹, D. Fertitta³, D. Hebert¹, R. Helber¹, P. Martin¹, J. May¹, H. Ngodock¹, J. Osborne^{1,3}, C. Rowley¹, J. Shriver¹, T. Smith¹, I. Souopgui⁶, P. Spence⁵, and M. Yaremchuk¹

¹*Naval Research Laboratory, Stennis Space Center, MS*

²*Naval Research Laboratory, Monterey, CA*

³*American Society for Engineering Education, Stennis Space Center, MS*

⁴*University of Southern Mississippi, Stennis Space Center, MS*

⁵*Qineti! North America, Stennis Space Center, MS*

⁶*University of New Orleans, Stennis Space Center, MS*

Rogue Wave Probability Estimator for WAVEWATCH III.....112

M. Orzech¹, J. Simeonov¹, and M. Manolidis²

¹*Naval Research Laboratory, Stennis Space Center, MS*

²*National Research Council Postdoctoral Research Naval Research Laboratory, Stennis Space Center, MS*

Multi-scale Characterization and Prediction of the Global Atmosphere from the Ground to the Edge of Space using Next-Generation Navy Modeling Systems.....114

J.P. McCormack¹, S.D. Eckermann¹, C.A. Barton^{1,4}, F. Sassi¹, M.A. Herrera^{1,3}, K.W. Hoppel¹, D.D. Kuhl¹, D.R. Allen¹, J. Ma², and J. Tate²

¹*Naval Research Laboratory, Washington, DC*

²*Computational Physics Inc., Springfield, VA*

³*National Research Council Postdoctoral Research Fellow, Washington, DC*

⁴*Karles Fellow*

| | |
|--|------------|
| Dynamics of Coupled Models | 116 |
| I. Shulman, B. Penta, S. Cayula, and C. Rowley <i>Naval Research Laboratory, Stennis Space Center, MS</i> | |
| Probabilistic Prediction to Support Ocean Modeling Projects..... | 118 |
| C.D. Rowley ¹ , L.F. Smedstad ¹ , C.N. Barron ¹ , R.S. Linzell ² , P.L. Spence ² , T.L. Townsend ¹ , Z.W. Lamb ¹ , M. Yaremchuk ¹ , J.C. May ¹ , J.M. Dastuque ¹ , T.A. Smith ¹ , J.J. Osborne ¹ , G.G. Penteliev ¹ , B.P. Bartels ² , B.R. Maloy ¹ ¹ <i>Naval Research Laboratory, Stennis Space Center, MS</i> ² <i>Perspecta, Stennis Space Center, MS</i> | |
| Guidance for Heterogeneous Observation System (GHOST) | 120 |
| L.F. Smedstad ¹ , C.N. Barron ¹ , G.A. Jacobs ¹ , P.L. Spence ² , J.M. D’Addezio ¹ , B.P. Bartels ² , C.D. Rowley ¹ , Z.W. Lamb ¹ ¹ <i>Naval Research Laboratory, Stennis Space Center, MS</i> ² <i>Perspecta, Stennis Space Center, MS</i> | |
| High Resolution Global Ocean Reanalysis | 122 |
| P.J. Hogan <i>Naval Research Laboratory, Stennis Space Center, MS</i> | |
| Bio-Optical Modeling and Forecasting | 124 |
| J.K. Jolliff, S.Ladner, S. Ladner, T. Smith, and C. Wood <i>Naval Research Laboratory, Stennis Space Center, MS</i> | |
| Atmospheric Process Studies | 126 |
| N. Barton ¹ , T. Whitcomb ¹ , J. Ridout ¹ , K. Viner ¹ , J. McLay ¹ , W. Crawford ² , M. Liu ¹ , and C. Reynolds ¹ ¹ <i>Naval Research Laboratory, Monterey CA</i> ² <i>American Society for Engineering Education, Washington, DC</i> | |
| Eddy-resolving Global/Basin-Scale Ocean Modeling..... | 128 |
| E.J. Metzger and J.F. Shriver <i>Naval Research Laboratory, Stennis Space Center, MS</i> | |
| Coastal Mesoscale Modeling – COAMPS-TC | 130 |
| W.A. Komaromi and P.A. Reinecke <i>Naval Research Laboratory, Monterey, CA</i> | |
| The Effect of Langmuir Turbulence in Upper Ocean Mixing..... | 132 |
| Y. Fan <i>Naval Research Laboratory, Stennis Space Center, MS</i> | |

Signal Image Processing (SIP)

Reducing the Burden of Massive Training Data for Deep Learning136
L.N. Smith, E.A. Gilmour, S.N. Blisard, and K.M. Sullivan
Naval Research Laboratory, Washington, DC

Space and Astrophysical Science (SAS)

Meteorology and Climatology of the Thermosphere140
D.P. Drob, M. Jones, and M. Dhadly
Naval Research Laboratory, Washington, DC

Radiative Signatures and Dynamical Interactions of AGN Jets142
M.T. Wolff¹ and J.H. Beall²
¹*Naval Research Laboratory, Washington, DC*
²*St. John's College, Annapolis, MD*

Development of a Weather Model of the Ionosphere144
S.E. McDonald¹, F. Sassi¹, C.A. Metzler¹, D.P. Drob¹, J.L. Tate², and M.S. Dhadly³
¹*Naval Research Laboratory, Washington, DC*
²*Computational Physics, Inc., Springfield, VA*
³*George Mason University, Fairfax, VA*

Navy Ionosphere Model for Operations146
S.E. McDonald¹, C.A. Metzler¹, J.L. Tate², R.K. Schaefer³, P.B. Dandenault³, A.T. Chartier³, G. Romeo³, G.S. Bust³, and R. Calfas⁴
¹*Naval Research Laboratory, Washington, DC*
²*Computational Physics, Inc., Springfield, VA*
³*The Johns Hopkins Applied Physics Laboratory, Laurel, MD*
⁴*The University of Texas at Austin Applied Research Laboratories, Austin, TX*

Electromagnetic Pulses from Hypervelocity Impacts on Spacecraft148
A. Fletcher
Naval Research Laboratory, Washington, DC

Global Kinetic Simulations of Space Plasma Waves and Turbulence150
A. Fletcher
Naval Research Laboratory, Washington, DC

Dynamic Phenomena in the Solar Atmosphere152
M.G. Linton
Naval Research Laboratory, Washington, DC

Modeling Propagation of Ionospheric Disturbances Initiated by Magnetospheric Substorms154

J. Haiducek and J. Helmboldt

Naval Research Laboratory, Washington, DC

Radio and Gamma-ray Searches for Millisecond Pulsars and Radio Transients ...156

P.S. Ray and J. Deneva

Naval Research Laboratory, Washington, DC

Other (OTH)

Simulation of High-Energy Radiation Environments160

J. Finke and A. Hutcheson

Naval Research Laboratory, Washington, DC

Author Index163

Division Index.....166

Site Index168



Computational Structural Mechanics

CSM covers the high resolution multidimensional modeling of materials and structures subjected to a broad range of loading conditions including quasistatic, dynamic, electromagnetic, shock, penetration, and blast. It also includes the highly interdisciplinary research area of materials design, where multiscale modeling from atomistic scale to macro scale is essential. CSM encompasses a wide range of engineering problems in solid mechanics, such as material or structural response to time- and history-dependent loading, large deformations, fracture propagation, shock wave propagation, isotropic and anisotropic plasticity, frequency response, and nonlinear and heterogeneous material behaviors. High performance computing for CSM addresses the accurate numerical solution of conservation equations, equation of motion, equations of state, and constitutive relationships to model simple or complex geometries and material properties, subject to external boundary conditions and loads. CSM is used for basic studies in continuum mechanics, stress analysis for engineering design studies, predicting structural and material response to impulsive loads, and modeling response of heterogeneous embedded sensors/devices. DoD application areas include conventional underwater explosion and ship response, structural acoustics, coupled field problems, space debris, propulsion systems, structural analysis, total weapon simulation, weapon systems' lethality/survivability (e.g., aircraft, ships, submarines, and tanks), theater missile defense lethality analyses, optimization techniques, and real-time, large-scale soldier- and hardware-in- the-loop ground vehicle dynamic simulation.

Title: Geometric, Constitutive and Loading Complexities in Structural Materials

Author(s): S.A. Wimmer, ¹ R.N. Saunders, ¹ A. Arcari, ² D.J. Hasler, ³ and J.G. Michopoulos, ¹

Affiliation(s): ¹Naval Research Laboratory, Washington, DC; ²Excet, Inc., Springfield, VA; and ³Naval Operational Support Center, Green Bay, WI

CTA: CSM

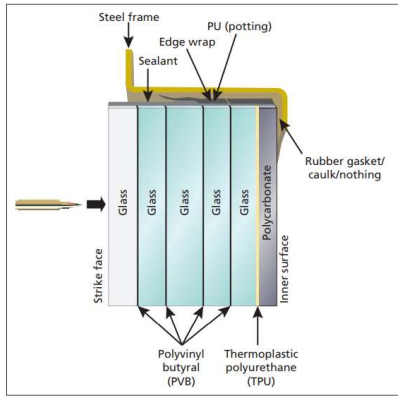
Computer Resources: HPE SGI 8600, SGI ICE X [AFRL, OH]

Research Objectives: The research strives to develop rational bases and mathematical descriptions of complex material responses for structural and novel evolving materials. Structural integrity and life cycle evaluations require an understanding of material responses. Analytical models and techniques cannot describe complex materials and often do not account for interactions, complex geometries, or multiphysics loading. Finite element methods are used to develop models involving multifunctional materials, novel evolving materials, and multiphysics. In order to accurately model the nonlinear response of conventional structural materials, rate dependence, large deformation, and damage accumulation mechanisms must be understood and accurately represented. The performance of the overall structure or system is also examined via parameters such as kinematics, geometric complexities, loading path dependencies, and interaction between loading types.

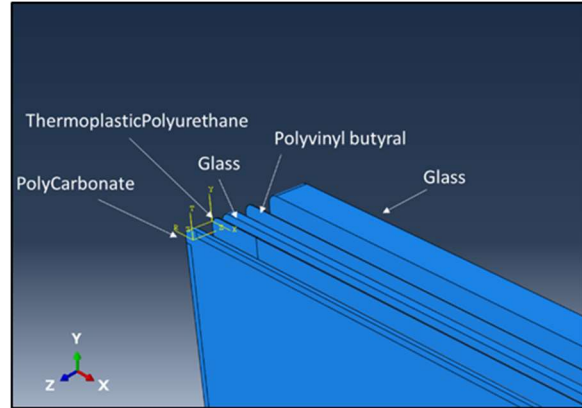
Methodology: The project uses finite element methods extensively. Nonlinear material constitutive response features are highlighted in much of the work. Implicit and explicit solutions methods are used as appropriate. The primary finite element code used is ABAQUS. Coupled material responses, such as electric-thermal or electrical-mechanical-thermal, are exercised for evaluation of these effects. Model development is done with CUBIT, ABAQUS/CAE, SimpleWare, or in-house software. Large run times and large model size are often required for the multistep nonlinear finite element analysis jobs.

Results: This project involves work in several topical areas. Work has been performed on creating image-based microstructural models, modeling multilayer ceramic structures, modeling stress corrosion cracking, modeling biofoulants, and modeling transparent armor delamination. Representative results for the topic of transparent armor delamination are discussed. Transparent armor is a laminated glass material bonded together with a soft polymer interlayer (see Fig. 1a). The innermost layer is a polycarbonate (PC) bonded to the glass with a rubbery thermoplastic polyurethane (TPU). The PC layer prevents shards and debris from entering the protected area after impact. The bond between the PC and the TPU degrades until temperature-induced stresses cause delamination, thus degrading visibility. Finite element modeling of a full three-dimensional (3D) windshield (Fig. 1b) was done to determine if the delamination is from the temperature maxima or minima, temperature gradient, or the rate of temperature change. Thermo-mechanical analyses were done with three different input cycles based on experiments using viscoelastic material properties measured experimentally (Fig. 2a). An example of the resulting stresses is shown in Fig. 2b as a contour plot. Fig. 3 shows the stress time-history at two critical windshield locations in the bond layer between PC and TPU. The three load cycles collapse onto a uniform line (Fig. 3a) when plotted against temperature gradient, showing a strong correlation. Also seen in Fig. 3b is a secondary effect in which the hot temperature cycles collapse on one line, and the cold cycles result in a shift upward in the stresses.

DoD Impact/Significance: Delamination in transparent armor costs the DOD tens of millions of dollars annually. Ongoing government and industry research into materials and testing will be greatly improved by clear understanding of the internal stresses that occur in the full components. This modeling work is being combined with other experimental and analytical efforts to provide a path forward to develop more aggressive inputs for accelerating delamination testing and metrics to identify the minimum needed PC-TPU bond strength to eliminate delamination in real-world environments.

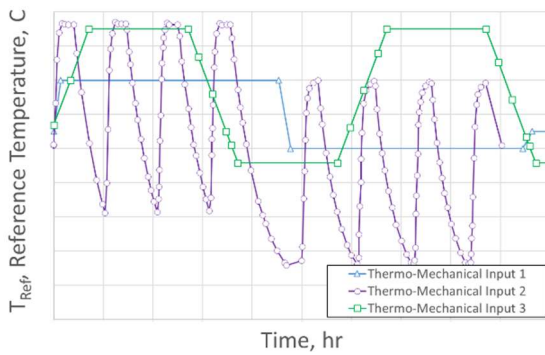


(a)

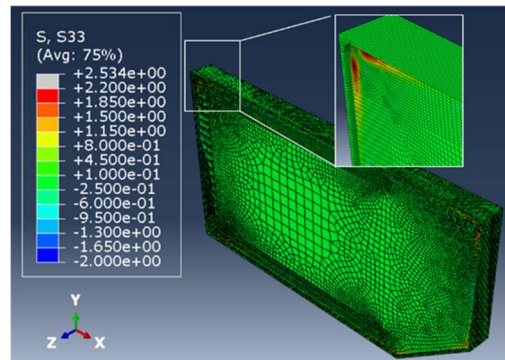


(b)

Figure 1. Schematic representation of transparent armor laminate (a), and corresponding model (b) of the full size component.

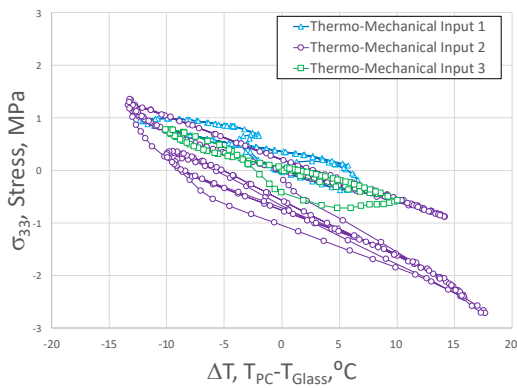


(a)

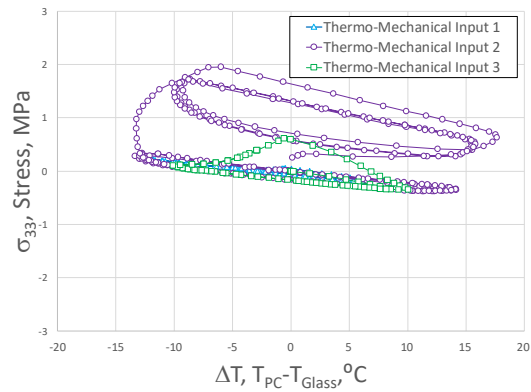


(b)

Figure 2. Three thermal inputs applied to the model external surfaces to simulate critical exposure conditions (a), and resulting stresses (b).



(a)



(b)

Figure 3. Opening stresses for three thermal inputs at two critical locations of the model, representing the highest delamination-driving forces.

Title: Computational Analysis of Warfighter Brain Injury and Protective Equipment

Author(s): X.G. Tan and R.N. Saunders

Affiliation(s): Naval Research Laboratory, Washington, DC

CTA: CSM

Computer Resources: SGI ICE X [AFRL, OH]; Cray XC40 [ARL, MD]; SGI Altix ICE [NRL, DC]; Cray XC40/50, SGI ICE X [ERDC, MS]

Research Objectives: The research objective of this project is developing methods to prevent and mitigate injury to warfighters. This involves computational analysis of ballistic/blunt impacts on personal protective equipment (PPE) and blast-induced traumatic brain injury (TBI). Computational methods, such as finite element analysis, are used to conduct the computational analysis. The use of HPC resources is vitally important to this project due to the high fidelity of the models of interest. A typical model to analyze traumatic brain injury requires approximately 24 hours on 216 computer cores. One of the primary outcomes of this research will be the accumulation of a significant number of simulations, which will be used to construct biomechanical correspondence relationships between humans, animals, and their surrogates.

Methodology: The project uses finite-element methods extensively, but the work is not restricted to finite-element methodologies. Nonlinear material mechanical constitutive response features are highlighted in much of the work performed. Implicit and explicit solutions methods are used as appropriate. The primary finite-element codes used are Abaqus and CoBi. User subroutines are used for specialized material constitutive response when applicable. Multiphysics modeling capability is used to couple the fluid and structure analysis. Typically ParaView, Abaqus/Viewer, IDL, Matlab, and Tecplot are used for visualization of results, including the animation. For model development, the project typically uses CUBIT, Abaqus/CAE, SimpleWare, IDL, and in-house software. Large run times and large model size are often required for the multiphysics/multistep nonlinear finite-element analysis jobs.

Results: This project involves work in several topical areas. Work has been performed on creating image-based high-fidelity head and helmet models, modeling biological tissues and biomechanics of trauma, and modeling ballistic shell and suspension pad materials. Representative results for the analysis of the TBI and combat helmet protection in the blunt impact are presented. We used the multifidelity modeling approach by integrating the fast-running, articulated human with personal protective equipment (PPE) biodynamics model with the high-fidelity human head with helmet finite-element model. The biodynamics model was employed to reconstruct the fall of a human body with PPE caused by the explosive blast wave (Fig. 1). We then simulated the blunt impact of the head with helmet on the ground by utilizing the biodynamics results (Fig. 2). It was found that the helmet helps lower the head acceleration, reduces stresses and strains in the brain, and thus mitigates the severity of brain injury when compared with the head without helmet under the same impact condition.

DoD Impact/Significance: Insights gained from this project are necessary for the advancement from concept to application. Navy/DOD expected results are an improved understanding of traumatic brain injury for Naval/DOD applications. New insights will be gained through quantifying the effects of geometry and material property differences on the mechanical response of quantities correlated with traumatic brain injury, which will impact warfighter health in terms of improved protective gear and improved understanding of the correlation between mechanical response thresholds and traumatic brain injury. The development of techniques to model population-wide anatomical variability will provide insight into the importance of the fit of protective gear.



Figure 1. Snapshots of articulated human body with PPE biodynamics due to blast loading, at 0.3 seconds, 1.1 seconds, and 1.3 seconds.

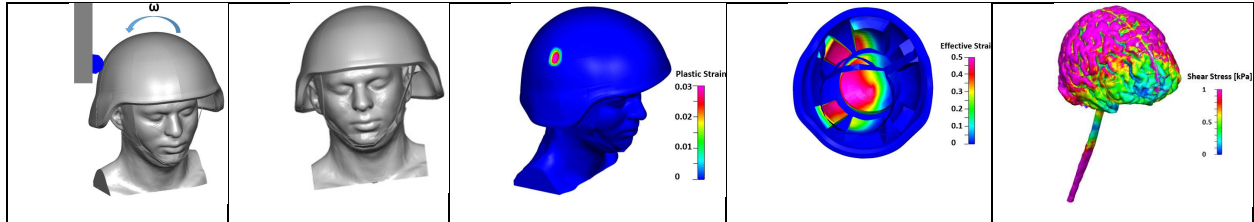


Figure 2. FE analysis of head with helmet hitting a small, solid object on the ground, showing the deformation of head-and-helmet system, plastic strain on the helmet, the effective strain of energy-absorbing pads, and maximum shear stress on the brain.

Title: Stochastic Methods for Uncertainty Quantification in Computational Mechanics
Author(s): K. Teferra and R.N. Saunders
Affiliation(s): Naval Research Laboratory, Washington, DC
CTA: CSM

Computer Resources: SGI ICE X [AFRL, OH]; HPE SGI 8600 [NAVY, MS]

Research Objectives: The research objective is to develop and integrate uncertainty quantification methods into computational mechanics simulations in order to understand the effects of input uncertainty on response quantities of interest. Structural mechanics problems inherently contain many uncertainties, including variability in material properties, boundary conditions, material interfaces, and component morphologies. Additionally, modeling errors are present for meso- and macro-scale simulations primarily because it is too computationally intractable to resolve all length and time scales of the physical processes of interest. In order to understand the effects of these uncertainties on mechanical response quantities of interest, the uncertainties must be characterized, parameterized, and then simulated. Deterministic analysis predicts the system response of a single instantiation of many possible states. Since it is desired to understand the mechanical response for the ensemble of possible system states, extensive simulations must be conducted along with the development of optimal sampling techniques, accurate stochastic simulation algorithms, and reduced order models.

Methodology: The project extensively uses finite element methods along with in-house-developed scripts and compiled codes. Nonlinear material constitutive response, complex-component and microstructure geometry, and large mechanical deformations are common features of the scenarios simulated. Implicit and explicit solutions methods are used as appropriate. The range of finite element codes used at Abaqus, CoBi, Sierra, and Moose. Model development is done with CUBIT, Abaqus/CAE, SimpleWare, or in-house software. Large run times and large model size are often required for the multi-step nonlinear finite element analysis jobs.

Results: While this project involves work in several research areas, the topic of modeling the microstructure evolution of additively manufacturing (AM) materials is highlighted. Material properties are derived from its composition as well as microstructural configuration, which depends on the processing technique used in fabrication. The layer-by-layer deposition process in AM is a significant departure from traditional wrought processing, resulting in unique microstructures. This project focuses on using the cellular automata finite element model to simulate the melting and grain growth due to the rastering laser. The laser parameters include power, intensity, and scanning velocity, which affect the shape of the melt pool, ultimately affecting the grain solidification structure. The results of applying this model are shown for a single scan in Figure 1. These results show that as the material solidifies, the grain growth follows the melt pool as the material cools below the melting temperature. While these results are preliminary, they show that the grain growth direction is aligned with the direction of maximum temperature gradient, which is to be expected.

DoD Impact/Significance: Enhanced structural material performance in terms of durability and strength-to-weight ratio, as well as manufacturability are essential ingredients toward transforming fleet capabilities. Additive manufacturing (AM) may eventually become a commonplace manufacturing technique for both military and civilian applications. Understanding the relationship between AM processing parameters and microstructure morphology can provide guidance to material designers to achieve manufacturing of materials with desired properties.

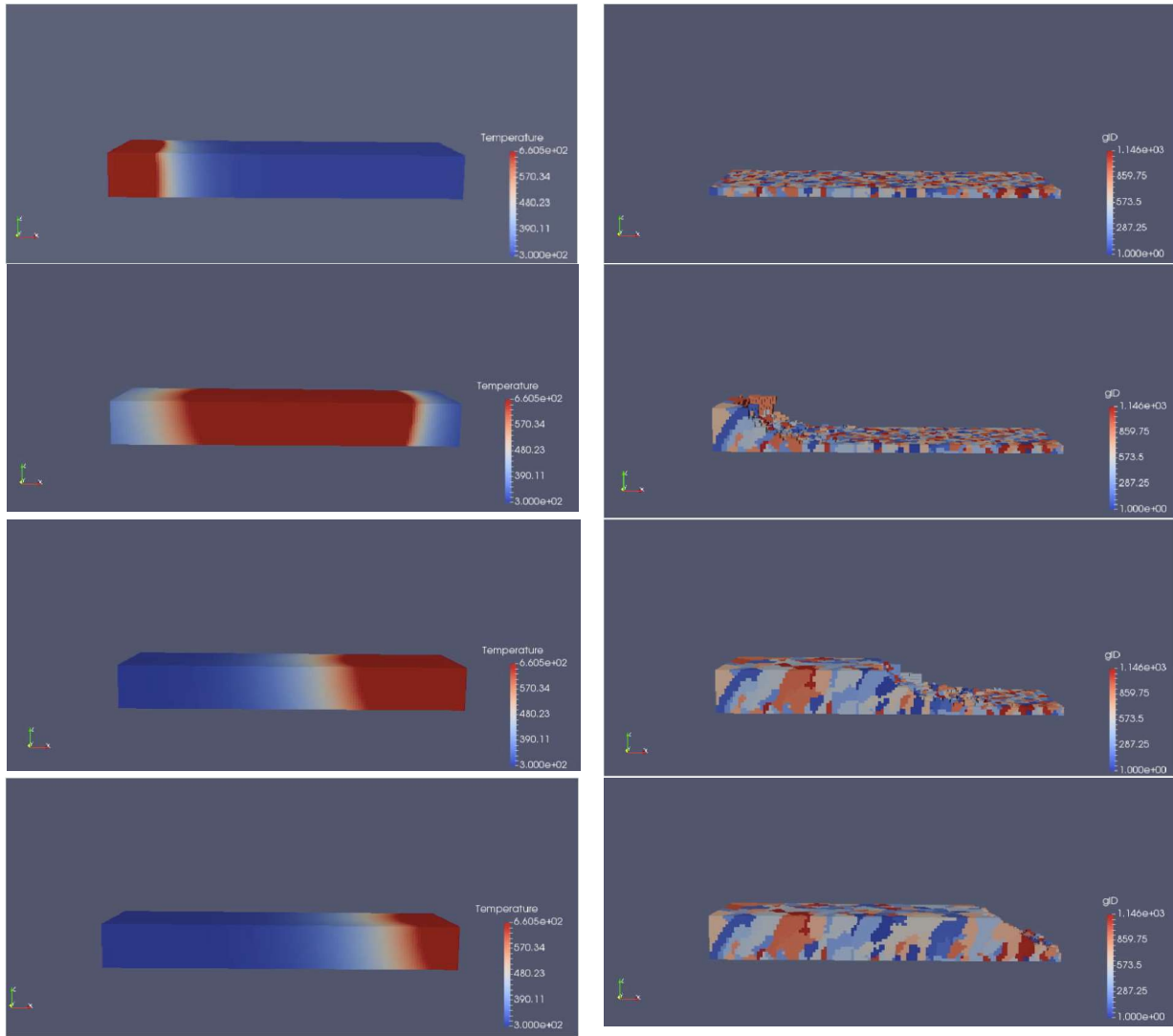


Figure 1. Results of a cellular automata finite element simulation of a single scan. The left figures show time snapshots of the temperature field, and the right figures show the ensuing competitive grain growth as the material cools.

THIS PAGE INTENTIONALLY LEFT BLANK

CFD

Computational Fluid Dynamics

CFD covers high-performance computations whose goal is the accurate numerical solution of the equations describing fluid motion and the related use of digital computers in fluid dynamics research. CFD is used for basic studies of fluid dynamics for engineering design of complex flow configurations and for predicting the interactions of chemistry with fluid flow for combustion and propulsion. It is also used to interpret and analyze experimental data and to extrapolate into regimes that are inaccessible or too costly to study. Work in the CFD CTA encompasses all Reynolds number flow regimes and scales of interest to the DoD. Incompressible flows are generally slow (e.g., governing the dynamics of submarines, slow airplanes, pipe flows, and air circulation) while compressible flows are important at higher speeds (e.g., controlling the behavior of transonic and supersonic planes, missiles, and projectiles). Fluid dynamics, itself, involves some very complex physics, such as boundary layer flows, transition to turbulence, and turbulence dynamics that require continued scientific research. CFD also must incorporate complex additional physics to deal with many real-world problems. These effects include additional force fields, coupling to surface atomic physics and microphysics, changes of phase, changes of chemical composition, and interactions among multiple phases in heterogeneous flows. Examples of these physical complexities include Direct Simulation Monte Carlo and plasma simulation for atmospheric reentry, microelectromechanical systems (MEMS), materials processing, and magnetohydrodynamics (MHD) for advanced power systems and weapons effects. CFD has no restrictions on the geometry and includes motion and deformation of solid boundaries defining the flow.

Title: Advanced Computational Models that Exploit Emerging Computer Architectures
Author(s): K. Obenschain and G. Patnaik
Affiliation(s): Naval Research Laboratory, Washington DC
CTA: CFD

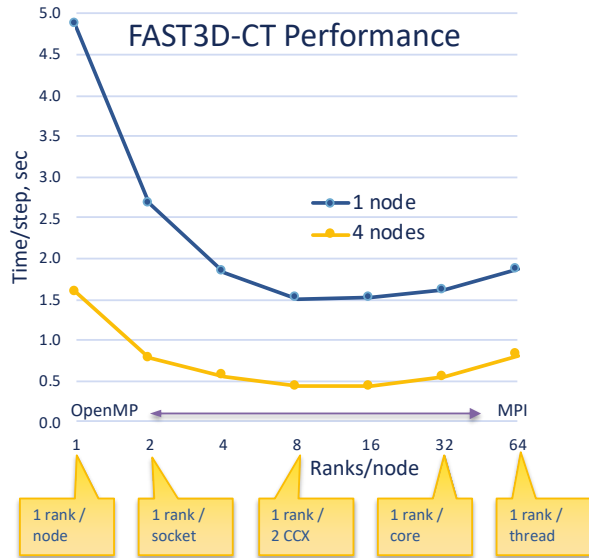
Computer Resources: HPE SGI 8600, SGI ICE X [AFRL, OH]

Research Objectives: This project aims to expand the use of many-core devices in high-performance computing environments while creating specific needed research capabilities that these devices enable. Specifically, 1: Develop methodologies to enable existing codes to exploit the performance of rapidly evolving many-core devices (MCD) to solve current roadblock problems. 2: Develop approaches to exploit the improved high-bandwidth communication architectures that are becoming available currently.

Background: The Laboratories for Computational Physics and Fluid Dynamics (LCP&FD) maintains an edge in computational physics by exploiting novel computer systems. Thus, NRL has been able to tackle and solve the hard problems using limited resources well before others in the field. The results from our previous 6.1 research proved that many-core architectures such as Graphical Processing Units (GPUs) could be exploited successfully for research computing and have observed that MCD architectures are evolving rapidly. To extend our lead, we must embrace this uncertainty and develop MCD-friendly methodologies that allow all of our codes to benefit from MCD architectures to start new initiatives and to solve currently intractable problems. A large number of legacy codes exist throughout the DoD that are still relevant and continue to be developed. Unfortunately, the resources to fully rewrite these codes for MCD architectures are not available.

Methodology/Results: HPCMP's resources are utilized to define a baseline for performance comparisons with exploratory architectures. The 6.1 project this effort supports in turn looks at different approaches such as different architectures and tactics to allow legacy codes to exploit the additional computing power on leading-edge hardware. Figure 1 demonstrates an example of tuning legacy codes to newer hardware (AMD EPYC). Currently deployed HPCMP systems (e.g. Intel Skylake – Mustang) have different memory topologies and less complex non-uniform memory architectures, hybrid codes (OpenMP+MPI) such as FAST3D-CT need to be cognizant of this additional complexity.

DoD Impact/Significance: The proposed work and applications proposed above are relevant to: Expeditionary & Irregular Warfare (Counter IED, sensors, lethality & survivability), Computational Environment Architecture (open architecture) Platform Design and Survivability (advances platform design, survivability, unmanned vehicles, and high-speed platforms), Power and Energy (energy security, power systems), Computational Materials Science and Fluid Dynamics.



Sweet spot corresponds to 1 rank per 2 CPU complexes (CCX), so no communications needed within rank

Figure 1. Performance Tuning for AMD EPYC.

Title: Simulations of Laser-Plasma Interactions and the Radiation Hydrodynamics of High-Velocity Laser-Accelerated Matter

Author(s): J.W. Bates, A.J. Schmitt and K. Obenschain

Affiliation(s): Naval Research Laboratory, Washington, DC

CTA: CFD

Computer Resources: HPE SGI 8600 [AFRL, OH]; Cray XC40 [ARL, MD]; Cray XC40/50 [ERDC, MS]

Research Objectives: Hydrodynamic and laser-plasma instabilities are the two main physics obstacles limiting thermonuclear ignition and high yield with laser-driven implosions. The goal of this work is to gain a better understanding of these phenomena and to develop practical strategies for their mitigation using the codes FastRad3D, ASTER and LPSE.

Methodology: LPSE is a wave-based, massively parallel computer code designed to solve the nonlinear Zakharov equations in the context of high-energy density plasmas. LPSE is highly useful because it can be used to study laser-plasma instabilities (including the generation of suprathermal electrons that can spoil the high compression of the thermonuclear fuel) such as two-plasmon decay, cross-beam energy transfer (CBET) and Brillouin and Raman scattering — all of which are presently key challenges in the quest for successful inertial confinement fusion (ICF). (CBET, in particular, has recently been identified by the NNSA as a critical LPI issue in the U.S. laser-direct-drive program.) FastRad3D and ASTER, on the other hand, are Eulerian-based radiation-hydrodynamics codes that are used to simulate a complete ICF implosion. These codes are also massively parallel — and while they do not address laser-plasma instabilities — they do model a variety of other complex physical processes important for laser fusion such as laser absorption, radiation transport and thermonuclear burn. We are using all three of these codes to improve our understanding of the physics of ICF implosions.

Results: Our primary results for FY2019 were obtained using the LPSE code in two and three spatial dimensions. Using the LPSE code, we modeled frequency-tripled, Nd:glass laser beams with realistic features such as random speckle patterns, distributed phase plates and polarization smoothing and showed that broadband laser light can significantly mitigate CBET at a bandwidth of about 8 THz ($\Delta\omega/\omega_0 \simeq 1\%$, where $\Delta\omega/2\pi$ and ω_0 are the bandwidth and angular frequency, respectively) for plasma conditions that are similar to those on the National Ignition Facility. We also demonstrated in our study that “frequency detuning” (i.e., utilizing two or three discrete “colors” of narrowband laser light), does suppress CBET to a degree, but its efficacy as a mitigation strategy is limited. Although the bandwidths of existing, high-power ICF lasers are too small to suppress CBET directly, there are now experimental efforts underway to develop broadband laser drivers for ICF applications. The results of our simulations of CBET have helped to justify the necessity for such laser development and also to quantify the bandwidth levels needed. It is expected that broadband lasers will be beneficial for mitigating other varieties of laser-plasma instabilities as well, which is a subject of ongoing research.

DoD Impact/Significance: Suppression of hydrodynamic and laser-plasma instabilities will expand the design space available for viable ICF target designs, which will benefit the National ICF program and auxiliary research efforts related to stockpile stewardship.

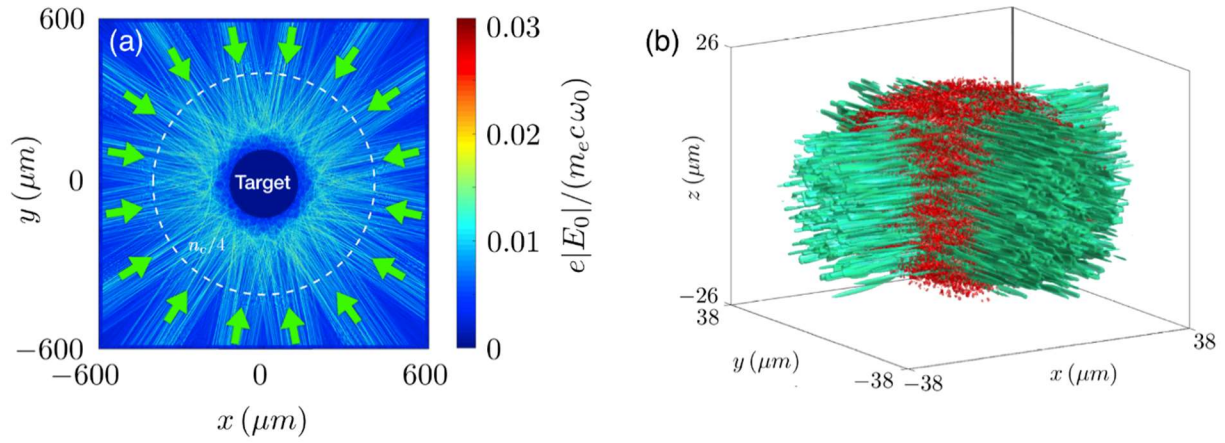


Figure 1. Examples of CBET simulations performed with the LPSE code in (a) two and (b) three dimensions. The plot in (a) shows the electric-field magnitude of 16 laser beams impinging on a spherical, full-scale ICF target where each beam is modeled with discrete speckles, distributed phase plates and polarization smoothing, and an outward plasma flow velocity enables CBET scattering to occur, as indicated by the bright areas in the figure. (Note that the dashed, white line denotes the quarter-critical surface of the plasma.) The surface plot in (b) shows iso-contours of the magnitude of the electric field for two lasers (shown in green) crossing at 90 degrees in an ICF plasma and exchanging energy by the CBET process. The red areas in this figure denote the density perturbations of the ion acoustic waves coupling the two beams.

Title: Dynamics of Compressible Turbulent Flames and the Deflagration-to-Detonation Transition

Author(s): V.N. Gamezo¹ and A.Y. Poludnenko²

Affiliation(s): ¹Naval Research Laboratory, Washington, DC; ²University of Connecticut, Storrs, CT
CTA: CFD

Computer Resources: SGI ICE X, HPE SGI 8600 [AFRL, OH]; Cray XC40/50, Cray XE6m, SGI ICE X, [ERDC, MS]

Research Objectives: Recent years have seen a resurgence of interest in rotating detonation engines (RDE) in the context of rocket propulsion. The goal of this project is to model, understand, and predict complex reactive-flow phenomena leading to the detonation initiation, including the DDT, from first principles both in combustion systems on Earth and in astrophysical contexts.

Methodology: We carry out fully resolved simulations with single-step and multistep kinetics to compute the interaction of a fully resolved, premixed flame with a subsonic turbulence. We solve compressible reactive-flow equations on a uniform mesh using a fully unsplit corner transport upwind scheme with the PPM spatial reconstruction and the Harten-Lax-van Leer-contact (HLLC) Riemann solver implemented in the code Athena-RFX. We consider both the canonical “flame-in-a-box” configurations, as well as the setup based on the realistic geometry and experimental conditions that correspond to the Turbulent Shock Tube (TST) facility developed at the University of Central Florida. We consider chemical burning in H₂-air and CH₄-air mixtures described by one-step Arrhenius or detailed reaction kinetics models, as well as thermonuclear burning of C¹² and O¹⁶ in relativistic, degenerate plasmas typical of stellar interiors during Type Ia supernova (SNIa) explosions. The thermonuclear burning is implemented using an α -chain network.

Results: The simulations show that the interaction of highly subsonic chemical or thermonuclear flames with a highly subsonic turbulence can produce strong shocks and detonations. A rapid runaway process resulting in a pressure buildup occurs once the flame speed exceeds the critical Chapman-Jouguet (CJ) deflagration threshold. In a paper published in *Science*³, we developed a general analytical theory of turbulence-driven DDT (tDDT) in unconfined systems. This universal mechanism allows a detonation to form while the flame remains in the flamelet regime, in which the turbulent flame brush can be viewed as a folded laminar flame sheet with the internal structure minimally affected by turbulence. We describe an experimental confirmation of this process in terrestrial H₂-air flames in the TST facility at the University of Central Florida. Next, we used numerical simulations of a fully resolved turbulent thermonuclear flame in a degenerate ¹²C stellar plasma to show that under conditions representative of those in a SNIa explosion, this mechanism also can result in the spontaneous formation of strong shocks triggering a detonation (Fig. 1). We also recently carried out direct numerical simulations of the tDDT process in the TST facility (Fig. 2). This resulted in the largest simulation of a reactive-flow system to date with the grid size of ~90 billion cells.

DoD Impact/Significance: Understanding the mechanisms of flame acceleration and DDT provides insights for further development of turbulent combustion models for large-eddy simulations of high-speed regimes. These models are important for the theory of Type Ia supernova explosions, and are critical for the design of the next generation of propulsion and energy-conversion systems, such as scramjet engines, rotating-detonation engines, high-pressure turbines, etc.

³Poludnenko, A.Y., Chambers, J., Ahmed, K., Gamezo, V.N., Taylor, B.D., A unified mechanism for unconfined deflagration-to-detonation transition in terrestrial chemical systems and type Ia supernovae. *Science* 366, eaau7365 (2019).

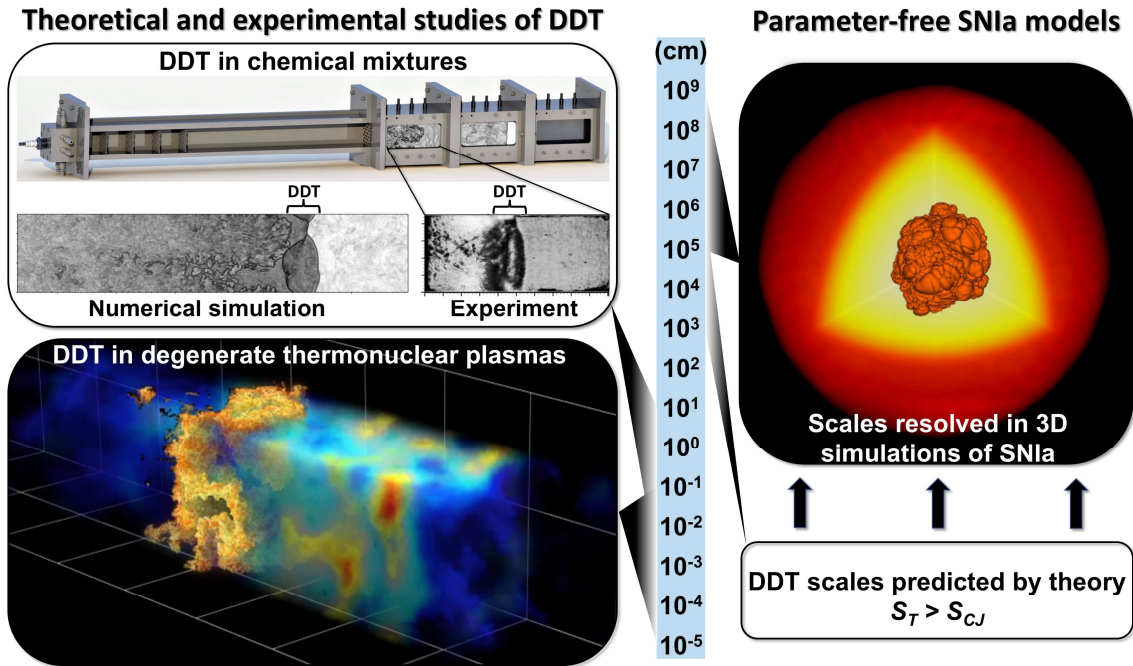


Figure 1. The DDT in SNIa is predicted to occur on scales of $\sim 10^3$ to 10^6 cm, which is well below the characteristic scale of a WD star (10^9 cm) and mostly below the smallest scales resolvable in three-dimensional simulations, $\sim 10^5$ cm. To demonstrate the turbulence-driven, unconfined DDT in experiments and DNS, we considered turbulence-flame interaction on small scales of $\sim 10^{-5}$ to 10 cm. The synergy between the experiments and DNS of chemical and thermonuclear flames led to the unified theory of DDT.

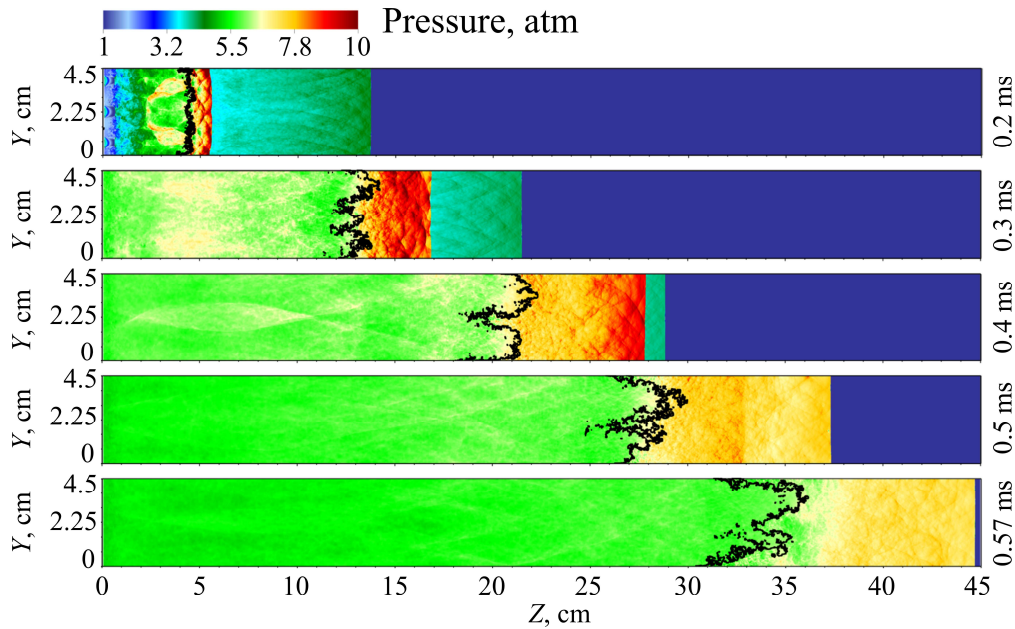


Figure 2. Two-dimensional cuts of pressure in the DNS of the TST facility.

Title: Advanced Two-Phase CFD Model
Author(s): T.D. Holman
Affiliation(s): Naval Research Laboratory, Washington DC
CTA: CFD

Computer Resources: Appro Cluster [ARL, MD]

Research Objectives: Two-phase heat-transfer devices are the state of the art in thermal system architecture, especially the Loop Heat Pipe (LHP) architecture. Due to not having moving parts, these devices are ideal for use in space environments. Numerically simulating the internal flow of two-phase heat-transfer devices will give a better understanding of their behavior in different environments that they are tested and operated in. The primary objectives are verifying physical oscillation mechanisms, designing to minimize instability regions, and implementing control methods to mitigate unavoidable instability regions through numerical modeling and experimental testing. These oscillations have been shown to precede/cause loop heat pipes to inadvertently shut down, a most undesirable occurrence that is not addressed by existing loop heat pipe theory. This inadvertent shutdown is often referred to as a LHP failure.

Methodology: To achieve this goal, there are continued development of numerical and analytical models, continued experimental program to confirm the accuracy of the analytic and numerical models, and the utilization of these models to study and design loop heat pipes to mitigate the effects of oscillatory behavior. The end results are tools that will be utilized for design of LHPs for future space assets. The basic approach is: 1) Utilize analytical model predicts of oscillations in closed-loop two-phase heat-transfer systems and experience to narrow down parameter space of mechanisms that cause oscillations. 2) Mitigate unavoidable oscillations through closed-loop control. 3) Utilize the analytical and numerical models to design proof-of-concept robust LHP. 4) Test proof-of-concept robust LHP design. This is expected to be an iterative process.

Results: A significant numerical modeling effort went into determining the viability and sizing of a condenser bypass tube and its effect on thermal fluid oscillations in a loop heat pipe — see Fig. 1. These numerical efforts led to the conclusion that a condenser bypass tube will control thermal fluid oscillations in a loop heat pipe. An experiment started to prove a condenser bypass tube could control oscillations in a loop heat pipe. A large loop heat pipe with a condenser bypass tube, and a small valve to close the condenser bypass tube, has been tested in the environmental chamber at NRL. The large loop heat pipe has been tested previously in the environmental chamber at NRL and showed thermal fluid oscillations — see Figs. 2 and 3. The test was conducted with and without the condenser bypass, the valve can be opened and closed, and it was observed that the condenser bypass eliminated oscillations that were observed between 500W and 600W without the bypass.

Four papers have been published and all have been well received, one journal article has been written but is still under review. One patent has been submitted.

DoD Impact/Significance: A unique model has been created that can predict where oscillatory behavior in LHPs can occur and can predict the frequency/amplitude of the oscillations. The model is still being developed to add more features, but this unique tool allows NRL to design more robust LHPs.

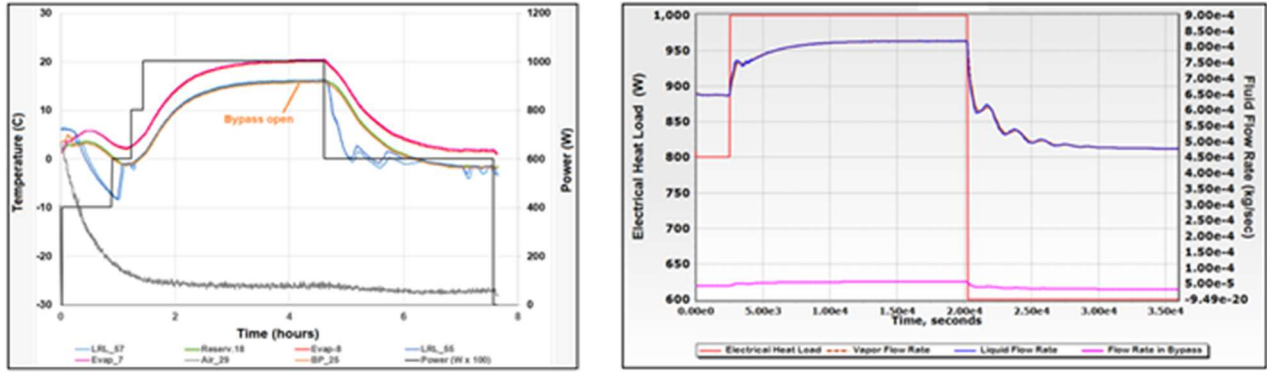


Figure 1—Comparison of LHP model and LHP experimental data.

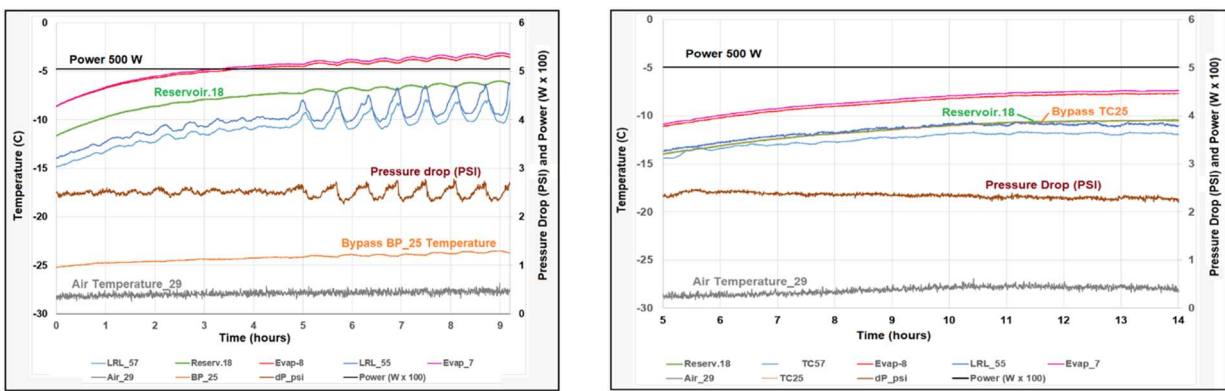


Figure 2. LHP oscillations with and without condenser.

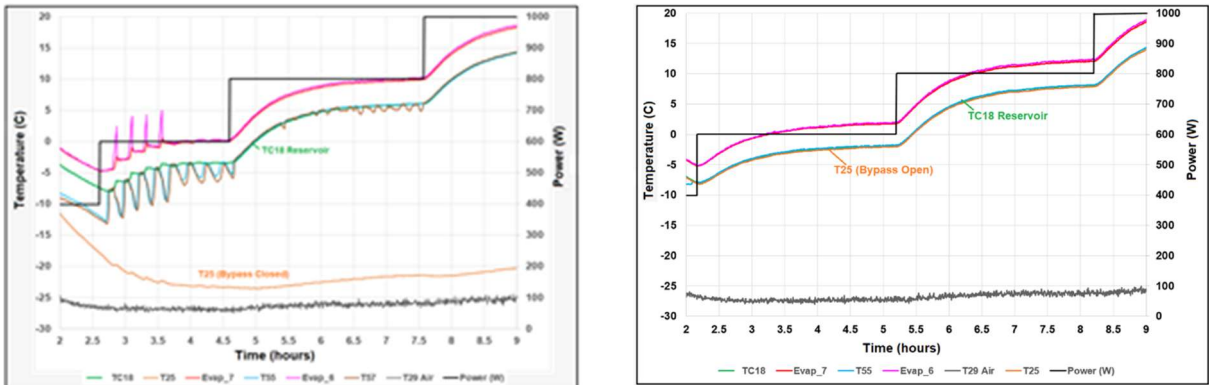


Figure 3. LHP operation with and without condenser bypass.

Title: The Impact of Foam and Aerosol Dynamics on Fire, Explosion Safety, and Suppression (Mechanisms of Water Mist Suppression of a Burning Solid Surface)

Author(s): X. Zhuang¹ and R. Ananth²

Affiliation(s): ¹ASEE Postdoctoral Fellow, Naval Research Laboratory, Washington, DC; ²Naval Research Laboratory, Washington DC

CTA: CFD

Computer Resources: SGI ICE X [AFRL, OH]

Research Objectives: The objective of this work is to develop a computational model to study the interfacial properties of the surfactant monolayers at fuel/water and air/water interfaces, and their interactions with heptane and gasoline fuels.

Methodology: The molecular dynamics (MD) simulations were performed on surfactants to simulate a heptane/surfactant-monolayer/water interface with a constant number of molecules, pressure, and temperature (*NPT*) ensemble. NAMD is used to run the MD simulations, and VMD, CHARMM, and Python were used for the trajectory analyses and properties calculations. A large variety of siloxane surfactants were studied to investigate the effects of changes to surfactants' tail and head structures on the interfacial properties relating to lamella stability and fuel/surfactant packing at the interface. Beside pure surfactants, surfactant mixtures also were studied to investigate their effect on interfacial properties.

Results: Packing of surfactants at an interface is quantified by calculating order parameter, number of hydrogen bonds, and the atomic number density of heptane fuel (AND_h), which may be related to the heptane transport rate. We also calculated the ratio of the number of heptane fuel molecules to surfactant molecules (R_h), which may be related to degradation rate. Figure 1a shows simulation results for mixtures of zwitterionic fluorocarbon surfactant (Capstone) and a hydrocarbon surfactant (nonylglycoside with one glycoside head and a nine-carbon-length tail). The order parameter of the capstone/glycoside surfactant mixture as a function of atom position in the nonylglycoside molecular structure. Figure 1a shows that the order parameter is the highest when the mass fraction of Capstone (f) equals 0.6. By using Capstone/glycoside as reference, we may target to find a fluorine-free surfactant with high order parameter of the tail and tight packing. Polyoxyethylene trisiloxane/glycoside surfactants were studied to investigate surfactant packing. As shown in Fig. 1b, a polyoxyethylene trisiloxane surfactant (H10) with ten oxyethylene (OE) units has higher order parameter at a mass fraction of 0.2, which may result in tighter packing and possibly high interfacial stability. The results show that the trisiloxane/Glucopon with smaller OE unit has smaller AND_h ; the smallest value occurs at OE unit $n=8\sim 9$. We also simulated siloxanes with a large variety of head groups to have a general idea on interfacial properties of the novel siloxane surfactant. The results show that the trisiloxanes with two glucosides as a head group have the lowest AND_h . Therefore, they may have similar heptane transport rate as capstone and may be potentially good surfactant candidates.

DoD Impact/Significance: Per- and polyfluoroalkyl substances (PFAS) in Aqueous Film Forming Foams (AFFF) for firefighting pose environmental and health problems. Therefore, PFAS must be replaced, but without sacrificing their high fire-suppression performance for pool fires. Computational models of fluorine-free siloxane surfactants are developed to optimize their molecular structures for increased packing at an interface. Increased packing can create better barriers for fuel traveling through a foam layer and feeding the fire. This will provide structural features of potential surfactants for synthesis and experimental investigations, and facilitate the development of environmentally safe and effective firefighting foams.

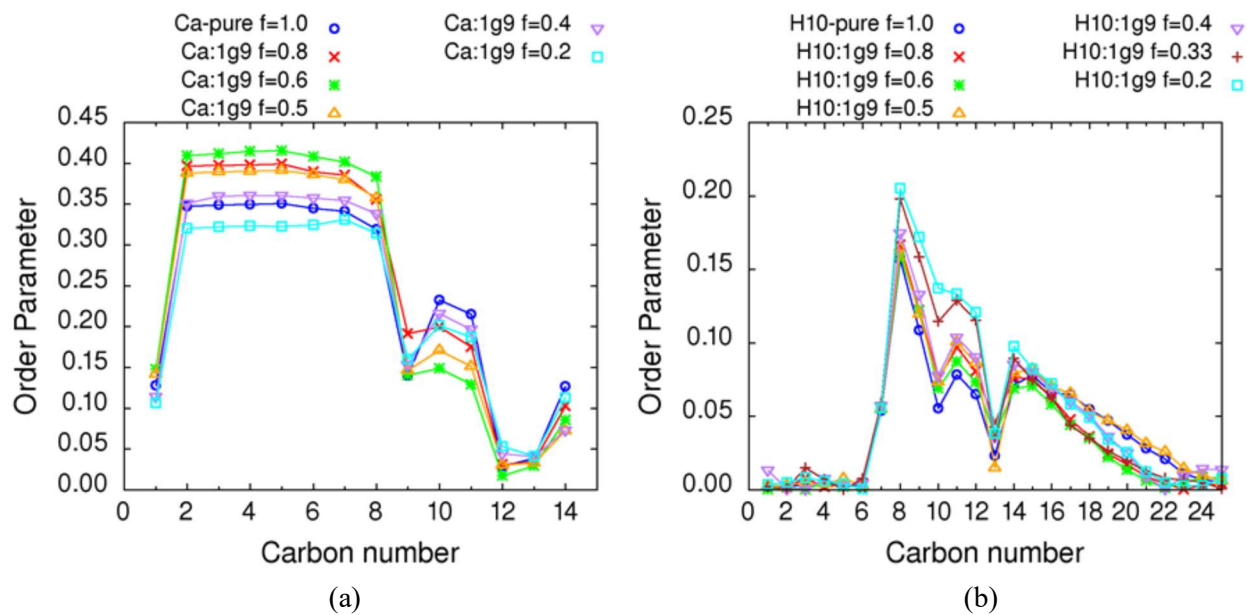


Figure 1. (a) Order parameter of Capstone/glycoside as a function of atom position in glycoside's molecular structure at varied capstone mass fraction f . Ca is Capstone, and 1g9 is nine-carbon-length tail with one glycoside head. (b) Order parameter of trisiloxane (H10)/glycoside (1g9) as a function of atom position on trisiloxane with ten oxyethylene units at varied trisiloxane mass fraction f .

Title: High-Temperature and Rarefied Gas Dynamics in Hypersonic Flows
Author(s): J.R. Maxwell, E.W. Hyde, and R.E. Rogers
Affiliation(s): Naval Research Laboratory, Washington, DC
CTA: CFD

Computer Resources: SGI ICE X [ARL, MD]; Cray XC40 [NAVY, MS]

Research Objectives: The objective of the investigations is to develop a quick and efficient tool to predict aerothermodynamics about bodies in hypersonic flows. The verification and validation of the analytical tool, WRAITH, will be verified using CFD.

Methodology: This research has utilized the CFD code ANSYS Fluent, which requires significant parallel computing to achieve high-fidelity results. To achieve this, flight domains must be created and meshed intelligently with the geometric complexity of the flight vehicle and domain considered. Numerical solutions utilizing high-performance parallel computing then are initiated to solve the domain. For the present research, hypersonic flow about a waverider was studied to investigate the aerodynamic and transient thermal effects on the body and to use those results to verify a reduced-order analytical model, called WRAITH.

Results: High-fidelity LES simulations were used to verify the results of an NRL-developed analytical code, WRAITH, for the prediction of aerodynamic forces, moments, and heating on a conical waverider. Flow and vehicle conditions predicted using WRAITH are generated in a matter of seconds, while the CFD took significantly longer. However, CFD typically agreed with the analytical tool to within 10% for variables of interest.

DoD Impact/Significance: This research has contributed to the understanding of heating and aerodynamic affects in hypersonic flows. Specifically, it has fostered the creation of an analytical tool that yields approximate results for vehicle heating and aerodynamic forces and moments for a candidate vehicle across its entire flight path. This tool can produce results in seconds while the alternative CFD methods may require millions of CPU-hours. Expanding on this newfound knowledge, better modeling of aerodynamic entry vehicles, meteorites, and low-Earth-orbit satellites will be possible.

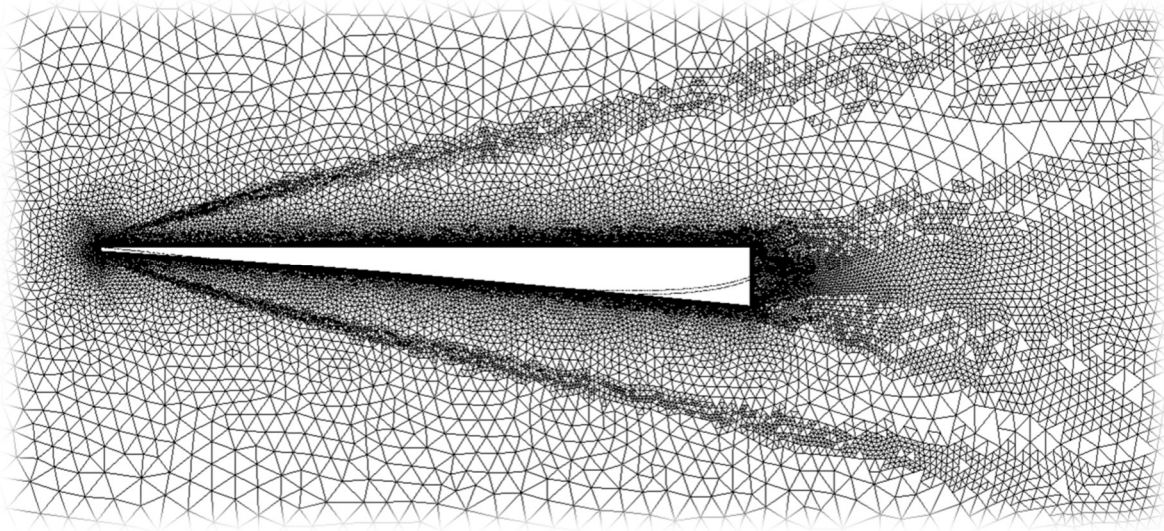


Figure 1. High-resolution and adaptively refined mesh for a hypersonic waverider.

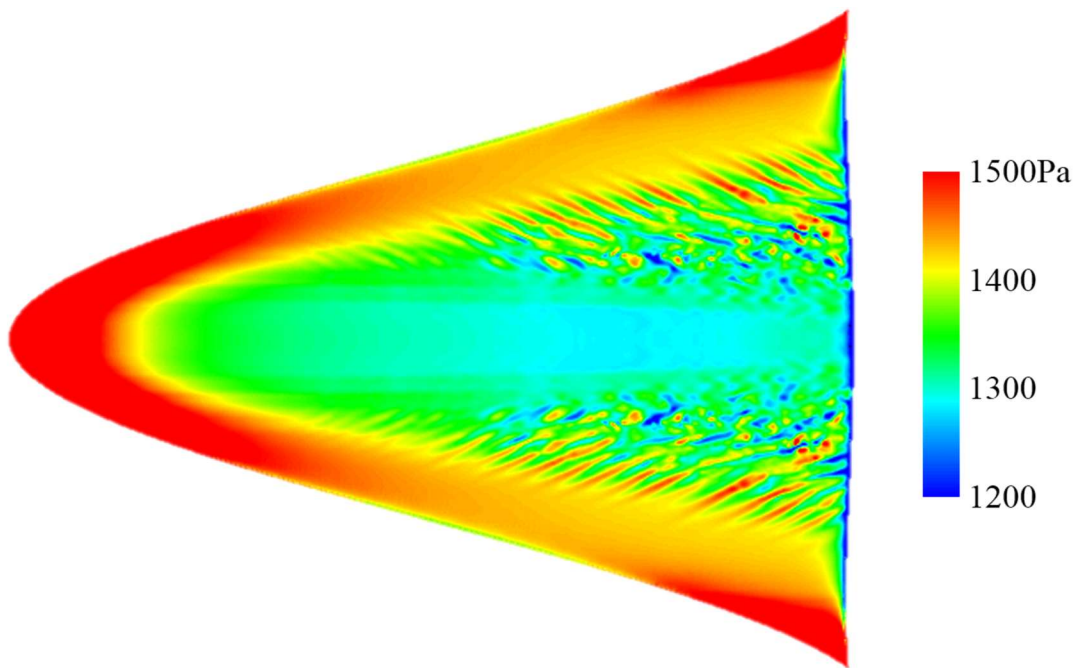


Figure 2. Simulations of pressure contours of the waverider illustrating the transition to turbulence.

Title: Direct Numerical Simulation of Fluid-Sediment Wave Bottom Boundary Layer

Author(s): A. Penko, S.P. Bateman, J.A. Simeonov, and J. Calantoni

Affiliation(s): Naval Research Laboratory, Stennis Space Center, MS

CTA: CFD

Computer Resources: SGI ICE X [AFRL, OH]; Cray XC40 [ARL, MD]; Cray XC40/50, Cray XE6m [ERDC, MS]

Research Objectives: Predictive models for nearshore bathymetric evolution require a complete understanding of the physics of fluid-sediment interactions in the wave bottom boundary layer (WBBL). Since such processes are difficult, if not impossible, to measure in situ, we performed coupled fluid-sediment numerical simulations to increase our understanding of the sediment and hydrodynamics in the WBBL. Fundamental concepts used in describing the phenomena of sediment transport such as mixture viscosity and diffusivity, hindered settling, reference concentration, bed failure criterion, and the concept of acceleration-induced transport are addressed with our models. The models produce high-resolution results necessary to gain insight into the small-scale boundary layer processes and to clarify new directions for measurement techniques needed to improve predictive capabilities.

Methodology: Utilization and development of a suite of discrete and continuum WBBL models for simulating sediment transport in the nearshore environment from the microscale (cm-m) to the mesoscale (km) is ongoing with HPC resources. At the microscale (<10 cm), the three-dimensional sediment phase is simulated with discrete element method (DEM) that allows individual grains to be uniquely specified (e.g., size, density, and shape). The fluid phase model varies in complexity from a simple one-dimensional eddy viscosity to a fully three-dimensional direct numerical simulation (DNS). Coupling between the fluid and sediment phases varies from one-way coupling to a system fully coupled at every fluid time step. Between the micro- and mesoscale (1-50 m), a spectral seafloor model simulates seafloor roughness dependent on changing wave conditions. At the mesoscale (1-10 km), a model simulates high resolution three-dimensional flow over the inner continental shelf in domains $O(4 \times 10^4 \text{ m}^2)$. Also at the mesoscale, nearshore hydro- and morphodynamics are simulated with the coupled wave-circulation morphology model, Delft3D.

Results: Simulations of oscillatory flow over a two-dimensional rippled sediment bed used sedFoam, an open-source solver based on OpenFOAM, which incorporates two-phase Euler-Euler coupling between the fluid and sediment phases, where the sediment phase was modeled using kinetic theory. Simulations were run from both initial flat bed and initial ripple conditions. Sediment grain size and oscillatory flow conditions were selected to match laboratory experiments by Frank-Gilchrist et al. (2018). Preliminary results for velocity, sediment concentration, and fluid shear stress (Fig. 1) demonstrate the fluid flow and sediment suspension over the ripple. Results are utilized for a machine learning approach for sediment transport prediction.

DoD Impact/Significance: Ultimately, all process-based models for nearshore bathymetric evolution are limited by shortcomings in fundamental knowledge of multiphase-boundary-layer physics. The microscale simulations provide an unprecedented level of detail for the study of fluid-sediment interactions that is impossible to obtain with available measuring technologies in the field or the laboratory. These results are utilized to improve parameterizations of small-scale processes in larger-scale models. At the mesoscale, our models are highly efficient and well suited for coupling to regional operational hydrodynamic models in order to include the effects of an evolving seafloor bottom.

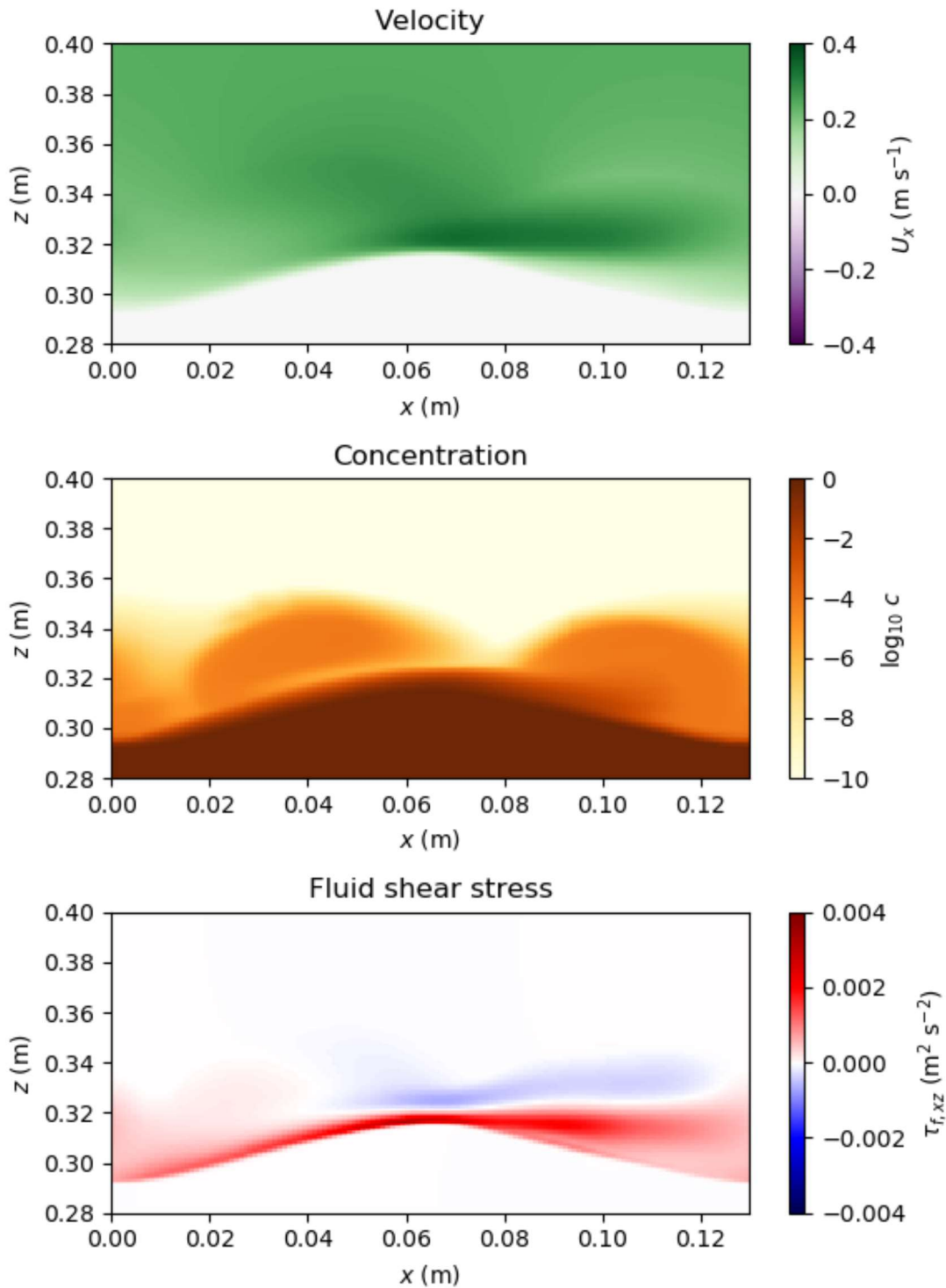


Figure 1. Visualization of two-dimensional (a) velocity, (b) sediment concentration, and (c) fluid shear stress output from a sedFoam simulation. The time shown is at $t = 2.75$ sec, just before the onshore peak of bottom velocity generated by the propagation of a surface wave over a sand ripple on the seafloor. The simulation domain was 71,500 grid cells and was run for 10 wave periods, using ~ 1900 CPU-hours on 128 processors on the Excalibur Cray XC40 system at ARL DSRC.

Title: Bathymetry Prediction System

Author(s): A. Penko¹, J. Veeramony¹, M. Palmsten¹, S. Harrison¹, K. Edwards¹, S. Trimble², and W. Lee²

Affiliation(s): ¹Naval Research Laboratory, Stennis Space Center, MS; ²National Research Council Postdoctoral Fellow

CTA: CFD

Computer Resources: Cray XC40 [ARL, MD]

Research Objectives: Rapid changes in nearshore bathymetry (such as sandbar migration) occurring during the daily-to-weekly passage of weather fronts impact navigation and trafficability in very shallow water (VSW). A major challenge for bathymetric models is high sensitivity to the initial bathymetry and spatial variability of sediment type. Such information is typically out of date or does not exist for VSW in denied areas. This project combines state-of-the-art remote sensing, data assimilation, and ensemble numerical modeling to produce a new coastal prediction system that forecasts waves, circulation, and bathymetric evolution including uncertainty estimates on operational length and time scales without the need for high-resolution in situ measurements.

Methodology: We developed an ensemble bathymetric modeling system that can be set up and run in areas with sparse to no observational data. This approach differs from the heuristic approach frequently taken in numerical modeling, in which models are set up and calibrated to match a single set of observations at a particular site. In contrast, this approach takes into account the uncertainty in model inputs and parameters to produce a robust probabilistic forecast of waves, currents, and sediment transport in the nearshore, which is particularly useful when the likelihoods of hydrodynamic conditions and bathymetric change are required for operations. Ensemble simulations were run using a range of parameters and initial conditions. The ensemble simulations of hydro- and morphodynamics were performed using a nested Delft3D setup at the U.S. Army Corps of Engineers Field Research Facility (FRF) in Duck, NC. First, the sensitivity of the model parameters to the simulated hydro- and morphodynamics at the FRF site was tested by running more than 3300 hindcast ensemble simulations with varying parameter values. These simulations ran for approximately 20 hours on 32 processors, utilizing more than 2.1 million CPU hours of the DoD HPCMP.

Results: We tested the system in a weeklong hindcast simulation at the FRF during Hurricane Joaquin in 2015. The parameter ranges that contributed the most variation in the flow and sediment transport results then were used in the ensemble system to produce probabilistic outputs of waves, currents, and sediment transport. The ensemble simulation results showed that the specified sediment transport formula chosen within the simulation yielded the largest variability between simulations. We calculated the standard deviation of the seafloor elevation of all the ensemble simulations and plotted to show where the model varied the most in its predictions of bed-level change (Fig. 1). Using ensemble simulations with varying model parameters and inputs can provide an estimate of model uncertainty and insight into where the greatest amount of bed change is likely to occur.

DoD Impact/Significance: Littoral bathymetry evolves rapidly due to the passage of weather fronts, impacting navigation and trafficability as well as mine countermeasures. Due to the continual fluctuations in the littoral zone, forecasting systems coupled with data assimilation and uncertainty estimation are necessary to provide the most accurate information possible for quantitative decision making. In the long term, predictions of nearshore coastal bathymetric change will improve wave and current predictions that will aid in the navigation and trafficability of the Navy and will provide valuable information about mine burial/exposure.

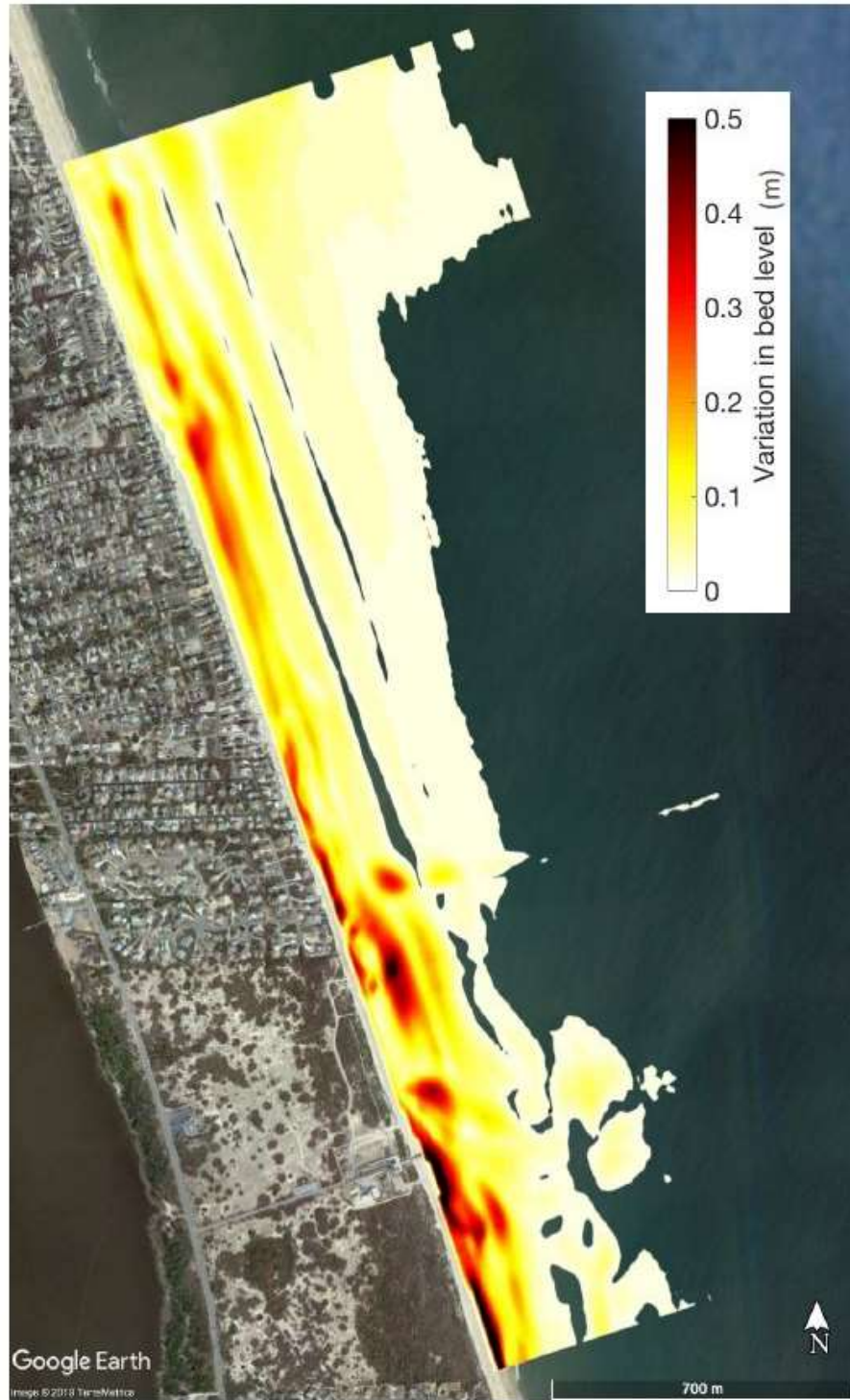


Figure 1. Shown is a plot of the standard deviation of the seafloor elevation of all 3300 ensemble simulations run at Duck, NC, representing the variation of the predicted bed level change. The results can be used to provide insight into where significant changes in seafloor elevation can occur in a particular region.

Title: Predicting Fluid-Structure Interaction for Military Applications

Author(s): D.R. Mott, A.D. Kercher, R.F. Johnson, A. Corrigan, and D.A. Kessler

Affiliation(s): Naval Research Laboratory, Washington, DC

CTA: CFD

Computer Resources: SGI ICE X [AFRL, OH]; Cray XC40, SGI ICE X [ARL, MD]

Research Objectives: Create the computational capability to predict the interaction of fluids with complex structures that also can be flexible, including large, high-rate deformations due to blast loading. Flows may include advection and diffusion of multiple materials and may include convective and evaporative heat transfer and species transport at ambient atmospheric conditions. Use the new capability to study other problems of defense relevance including helmet design and microfluidic transport applied to additive manufacturing.

Methodology: A discontinuous Galerkin solver for incompressible flows, developed at NRL's Laboratories for Computational Physics and Fluid Dynamics within the JENRE® software framework, was used to simulate transport (convection and diffusion) of multiple materials within a fluid flow.

Results: FY19's highlighted result is from microfluidics: approaches to microfluidic "spinning," i.e., forming fibers with tailored composition and shape by manipulating the material flow that creates them, are explored for application in extrusion-based additive manufacturing applications (popularly referred to as 3D printing). The microfluidic spinning processes explored here are performed at low temperatures, making them compatible with biological materials that would be damaged or destroyed by common extrusion techniques that require melting a material feed for printing. Using a sheath fluid to encapsulate the core "ink" material as it travels through the print nozzle enables the delivery of high-viscosity inks that would clog the nozzle if delivered alone, and the width of the delivered material stream can be shrunk well below the physical size of the nozzle by increasing the relative amount of sheath flow encasing it. Figure 1 includes a representative calculation for the first step in this process, namely, creating the sheath-core arrangement of fluids. For the materials studied, prior to the initiation of solidification of the core material, both the core and sheath fluids can be approximated as Newtonian, and the pressure-driven flow through the microfluidic components is computed by solving the incompressible Navier-Stokes equations.

DoD Impact/Significance: Improvements in manufacturing capabilities will enable more capable systems to be fielded for our warfighters. Additive manufacturing approaches are being explored to push small-scale, targeted manufacturing activities closer to the theater of engagement, with the possibility of greatly reducing the logistical footprint for delivering and stocking spare parts. Leveraging seemingly disparate applications (like body armor cooling, chemical detection, microfluidic design) that share common underlying physics enables us to amplify the impact of our computational efforts and to employ capabilities across a range of Navy and Marine Corps applications, as well as to meet needs in the larger DoD and defense communities.

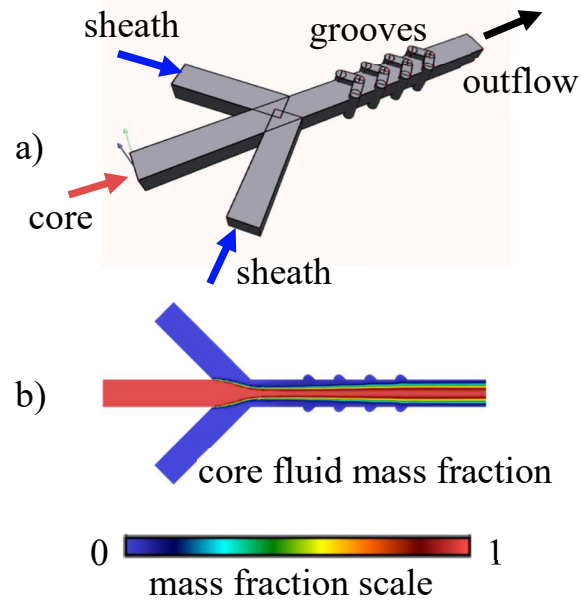


Figure 1. Representative flow simulation for the sheath-flow generation: a) Geometry and identification of core and sheath inflow ducts. Each rectangular channel is 1000 microns wide and 750 microns deep. b) Cross-section at half-height between duct floor and ceiling showing the distribution of core and sheath fluid, including the effects of mass diffusion in this particular simulation.

Three streams enter the rectangular duct, layering the sheath material on either side of the core material. Chevron-shaped grooves that are cut into the floor and ceiling of the duct carry sheath fluid toward the centerline above and below the core material, isolating the core material from all four channel walls. Molding of the flows via strategically placed divots and bumps within the channel that alter the flow path can be used to redistribute the fluids within the channel cross section and hence dictate the shape of the fiber formed.

Title: Multidimensional Chemically Reacting Fluid Dynamics with Application to Flameless Combustors
Author(s): R.F. Johnson
Affiliation(s): Naval Research Laboratory, Washington, DC
CTA: CFD

Computer Resources: Cray XC40, SGI ICE X [ARL, MD]; Cray XC40/50, SGI ICE X [ERDC, MS]

Objectives: Use the HPC computational resources to simulate the computationally expensive chemically reacting fluid dynamics in various multidimensional configurations with the goal of better understanding various complex, multi-scale, combustion phenomenon.

Methodology: The codes currently in use at The Laboratories for Computational Physics and Fluid Dynamics can accurately predict the flow field in many configurations. These codes employ high-order methods, which are capable of simulating unsteady flows with strong shocks, chemical reactions, and other complex features. This work focuses on developments that are currently underway that will allow for the simulation of high-speed and low-speed reacting flows using state-of-the-art numerical methods. This year, we produced several important results as well as began to simulate experimental configurations for validation purposes.

Results: In the past three years, we dedicated research time to simulating flameless combustion, particularly a configuration developed by the University of Cincinnati (UC). UC's combustion experiments were sensitive to invasive measurement techniques, so accurate CFD results were seen as a way to assist in providing advanced diagnostics that UC's experiments would be incapable of measuring without perturbing the flow. Our simulations have assisted in guiding modifications to experiments that would result in a more ideal flameless combustion.

Figure 1 shows an instantaneous result of the flameless combustor simulated. Plane cuts are taken at various heights above the fuel injectors. The unsteady fluid dynamics couple with the fuel injector and cause a shedding mode that is evident in the higher axial plane cuts. Some of the six fuel streams were less present in the downstream locations and time-accurate results showed that the prominent fuel streams would alternate, indicating a shedding mode within the combustor. The UC combustor is a practical configuration that could be used for propulsion devices, as the pressure loss is on the order of modern propulsion devices, $\Delta p \sim 4\%$. However, the details of the combustion phenomena in flameless or distributed combustion still have unanswered questions. The chemical kinetics to understand the detailed combustion would be incredibly expensive to model fully in the UC combustor. To better understand the link between chemical kinetics and fluid dynamics in distributed combustion, we have started to simulate a smaller combustion experiment performed by North Carolina State University (NCSU). The type of distributed combustion is related to the flameless combustion and is known as MILD.

Figure 2 shows a diagram of the experimental configuration and early simulation results. The combustion in the NCSU experiments transitions from a distributed, MILD, combustion zone to a conventional flame farther downstream. We plan to assess the chemical models necessary to reproduce this configuration. Not only will the case act as validation, but also will highlight what features are necessary to model in the larger UC combustor case.

DoD Impact/Significance: Accurately predicting combustion has benefits to Navy engine technologies. The research in flameless combustion will yield a better grasp of a not-well-understood phenomenon that promises better combustion efficiency and lower heat signatures of Navy/DoD aircraft.

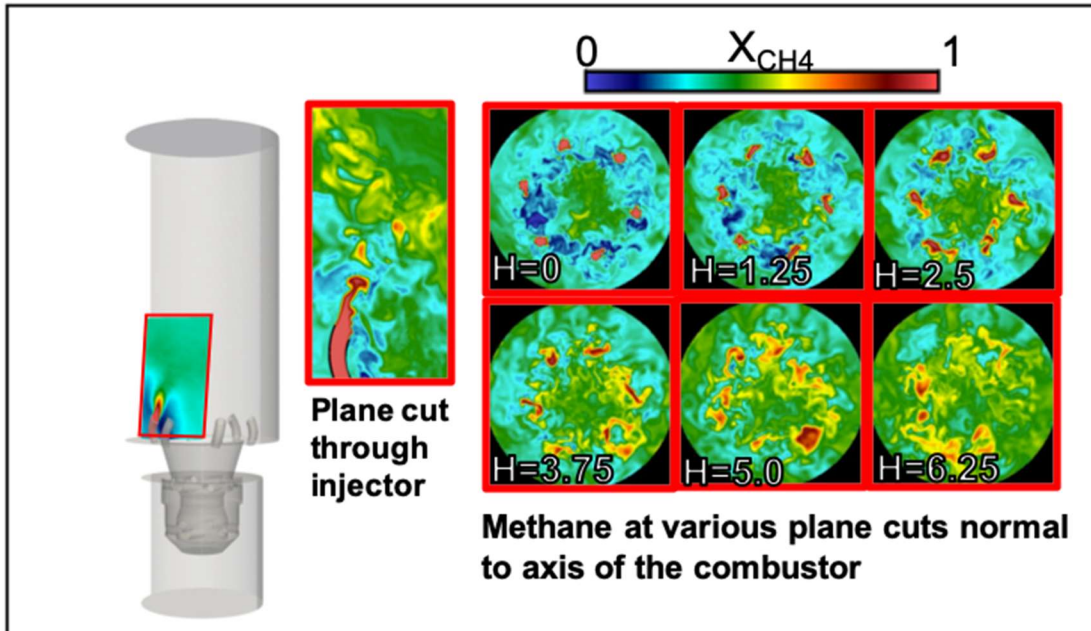


Figure 1. Time-accurate results for the six methane injectors.

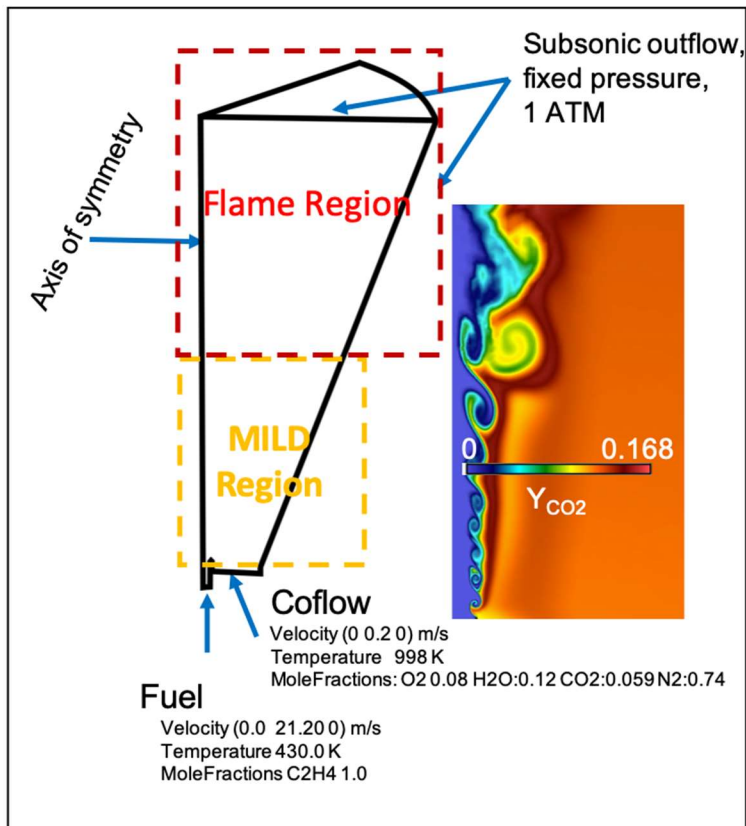


Figure 2. NCSU MILD combustion experiments and NRL preliminary simulation.

Title: Applications of FEFLO Incompressible Flow Solver
Author(s): R. Ramamurti
Affiliation(s): Naval Research Laboratory, Washington, DC
CTA: CFD

Computer Resources: SGI ICE X [ARL, MD]

Research Objective: Perform three-dimensional (3D) numerical simulations of flow past complex configurations. The proposed studies will investigate the use of bio-inspired wings for propulsion and will characterize the thrust generated by these propulsive flapping surfaces with a focus on the interaction between fluid forces and the structural response.

Methodology: A finite element solver, called FEFLO, for 3D incompressible flows based on unstructured grids is used. The flow solver is combined with adaptive remeshing techniques for transient problems with moving grids and also is integrated with the rigid body motion in a self-consistent manner which allows the simulation of fully coupled fluid-rigid body interaction problems of arbitrary geometric complexity in three dimensions. NRL has developed a flapping-fin UUV for effective low-speed operations. We have developed and validated two additions to our proven computational fluid dynamics (CFD) solver: first, a fluid-structure interaction (FSI) solver involving a beam structure, and second, a structure involving a membrane. Both of these cases are important components in the fluid-structure interaction problems for small, unmanned vehicles with flapping wings, and are validated against two benchmark test cases. A generalized structural solver also is coupled to the fluid solver and is tested for notional air vehicles.

Results: Most natural flyers such as bats use an articulated skeleton covered with an elastic membrane for morphing their wings during flight. Therefore, we consider bio-inspired wings comprising carbon-fiber structures and elastic Mylar membranes between them. In order to validate the coupled solver, the problem is broken into two: one for the coupled fluid-and-beam case, and the second for the coupled fluid-and-membrane case. For the former, the benchmark case described by Turek and Hron [1], the flow around a cylinder with an elastic beam behind the cylinder was simulated. The flow around the cylinder is in the laminar regime ranging from Reynolds number, $Re = 20$ to 200. The latter case was validated against the numerical results reported by Gordnier [2] for various angles of attack and are in good agreement. Some of these results, shown in Figs. 1-3, were reported in the paper presented at the coupled fluid dynamics conference [3], Conference on Coupled Problems in Science and Engineering, Sitges (Barcelona), Spain, June 2019.

DoD Impact/Significance: We have developed a computational methodology for studying the crucial coupling between the fluid dynamics loading and wing shape response effects of flexible, flapping wings that can guide the design of small, unmanned vehicles and their control systems.

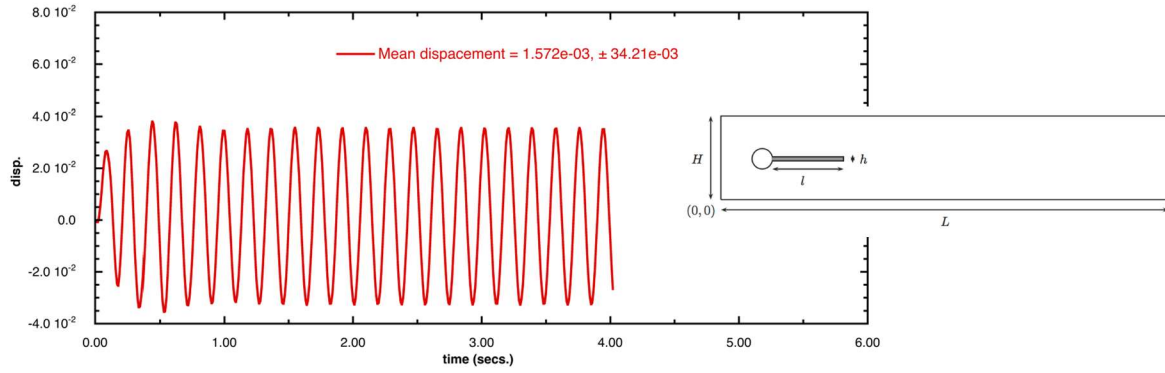


Figure 1. Displacement time history for the Turek-Hron benchmark case, $Re = 200$.

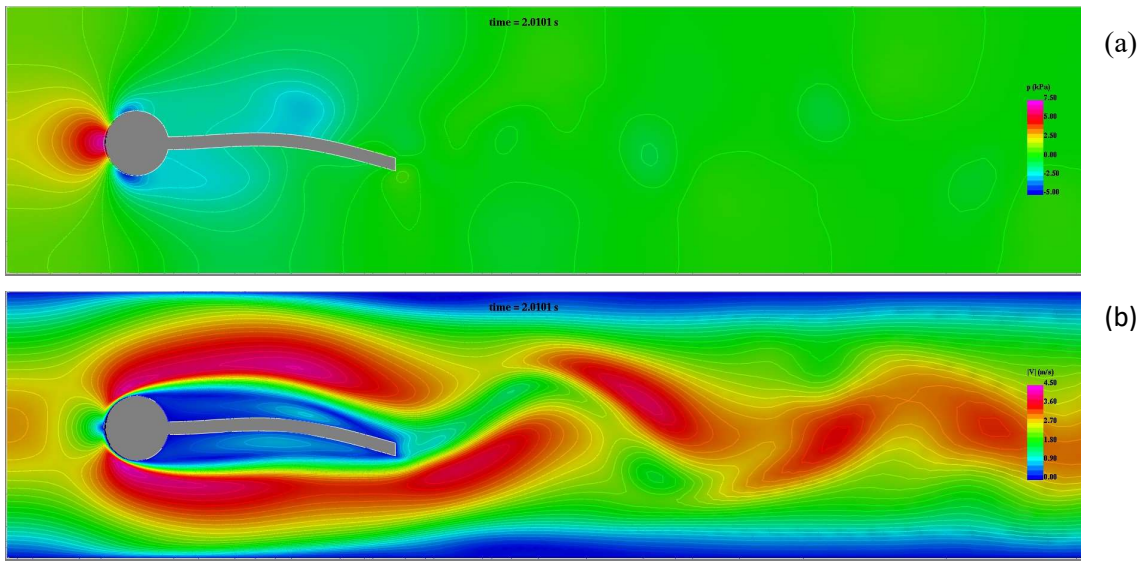


Figure 2. Flow results for Turek-Hron benchmark case, $Re = 200$, (a) pressure distribution and (b) magnitude of velocity.

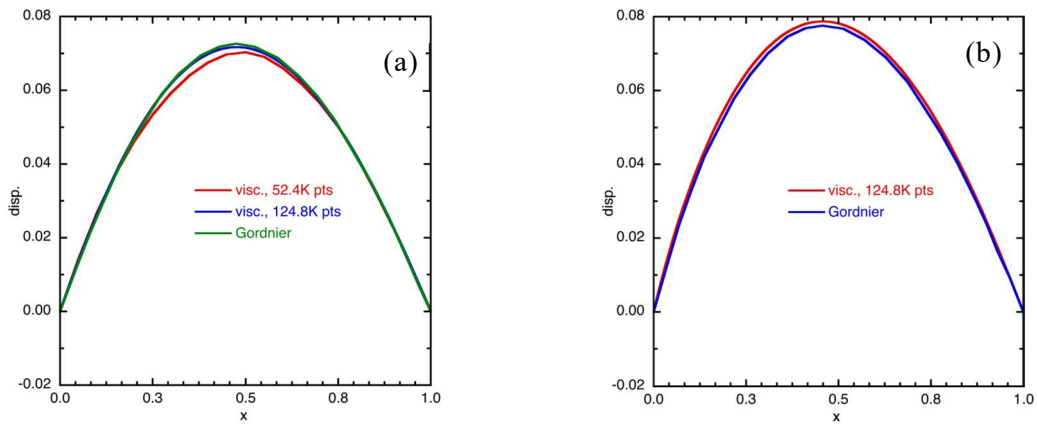


Figure 3. Comparison of deflection of the membrane, $Re = 2500$, (a) $\alpha = 4^\circ$ and (b) $\alpha = 8^\circ$.

Title: Numerical Simulations of Turbulence Impact on Optical Signal Transmission and Near-Surface Turbulence

Author(s): S. Matt, W. Hou, and A. Perez

Affiliation(s): Naval Research Laboratory, Stennis Space Center, MS

CTA: CFD

Computer Resources: SGI ICE X [AFRL, OH]; Cray XC40 [ARL, MD]

Research Objectives: The objective is to expand on the computational fluid dynamics (CFD) representation of the numerical tanks that are part of the Simulated Turbulence and Turbidity Environment (SiTTE) laboratory, in particular, the new laminar-to-turbulent-flow tank flowSiTTE. The flow tank is designed for the study of boundary-layer dynamics, in particular, the impact of actuated membranes on boundary-layer turbulence and frictional drag. CFD simulations support the laboratory work: The use of a wavelike boundary condition in OpenFOAM emulates actuated boundary motion, and combining ANSYS Mechanical and Fluent allows testing the impact of viscoelastic boundary materials on the flow through the use of full two-way fluid-structure interaction. Another numerical tank supports laboratory experiments at a large wind-wave tank to study laboratory-scale Langmuir circulation. The numerical simulations support work on a new underwater imager, novel methodologies and mechanisms for active boundary-layer control, as well as insight into the dynamics underlying near-surface turbulence and boundary-layer processes.

Methodology: To accurately reproduce the turbulence dynamics, the representation of the numerical tanks is accomplished using large-eddy simulation (LES) and the physical domain size of the respective tanks. The numerical experiments build on our previous work based on LES models using the open-source CFD code OpenFOAM, including custom developments to simulate Langmuir turbulence, and a wavelike boundary condition emulating boundary actuation. To explore the impact of viscoelastic boundary materials on the flow, full two-way fluid-structure interaction was implemented combining CFD (Ansys Fluent) and Computational Solid Mechanics (Ansys Mechanical).

Results: Two-way fluid-structure interaction is employed to investigate the dynamics of a viscoelastic membrane embedded in a hydrofoil. The LES model (Fluent) is used to explore flow near the membrane and the impact on transition to turbulence, whereas the Solid Mechanics model (ANSYS Mechanical) describes the deformation in the elastic material (Fig. 1). The models are fully coupled and exchange information via the ANSYS Workbench interface. To test the impact of an actuated boundary on the flow, a wavelike, undulating boundary condition was developed for OpenFOAM (Fig. 2). For the study of Langmuir turbulence, a multiphase LES model and a rigid-lid LES model with added Craik-Leibovich vortex force were used to test the performance of Langmuir turbulence parameterization.

DoD Impact/Significance: CFD simulations of flowSiTTE with viscoelastic and actuated boundaries support the development of novel methodologies for active boundary-layer control and drag reduction. The work on numerical tanks also benefits research on optical communication, lidar sensing of turbulence, new fiber-optics sensor development (temperature, flow), near-surface turbulent flows, including air-sea interface, and boundary-layer processes.

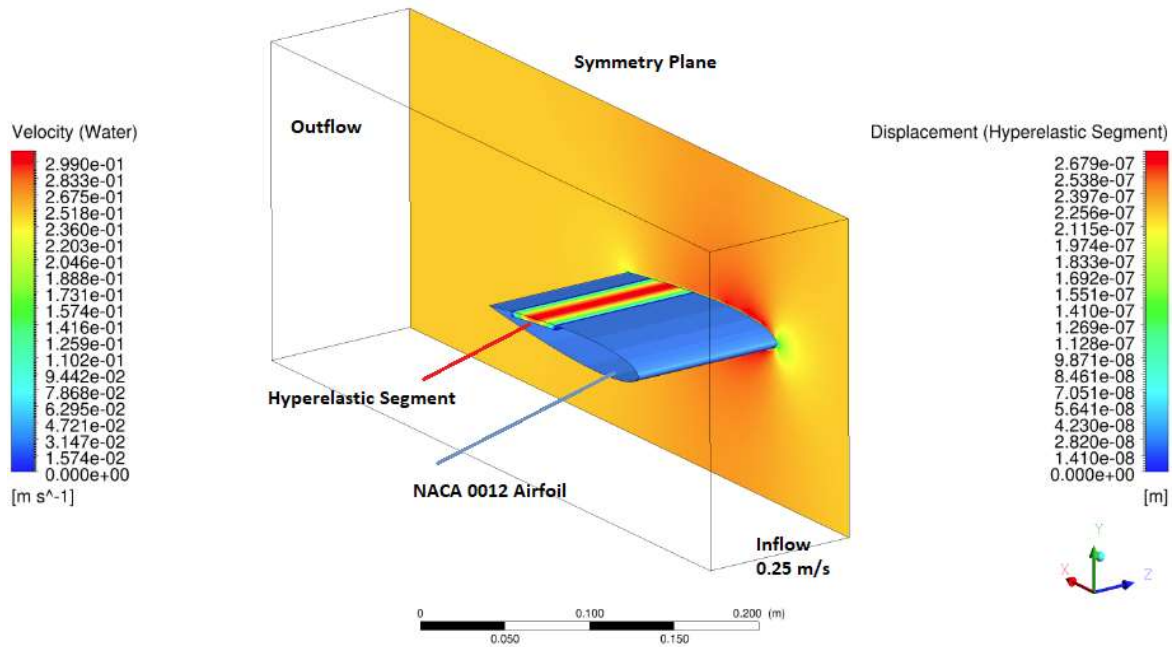


Figure 1. Computational Fluid Dynamics (Ansys Fluent) and Computational Solid Mechanics (Ansys Mechanical) are coupled to study the impact of viscoelastic boundary materials on flow transition for the development of novel methods to reduce frictional drag. A hyperelastic segment (neoprene) is embedded in a hydrofoil (NACA 0012 airfoil) and the deformation of the material in response to the flow over the hydrofoil, as well as the impact of the elastic material on the flow dynamics, are investigated.

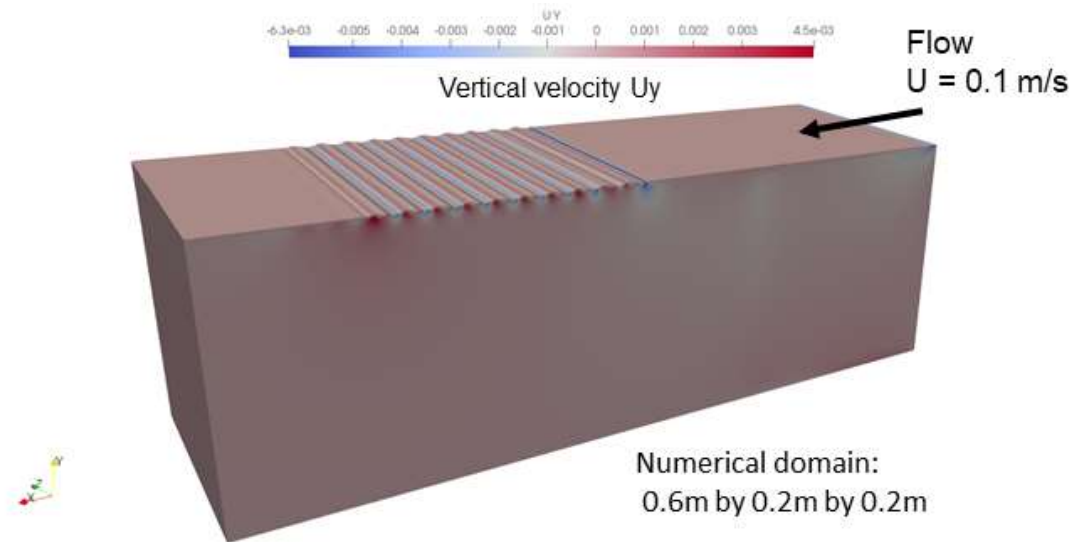


Figure 2. A wavelike boundary condition is implemented for the OpenFOAM representation of flowSiTTE to emulate and investigate the impact of actuated boundary motion on the flow. The numerical domain is the full size of the flowSiTTE test section. Color scale is in m/s and shows vertical velocity.

Title: Detonations with Multi-Phase Flows for Propulsion
Author(s): D.A. Schwer
Affiliation(s): Naval Research Laboratory, Washington, DC
CTA: CFD

Computer Resources: HPE SGI 8600 [AFRL OH]; Cray XC40 [ARL, MD]

Research Objectives: The main research goal of the present HPC project is to study high- and low-speed multiphase reacting flows for further understanding advanced engine concepts, with the specific application for detonation engines.

Methodology: We have used two modeling codes for our research into blast and detonation engine simulations. Our main development and simulation code is the JENRE® code. Due to our extensive experience with using the DET3D codes for detonation propulsion, we will continue to use them as a benchmark for comparison with the JENRE® code. JENRE® is a new code utilizing unstructured meshes and the discontinuous-Galerkin-FEM techniques to solve a wide variety of complex fluid dynamical phenomena. It has been built from the ground up at NRL to make efficient use of CUDA, Thread-Building-Blocks, OpenMP, and MPI through the use of the Thrust library. By utilizing unstructured meshes, the solver can be coupled to solid structural models easily and provides a pathway for doing fluid-structure interaction. Both gas-phase and multiphase models from our DET3D codes have been incorporated into the JENRE® code.

Results: Because detonation engines are a radical departure from the constant-combustion processes in current engines and power-generation devices, integration of the combustion chamber into those devices requires special care and investigation. Practical RDEs require direct injection of liquid fuels for efficient operation. Research was conducted this year to better understand the differences between gaseous and fuel spray JP10/oxygen detonations in multiple dimensions. The simulations confirm the formation of cellular structures for multidimensional liquid fuel sprays. The sizes of the cellular structures are closely tied to the droplet sizes of the fuel spray due to the vaporization time. Also present in the fuel spray detonations are regions of fuel vapor that persist long after the detonation wave has passed (Fig. 1). This results in a slower detonation wave compared with the fully mixed gaseous case. Parametric studies were done for the droplet size using both monodispersed and log-normal distributions, and also by varying the equivalence ratio. This year's research also was focused on validating RDC computations with JENRE® using both detailed and IPM models. JENRE® codes use a discontinuous-Galerkin approach to solve the conservation equations, allowing a great amount of flexibility in improving the numerics and introducing new techniques such as adjoints to examine optimization in complex domains. DG methods tend to be very computationally expensive, but the local, compact nature of the calculations map well to multiple-GPU computing resources. A hydrogen/oxygen/argon detonation is examined and compared with previous continuous-Galerkin methods, and timings for GPU performance also were made.

DoD Impact/Significance: The physics involved in RDEs and other detonation engines is substantially different than for gas-turbine engines, and also different from more traditional, premixed detonation calculations, requiring research into how an RDE can fit into existing frameworks for propulsion and power generation. Our work in computing RDE flow fields in conjunction with experimental work at the Naval Postgraduate School has helped us better understand the physics and verify our physical models, and our development of JENRE® gives us the capability to explore how best to fit RDEs into these existing frameworks. Through this research, the potential of significant efficiency gains for detonation engines can be realized in propulsion and power-generation devices.

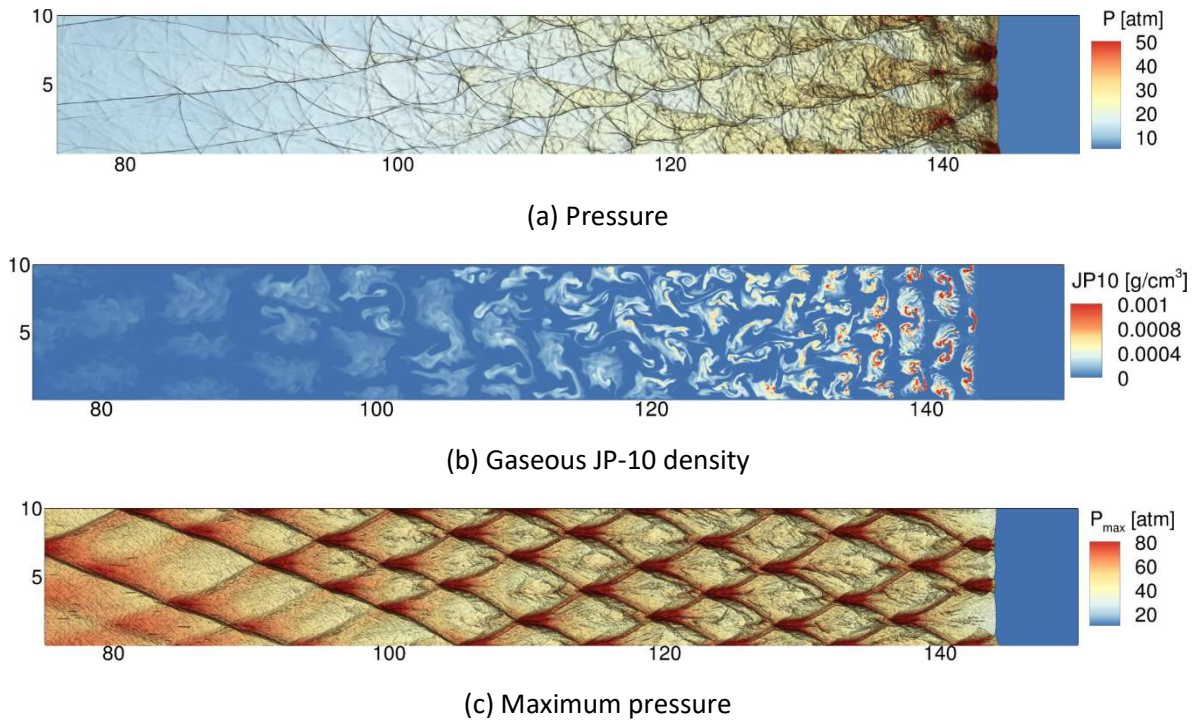


Figure 1. Two-dimensional detonation structure for (a) pressure and (b) JP-10 gas density, showing strong transverse waves in the simulation along with pockets of fuel-rich gases that persist far downstream from the detonation wave. Maximum pressure is shown in (c). $D_n=5$ mm, $f=1$, $t=0.7$ ms.

Title: Numerical Investigation of Advanced Military Aircraft Noise Reduction Concepts

Author(s): J. Liu, A. Corrigan, R.F. Johnson, and R. Ramamurti

Affiliation(s): Naval Research Laboratory, Washington, DC

CTA: CFD

Computer Resources: HPE SGI 8600, SGI ICE X [AFRL, OH]; Cray XC40, SGI ICE X [ARL, MD]; Cray XC40/50, SGI ICE X [ERDC, MS]; HPE SGI 8600 [NAVY, MS]

Research Objectives: Use HPC computational resources to predict details of turbulent flow structures and noise generation in supersonic exhaust jets from representative military aircraft jet engine nozzles and to use this information to investigate and assess promising jet noise-reduction concepts in support of the ongoing testing program.

Methodology: The flow solver is JENRE[®], a Navy-based and NRL-developed nodal finite-element code. JENRE[®] can take structured meshes and unstructured meshes with arbitrary cell types and has multiple levels of parallelism: multicore CPUs or multicore GPUs, and MPI for interprocessor communication. JENRE[®] has achieved an exceptional computational performance and scalability. Since using large-eddy simulations (LES) to fully resolve wall-bounded flows at high Reynolds numbers is computationally prohibitive due to the limitations of the available numerical methods and computational resources, the wall-layer-model approach is used to simulate the boundary-layer effect of the wall-bounded flows. The far-field noise-prediction tool, which uses the Ffowcs Williams & Hawkins (FW-H) Surface Integral method, also has been implemented in JENRE[®]. To simulate the high-temperature effect observed in realistic jet engine exhausts, a temperature dependent function of the specific heat ratio is developed and implemented in JENRE[®].

Results: LES has become an important tool to enhance the understanding of the jet noise-generation mechanism and to assist the jet noise-reduction effort. We have used LES to examine the flow field and jet noise generation of supersonic jets emanating from laboratory-scale simplified nozzle configurations. To move toward more realistic jet engine exhaust conditions, it is important to include nozzle geometries that mimic those used in the Navy-relevant applications, for example, the F400 series nozzle used in the F404-GE-F400 engine, which powers the F/A-18 aircraft. Figure 1(a) shows a model-scale nozzle surface contour that mimics their F404 nozzle. This nozzle is a faceted biconic convergent and divergent nozzle made of 12 flaps. Figure 1(b) shows the bypass cooling system and a center body inside the nozzle. In the past year, we had examined the effect of the nozzle boundary layer and a bypass cooling flow on the flow field and noise at overexpanded conditions at a temperature comparable to those observed at the maximum non-afterburning power settings. This year, we have examined a much higher jet temperature at an afterburning power level. Since the temperature is very high, a temperature-dependent specific heat ratio has to be used. It is found that using a constant specific heat ratio will underestimate the downstream shock-cell size even at an intermediate jet temperature as shown in Fig. 2. It is also found that the instability waves are more visible when the jet temperature is high, as shown in Fig. 3, and this can be predicted only by a temperature-dependent specific heat ratio.

DoD Impact/Significance: There is a growing need to reduce significantly the noise generated by high performance, supersonic military aircraft. The noise generated during takeoff and landing on aircraft carriers has direct impact on shipboard health and safety issues. It is estimated that the US Veterans Administration pays \$4.2 billion or more for hearing-disability claims each year. The results of our work will provide better understanding of the noise production for both industrial and military aircraft, and will aid the current effort of noise reduction, especially for supersonic aircraft.

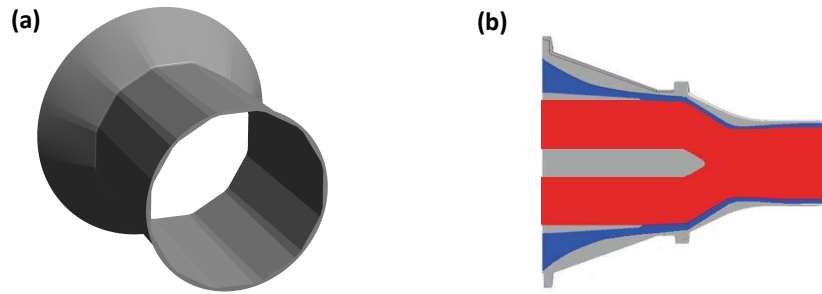


Figure 1. Nozzle geometry. (a) F-400 series model nozzle geometry. (b) The bypass cooling system and the centerbody inside the nozzle.

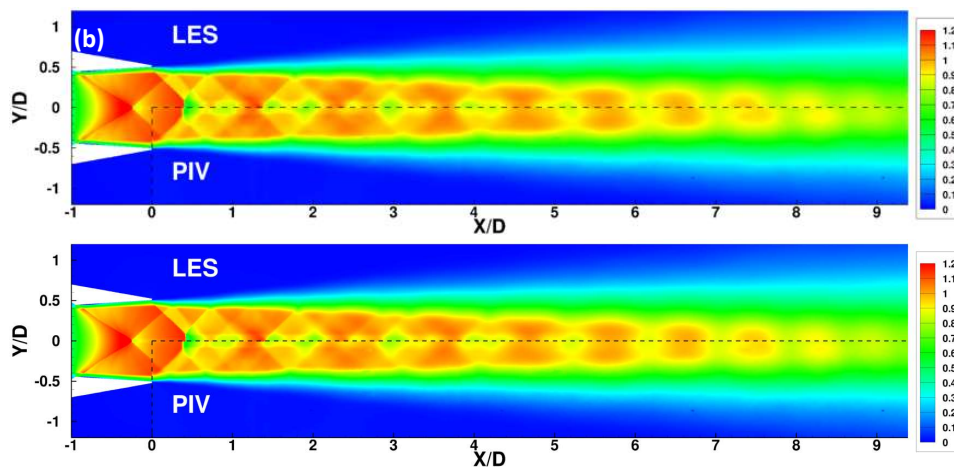


Figure 2. Comparison of axial velocity contours between LES predictions and NASA PIV measurement data (Ref. 1) at a jet temperature of 844K of an overexpanded jet.

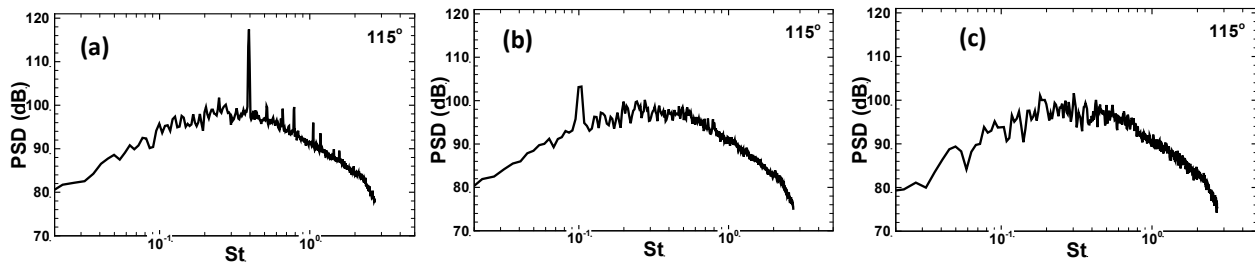


Figure 3. Far-field noise spectral distributions of an overexpanded jet at a temperature of 2,100 K in the peak radiation direction. (a) The shear layer between the bypass cooling flow and the main hot core inside the nozzle is laminar. (b) The shear layer between the bypass cooling flow and the main hot core inside the nozzle is turbulent. (c) A buffer zone is added around the nozzle inlet to eliminate any inlet pressure wave reflections.

¹Bridges, J., Wernet, M. P., and Frate, F. C., PIV Measurements of Chevrons On F400-Series Tactical Aircraft Nozzle Model," AIAA Paper No. 2011-1157, January 2011

Title: Investigation of Jet Noise Reduction Optimization
Author(s): J. Liu
Affiliation(s): Naval Research Laboratory, Washington, DC
CTA: CFD

Computer Resources: Cray XC40 [ARL, MD]

Research Objectives: Use HPC computational resources to predict details of turbulent flow structures and noise generation in supersonic exhaust jets from representative military aircraft jet engine nozzles and to use this information to investigate and assess promising jet noise-reduction concepts in support of the ongoing testing program.

Methodology: The flow solver is JENRE[®], a Navy-based and NRL-developed nodal finite-element code. JENRE[®] can take structured meshes and unstructured meshes with arbitrary cell types and has multiple levels of parallelism: multicore CPUs or multicore GPUs, and MPI for interprocessor communication. JENRE[®] has achieved an exceptional computational performance and scalability. Since using large-eddy simulations (LES) to fully resolve wall-bounded flows at high Reynolds numbers is computationally prohibitive due to the limitations of the available numerical methods and computational resources, the wall-layer model approach is used to simulate the boundary-layer effect of the wall-bounded flows. The far-field noise prediction tool, which uses the Ffowcs Williams & Hawkings (FW-H) Surface Integral method, has also been implemented in JENRE[®]. To simulate the high-temperature effect observed in realistic jet engine exhausts, a temperature dependent function of the specific heat ratio is developed and implemented in JENRE[®].

Results: Strategic environmental research and development program (SERDP) has issued a statement of need (SON) of aircraft engine noise-reduction technology, and this work is part of the project associated with that SON. Since this is the first year in this SERDP project, the focus is the baseline nozzle validation. LES has been used to simulate the jet plume and noise generated by a model-scale F404 nozzle, which is a faceted biconic convergent and divergent nozzle made of 12 flaps, as shown in Fig. 1. An equivalent circular nozzle also is designed and simulated to examine the effect of the faceted nozzle surface. Figure 2 shows the axial velocity contours inside and the near the nozzle for both nozzle geometries. It can be seen that both simulations show a similar, diamond-like, shock-cell structure in the jet core, but the faceted nozzle also displays some small shock waves inside the nozzle. Figure 3 shows the axial velocity contours near the faceted nozzle surface. It is clear that there are small expansion and compression waves generated inside the faceted nozzle. It is found that those are associated with the discontinuity between the neighboring seal surfaces. But the effect of those small shock waves is found small on the downstream shock-cell formation and the jet plume development in both LES predictions and the experimental measurement data.

DoD Impact/Significance: There is a growing need to reduce significantly the noise generated by high-performance, supersonic military aircraft. The noise generated during takeoff and landing on aircraft carriers has direct impact on shipboard health and safety issues. It is estimated that the US Veterans Administration pays \$4.2 billion or more for hearing-disability claims each year. The results of our work will provide better understanding of the noise production for both industrial and military aircraft, and will aid the current effort of noise reduction, especially for supersonic aircraft.

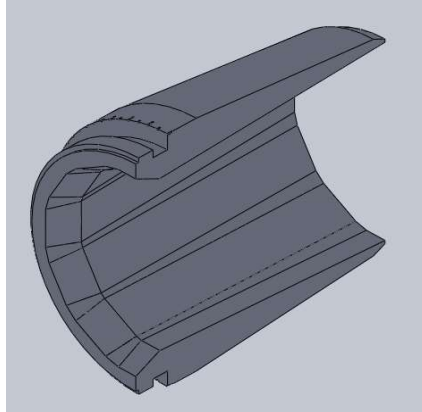


Figure 1. A model-scale F404 nozzle geometry.

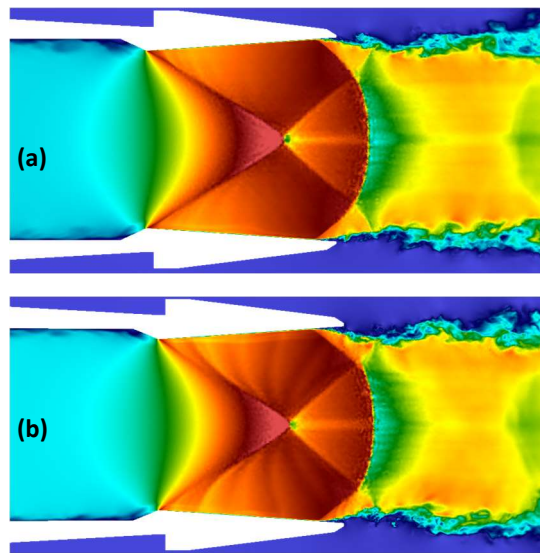


Figure 2. Axial velocity inside and near the nozzle. (a) Circular nozzle where the nozzle surface is smooth. (b) Faceted nozzle where the nozzle surfaces are made of flat panels as shown in Figure 1.

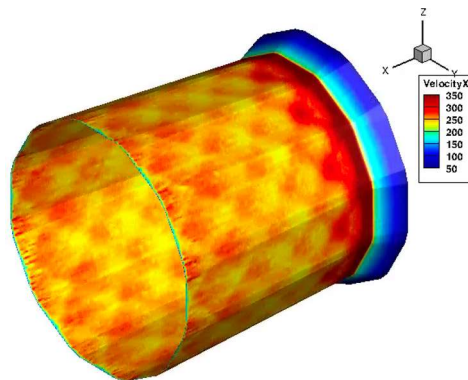


Figure 3. Axial velocity contours close to the nozzle surface of the faceted nozzle.

Title: Numerical Simulations of Noise Generated by Non-Circular Advanced Military Aircraft Nozzles
Authors: K. Viswanath and R. Ramamurti
Affiliations: Naval Research Laboratory, Washington, DC
CTA: CFD

Computer Resources: Cray XC40, SGI ICE X [ARL, MD]; Cray XC40/50, SGI ICE X [ERDC, MS]

Research Objectives: Use HPC computational resources to predict details of turbulent flow structures and noise generation in supersonic, noncircular, asymmetric exhaust jets from representative military aircraft jet engine nozzles. This information will be used to investigate and assess promising jet noise-reduction concepts in support of the ongoing testing program.

Methodology: Simulations are performed using the Jet Noise Reduction (JENRE®) code developed at the Naval Research Laboratory. JENRE® provides unsteady compressible flow solver capabilities that support various numerics, cell-centered finite volume or nodal finite element method, while delivering high throughput on calculations. It was developed with an emphasis on raw performance and the ability to exploit emerging massively parallel, high-performance computing (HPC) architectures. It supports different HPC parallel programming paradigms for message passing such as MPI, OpenMP, CUDA, and hybrid models depending on the HPC cluster architecture. A key bottleneck of HPC throughput is data input-output (IO). JENRE® supports parallel IO via MPI/IO or the adaptable IO system (ADIOS) to further complement the multiple levels of parallelism. JENRE® uses an edge-based formulation for all flux integration and limiting algorithms. Taylor-Galerkin finite element method with second-order spatial accuracy, for tetrahedral cells, is used with the Finite Element Flux Corrected Transport (FEM-FCT) method. The multidimensional FCT flux limiter provides an implicit subgrid stress model, which ensures monotonicity at shocks and sharp gradients with minimal artificial dissipation. JENRE® also features a Wall Model that supports high-speed flows and surface roughness effects while significantly reducing grid-resolution requirements.

Results: Simulations of supersonic jets for various operating conditions and different nozzle configurations were investigated to understand their asymmetric noise characteristics and to evaluate noise-reduction techniques. A twin-jet rectangular nozzle (equivalent diameter $D = 0.018$ m), with an aspect ratio of 2 and centerline nozzle separation distance of $2.3D$ shown in Fig. 1, was simulated and its noise production and flow features compared with experimental data from the University of Cincinnati. The simulation predicted the far-field noise and the spatial variation of the noise agreeably. Figure 2 shows the temperature contours of the developed cold jet plume at ideally expanded operating conditions. The jets start interacting about $3D$ from nozzle exit in the symmetry plane. Both plumes have double-diamond shock cells at the beginning and there is a normal shock along the centerline for the first two cells. Figure 3 shows the comparison with experiments, and an overlay of the centerline velocity profiles with time-averaged flow field. The core breakdown happens about $8D$ downstream in both simulations and experiments, while the initial shock-cell structures differ.

DoD Impact/Significance: The results of our work will provide better understanding of the noise production for both industrial and military aircraft, and will aid the current effort of noise reduction, especially for supersonic aircraft, to reduce the impact of the jet noise on shipboard health and safety issues. Futuristic nozzles are tending towards noncircular geometries for flexibility in airframe integration, capabilities such a SERN profile, and other potential advantages.

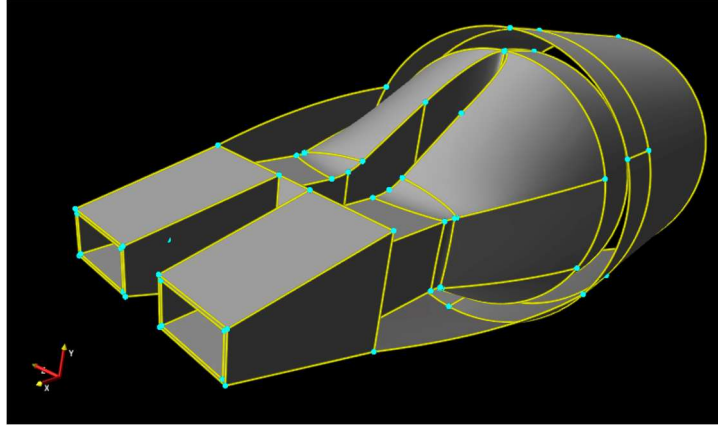


Figure 1. Twin-jet-nozzle geometry, aspect ratio 2 nozzles with separation distance of $2.3D$.

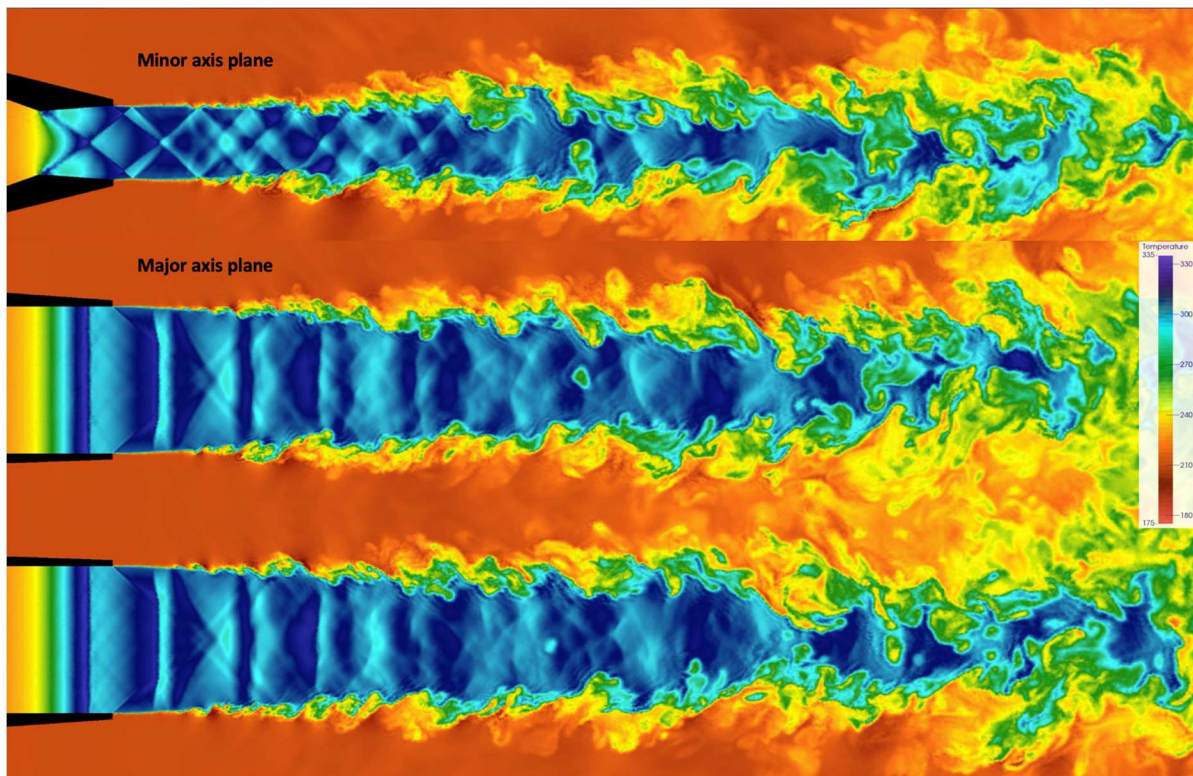


Figure 2. Instantaneous temperature contours of the twin jet plume. Top shows the minor axis plane with one jet behind the other. Bottom shows both jets in the major axis plane.

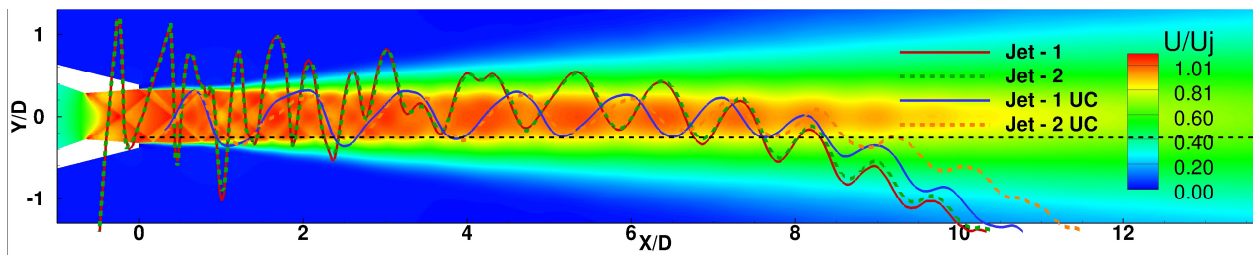


Figure 3. Overlay with centerline jet velocity of the time-averaged flow field from JENRE® simulation showing shock-cell structures and plume core-breakdown length.

Title: Hypersonic Reactive Flow Modeling
Author(s): G. Goodwin
Affiliation(s): Naval Research Laboratory, Washington, DC
CTA: CFD

Computer Resources: SGI ICE X [ARL, MD]

Research Objectives: The objective of this research is to characterize the effect of a high-speed flowfield and unsteady/nonuniform boundary conditions on the ignition and combustion processes in hypersonic airbreathing engines. This research encompasses a broad range of system types, sizes, and scales, from smaller combustors used for analyzing the fine details of the underlying combustion physics to larger applied systems such as ramjets and supersonic combustion ramjets (scramjets) in which quantification of combustor efficiency and reliability is a primary goal.

Methodology: One of the predominant challenges in using airbreathing engines for hypersonic flight (typically greater than five times the speed of sound) is that the extremely fast flow speeds through the engine present a challenging environment for reliable ignition of the fuel and stable combustion. The methodology for this research is to use high-fidelity computational fluid dynamics (CFD) to simulate the high-speed reactive flow in the combustors of airbreathing hypersonic vehicles. Boundary conditions, fuel chemistry, combustor geometry, and turbulence levels are varied to catalog the effects of these phenomena on achieving stable ignition and complete combustion. For the results described in this paper, the combustor of a dual-mode scramjet with an inflow Mach number of 0.6 was used as the computational domain. The inflow is a mixture of ethylene and air at an equivalence ratio of 0.6, a pressure of 1.72 atm, and a temperature of 1,125 K (Fig. 1). A synthetic turbulence generator was implemented to generate isotropic turbulence at the inflow boundary such that the turbulence intensity in the combustor ranges from 10% to 15%.

Results: The combustor is ignited by simulated spark ignition and a flame quickly anchors to the leading edge of the cavity. The high-frequency pressure waves generated by the turbulent inflow gradually diffuse as they propagate farther into the domain. The pressure waves collide with and perturb the flame, causing the formation of turbulent structures along the flame surface. Despite the distortion to the flame surface, the flame remains anchored to the cavity lip indefinitely. Downstream of the cavity, in the expanding section of the combustor, the flame travels far into the core flow above the lower cavity wall. This results in the majority of the fuel being consumed over a short distance, indicating that the inflow turbulence improves mixing and combustor efficiency. The local extinction of the flame as it traverses the intersection of the cavity ramp wall and the expanding wall is caused by the sharp turning angle. Future work will focus on optimizing the smoothness of the turning angle to mitigate local flame extinction.

DoD Impact/Significance: The impact of this research is an increased fundamental understanding of the fine-scale ignition and combustion physics in scramjet engines. The air flow into scramjet engines is typically highly turbulent and the ability to simulate a realistic turbulence profile at the combustor inlet is paramount to accurately characterizing flame stability within the engine under flight conditions. Using high-fidelity computational fluid dynamics to simulate scramjet combustion is a critical step in the engine development process, as ground test facilities cannot achieve the full range of relevant test conditions that can be captured in simulations.

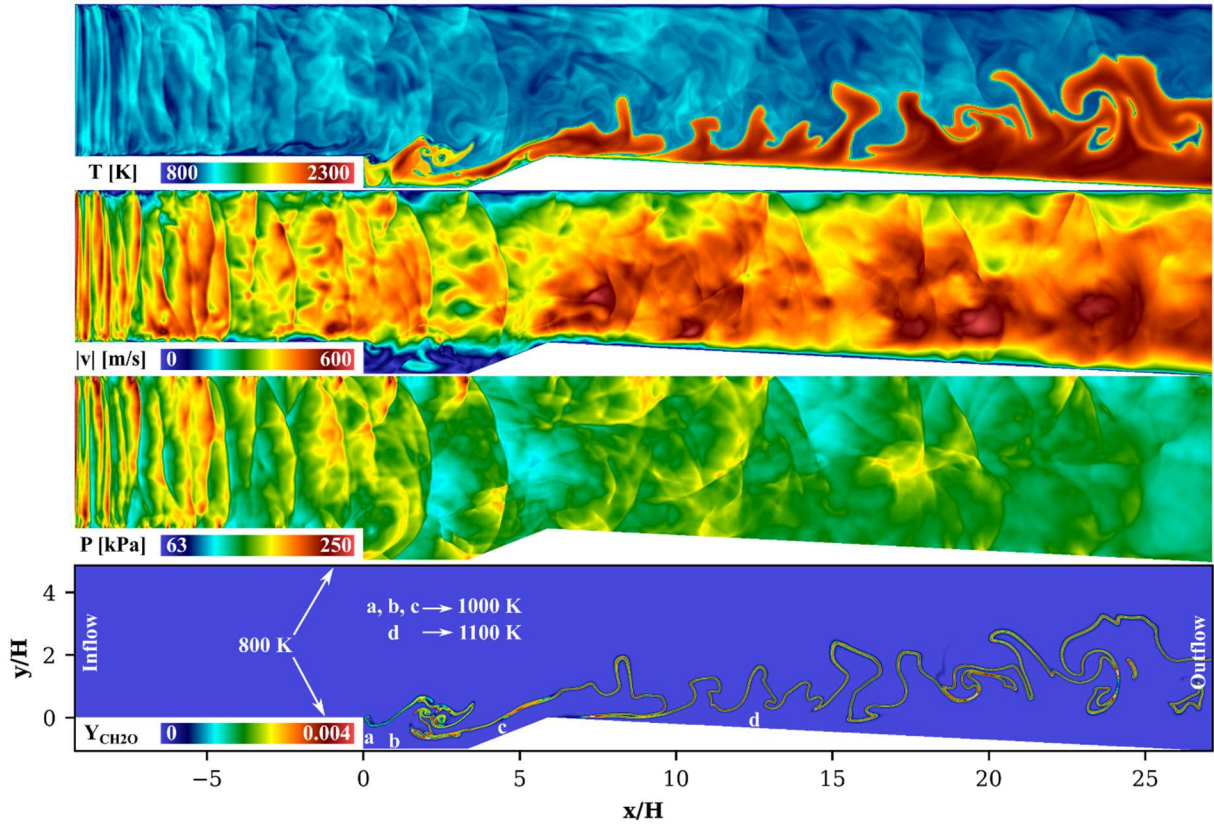


Figure 1. Computational fluid dynamics simulation of combustion in a dual-mode scramjet engine with a Mach 0.6 inflow of turbulent ethylene-air mixture. The flame is stabilized within the cavity flameholder and anchored to the cavity lip. Shown from top to bottom: temperature, velocity magnitude, pressure, and mass fraction of formaldehyde (an intermediate species of ethylene-air combustion). Axes normalized by cavity height H , and isothermal wall temperature is shown.

Title: Simulations of the Ionosphere and Magnetosphere

Author(s): J. Krall¹ and J.D. Huba²

Affiliation(s): ¹Naval Research Laboratory, Washington, DC; ²Syntek Technologies, Fairfax, VA

CTA: CFD

Computer Resources: SGI ICE X [AFRL, OH]; Cray XE6m, SGI ICE X [ERDC, MS]

Research Objectives: Develop space weather-forecasting capability. Simulate geomagnetic storms and other events of interest in order to understand geospace. Develop coupled ionosphere/plasmasphere/thermosphere models for ionospheric specification. Develop a first-principles model of Earth's ionosphere/plasmasphere/thermosphere system.

Methodology: The research uses the NRL code SAMI3, which is a comprehensive 3D simulation model of Earth's ionosphere/plasmasphere system. We have developed a model of SAMI3 that includes heavy metal ions (Fe^+ and Mg^+). SAMI3 has also been coupled to magnetosphere models, such as the RCM code and thermosphere simulations, such as the GITM model. These simulations use measured solar wind and irradiance data as inputs that drive the system.

Results: The models SAMI3 and RCM have been self-consistently coupled via the electrostatic potential equation and were used to study the ionosphere-plasmasphere system response to the March 17, 2015 geomagnetic storm. The novel feature of this work is that it captured the important storm-time dynamics of the ionosphere on a global scale and its manifestation in the plasmasphere. We find that the penetration electric fields associated with the magnetic storm lead to a storm-time enhanced density (SED) in the low- to mid-latitude ionosphere. Additionally, we observe the development of polar cap ‘tongues of ionization’ and the formation of sub-auroral plasma streams (SAPS) in the post-sunset, pre-midnight sector and its impact on the plasmasphere. Additionally, SAMI3/RCM has been ‘one-way’ coupled to GITM in that GITM provides the neutral density, temperature and winds to SAMI3/RCM but the ion dynamics are not coupled to GITM. This and related work were reported at the 2018 Fall AGU Meeting and the EGU General Assembly 2019.

In our work on ionosphere-magnetosphere coupling, we improved the high-altitude dynamics of SAMI3. Using the single-longitude SAMI2 code as a testbed, we developed a version of SAMI2 that allows counter-streaming H^+ ions to flow through each other at high altitude, addressing a longstanding concern and allowing the first comprehensive fluid simulation of early-stage plasmasphere refilling. The updated SAMI2 code enabled us to complete a study of the limiting H^+ outflow from the topside ionosphere. This and related work were reported at the EGU General Assembly 2019 and the 2019 GEM Summer Workshop and was published in *Geophys. Res. Lett.* and *J. Geophys. Res.*

In addition to the above, we have accomplished the first global simulation of metal-ion dynamics in both the E and F regions, showing that direct wind forces and global electric fields dramatically redistribute metal ions in the ionosphere. This can be a significant factor in the formation of the “sporadic E” layers in the ionosphere E region (90-150 km) that interfere with communication and navigation signals. We showed that high Fe^+ and Mg^+ densities can occur at low- to mid-latitudes as well as at the polar caps. This and related work were reported 2018 Fall AGU Meeting and published in *Geophys. Res. Lett.*

DoD Impact/Significance: Potential protection of communication satellites and the power grid. Support of ongoing experiments in remote sensing of the space environment. Provide input to ionospheric and thermospheric models.

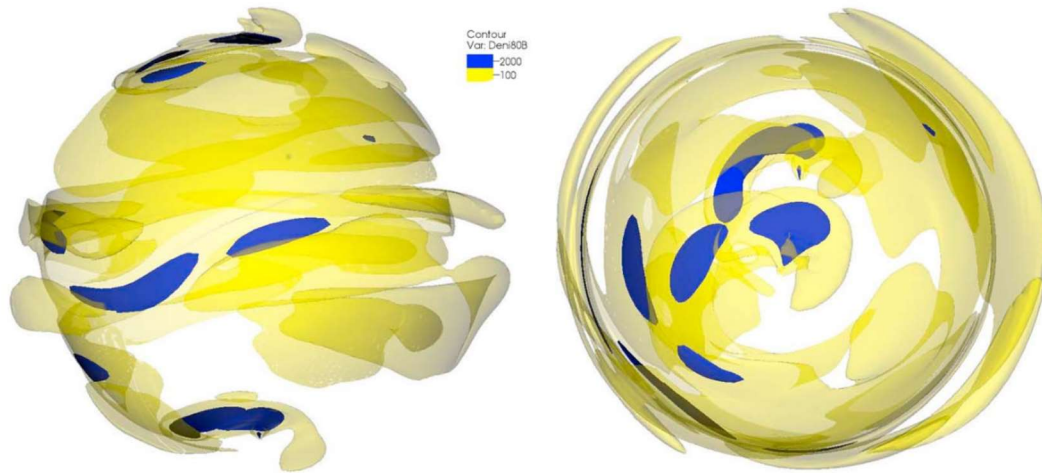


Figure 1. Isodensity surfaces of ionosphere Mg⁺ ion density modeled by SAMI3. Isosurfaces are at 2000 cm⁻³ (blue) and 100 cm⁻³ (yellow). Earth radius is artificially reduced by a factor of 10 to better show the three-dimensional ion structure.

Title: Electron Scattering Cross Sections for Plasma Response Models

Author(s): P.E. Adamson, S.B. Swanekamp, and A.S. Richardson

Affiliation(s): Naval Research Laboratory, Washington, DC

CTA: CFD

Computer Resources: SGI ICE X [AFRL, OH]; Cray XC40 [ARL, MD]; SGI Altix ICE [NRL, DC]

Research Objectives: The goal is to calculate electron scattering cross sections to improve plasma response models for intense electron-beam-driven plasmas.

Methodology: NRL has been studying the interaction of intense electron beams with air and other gases since the 1980s and has been developing advanced plasma-chemistry models for various defense applications since 2005. The focus of current efforts is to improve plasma-chemistry algorithms to increase the range of validity of models and to improve code performance for modeling plasmas in highly ionized states produced by an intense electron beam. This work includes gathering the necessary cross section information. For reactions from the ground state, the cross sections are often measured directly. For other reactions involving excited molecular or atomic states, cross sections are difficult to measure. For these processes, we are developing semi-classical approximate methods and also using the fully quantum R-Matrix scattering code UKRMol+ to compute the cross sections. The scattering code relies on accurate representations of the unperturbed wave functions of the target atom or molecule for which we are using Molpro, a comprehensive system of ab initio programs for advanced molecular electronic structure calculations. The FY19 goal of this work was to determine the feasibility of using UKRMol+, and its commercial variant Quantemol-EC, for determining cross section values for the difficult-to-measure excited-state-to-excited-state transitions.

Results: UKRMol+ was obtained and compiled on the SGI Altix ICE and Cray XC40 Excaliber systems. Proof of principal calculations were performed to exercise the process of computing electronic wave functions with Molpro on Excaliber and using the resulting wave functions to perform electron-scattering calculations with UKRMol+ on the DSRCs.

DoD Impact/Significance: The outputs from nuclear weapons can drive intense electron beams, which produce plasmas with varying characteristics. Understanding the nature and evolution of intense electron-beam-driven plasmas is fundamental to understanding the nuclear weapon effects that can interfere with or permanently damage devices, leaving desired missions uncompleted. The choice of plasma chemistry and plasma dynamics (referred to collectively as the plasma response model) divides the parameter space of electron-beam-driven plasmas into four regions. The division of phase space into these four regions is shown in Fig. 1. At present, good models only exist in the lower-right-hand side of the figure, where the plasma dynamics is treated as a fluid and the chemistry is treated as a weakly ionized plasma. The primary productivity measure of this research is the development of plasma response models and computational algorithms that are applicable in all four regions of phase-space. Another measure is the clear definition of the boundaries that separate each of the regions.

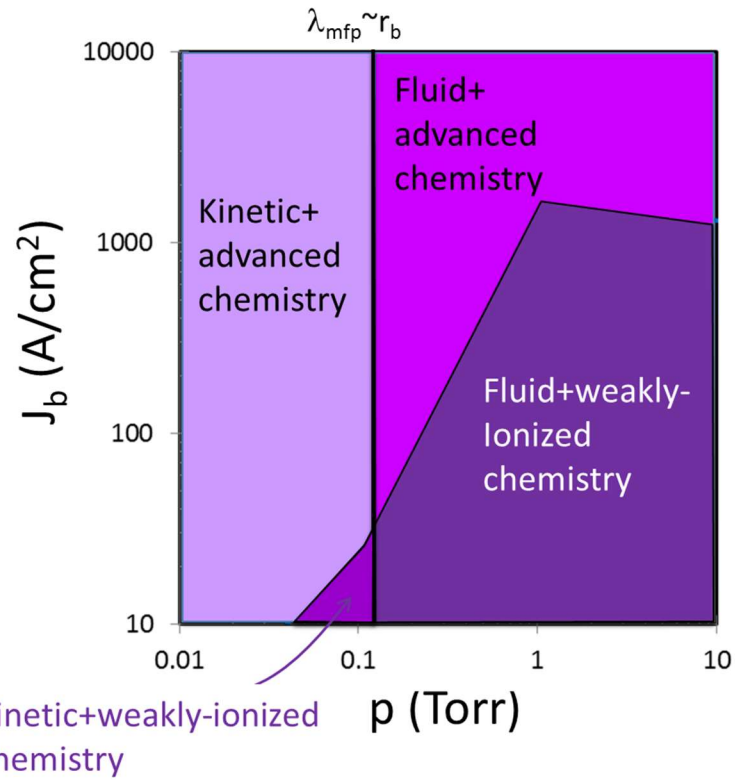


Figure 1. A phase-space map that shows the approximate boundaries between the four regions determined by the plasma chemistry and the plasma dynamics models, referred to collectively as plasma response models.

Title: Radiation Field Characteristics and Interaction in High Energy Density Z-Pinch Plasmas¹

Author(s): Y.K. Chong

Affiliation(s): Naval Research Laboratory, Washington, DC

CTA: CFD

Computer Resources: HPE SGI 8600, SGI ICE X [AFRL, OH]; Cray XC40 [ARL, OH]; Cray XC40/50 [ERDC, MS]

Research Objectives: The intense radiation sources such as the pulsed thermonuclear neutrons emitting from deuterium Z-pinch plasmas in high-power pulsed generators play an important role in the support of the DoD missions such as the nuclear weapon effects study and nuclear nonproliferation assays. In general, the radiation yield performance is strongly affected by the formation and evolution of RT instability and multidimensional gradients and nonuniformities. The control and mitigation of their development toward a uniform high density and temperature Z-pinch implosion toward the radiation yield optimization, therefore, remain an important focus of the current and future work. The objective of this study is to investigate the effects of an external axial magnetic field on the physics and energetics of deuterium Z-pinch plasmas and to optimize their design and performance as a pulsed neutron source using a multiphase multidimensional radiation magnetohydrodynamics (RMHD) model.

Methodology: The multimaterial, multidimensional version of Mach2 MHD code with the dynamical domain tabular collisional radiative equilibrium (DDTCRE) radiation transport model will be employed in the study of the multimaterial Z-pinch plasma load experiments with and without the axial magnetic field on the Sandia ZR pulsed accelerator (Fig. 1). The material interface tracking and interaction physics control needed for the multimaterial Z-pinch plasmas are possible through a PLIC volume-of-fraction model. The multiphase version of the DDTCRE transport model provides an accurate treatment of the radiation transport and non-LTE ionization dynamics in a computationally efficient manner. The ray-based 3D integral radiation transport and detailed configuration non-LTE ionization postprocessor model code suite, SPECAM/AXSTRAN, can be applied to understand and analyze the spectral signature emanating from any diagnostic trace elements.

Results: The Mach2+DDTCRE radiation MHD model was employed to investigate the effects of the external axial magnetic field on the implosion physics and dynamics of multishell deuterium gas-puff Z-pinch loads on the ZR accelerator at the Sandia National Laboratories. Our simulation study indicates that the thermal neutron yield of DD Z-pinch plasmas is strongly influenced by the multidimensional structure and nonuniform gradients formation and development due to the RT instabilities. The study identified the potential optimal external axial magnetic field application in magnitude, distribution, and duration that can lead to the reduction of the RT instabilities and the improved uniform implosion quality that can lead to an enhanced thermal neutron emission behavior.

DoD Impact/Significance: The optimization study of the thermal neutron emissions from hot, dense deuterium Z-pinch plasmas via an externally applied axial magnetic field to improve the uniform high density and temperature implosion process from the RMHD simulations is an essential step toward their utilization as a choice tool for the DoD nuclear weapons effect and nonproliferation mission study. The post process diagnostic investigation of the radiation trace element provides an additional tool for understanding and controlling their implosion physics and dynamics toward their optimal design and performance as a pulsed neutron source.

¹This work is supported by DOE/NNSA. Sandia is a multiprogram laboratory operated by Sandia Corporation, a Lockheed Martin Company, for the U.S. DOE's NNSA under contract DE-AC04-94AL85000.

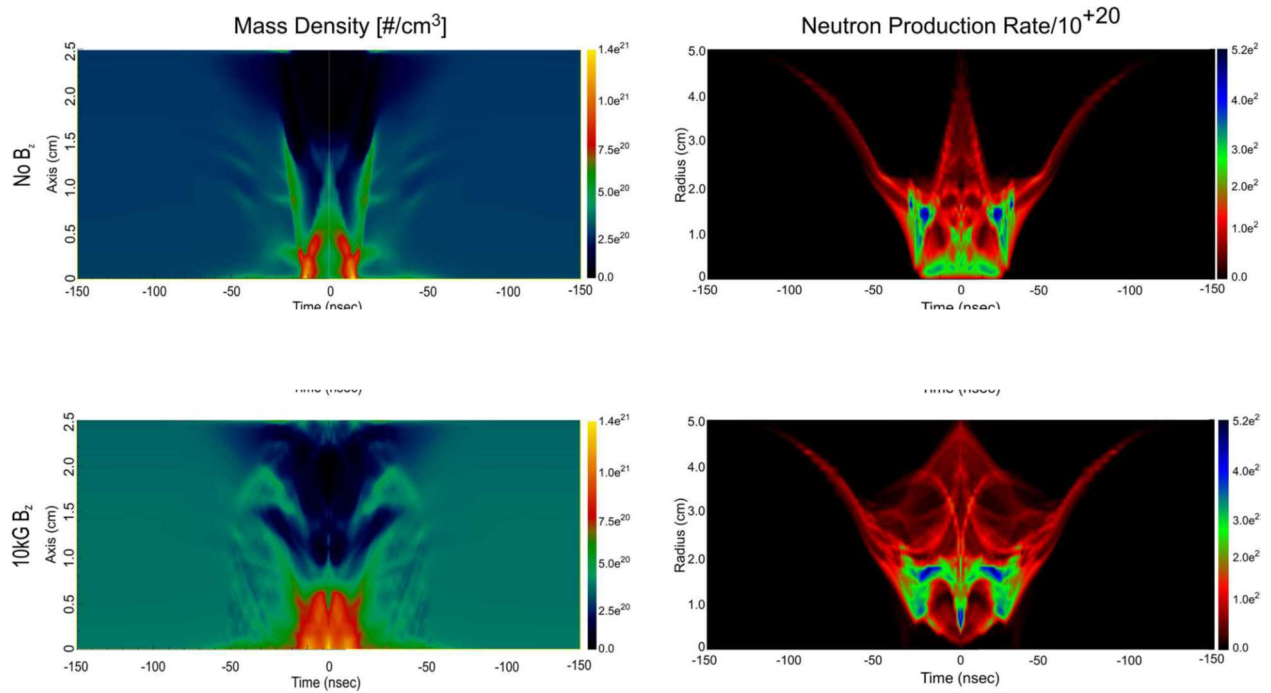


Figure 1. Mach2+DDTCRE 2-D Radiation MHD prediction of the ion density and the total thermal neutron yield for Sandia 1234 D-on-D nozzle gas puff Z-pinch load experiment on the ZR accelerator without (top row) and with (bottom row) the axial magnetic field of 10kG: (left) radially integrated linear mass density, and (right) axially integrated thermal neutron production rate as a function of time as referenced from the peak neutron yield time 0.

THIS PAGE INTENTIONALLY LEFT BLANK



Computational Biology, Chemistry, and Materials Science

CCM covers computational tools used to predict basic properties of chemicals and materials, including nano- and biomaterials. Properties such as molecular geometries and energies, spectroscopic parameters, intermolecular forces, reaction potential energy surfaces, and mechanical properties are being addressed. Within the DoD, quantum chemistry, molecular dynamics, statistical mechanics, and multiscale methods are used to design new chemical, polymer, nano- and biomolecular systems, for fuel, lubrication, laser protection, explosives, rocket propulsion, catalysis, structural applications, fuel cells, and chemical defense. Solid-state modeling techniques are employed in the development of new high-performance materials for electronics, optical computing, advanced sensors, aircraft engines and structures, semiconductor lasers, advanced rocket engines components, and biomedical applications. Of recent emerging interest in the Computational Biology, Chemistry, and Materials Science (CCM) CTA are methodologies that cover bioinformatics tools, computational biology, and related areas, such as cellular modeling.

Title: *Ab initio* Molecular Dynamics Simulations of High-energy-density Molecular Crystals

Author(s): I.V. Schweigert

Affiliation(s): Naval Research Laboratory, Washington, DC

CTA: CCM

Computer Resources: HPE SGI 8600 [AFRL, OH]; SGI ICE X, [ARL, MD]

Research Objectives: To demonstrate the utility of *ab initio* molecular dynamics (MD) in application to thermal and mechanical properties of high-energy-density molecular crystals.

Methodology: Molecular dynamics (MD) simulations can provide *a priori* predictions for thermal and mechanical properties of explosives and propellants. Classical MD methods rely on interatomic potentials to compute forces between atoms, but accurate potentials are rarely available for high-energy-density molecular crystals. *Ab initio* MD (AIMD) eliminates the need for the interatomic potentials by relying instead on the electronic Schrödinger equation, which is typically solved using density functional theory (DFT). AIMD offers much-improved accuracy and transferability compared with classical MD; however, solving the nonlinear equations of DFT at each MD step comes with a dramatic increase in the computational cost. The steep computational cost of AIMD can be partially mitigated by using a massively parallel implementation of DFT. Several open-source and commercial DFT codes offer such a capability, but differ dramatically in their efficiency and scalability. Within this Pathfinder project, we sought to evaluate the computational efficiency and numerical accuracy of different DFT implementations in application to temperature-dependent lattice parameters of high-energy-density molecular crystals.

Results: Typical computational costs associated with different MD approaches are illustrated in Fig. 1a. Shown are the wall-clock times necessary to simulate picosecond-long trajectories on a single, 40-core SGI ICE X node with MD and AIMD methods. Given the orders-of-magnitude differences in the computational costs, one can argue that AIMD should be used only when classical MD methods do not provide a sufficient accuracy for the properties of interest. We found this indeed to be the case for high-energy-density molecular crystals: As we show in a companion HPC report, only the DFT-based AIMD simulations were able to quantitatively capture the temperature dependence of various lattice parameters of CL-20 polymorphs. Nevertheless, the steep computational cost of AIMD requires a judicious choice of the DFT implementation and associated numerical settings. Figure 1b illustrates the weak scaling performance (i.e., how well an increase in the system size can be compensated by increasing the number of cores) for a number of DFT codes. We found that for molecular crystals, DFT implementations that use dual Gaussian-planewave basis sets (such as CP2K), generally outperform DFT implementations based on pure Gaussians, pure planewaves, or numerical orbitals. We also have tested the convergence of the predicted lattice parameters with respect to the primary basis set (Fig. 1c), planewave cutoff (not shown), size of the RDX supercell (not shown), trajectory length (Fig. 1d), and the number of AIMD trajectories (not shown) used to estimate ensemble averages. The resulting numerical settings were used in the simulations of the temperature-dependent lattice parameters of CL-20, which are described in the companion HPC report.

DoD Impact/Significance: AIMD simulations can provide *a priori* predictions for thermal and mechanical properties of high-energy-density molecular crystals, thus enabling *in silico* characterization of new compounds of interest to the DoD prior to investments in their synthesis and scale-up.

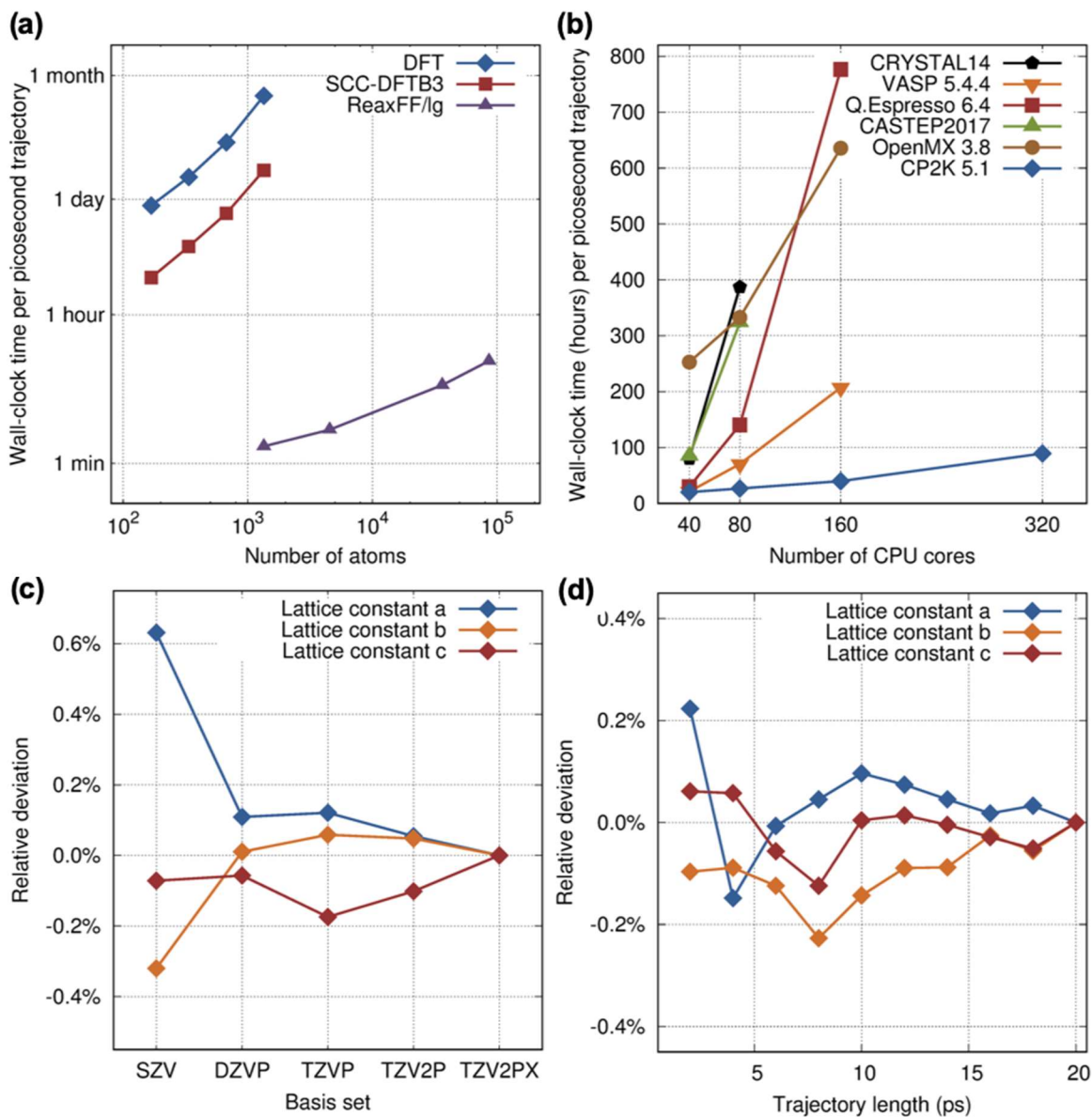


Figure 1. (a) Wall-clock times necessary to simulate the crystal unit cell of α -RDX on a single, 40-core SGI ICE X node with different MD approaches: a variable-charge, bond-order interatomic potential (ReaxFF/lg), a density functional tight binding method (SCC-DFTB3), and density functional theory (DFT). (b) Wall-clock times necessary to simulate multiple unit cells of α -RDX with various DFT codes, while keeping a fixed number of atoms (4) per CPU core. (c) Variations in the optimized 0 K lattice constants of α -RDX as a function of the Gaussian basis set used in DFT simulations with CP2K. (d) Variations in the simulated room-temperature lattice constants of α -RDX as a function of trajectory length in DFT-based AIMD simulations.

Title: First-Principles Simulations of Condensed-Phase Decomposition of Energetic Materials

Author(s): I.V. Schweigert

Affiliation(s): Naval Research Laboratory, Washington, DC

CTA: CCM

Computer Resources: HPE SGI 8600, SGI ICE X [AFRL, OH]; Cray XC40, SGI ICE X [ARL, MD]; SGI ICE X [ERDC, MS]

Research Objectives: To predict thermal, mechanical, and chemical properties of explosives subjected to elevated temperatures and pressures.

Methodology: Crystal structure optimizations and *ab initio* molecular dynamics (MD) simulations are being used to study physical and chemical changes in high-energy-density molecular crystals subjected to elevated temperatures and pressures. These calculations rely on density functional theory (DFT) and periodic-cell models to approximate bulk crystalline environment. Structure optimizations use variable-cell optimization algorithms to determine changes in crystal structures and lattice constants at elevated pressures. *Ab initio* MD simulations use constant-pressure, constant-temperature (NPT) and constant-volume, constant-energy (NVE) integrators combined with multiple replicas to simulate target thermodynamics conditions and to probe decomposition mechanisms triggered by these conditions. Python and Perl scripts are being developed to streamline the input deck preparation, job execution, and data analysis.

Results: This year, DFT-based *ab initio* MD simulations were completed to investigate the thermal expansion of CL-20 polymorphs. First, the convergence of the predicted lattice parameters with respect to the number of trajectories, trajectory lengths, and representative volume sizes were tested. It was found that ensemble averages over 5 trajectories, with each trajectory simulating 2x1x1 supercells for 10 picoseconds, were sufficient to closely reproduce the results from much larger simulations. Second, the MD methods based on the interatomic potentials (ReaxFF/lg) and on density-functional tight binding (DFTB) were tested to determine whether the steep computational cost of DFT-based simulations can be avoided. It was found that ReaxFF/lg and DFTB do not capture the known temperature dependences of the CL-20 lattice parameters (Figs. 1a and 1b). Only when dispersion-corrected DFT (PBE-D3) is used to compute the forces in the MD simulations, do these simulations agree well with the experimental values (Fig. 1a and 1b). Finally, DFT-based MD simulations were used to predict the temperature-dependent lattice parameters for temperatures not accessible in experiments. Overall, 45 trajectories were computed for each polymorphs, sampling temperatures from 5 to 400 K. The resulting temperature-dependent volumes of the primitive cells for the ϵ and γ polymorphs are shown in, respectively, Fig. 1c and 1d. These simulations predict that the volumetric thermal expansion of the CL-20 polymorphs is linear as a function of temperature. Therefore, the experimental values measured at cryogenic temperatures can be extrapolated above room temperature. Ongoing simulations are focused on thermal expansion in the high-pressure ζ polymorphs of CL-20 for which experimental data is not available.

DoD Impact/Significance: CL-20 is being considered as a replacement for HMX in several high-performance explosive formulations. Thermomechanical equation of states for the CL-20 polymorphs, including shock Hugoniot relationships, are needed to support physics-based modeling of initiation systems for CL-20-based explosives. The simulations completed this year ascertained the accuracy of DFT in application to CL-20. Future simulations will focus on the equations of state under elevated temperatures and pressures, for which experimental data is currently not available.

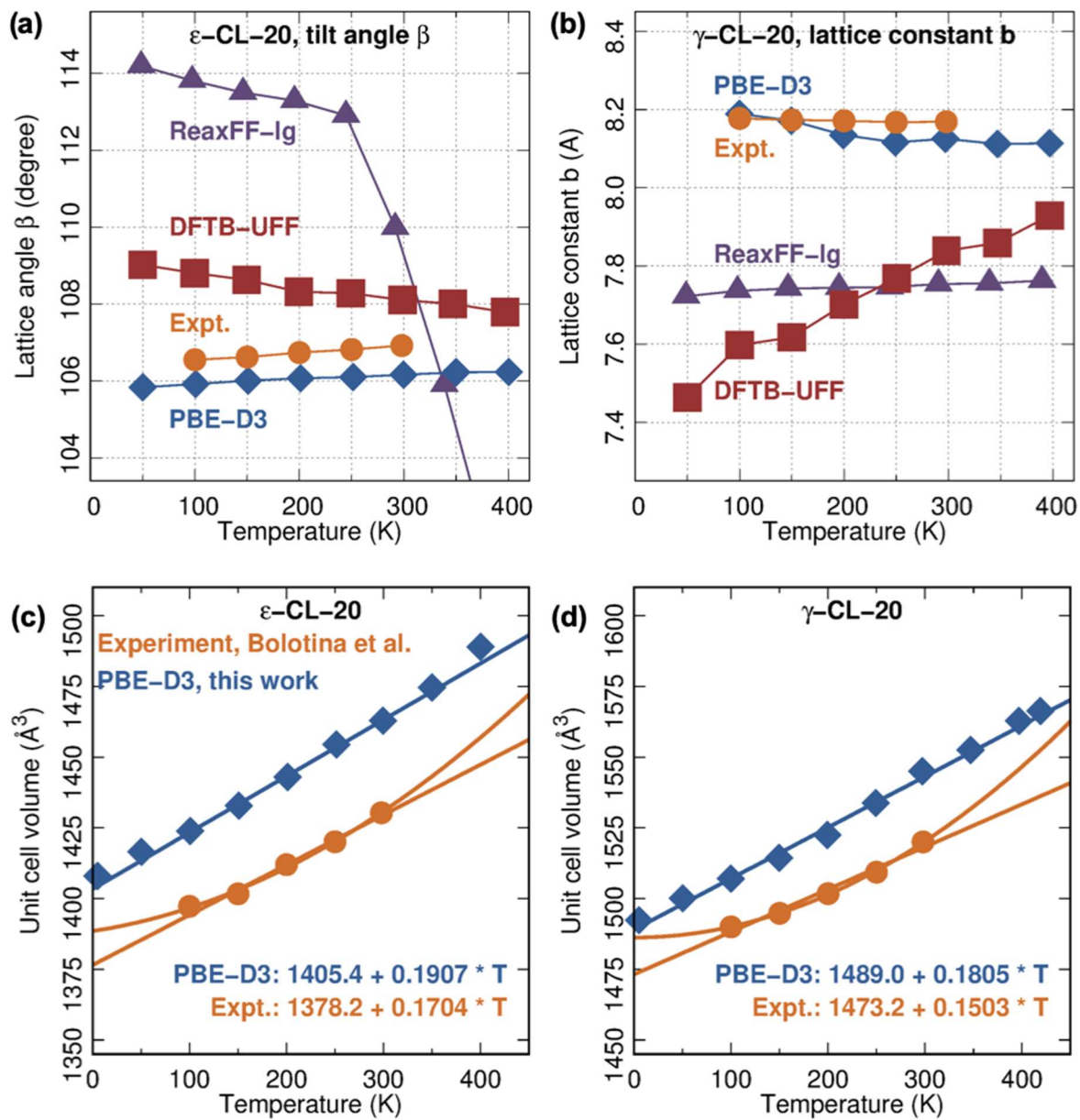


Figure 1. (a) Computed and experimental tilt angles in ϵ -CL-20 at various temperatures. (b) Same, but for the lattice constants b in γ -CL-20. (c) Computed and experimental primitive cell volumes of ϵ -CL-20 at various temperatures. Solid lines show linear and quadratic fits to the computed and experimental values. (d) Same, but for γ -CL-20.

Title: Quantum-Chemical Simulation of Surface-Science Experiments

Author(s): V.M. Bermudez

Affiliation(s): Naval Research Laboratory, Washington, DC

CTA: CCM

Computer Resources: SGI ICE X [AFRL, OH]; SGI Altix ICE [NRL, DC]

Research Objectives: The objective of this program is to perform quantum-chemical calculations as an aid in interpreting surface-science experiments and in understanding the structure and properties of surfaces.

Methodology: The QUANTUM ESPRESSO (versions 5.2 and higher) and CRYSTAL (2014) software packages are used for density functional theory (DFT) calculations on periodic structures. The GAUSSIAN-16 program suite is used for DFT calculations on isolated molecules and clusters.

Results: Charge trapping by intrinsic and extrinsic defects in Si_3N_4 thin films and at $\text{Si}_3\text{N}_4/\text{SiO}_2$ and $\text{Si}_3\text{N}_4/\text{Si}$ interfaces has been studied extensively due to the technological significance of this topic when Si_3N_4 is employed as a gate dielectric. A key aspect has been the use of *ab-initio* density functional theory (DFT) to develop a microscopic understanding of the structure and properties of such defects. However, little attention has been directed toward charge trapping by *intrinsic surface states*, which has been seen experimentally. For example, an increase in charge retention is found when Si_3N_4 films with low levels of surface contamination are stored in ultra-high vacuum (UHV) *vs.* under N_2 , which suggests charge trapping at surface sites that are sensitive to impurities in the N_2 . For atomically clean Si_3N_4 surfaces in UHV, the valence band (VB) is seen to shift rigidly by ~ 1.4 eV to lower kinetic energy following a small exposure to O_2 , which is consistent with the elimination of negatively charged surface traps.

Intrinsic surface states arise from coordinatively-unsaturated surface atoms. In the bulk of $\beta\text{-Si}_3\text{N}_4$, all Si atoms are equivalent, and there are two inequivalent types of N atoms, termed “ N_t ” and “ N_c ”. On the (0001) surface, each Si is missing one N_t ligand and each N_t is missing one Si ligand. Interaction between the dangling bonds on these atoms produces a dimer pair termed “ $\text{Si}=\text{N}_t$ ”, which forms an empty and slightly dispersive band of surface states at ~ 4.8 eV above the valence band maximum (VBM) with a computed band gap of $E_g = 6.7$ eV. Trapping of an electron can occur spontaneously by transfer from an oxygen substitutional impurity in the bulk. The accompanying figure shows the distribution of spin-polarized electron density (i.e., the difference between “spin-up” and “spin-down” densities) after electron transfer. Most of the density appears on a surface Si atom close to the O dopant with some contribution from the three N atoms bonded to this Si. This charge localization and the resulting displacement of the Si atom causes a localized state to “drop out of” the band of surface states. The effects on the surface electronic structure are significant, as shown in the figure. Structure (a) derives from the nonbonding lone-pair orbital on the N_t atom in the $\text{Si}=\text{N}_t$ at the trap site, which, before trapping, was positioned just below the VBM. Structure (b), which lies at the Fermi level, arises from the partially filled Si dangling bond, which, before trapping, was empty and was involved in an anti-bonding interaction with the surface N_t . Structure (c) results from other $\text{Si}=\text{N}_t$ sites that are perturbed by the presence of the trapped charge. These are the most important trap-related features. The results provide an explanation for the observed shift in surface charge when a clean surface becomes contaminated.

DoD Impact/Significance: Thin films of Si_3N_4 are used in a variety of applications including passivation layers for group-III nitride high electron mobility transistors, gate dielectrics in field-effect transistors, diffusion barriers, and as a host matrix for the integration of silicon nanocluster-based light-emitting diodes with silicon integrated circuits. Charge trapping is an important factor in all these applications, and the present work sheds light on a previously unknown mechanism by which this occurs.

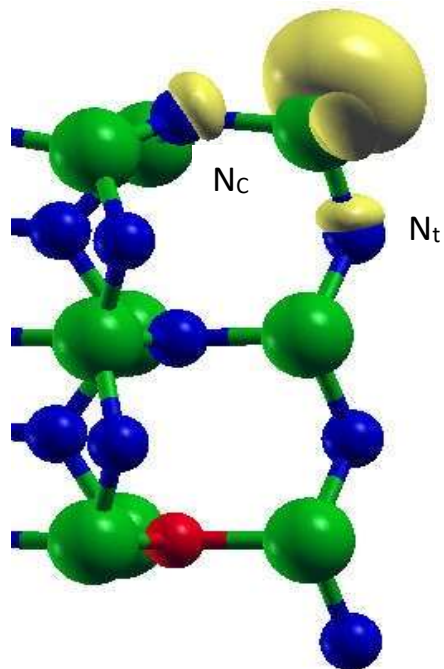


Figure 1. Diagram showing the spin-polarized charge density ($\delta\rho^{\uparrow\downarrow}$, in yellow) that results when an O atom substitutes for Nc within the slab. The view is approximately along the surface Si=Nt bond from the Nt toward the Si. For clarity, only a small section of the two-dimensionally-periodic slab model is shown, and the isosurface cutoff is set at $\sim 10\%$ of the maximum value. The surface Nc and the underlayer Nt bonded to the Si trap site are indicated. Si, N and O are shown in green, blue and red, respectively. The [0001] axis lies in the plane of the page.

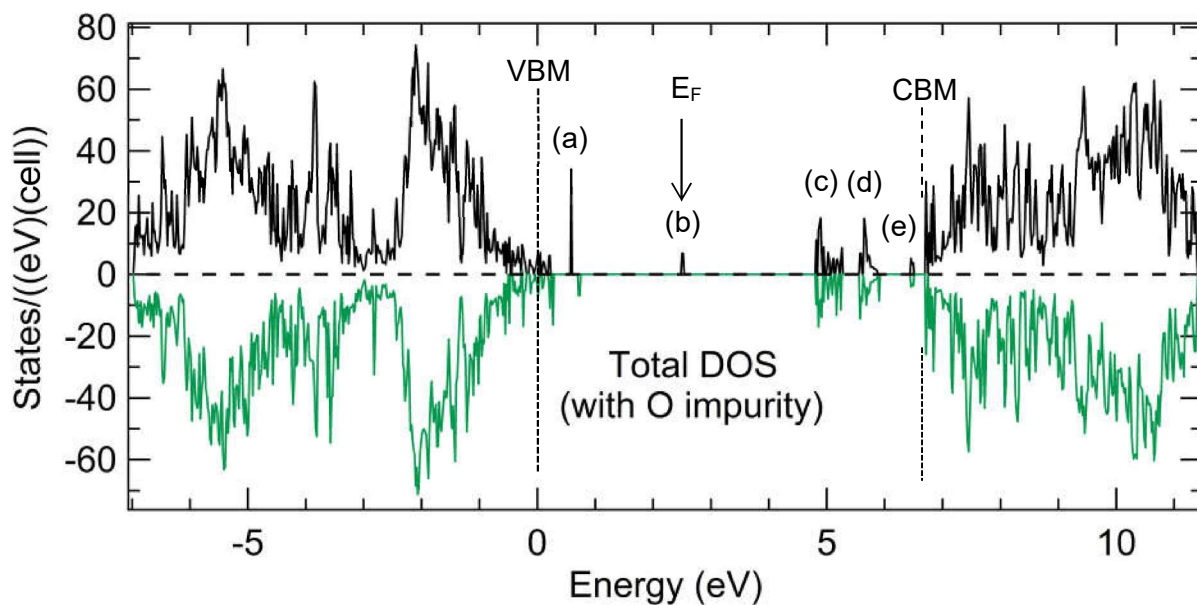


Figure 2. The total density of states (DOS) obtained when an O atom substitutes for Nc within the slab. Black and green traces show the majority- and minority-spin results, respectively, and the labels “(a)”, etc. indicate states lying within the bulk band gap, which is defined by the valence band maximum (VBM) and the conduction band minimum (CBM). The DOS is in units of states/eV per (1x1x5) slab unit cell, and the arrow marks the location of the Fermi level (E_F).

Title: Improved Calculation of Solid-Phase Heats of Formation Using Intermolecular Interactions Observed in Crystal Structures

Author(s): I.D. Giles and G.H. Imler

Affiliation(s): Naval Research Laboratory, Washington, DC

CTA: CCM

Computer Resources: Cray XC40 [ARL, MD]

Research Objectives: The discovery of novel high-energy-density materials (HEDMs) with improved properties in performance and safety is a major goal for researchers across the Department of Defense. Testing new materials for energetic properties such as pressure of detonation, velocity of detonation and sensitivity requires large quantities of material, proper testing facilities and safety considerations to the point that it is prohibitively expensive to test every potential material being researched. Predicting energetic material properties computationally is necessary to select the best energetic materials for scale-up and testing. Currently, thermochemical code programs such as Cheetah are used to calculate detonation parameters such as pressure and velocity of detonation. Cheetah requires density, molecular formula and solid-phase heat of formation to calculate detonation parameters. Accurate methods to calculate gas-phase heat of formation exist; however, calculating enthalpy of sublimation, which is needed for conversion to solid-phase heat of formation, is more difficult. This project will use atomic coordinates from crystal structures and DFT computations to calculate enthalpy of sublimation.

Methodology: DFT and Time-Dependent DFT (TDDFT) through the Gaussian package will be used to geometry-optimize a starting structure based on single-crystal X-ray diffraction data (XRD) using a suitable method and basis set (B3LYP and 6-311++g to start). Further energy and frequency optimization will ensure a global energy minimum as well as determine the electronic structure and heats of formation, and understand their vibrational spectra. TDDFT methods will be used with solvation models (H₂O and acetone to start) to understand the electronic transitions seen in their electronic spectra in the corresponding solvents. Default tolerances will be employed unless deemed insufficient. Energies of intermolecular interactions will be estimated based on internuclear distances (as seen in Fig. 1) and will be used to calculate enthalpy of sublimation. Scripts developed by Edward Byrd and Betsy Rice at ARL have been demonstrated to be very accurate and will be used for the calculation of gas-phase heat of formation. The Politzer method is currently used to calculate enthalpy of sublimation and will be used for comparison with the methods developed in this project.

Results: Initial studies have focused on calculating solid-phase heats of formation for a series of twenty energetic materials in the nitro-aromatics family. With the current model, root-mean-square deviations of calculated enthalpies of sublimation compared to experimental enthalpies of sublimation are comparable with methods currently used in literature. Examining additional families of energetic materials will allow further improvements to the model and have the potential to create a very accurate method with low computational demands.

DoD Impact/Significance: At the current iteration, this method approaches or matches the accuracy of popular methods used to calculate enthalpy of sublimation, which is needed to calculate solid-phase heat of formation. Additional improvements have the potential to surpass methods in use today. More accurate calculation of solid-phase heat of formation would assist researchers in identifying the best HEDMs for scale-up and additional testing.

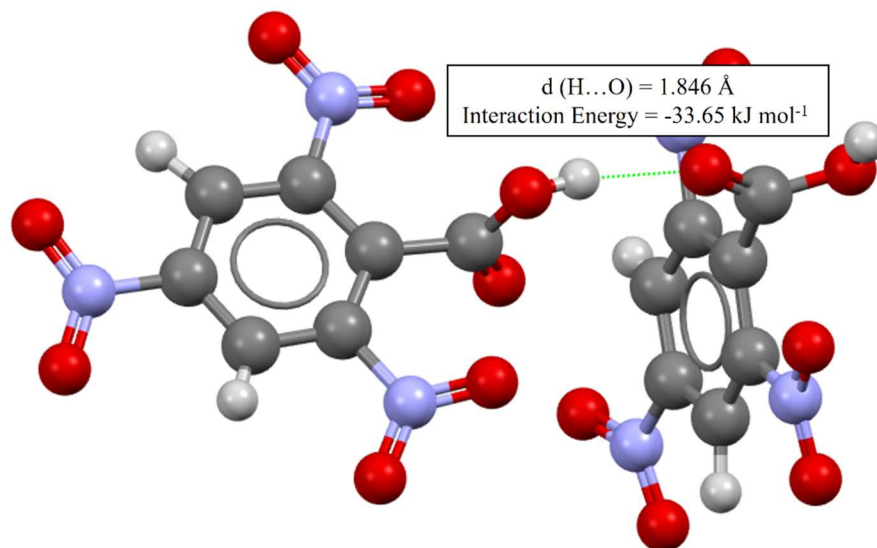


Figure 1. DFT computation demonstrating strong hydrogen bond in 2, 4, 6-trinitrobenzoic acid as identified in single crystal X-ray structure. Interaction energies have been quantified using intermolecular distances between hydrogen bond acceptors and donors.

Title: Synthetic Biology for Military Environments
Author(s): W.J. Hervey and G.J. Vora
Affiliation(s): Naval Research Laboratory, Washington, DC
CTA: CCM

Computer Resources: HPE SGI 8600, SGI ICE X [AFRL, OH]; Cray XC40 [ARL, MD]; Cray XC40/50, Cray XE6m, SGI ICE X [ERDC, MS]

Research Objectives: The primary goal of our synthetic biology research program is to design and implement molecular toolkits for microbial species (or target “chassis”) that are directly relevant to military environments, as opposed to solely functioning in laboratory settings. A prerequisite to engineering a synthetic biology platform for this purpose are characterizations and measurements of target microbial genomes (DNA), transcriptomes (mRNA), proteomes (proteins), and metabolomes (small molecules). These high-throughput molecular-level, “wet-lab” measurements allow researchers to compare and contrast synthetic modifications from unmodified microbial strains. Acquisition of disparate ‘-omics’ measurements by multiple analytical modalities results in a very large data volume. An additional objective of this research was to enable multiple Tri-Service co-investigators to access comparable software tools for data analyses via a multiple user “Proteomics Portal.”

Methodology: Synthetic biology is a highly multidisciplinary research area that imparts desirable (or “designer”) functions into cells from the introduction of simple genetic circuits to complex engineered genetic regulatory networks. Applications of synthetic biology range from design of DNA constructs for sensing and reporting target analytes to the manipulation of enzymatic pathways to improve yield of natural or synthetic products. Throughout FY19, we evaluated performance of a DNA operational envelope in the microbial species *Vibrio natriegens* and characterized protein expression from this operational envelope by multiple liquid chromatography tandem mass spectrometry (LC-MS/MS) approaches. These LC-MS/MS data, as well as data from other synthetic microbial chassis, were used as test input data for the Synthetic Biology for Defense (SB4D) Proteomics Portal.

Results: In FY19, HPC allocations resulted in 3 conference proceedings from NRL-DC, as well as additional proceedings from Tri-Service co-investigators on this subproject. Two manuscripts are in final preparation for submission that leveraged FY19 allocations from this subproject at NRL.

DoD Impact/Significance: Our HPC subproject is directly applicable to “Sense and Sense-Making” from large-scale biomolecular datasets of considerable DoD interest, namely biologically inspired materials design, synthetic biology, systems biology, and alternative energy sources.

a)



b)

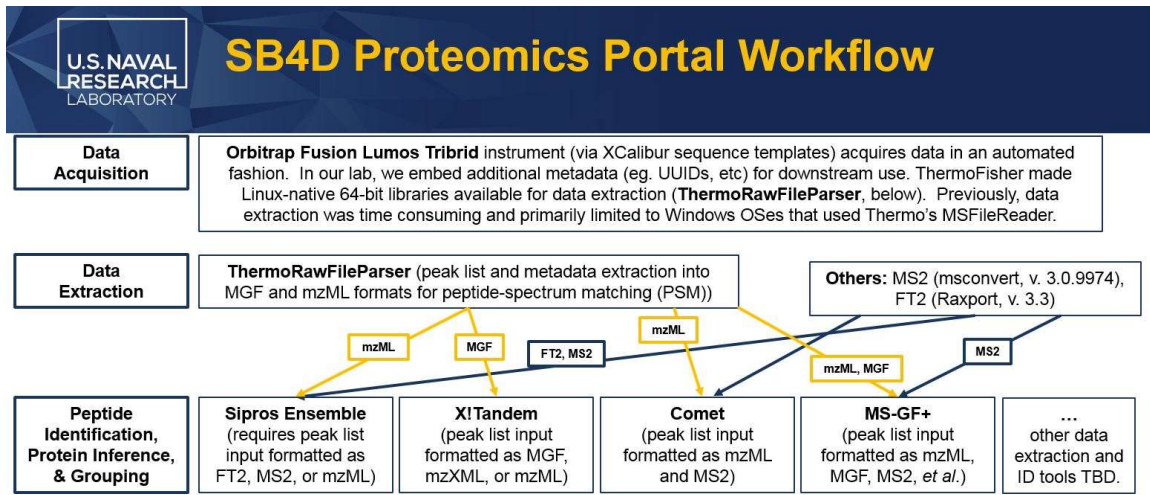


Figure 1. a) Proteomics Data Acquisition Instrumentation, Hardware, and Commercial Software: Data from an Orbitrap Fusion™ Lumos™ Tribid™ mass spectrometer (ThermoFisher Scientific) is recorded to computer under automated software control. Data are transferred to a NetApp storage device, which is mountable by a Dell R740 server (Red Hat Enterprise Linux 7 Server). Commercial software used for data analysis on the server include Mascot Server (Matrix Science), PEAKS X (Bioinformatics Solutions), and Scaffold Q+S (Proteome Software). The Dell R740 server also is capable of extracting data to open formats via the vendor's software and transferring them to HPCMP systems. b) Synthetic Biology for Defense (SB4D) Proteomics Portal Application Workflow: Post-acquisition and data extraction via ThermoRawFileParser, peptide peak lists in multiple open formats (mzML, Mascot Generic Format (MGF), MS2, FT2) can be transferred efficiently to HPCMP resources. To demonstrate Portal proof-of-principle, the Sipros Ensemble application (Guo *et al.* *Bioinformatics* 2018) was used to search mass spectrometry data. However, as shown above, a number of software tools in the public domain may be used to infer peptide-spectrum matches from proteomics data.

Title: Marine Biofilm Metaproteomics
Author(s): W.J. Hervey and G.J. Vora
Affiliation(s): Naval Research Laboratory, Washington, DC
CTA: CCM

Computer Resources: HPE SGI 8600, SGI ICE X [AFRL, OH]; Cray XC40 [ARL, MD]; Cray XC40/50 [ERDC, MS]

Research Objectives: To implement, maintain, and adapt a modular data analysis workflow of selected bioinformatics software applications from the public domain. This effort maintains an HPC Application Software Initiative (HASI) previously awarded for biomolecular characterization of microbiomes relevant to the Department of Defense, such as the warfighter gut microbiome, marine biofilms, and biofouling microbial consortia. Integration of disparate, large-scale data tiers of biological information on genomic (DNA), transcriptomic (RNA), proteomic (protein), and metabolomics (metabolite) levels is a prerequisite to understanding microbiomes, such as biofilms, at the molecular level.

Methodology: The process of creating large-scale metaproteome inventories of proteins predicted to be present among microbiomes is threefold: assembly of small DNA pieces into larger contiguous segments (or “contigs”), prediction of protein-coding regions from contiguous DNA segments, and in silico translation of the genetic information into protein sequence data. Two factors make this workflow computationally intensive and time-consuming: the large volume of data acquired from complex environmental samples (e.g. the number of DNA reads and MS/MS spectra acquired) and the diverse species complexity present in the environmental sample. FY19 saw publication of the software application MetaCarvel in the journal *Genome Biology’s* Microbiome special issue. MetaCarvel retains multiple microbial genome sequence variants by representing multiple connections among assembly graphs as SPQR trees. These sequence variants can resolve biological differences within microbiomes, such as potential gene loss or gene gain events (Fig. 1). Resolution of strain variants within microbiomes can be particularly insightful in detecting bacteria harboring antimicrobial resistance properties from bacterial strains that are susceptible to antimicrobial agents. We also reported an additional software tool, seqCAB (or sequence conversion & annotation with NCBI’s BLAST+), at a conference in order to improve performance and accuracy of biological sequence annotations. Both the MetaCarvel and seqCAB software tools have been included into the most recent iteration of our bioinformatics workflow, which spans applications for genome assembly, open-reading-frame prediction, transcriptome profiling, and proteome identification for both isolate species and complex microbial consortia, such as biofilms.

Results: In FY19, HPC allocations resulted in publication of two peer-reviewed journal articles and three conference proceedings, while also proving enabling to other research projects, such as characterization of acorn barnacle (*Amphiblanus amphitrite*) proteins and genome assembly between NRL Codes 6100/6900.

DoD Impact/Significance: Our HPC subproject is directly applicable to “Sense and Sense-Making” from large-scale biomolecular datasets of considerable DoD interest, particularly with respect to microbiomes, antimicrobial resistance, alternative energy sources, and the platform sustainability.

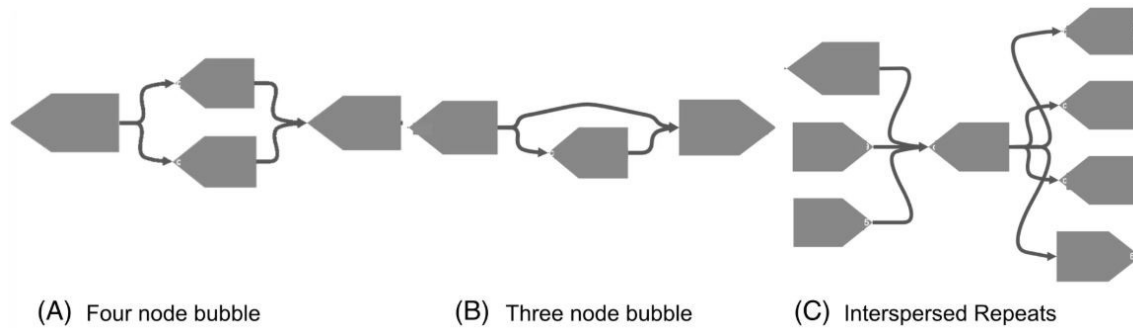


Figure 1. Different types of genome assembly motifs detected by MetaCarvel (from Ghurye *et al. Genome Biology*. 20: 174, 2019). (A) Four-node bubbles denote the variation between very similar sequences. They can result in the graph due to very high sequence similarity among microbial species. (B) Three-node bubbles potentially represent gene gain/loss events and horizontal gene transfers. They are formed due to the insertion or deletion of chunks between two otherwise similar genomes. (C) Interspersed repeats in the graph are denoted by the nodes with high centrality and usually tangle the graph.

Title: Preventing Corrosion by Controlling Cathodic Reaction Kinetics

Author(s): S.A. Policastro, C.M. Hangarter, and R.M. Anderson

Affiliation(s): Naval Research Laboratory, Washington, DC

CTA: CCM

Computer Resources: Cray XC40 [NAVY, MS]

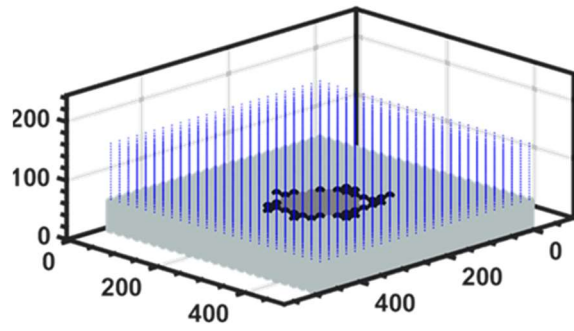
Research Objectives: Our goal is to devise and test a framework of corrosion-governing equations over a broad range of atmospheric conditions in order to develop an approach that will permit predictions of field exposure results and eventually improve damage tolerance forecasts.

Methodology: The simulation was developed in C# and was run on the Navy DSRC Cray XC40 asset using a recent revision of the Mono compiler, which compiles C# code to run on Linux-based operating systems. The custom partial differential equation solver, which was written to solve the diffusion and electromigration equations, uses one of the Intel Math Kernel Library routines included on the Navy HPC system to perform the sparse matrix inversions that are needed for Crank-Nicolson algorithm.

Results: A simulation of atmospheric corrosion for galvanic couples between a stainless-steel alloy, UNS S13800, and an aluminum alloy, UNS A92024, was developed that incorporated a model for atmospheric processes that influence thin-film-electrolyte evolution, a model for chemical processes occurring within the electrolyte, and a model for the galvanic corrosion interaction between the two alloys (Fig. 1). The electrochemical processes for the response of the two alloys to the chemical environment of the electrolyte were based from experimental measurements of the alloy behavior.

DoD Impact/Significance: This research directly supports the "Platform" category in the "Department of the Navy Goals and Objectives for FY 2016 and Beyond" document by developing prediction tools that support decreasing maintenance and life cycle costs. A successful program will result in a robust, predictive model of atmospheric corrosion phenomena, a laboratory-scale approach to predict the performance of naval materials in atmospheric conditions, and new methods to probe atmospheric corrosion with high spatial resolution.

a.



b.

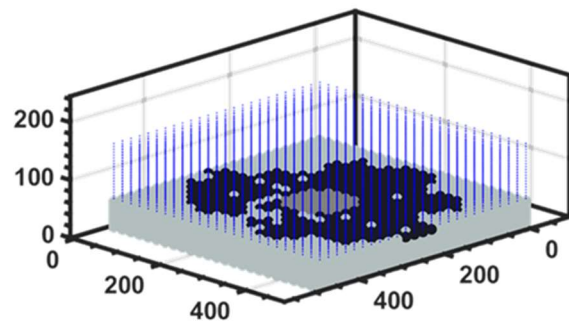


Figure 1. Plots of the predicted differences in extent of surface oxidation of the aluminum alloy UNS A92024 galvanically coupled to a disc made of UNS S13800 stainless steel for an electrolyte containing a) 0.6 M NaCl and b) 3.2 M NaCl.

Title: Surfaces and Interfaces in Oxides and Semiconductors

Author(s): C.S. Hellberg

Affiliation(s): Naval Research Laboratory, Washington, DC

CTA: CCM

Computer Resources: HPE SGI 8600, SGI ICE X [AFRL, OH]; Cray XC40, SGI ICE X [ARL, MD]; SGI ICE X [ERDC, MS]

Research Objectives: Determine how the oxygen content in the experimental chamber modifies the temperature of electric-field-assisted sintering (also known as flash sintering) and the resulting microstructure. Replacing air with argon has been shown to reduce the flash-sintering temperature of several oxides, including ZnO and yttria-stabilized zirconia (YSZ). Additionally, the sharp grain boundaries in the microstructure disappear when the oxygen pressure is reduced.

Methodology: We performed highly accurate first-principles density functional calculations of large (containing up to 376 atoms) YSZ computational cells to determine the ground state atomic shown in the Fig. 1 and various structures with defects. Initially, we relaxed 47-atom cells to determine the optimal arrangements of all atoms. Starting in the initial ZrO_2 structure, there are 128 arrangements of two Y substitutions and one oxygen vacancy. Once the optimal structure was found, we tiled it to create 376-atom supercells. In the large supercells, we introduced additional oxygen vacancies and interstitials, and computed all charge states of each. We used the VASP Density Functional Theory (DFT) code at the AFRL and ARL HPC centers. Finally, we computed the free energies using grand-canonical thermodynamics.

Results: We find that the formation energies of oxygen defects do not depend on the oxygen partial pressure for oxygen pressures that can be achieved experimentally. However, the oxygen partial pressure determines the Fermi energy for the electrons in the sample. The shift in Fermi energy changed the formation energies of Zn and Y defects, which, in turn, degrade the crystallinity of the samples sintered in argon.

DoD Impact/Significance: Discovered in 2010, flash sintering occurs much more quickly and at significantly lower temperatures than conventional sintering in most materials. It has the potential to allow sintering to be used to process many more materials due to these advantages. However, as with conventional sintering, our results show that the experimental atmosphere is critical for producing high-quality dense materials.

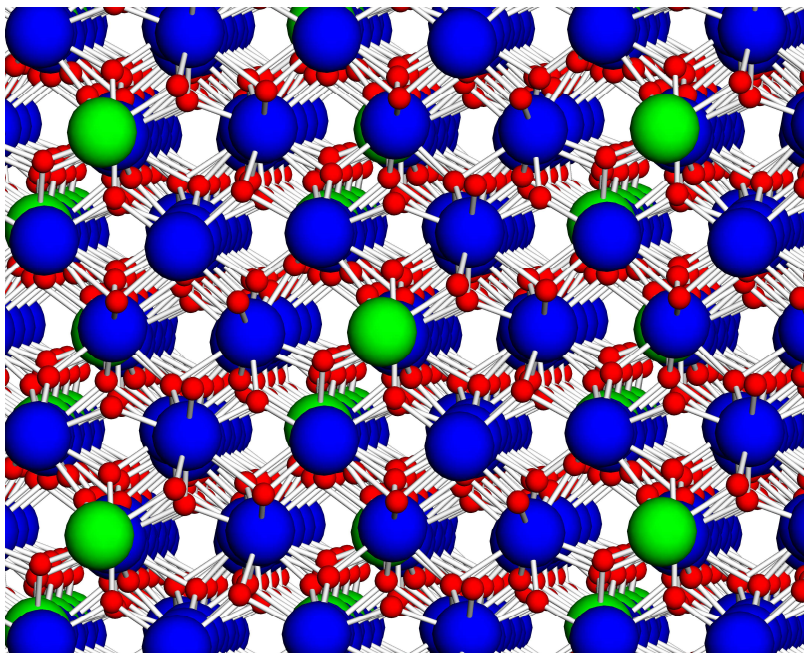


Figure 1. Computed ground-state structure of yttria-stabilized zirconia. Zr atoms are blue, Y atoms are green, and O atoms are red. This calculation used 14 Zr atoms, 2 Y atoms, and 31 oxygen atoms. Plenty of disorder is apparent. Nevertheless, the computed X-ray diffraction pattern is tetragonal, in agreement with experimental observation.

Title: High-Throughput Search for New Magnetic Materials and Noncollinear Magnetism

Author(s): I. Mazin¹ and J. Glasbrenner²

Affiliation(s): ¹Naval Research Laboratory, Washington, DC; ²George Mason University, Fairfax, VA
CTA: CCM

Computer Resources: SGI ICE X [AFRL, OH]; SGI ICE X [ERDC, MS]

Research Objectives: Understanding relativistic and nonrelativistic magnetism, including noncollinear magnetic systems.

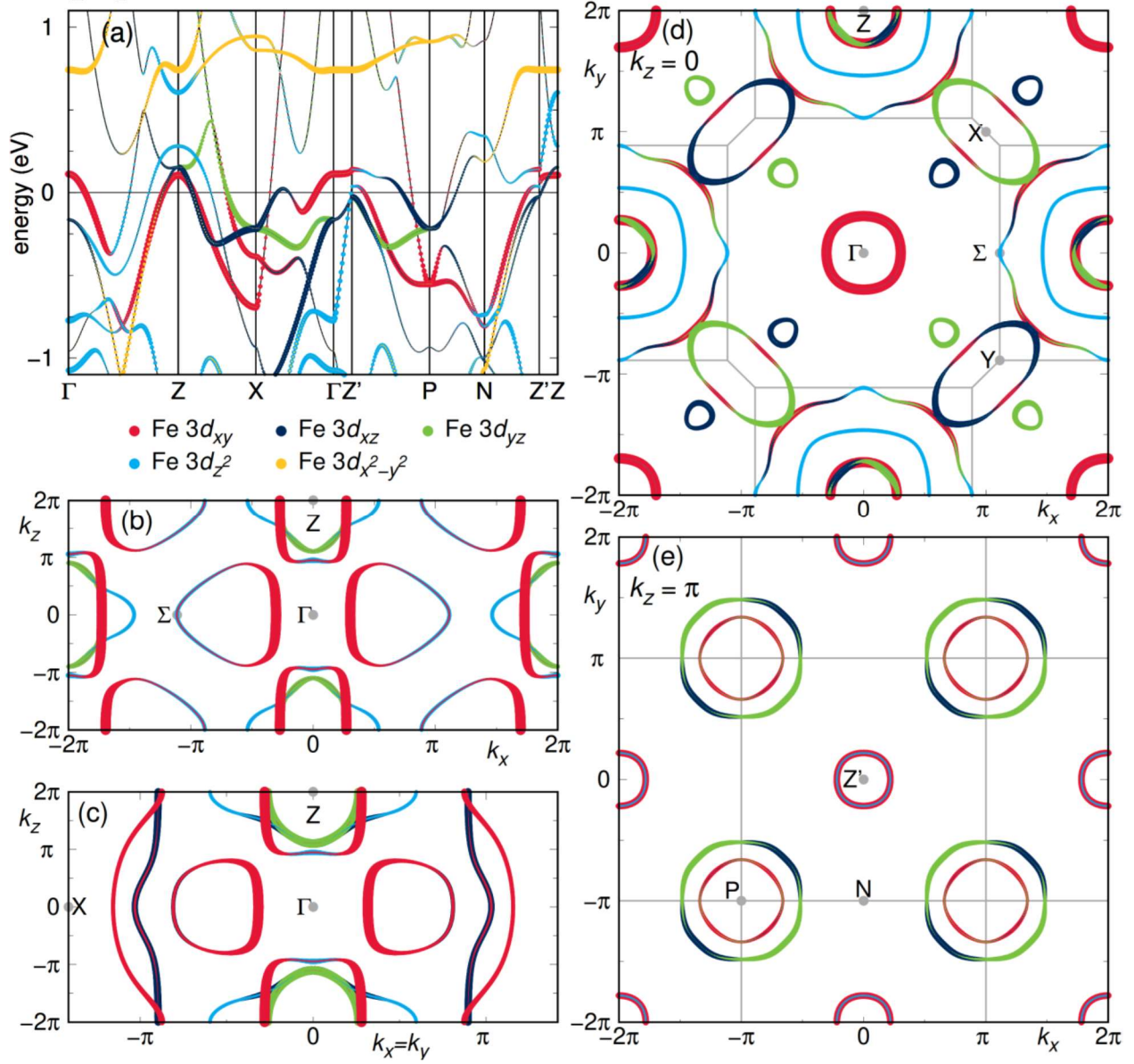
Methodology: We performed *ab initio* density functional theory (DFT) calculations, using the all-electron code WIEN2k and the pseudopotential code VASP at the AFRL and ERDC HPC centers. These codes can calculate the total energy for preset magnetic moment directions on each atomic site, as well as full self-consistent relaxation of both the amplitudes and directions of individual magnetic moments, and also can calculate the total energy of incommensurate magnetic spirals. VASP also can be used to optimize crystal structures efficiently.

Results: We have performed DFT calculations for several challenging materials with unconventional magnetism. One project was on newly discovered overdoped Fe-based superconductor LaFe₂As₂. We showed that (a) La d-bands cross the Fermi level, so that the actual doping level is smaller than nominal, and (b), that the topology of the Fermi surface is still beneficial for the s[±] superconductivity, despite different orbitals forming the Fermi surface pockets. In another project, we worked on magnetic properties of naturally occurring spin-Delta-chain mineral, acatamite, and explained its magnetic phase diagram (this work was performed in close collaboration with an international group investigating the same phase diagram experimentally). In a third project, we predicted a new noncollinear Kitaev system, IrO₂. According to our calculations, this material not only can be stabilized in a layered honeycomb form, but also would form a van der Waals crystal that could be exfoliated to produce magnetic monolayers. We also have computed the magnetic Hamiltonian of this system.

DoD Impact/Significance: Fe-based superconductors constitute the most intriguing family of unconventional high-temperature superconductors after the cuprates. Better understanding of this family eventually might lead to room-temperature ambient-pressure superconductivity, which would be very beneficial for Navy applications.

Frustrated quantum magnets, such as acatamites or the newly predicted IrO₂, have potential for quantum computing through their nontrivial topological properties.

LaFe₂As₂ (UT)



Title: Materials for Energy Storage and Generation
Author(s): M. Johannes
Affiliation(s): Naval Research Laboratory, Washington, DC
CTA: CCM

Computer Resources: SGI ICE X [AFRL, OH]; SGI ICE X [ERDC, MS]

Research Objectives: The objectives of this program are to use density functional theory (DFT) and its extensions, including molecular dynamics, to understand the materials properties that drive functionality in materials relevant to energy storage and generation, including new materials for low-power electronics.

Methodology: First-principles pseudopotential methods are employed to calculate quantities of interest. The majority of the work was done using the Vienna Ab-Initio Software Program (VASP), but a substantial minority was done using the Wien Code, which is a full-potential LAPW code. Postprocessing is done using personal codes. Both standard (static) $T=0$ DFT calculations and temperature-dependent molecular dynamics (MD) calculations were used.

Results: In FY19, the project's focus was on analyzing materials for photocatalysis in terms of both ionic and electronic transport and the effect of defects, particularly oxygen vacancies, on that transport. One major finding was that without any defects (*i.e.* in a perfect crystalline material), the Au nanoparticles that drive catalytic behavior at the surface of a TiO_2 substrate do not interact electronically with the substrate. No hybridization between Au and surface states occurs and consequently, no electronic relaxation into the metallic bands from the TiO_2 can take place. This limits electronic conduction, which is a major component of efficient catalysis. Another finding is that when oxygen-vacancy defects do exist, they migrate easily to surface or subsurface locations where they can participate most effectively in the catalytic process. This is fortuitous because it implies that processing conditions that lead to highly defective materials will lead to good catalytic properties, even though the defects initially might be far away from catalytic sites. Finally, we showed that water adsorption and proton dissociation and diffusion did not take place *at all* in the absence of subsurface oxygen vacancies. Thus, oxygen vacancies are crucial for nearly all aspects of catalysis in Au- TiO_2 materials.

A secondary project has been the analysis of strain effects in topological materials. In materials in which degeneracies are "accidental" due to band crossings but "protected" due to the symmetry of the bands, cone-like Dirac states form. Straining the materials, though, removes the symmetry protection and gaps out the band crossings. The newly gapped materials might be topologically trivial or nontrivial, depending on the relationship of the phase of the wavefunctions around a particular loop in the Brillouin zone. We have calculated the topological character of Cd_3As_2 as a function of strain and found that strain along the (110) direction significantly gaps the material, resulting in a strongly nontrivial topological materials with robustly protected, highly conductive surface states.

DoD Impact/Significance: The DoN has set a goal of 50% energy consumption from alternative sources in 2020. Catalysis, especially employing materials not containing Pt, Pd, or Rh (all of which are expensive, rare and found outside US mines), is a possible route not only to fulfill the DoN goal, but to provide greater energy security by centering the production of energy within US boundaries, using cheap materials.

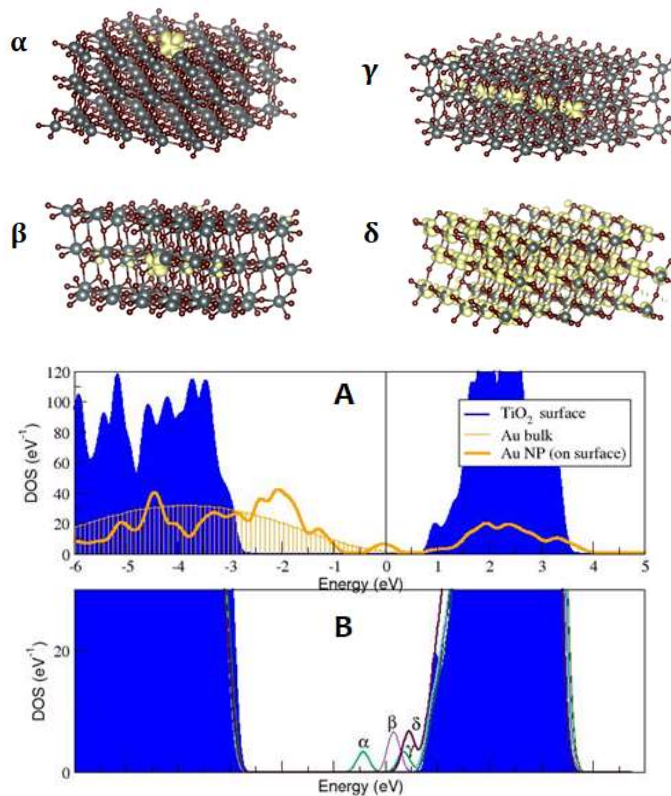


Figure 1. (*Top*) Density functional theory calculations of oxygen vacancy-generated localized electrons (polarons) at various depths (α - δ) in a TiO_2 slab. (*Bottom*) Comparison of electron energy states of an Au nanoparticle on a clean TiO_2 surface vs. in bulk (A) and electron energy states of localized defects in TiO_2 (B). Both degree of localization and depth of electron localization site affect the energy position of the defect states within the TiO_2 gap and determine the amount of hybridization that can take place.

Title: Multiple Length and Time Scale Simulations of Material Properties

Author(s): N. Bernstein

Affiliation(s): Naval Research Laboratory, Washington, DC

CTA: CCM

Computer Resources: HPE SGI 8600, SGI ICE X [AFRL, OH]; SGI ICE X [ARL, MD]

Research Objectives: To understand and predict mechanical, structural, and energetic material properties

Methodology: Molecular dynamics (MD) and Monte Carlo (MC) for the time evolution and sampling of atomic configurations. Trajectories use energies and forces from density functional theory (DFT) and interatomic potentials. Nested sampling used for calculating thermodynamic quantities and phase diagrams. Gaussian approximation potential (GAP) method for developing single- and multispecies interatomic potentials. The software implementing these methods included VASP for DFT simulations, LAMMPS for interatomic potential MD, ASE and libAtoms/QUIP for GAP development and interfacing between various programs, and pymatnest for nested sampling.

Results: The Gaussian Approximation Potential (GAP) machine-learning-based model for the potential-energy surface of silicon was used to simulate the formation of its amorphous phase from the quench of a liquid (Fig. 1). The computational efficiency of the potential made it possible to systematically vary the quench rates, and show that slower quenches lead to amorphous materials with lower defect densities and lower energies. These approach the experimental values at the slowest rate of 10^{10} K/s, showing that the method combines the efficiency and accuracy needed to describe experimentally relevant atomic structures. Further, the potential made it possible to examine individual atomic environments, and relate the local structure of defect atoms to their energy. The work on nested sampling continued with applications to different types of materials. Phase diagrams of open-network crystal structures, such as semiconductors and water, have proven unexpectedly challenging, and efforts focused on determining how to converge those simulations. Methods for multicomponent systems, including the semi-grand-canonical ensemble, made it possible to describe materials with phase-separated regions. The method was applied to a model alloy, PdAg, and is currently being prepared for publication before application to technologically relevant materials.

DoD Impact/Significance: Describing materials on the atomic scale is required for understanding their properties from microscopies, to shed light on experiments in which atomic-scale structure is not available, and to predict the behavior of new materials before they are synthesized. To enable the development of new materials for naval application, machine-learning interatomic potentials can provide accuracy comparable to state-of-the-art first principles methods, while being orders of magnitude faster, and providing local energy information that can be related to structure, unlike first-principles electronic-structure methods such as density functional theory. Amorphous silicon provides a challenging test system for the general class of amorphous materials, which have many applications, including phase-change-based nonvolatile storage and high-bandwidth switching, and is of also of inherent interest as an inexpensive solar-cell material. Most technologically relevant materials involve multiple chemical species, and as they are processed and used they experience a range of temperatures and mechanical states. Their phase diagram is therefore essential for understanding their behavior. It indicates the stability of various crystal structures and compositions, which control both bulk properties as well as microstructure such as second-phase particles that can enhance or detract from those properties. Alloys such as steels, used throughout the DoD for structural applications, are optimized by controlling this behavior, and these simulations are leading to new and robust methods for computationally designing new compositions.

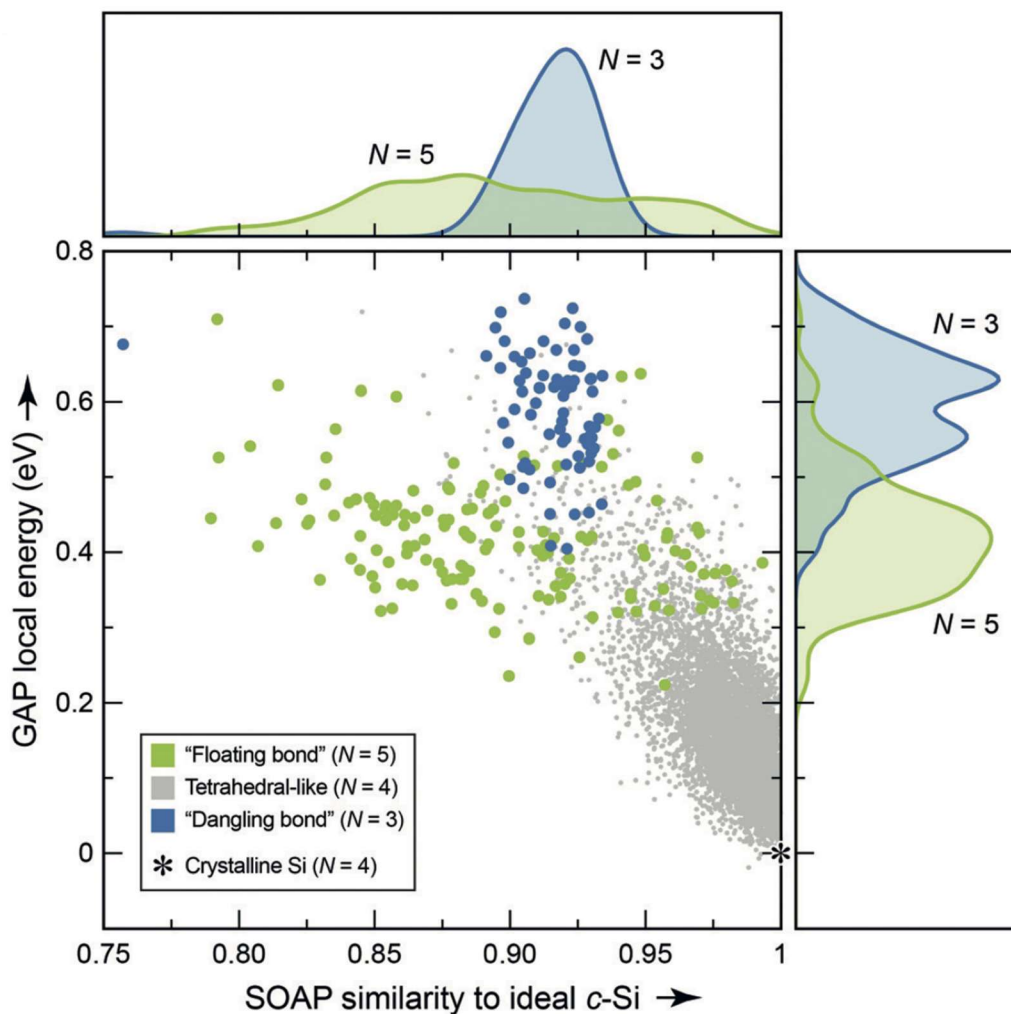


Figure 1. Distribution of local energies and atomic environments in amorphous silicon produced by quenching from the liquid at various rates. Grey dots indicate nominally non-defect (i.e. with 4 neighbors) atoms, showing a wide range of atomic energies and local structures (the ground state diamond structure is shown by an asterisk). Blue dots indicate undercoordinated (3 neighbor) atoms, which all show high energy and are all qualitatively different in local structure from the normal coordination atoms, while green dots indicate overcoordinated (5 neighbor) atoms, which overlap the distribution of local energies and structures present in normal coordination.

Title: Calculation of Materials Properties via Density Functional Theory and Its Extensions

Author(s): J.L. Lyons

Affiliation(s): Naval Research Laboratory, Washington, DC

CTA: CCM

Computer Resources: SGI ICE X [AFRL, OH]; Cray XC40 [ARL, MD]

Research Objectives: The main objective of the project is to understand the roles played by defects, dopants, and unintentional impurities in wide-band-gap semiconductor (WBGs) materials such as gallium oxide (Ga_2O_3) and novel materials such as cubic boron arsenide (c-BAs) using hybrid density functional theory (DFT) which accurately describes semiconductor defect properties.

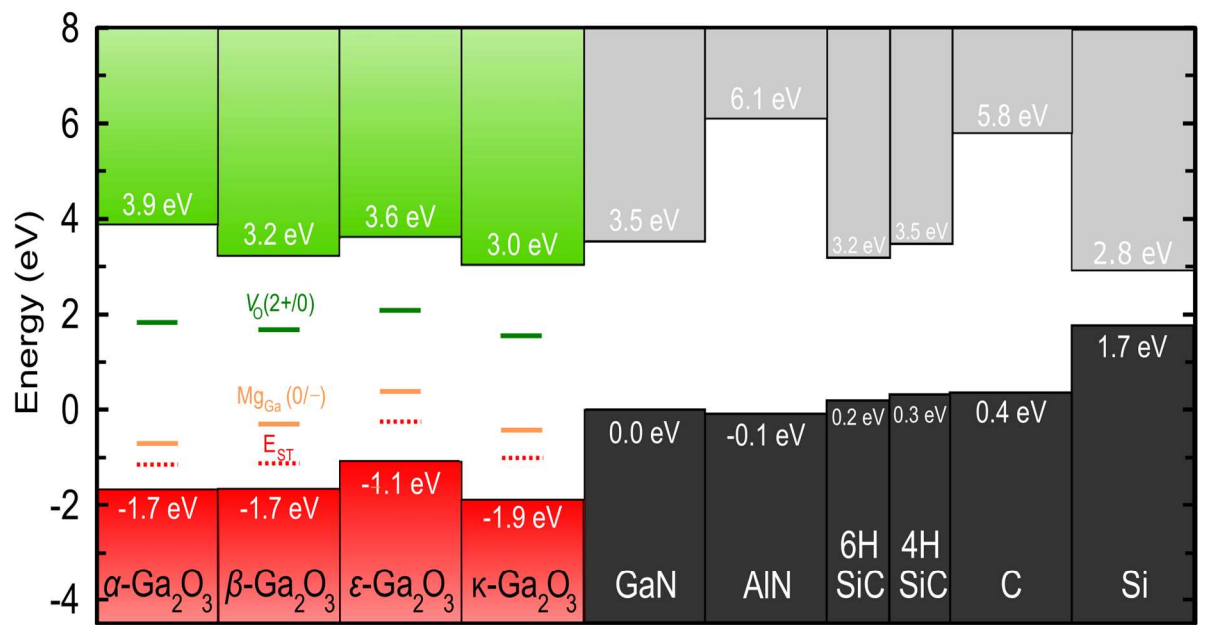
Methodology: DFT has long been a proven method for deducing semiconductor electronic structures. But when applied to WBGs, the so-called "band-gap problem" makes difficult the quantitative prediction not only of bulk band structures, but also of defect properties. To overcome these issues, we employ hybrid density functional theory. Hybrid functionals mix in a fraction of screened Hartree-Fock exchange into the exchange-correlation functional, and are capable of quantitative predictive accuracy for band gaps and defect transition levels, even in WBGs. Hybrid DFT is used to determine the charge-state transition levels, formation energies, and optical transitions associated with defects and impurities in WBGs.

Results: We investigated the band offsets of various phases of Ga_2O_3 using hybrid functional calculations and the VASP code. All phases were found to have low-lying valence bands, to exhibit spontaneous hole self-trapping, and to exhibit polaronic acceptor behavior as well as deep defect behavior for oxygen vacancies (V_o). We compared band offsets between gallium oxide and other semiconductors (such as Si, GaN, and AlN), which will be useful for future device designs (see report graphic).

All acceptor dopants in Ga_2O_3 previously have been found to be deep, but they can compensate donors and give rise to semi-insulating material, if incorporated. Using hybrid DFT, we explored the diffusivities of different acceptor dopants by calculating migration barriers and assessing diffusion pathways involving native defects. We found that Mg diffusion occurs with a low migration barrier and at low temperatures, and is assisted by gallium interstitials. In contrast, diffusion of N acceptors exhibits a much higher barrier, and occurs via an oxygen vacancy complex.

We also investigated sources of the unintentional *p-type* conductivity in the ultrahigh-thermal-conductivity c-BAs. Our results indicate that native defects, which are often invoked to explain this conductivity, are either deep acceptors or are high in energy. Our calculations instead point to impurities such as C and Si as likely sources of hole conductivity. We find these impurities incorporate into c-BAs as shallow acceptors with low formation energies, indicating that they can be expected to incorporate into this material and give rise to free hole concentrations.

DoD Impact/Significance: WBGs such as Ga_2O_3 are utilized in power electronics, which play a crucial role in many Navy-relevant applications, and afford significant SWAP-C savings when replacing components based on traditional semiconductor materials. Novel thermal conducting materials such as c-BAs can be incorporated into existing devices and afford significant gains in energy efficiency. Optimizing doping, understanding contaminants, and characterizing unintentionally incorporated defects are crucial steps for improving such materials.



Band offsets of Ga₂O₃ phases with other semiconductors. All band energies are referenced to the valence-band maximum of GaN (at 0 eV). Hole self-trapping energies (E_{ST}) are indicated with red dotted lines, Mg acceptor transition levels with orange lines, and oxygen vacancy donor transition levels with green lines.

Title: IR Absorption Spectra for Nerve Agent-Sorbent Binding Using Density Functional Theory

Author(s): S. Lambrakos, A. Shabaev, and Y. Kim

Affiliation(s): Naval Research Laboratory, Washington, DC

CTA: CCM

Computer Resources: Cray XC40/50 [ERDC, MS]

Research Objectives: Calculation of IR Absorption Spectra for molecular complexes of sorbent materials and a nerve agent simulant using Density Functional Theory.

Methodology: The present study examines calculation of IR spectra for custom sorbent materials, the nerve agent simulant dimethyl methylphosphonate (DMMP) and sorbent-DMMP molecular complexes using quantum-theory based calculations, i.e., density functional theory (DFT) and associated software technology, which provide complementary information to that obtained from spectroscopic measurements. This complementary information is both spectral features and their physical interpretation with respect to molecular structure, and thus prediction of spectral features that are difficult to measure in the laboratory. The present study adopts the software GAUSSIAN16 (G16) for the calculation of IR absorption spectra.

Results: The results of our study are relaxed or equilibrium configurations of the sorbent molecule based on a fluorinated bisphenol AF (o1eBPAF), nerve-agent simulant DMMP and the o1eBPAF-DMMP complex, ground-state oscillation frequencies and associated IR intensities for molecular geometries having stable structures, which are calculated by DFT [1,2]. A graphical representation of the molecular geometry of an o1eBPAF-DMMP complex is shown in Fig.1. DFT calculated IR intensities as a function of frequency for an isolated molecule of o1eBPAF and o1eBPAF-DMMP complex are shown in Fig. 2. As shown, there are two resonances near 3700 cm^{-1} , which are essentially degenerate. These two resonances correspond to two OH sites of the o1eBPAF molecule. In the spectrum of o1eBPAF-DMMP complex, one of these frequencies is about 300 cm^{-1} lower than the free OH resonance. This frequency corresponds to the OH site, which forms the hydrogen bond with the DMMP molecule. The other OH site remains free and its frequency is practically unchanged by hydrogen bonding with DMMP on the other side of o1eBPAF molecule, which is separated by a relatively large sorbent molecule.

DoD Impact/Significance: The properties of molecular complexes associated with nerve agent-sorbent binding are of major importance for detection of nerve agents using methods based on IR spectroscopy. Interpretation of predicted IR spectra using DFT should be more appropriate in terms of correlation between measured and calculated spectral features, rather than fingerprint-type matching of spectra. This follows, in that vibrational analyses using DFT are associated with zero, rather than finite, temperatures, and specific intermolecular configurations, rather than ensembles representing physically consistent samplings of phase space. Absorption spectra of relatively small molecular clusters represents a separate regime for dielectric response with respect to electromagnetic wave excitation.

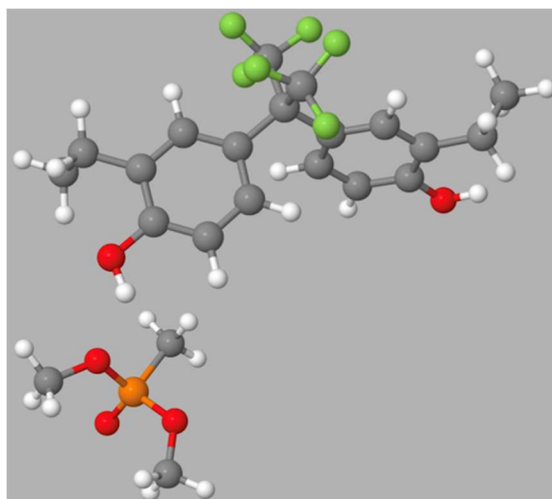


Figure 1. Graphical representation of molecular geometry for o1eBPAF-DMMP complex.

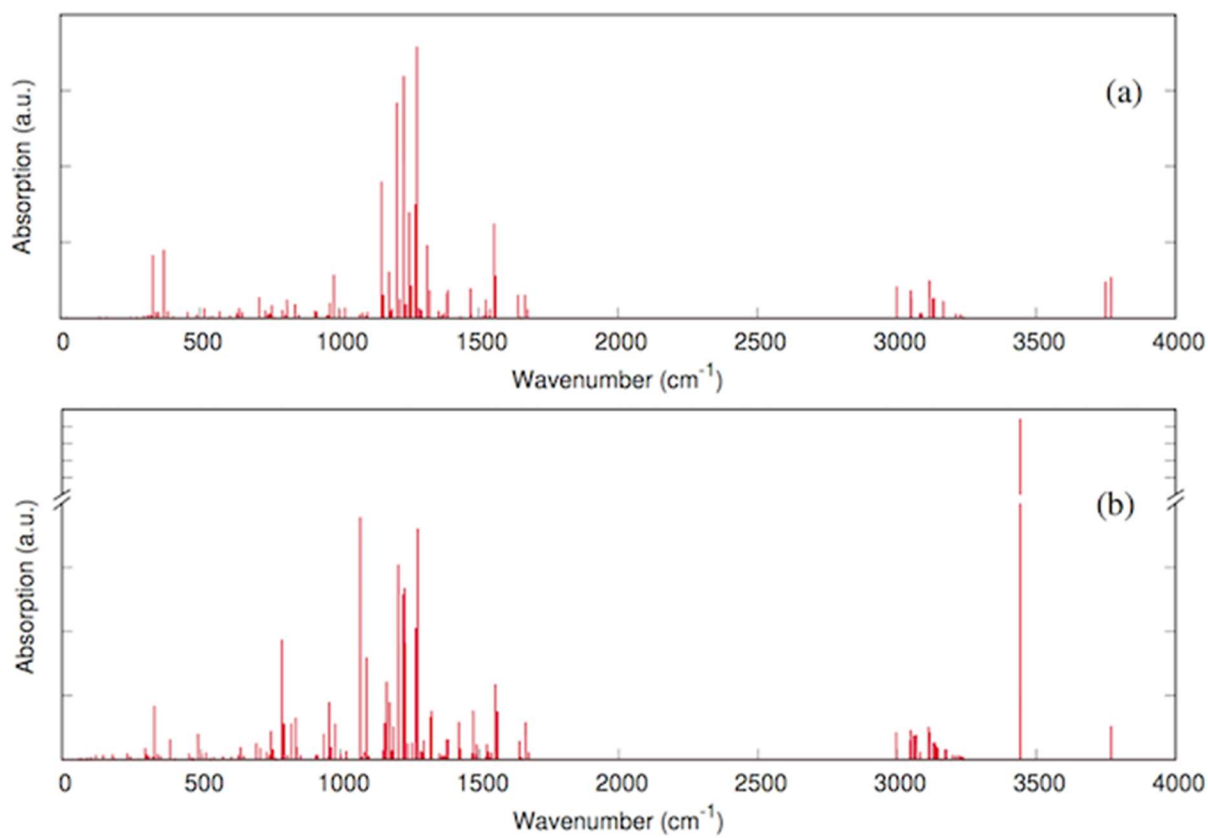


Figure 2. Comparison of DFT calculated absorption-spectrum resonances for (a) o1eBPAF and (b) o1eBPAF-DMMP complex.

Title: Numerical Studies of Semiconductor Nanostructures

Author(s): T.L. Reinecke¹ and S. Mukhopadhyay²

Affiliation(s): ¹Naval Research Laboratory, Washington, DC; ²National Research Council Postdoctoral Program, Washington, DC

CTA: CCM

Computer Resources: HPE SGI 8600, SGI ICE X [AFRL, OH]; Cray XE6m, Cray XC40/50 [ERDC, MS]

Research Objectives: To calculate the structures and the electronic properties of layered nanomaterials, to guide their chemical functionalizations, and to advance their use as chemical sensors and in advanced electronics. To make first-principles calculations of the thermal properties of semiconductors as a bases for new high-thermal-conductivity materials for cooling electronics and low-thermal-conductivity materials for high-efficiency thermoelectrics. To calculate the electronic and optical properties of solid-state quantum bit systems to advance their implementations in quantum information technologies.

Methodology: *Ab initio* density functional calculations are made of the structural and electronic properties of layered nanomaterials and their surface chemical functionalizations. *Ab initio* density functional methods are used to calculate the phonon frequencies and wavefunctions and the interactions between phonons in semiconductors and in semiconductor nanostructures, and inelastic Boltzmann equation methods are used to calculate their thermal conductivities. Electronic calculations are made using Quantum Espresso and VASP codes. The optical properties of quantum dots and other solid-state systems of interest in quantum information technologies are calculated using density functional theory, finite element techniques, and diagonalization of large matrices.

Results:

1. Surface phonon polaritons enhance light-matter interactions and the optical properties of materials of interest in IR nanophotonics, for high-resolution imaging and sensing. Most bulk materials have only narrow reststrahlen regions to support surface polaritons. Superlattices provide an opportunity to design materials with desirable optical properties. First-principles calculations have predicted materials and structures of interest, and experimental results are in agreement with calculations for the optical properties for AlN/GaN superlattices.
2. Quantum information has opened new opportunities in range of technologies, including quantum sensing, computing, and navigation. High-quality interfaces between spin qubits in solids and photons are central to many of these technologies. We have calculated the full time-dependent optical properties of Si vacancy qubits in SiC and have designed protocols for high-quality spin-photon interfaces with them.
3. New materials with high electrical conductivities and low thermal conductivities are needed for high-efficiency thermoelectrics in cooling and power generation. In recent work, we have made calculations for a range of new materials based on Tl_3VSe_4 and In_3VSe_4 . Exceptionally low thermal conductivities have been found in them and traced to their weak Tl and In bonding. The results agree with available experimental data, and these materials provide opportunities as high-efficiency thermoelectrics.

DoD Impact/Significance: Chemical functionalization of monolayer systems will open opportunities to control their properties for use in electronics and as chemical and biological sensors. New high-thermal-conductivity materials and systems make possible their exploitation in thermal management and in thermoelectrics. Understanding the role of interactions and couplings between quantum bits in solid systems opens opportunities to develop fast optical quantum technologies based on them.

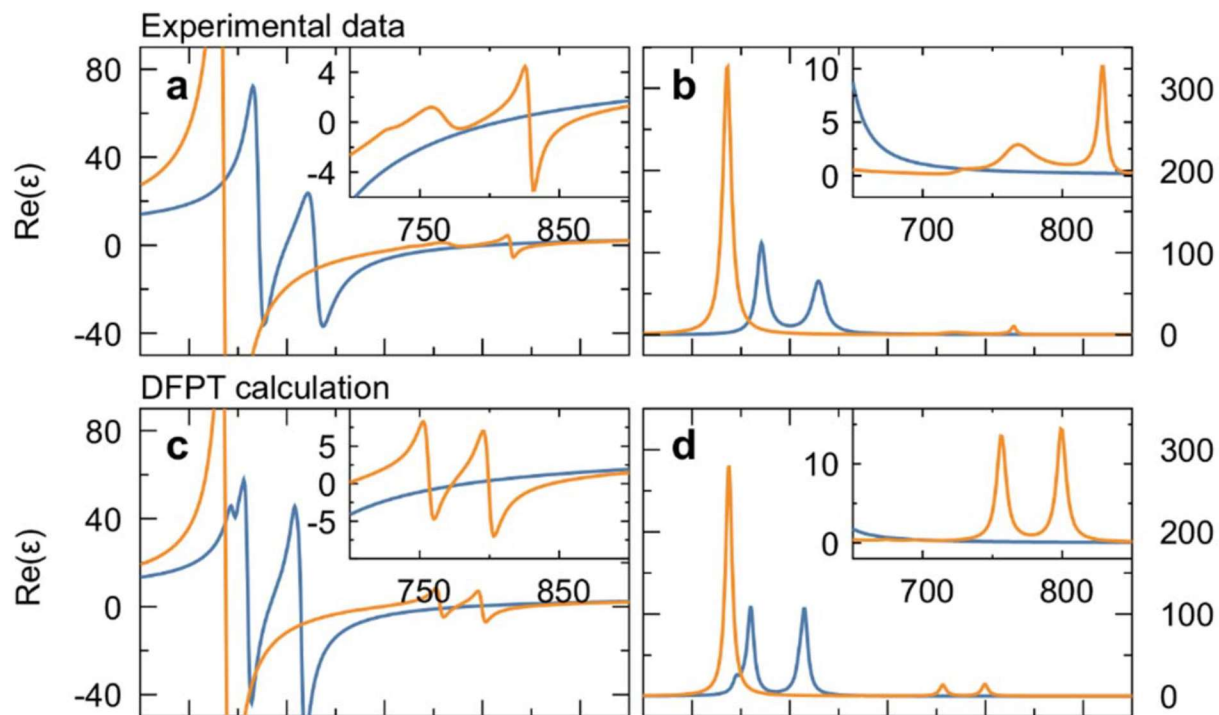


Figure 1. Calculated and measured, real (left) and imaginary (right), parts of dielectric function of the atomic-scale AlN/GaN superlattices.

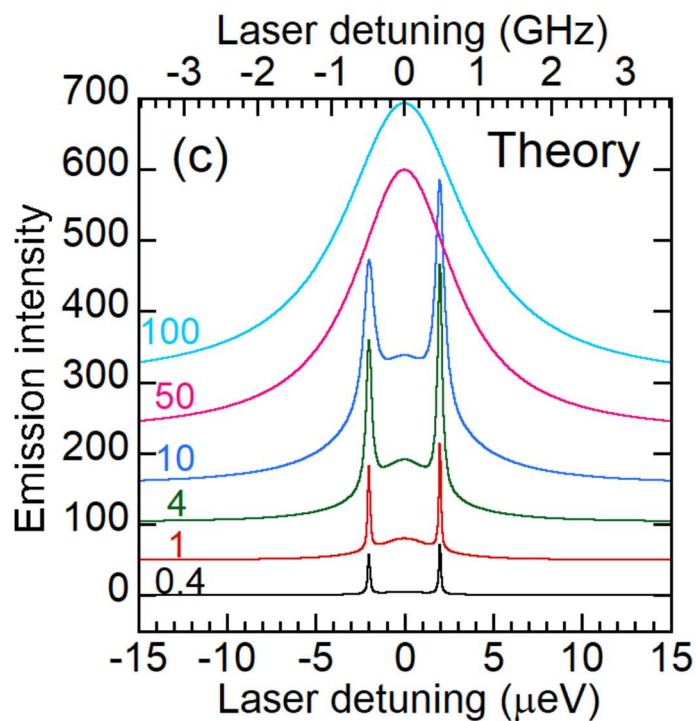


Figure 2. Calculated optical emission intensity from negatively charged Si vacancy qubit in 4H SiC for spin-photon interfaces.

THIS PAGE INTENTIONALLY LEFT BLANK



Computational Electromagnetics and Acoustics

CEA covers two primary computational disciplines. Computational Electromagnetics covers the high-resolution multidimensional solutions of Maxwell's equations. DoD applications include calculating radiofrequency (RF) sensor performance, radar scattering of tactical ground, air, and sea vehicles, the electromagnetic signature of buried munitions, high-power microwave performance, as well as the interdisciplinary applications in magnetohydrodynamics and laser systems. The Computational Acoustics area covers the high-resolution multidimensional solutions of the acoustic wave equations in solids and fluids. DoD applications include the modeling of acoustic fields for surveillance and communication, seismic fields for mine detection, and the acoustic shock waves of explosions for antipersonnel weapons.

Title: Flowfield and Transport Models for Navy Applications
Author(s): W.G. Szymczak, A.J. Romano, and S. Dey
Affiliation(s): Naval Research Laboratory, Washington, DC
CTA: CEA

Computer Resources: SGI ICE X [AFRL, OH]; SGI ICE X [ERDC, MS]

Research Objectives: Provide resources for computational fluid dynamics simulations, as well as optimization and inverse problems, supporting a variety of Navy applications. Examples include flow through acoustic sensors, flow and transport over passive filter shelters, and the extraction of anisotropic stiffness coefficients of white matter in brains of both healthy controls and patients with mild to severe traumatic brain injury (TBI).

Methodology: The extraction of stiffness parameters using wave guide elastography (WGE) was performed using a mixed model inversion (MMI) algorithm to treat both the anisotropic and isotropic regions within a human brain. WGE utilizes magnetic resonance elastography (MRE) and diffusion tensor imaging (DTI) measurements processed with an orthotropic anisotropic inversion algorithm. Within the anisotropic white matter regions, the orthotropic inversion provides nine independent stiffness coefficients including the three longitudinal terms C_{11} , C_{22} , C_{33} , three shear coefficients C_{44} , C_{55} , C_{66} , and three off-diagonal stiffness terms C_{12} , C_{13} , C_{23} . The algorithm was implemented using message passage interface (MPI) directives with work balancing based on the ratios of isotropic to non-isotropic voxels being sent to each processor. A surrogate finite element model with a simple anisotropic structure was also constructed using the STARS3D code. Results from this model are being used to provide an equivalent MRE displacement file, thereby providing a validation test for the inversion.

Results: The WGE-MMI code was run using 1152 cores (32 nodes with 36 cores per node) reducing the execution time from 48 hours (using a single node with 36 threads) to less than 15 minutes. In FY19, we used the stiffness results from 22 white matter structures as features for comparison between sets of healthy controls and TBI patients using datasets provided by the Mayo Clinic in Rochester, MN, Washington University in St. Louis, and Charité-Universitätsmedizin in Berlin. Orientation maps for the white matter structures within one of the healthy control brains are shown in Fig. 1. A comparison of mean shear stiffness values of the healthy controls to the TBI patients across 22 white matter segments are shown in Fig. 2.

DoD Impact/Significance: The WGE-MMI provide a unique capability in extracting anisotropic stiffness values of white matter structures. These values, within different segmented brain structures, provide features that currently are being prepared for machine-learning algorithms to distinguish between healthy controls and TBI patients. Thus, it has the potential to be used as a noninvasive test for diagnosing conditions of warfighters exposed to blunt, ballistic, or blast impacts.

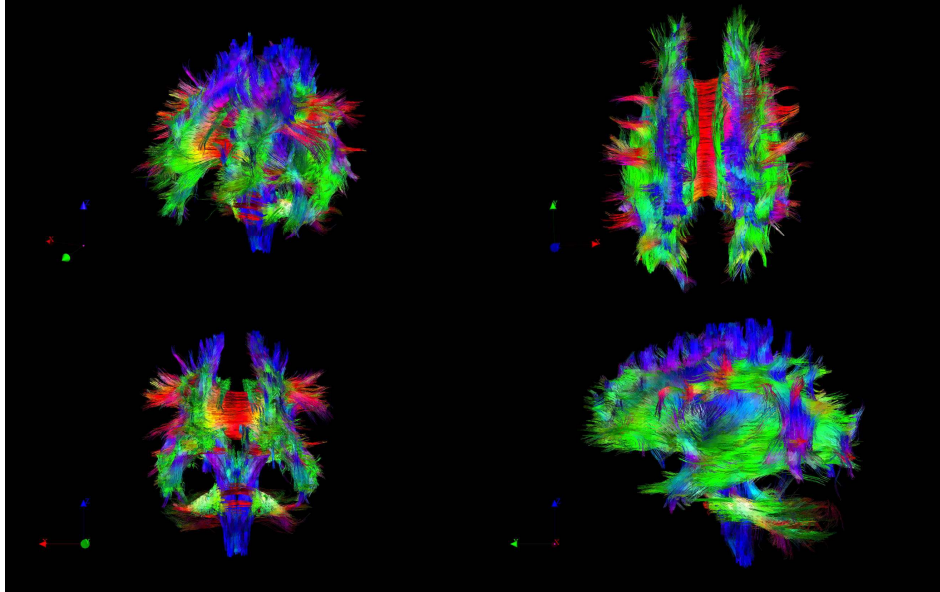


Figure 1. Different views of orientation maps for white matter pathways in a healthy brain.

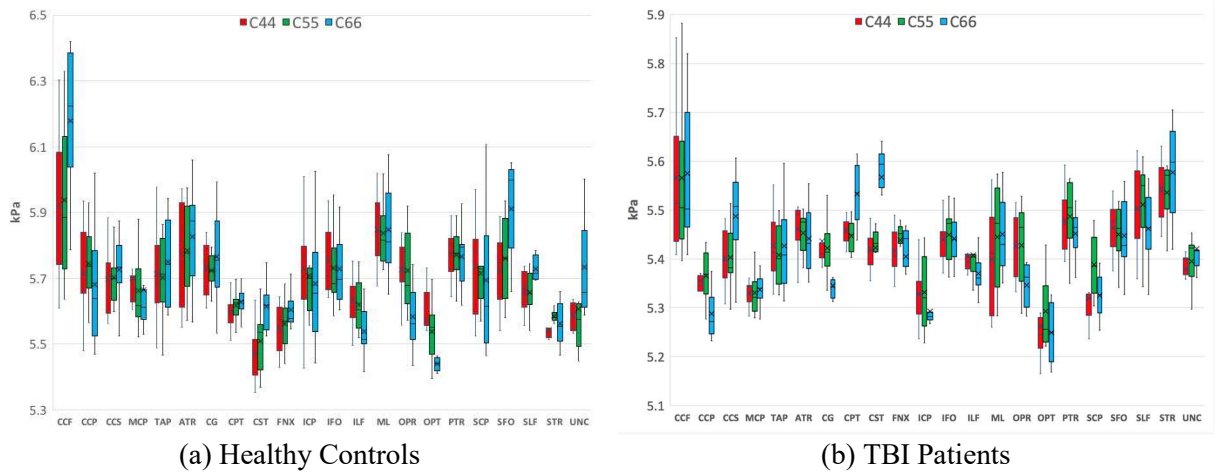


Figure 2. Comparisons of anisotropic shear stiffness values in different white matter segments for healthy controls and TBI patients.

Title: Small Slope Approximation (SSA) Rough-Surface Backscattering Analysis

Author(s): J. Alatishe

Affiliation(s): Naval Research Laboratory Washington, DC

CTA: CEA

Computer Resources: SGI ICE X [ARL, MD]

Research Objectives: To determine and characterize the spatial coherence effects inherent in sea clutter by numerically analyzing the associated response at the antenna port of a monostatic radar. The sea surface coherence effects are examined with respect to the associated antenna characteristics and the surface properties.

Methodology: The surface model used is based on a simple periodic surface representing the gravitational component of the ocean surface: a notional sea surface. Once the response from the surface has been computed, the properties of the simulated sea clutter responses are characterized. The surface scattering amplitude (SA) characterizes the spatial coherence. A version of the small-slope approximation (SSA), which approximates the induced field distribution on the sea surface, is employed in the SA. Once the SA has been computed, the response at the antenna port is determined and the coherence effects due to the surface are examined. Numerical integration is used to determine the antenna response from the rough-surface profile. The notional sea surface is derived from a sinusoidal surface using as surface parameters the significant wave height, gravitational wave period, and wavelength, all based on the Pierson-Moskowitz ocean wave-number spectrum for wind speeds at 5 and 10 m/s for an upwind direction. With both the SA and the surface model calculated, the response at the antenna port was computed for each antenna aspect angle. The codes used to execute these steps first were written in MATLAB and then were converted into FORTRAN 90. The codes then were parallelized using the message-passing interface and were run on 1024 processors or up to 32 graphics processing units (GPUs) at the Naval Research Laboratory (NRL) high-performance computing facility. Simulations were conducted at X-band (10 GHz).

Results: Data obtained from published accounts of the simulated response from a sinusoidal surface were used as the baseline for comparison. These sea clutter values were measured at various phase speeds and wind directions for given antenna aspect angles (elevation and azimuth) and polarizations of the antennas. The simulated received sea clutter responses were computed for elevation angles of 65° and 75° for both vertical and horizontal polarizations. The simulation generated a 2048-point frequency response of the notional sea surface for a given wind speed for an observed time increment. Fast Fourier transform convolution was used to generate the complex time-dependent echo, which is the spectral product of the associated sea surface frequency response and the transmitted waveform. As a result of the previous step, multiple coherent processing intervals were generated for analysis as depicted in Fig. 1. The number of spatial samples of the sea surface was set to 8,191 in the down-range, and 8,191 in the cross-range dimensions. The simulation results showed that the range-Doppler properties are similar to real-sea clutter in that the single rough scale of the notional sea surface is represented by the correct frequency offset (no mean current) and spectral structure (see Fig. 2). In addition, some clutter phenomena present in the simulated data and the statistics of the clutter appear to give insight into understanding real-sea clutter data. Further investigation of the simulated data is still required.

DoD Impact/Significance: Understanding the spatial coherence effects in radar sea clutter provides further insight into the phenomenology of backscattering from the ocean. This will be useful in devising new algorithms for detecting threats over the sea.

Example results:

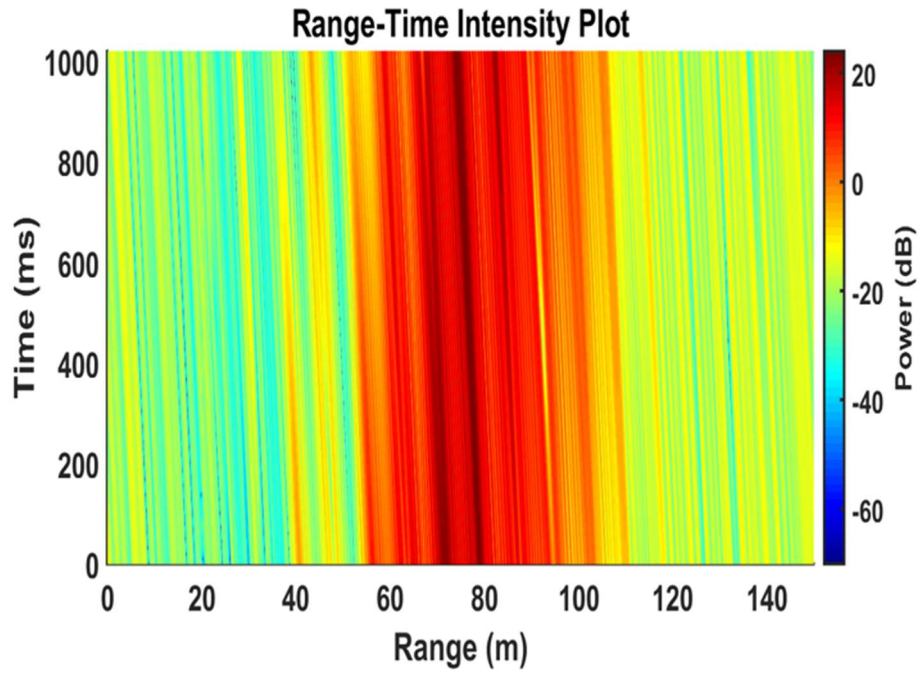


Figure 1. Range-time intensity plot of X-band sea clutter returns for VV polarization at 75° elevation. Pulsewidth is 2 ns, pulse repetition interval (PRI) is 2 ms, and wind speed is 5 m/s toward the radar.

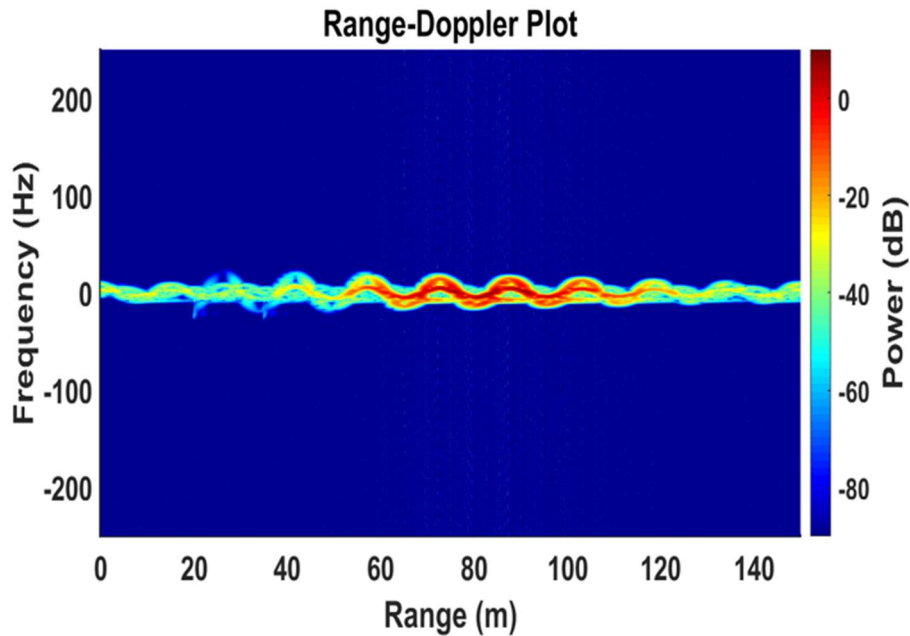


Figure 2. Range-Doppler plot of X-band sea clutter returns for VV polarization at 75° elevation. Pulsewidth is 2 ns, PRI is 2 ms, and wind speed is 5 m/s toward the radar.

Title: Diffusive Wave Spectroscopy of Underwater Sound
Author(s): D. Photiadis and N. Valdivia
Affiliation(s): Naval Research Laboratory, Washington, DC
CTA: CEA

Computer Resources: SGI ICE X [AFRL, OH]

Research Objectives: Develop forward numerical simulation models in disordered, acoustic media that can be used to test and further develop diffusive wave based detection algorithms.

Methodology: Effective multipole expansion method for the prediction of the late-time response in a medium with random disorder.

Results: The straightforward simulation of diffusive-wave algorithms fails because the required medium size, determined by the mean free path of the random medium, is too large. In the current year, simulations based on an effective multipole expansion for randomness described by point scatterers were carried out. The matrix equations that result from the multipole expansion have some specific properties of random matrix theory that we can take advantage for their numerical solution. The resultant eigenvalues are clustered around a specific circular area in the complex plane, which means that the majority of the spectrum can be solved using Krylov subspace approximations. Indeed, we discover that the solution of the matrix system can be successfully approximated using a few conjugate gradient iterations. This means that this approach is useful for smaller problems of Navy interest with current high-performance computing resources.

DoD Impact/Significance: The simulation results testing the diffusive wave algorithm discussed above are the first such reported numerical simulations.

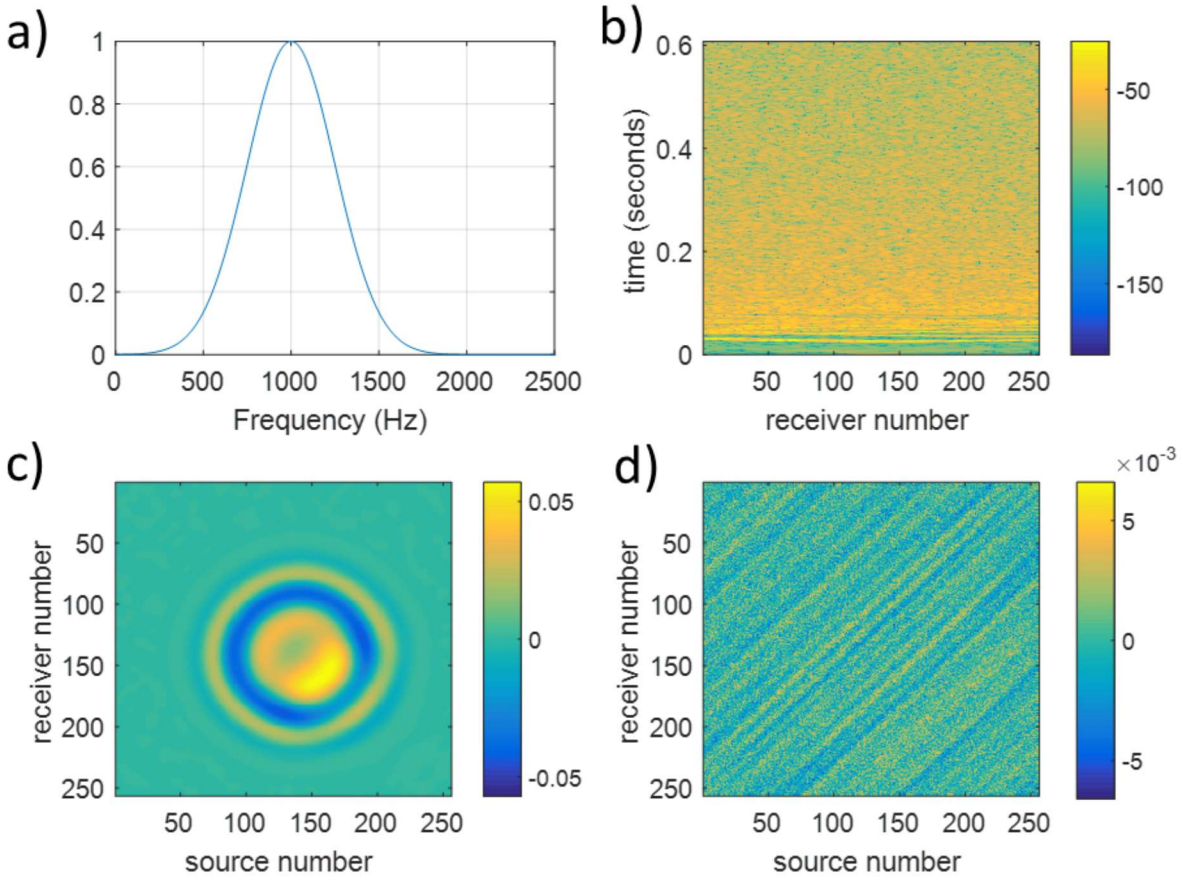


Figure 1. Resultant scattering matrix G_{pq} , $p, q = 1, \dots, 256$ for mean free path of 150m that results from a Gaussian pulse: a) Gauss pulse density function, b) view of the scattering matrix at fixed source $q = 128$, c) image of scattering matrix at $t=0.023$ (single scattering contribution is dominant) and d) image of scattering matrix at $t=0.324$ (multiple scattering occurs).

Title: Intense Laser Physics and Advanced Radiation Sources

Author(s): D.F. Gordon¹, J. Penano¹, L. Johnson¹, J. Isaacs¹, D. Kaganovich¹, B. Hafizi¹, and A. Davidson²

Affiliation(s): ¹Naval Research Laboratory, Washington, DC; ²National Research Council Research Associateship Program (RAP) Postdoctoral Program, Washington, DC

CTA: CEA

Computer Resources: HPE SGI 8600, SGI ICE X [AFRL, OH]; Cray XC40 [ARL, MD]; Cray XC40/50 [ERDC, MS]

Research Objectives: The primary objectives of this program are to model the propagation of intense, short-pulse lasers in plasmas and other nonlinear media, and to provide computational support for experiments on the NRL MATRIX laser. Current areas of research include nonlinear laser propagation, plasma-based accelerators, novel sources of short-pulse infrared radiation, and ultra-high-field physics.

Methodology: High-performance computing resources are utilized using several codes. turboWAVE is an object-oriented framework that contains modules designed to solve a variety of problems. Both fully explicit and ponderomotive guiding center particle-in-cell modules are used to model relativistically intense laser pulses propagating in plasmas (Figure 1). Quantum optics modules are used to describe the interaction of the laser pulse with atoms or ions. Fluid modules (SPARC) are used to describe hypersonic flow and shock propagation in gas targets. Optimization for the latest computer architectures requires exploiting three levels of hardware parallelism: vector arithmetic units, shared memory threads, and distributed memory processes. The framework universally supports all of these using a combination of OpenMP directives for vector and loop parallelism, and the message passing interface (MPI) for distributed processes. Some modules support general-purpose graphical processing units via OpenCL.

HELCAP solves a paraxial wave equation with a large number of source terms representing atmospheric turbulence, dispersion, and various nonlinear processes. HELCAP simulates the propagation of short-pulse and high-energy laser pulses, including adaptive optics. It is often useful to run a large statistical ensemble of initial conditions. For this purpose, embarrassingly parallel methodology is effective.

Results: We made improvements to the ponderomotive guiding center algorithm in turboWAVE that allow for rapid modeling of multipetawatt laser-plasma interactions in which electrons are expected to be accelerated to about 10 gigavolts. The model is efficient enough to be scripted so that two-dimensional parameter scans can be carried out with independent models running on each of several hundred nodes. Within a node, hybrid MPI-OpenMP are used to parallelize each job. This allows the effect of plasma parameters and focusing conditions on the electron beam quality to be studied in more detail than ever before.

DoD Impact/Significance: Laser propagation in turbulent atmospheres is relevant for directed energy. High-power pulsed sources of long wavelength radiation may also be relevant for directed energy. Laser-driven accelerators and radiation sources have potential applications for ultrafast (femtosecond) imaging of chemical and biological systems. High-energy electron beams might be useful as gamma ray sources for detection of special nuclear materials (SNM). High-energy ions might also be useful for SNM detection or for cancer therapy.

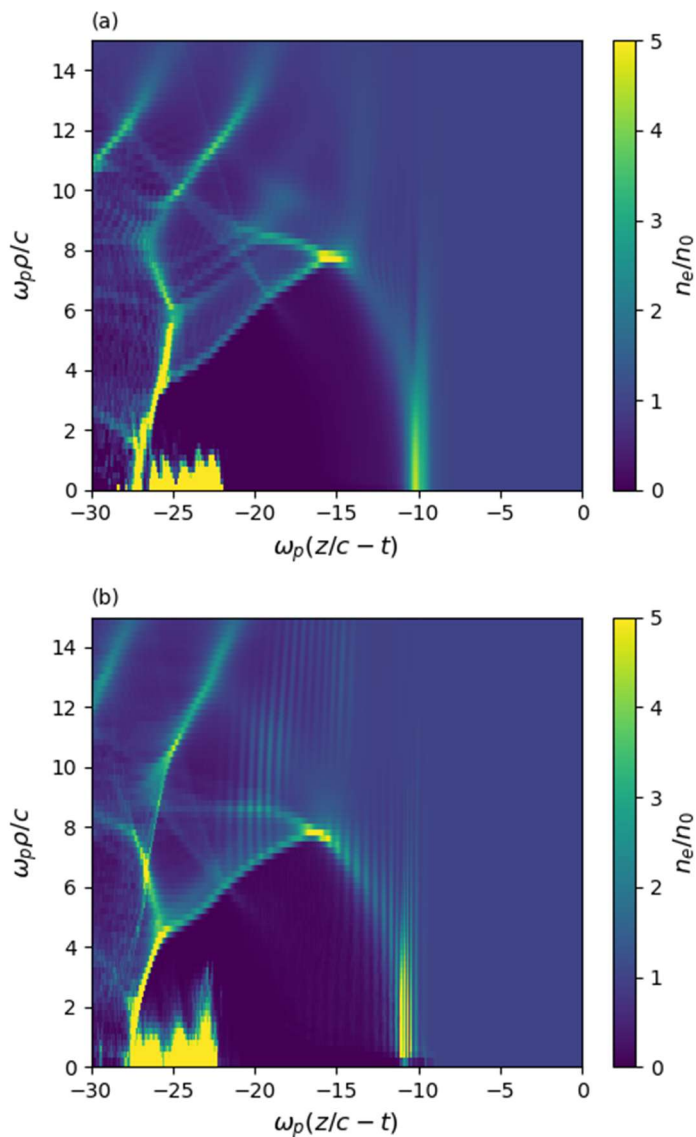


Figure 1. Comparison of (a) turboWAVE ponderomotive guiding center model and (b) OSIRIS fully explicit quasi-3D model. The color scale represents the electron density in a strongly driven laser plasma. The turboWAVE case runs in about 10 core-hours, while the OSIRIS case takes about 1,500. The efficiency of the turboWAVE model allows dense parameter scans to be carried out, which are useful in understanding near-term experiments that will be performed at the Extreme Light Infrastructure.

Title: Low-Grazing Angle Radar Backscatter
Author(s): J.V. Toporkov, J.D. Ouellette, and M.A. Sletten
Affiliation(s): Naval Research Laboratory, Washington, DC
CTA: CEA

Computer Resources: Cray XC40 [ARL, MD]; Cray XC40/50 [ERDC, MS]

Research Objectives: Coastal, shipborne, and airborne radar systems routinely encounter signal reflections from sea surface, often under low-grazing-angle (LGA) conditions. This surface signature is frequently regarded as clutter that masks target echoes, yet it can also be a source of information about local ocean conditions. Understanding the properties of sea backscatter and how they depend on the environmental parameters, as well as identifying their distinctions from those of man-made target echoes, is key to improving or even enabling performance of such radar systems and applications. This project investigates detailed characteristics of radar returns from ocean surface under both monostatic and bistatic observation geometries.

Methodology: The approach combines a physics-based model for evolving ocean surface with computationally efficient, exact evaluation of the scattered electromagnetic field. A wind-driven surface is represented by realizations of a Gaussian random process defined by the Elfouhaily wave spectrum. Interactions between surface harmonics affecting shape and motion of smaller ripples (that have great impact on scattering of decimeter- and centimeter-scale electromagnetic waves) are modeled by the Creamer transformation applied to a Gaussian realization. The electromagnetic field scattered by a “time-frozen” scene at a particular frequency is found by iteratively solving a boundary integral equation for the induced surface current. The formulation is based on first principles and automatically accounts for many phenomena (multiple scattering, shadowing) known to be problematic for analytical treatment. The calculations can be conducted at a number of frequencies covering certain bands to simulate pulse scattering. The procedure is repeated for every surface profile in the sequence representing temporal evolution. The simulations are limited to the two-dimensional (2D) space but have direct relevance to commonly occurring three-dimensional (3D) geometries (e.g. oncoming or receding long-crested waves).

Results: To help determine feasibility of passive remote sensing of a sea state utilizing illumination from geostationary communications satellites, time-varying simulations were performed for continuous-wave, time-harmonic S-band signals with vertical (VV) and horizontal (HH) polarizations. The employed bistatic setup is shown in Fig. 1. Consistent with the anticipated satellite position, the incidence angle was set to 45° . All scattering directions within the upper half-space were considered, although low grazing angles near $\theta_s = \pm 80^\circ$ could be of most practical interest. Average Doppler spectra such as those shown in Fig. 2 were obtained from a Monte Carlo ensemble of 2000 simulated 5-second data records. The angular behavior of the first two moments of the Doppler spectra and their sensitivity to wind speed are explored in Fig. 3. The performance of the two popular approximate scattering approaches, the 2nd-order Small Slope Approximation (SSA2) and the Coherent Two-Scale Model (CTSM), was evaluated against the exact simulations data, cf. Fig. 4. Several values for the scale separation length (that is inherent to the CTSM but is not firmly defined) were investigated. The choice of the reliable approximate model will be important for full 3-D scattering studies where costs of the exact solution may be prohibitive.

DoD Impact/Significance: More comprehensive and detailed characterization of sea clutter will help in design and performance assessment of the Navy radar systems operating in LGA regime. Bistatic configurations provide covertness for a passive receiver asset and could yield further performance enhancements due to peculiar scattering characteristics of surface and targets that do not emerge in the conventional monostatic case.

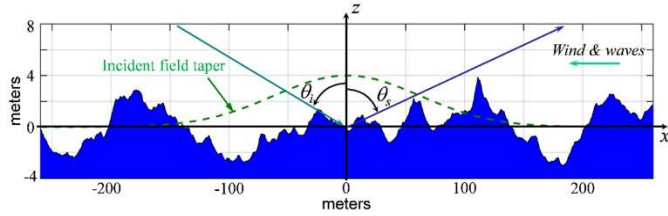


Figure 1. Setup for bistatic scattering simulations from evolving sea surface. All calculations are conducted at S band (2.3 GHz), with the incidence angle θ_i set to 45° , while averaging over 2000 realizations.

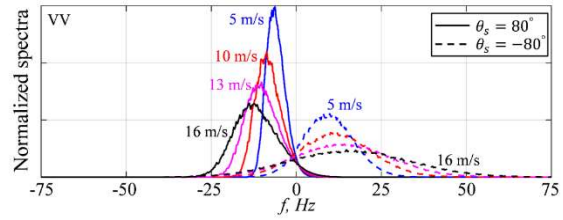


Figure 2. Simulated Doppler spectra at vertical polarization for near-grazing scattering directions in forward (positive θ_s) and backward half-planes. Wind speed is 13 m/s.

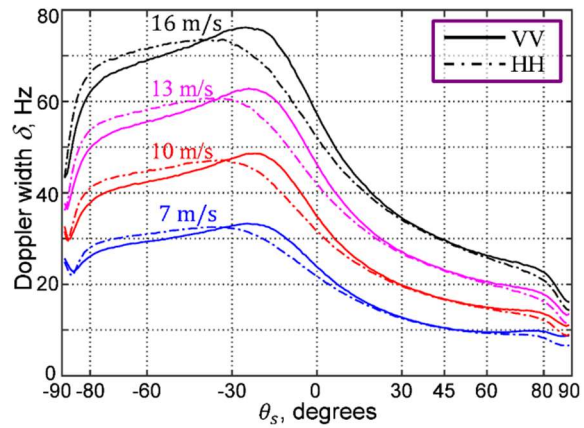
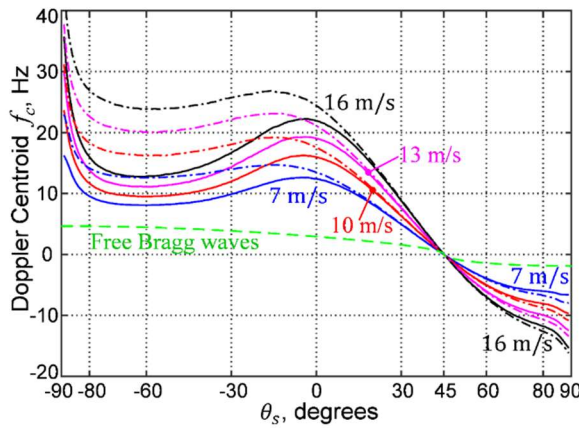


Figure 3. Centroids (shifts) and widths of Doppler spectra obtained using the exact numerical solution for different wind speeds. Extra vertical grid lines highlight forward scattering direction $\theta_s = 45^\circ$ as well as the near-grazing scattering angles $\theta_s = \pm 80^\circ$ considered in Fig. 2.

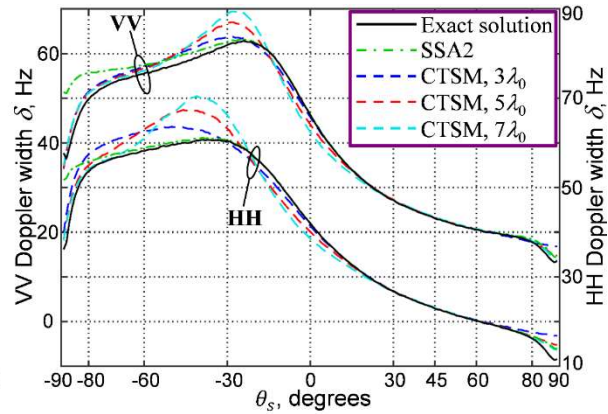
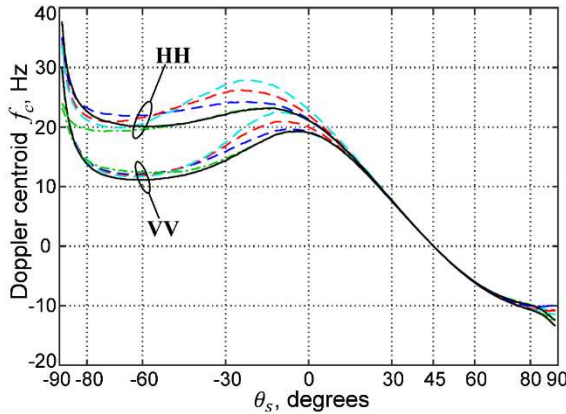


Figure 4. Centroids (shifts) and widths of Doppler spectra simulated using exact numerical solution and approximate scattering models (several scale-separation values in terms of the carrier wavelength $\lambda_0 = 13$ cm are considered for the CTSM). Wind speed is 13 m/s, and the same set of 2000 surface realizations is used in all cases. In the Doppler widths panel, axis labels on the right refer to the HH curves.

Title: Structural-Acoustic Response of Stiffened Elastic Cylindrical Shell

Author(s): S. Dey¹, E.L. Mestreau², R.M. Aubry², M. Williamschen², and D. Williams²

Affiliation(s): ¹Naval Research Laboratory, Washington, DC; ²KeyW Corp., Hanover, MD
CTA CEA

Computer Resources: Cray XC40 [ARL, MD]; SGI ICE X [ERDC, MS]

Research Objectives: Develop and validate the acoustic-scattering response of a parametric model for a stiffened elastic cylindrical shell.

Methodology: We utilized a high-order hp-infinite and infinite element based solver (STARS3D) developed at NRL for solving the coupled elasto-acoustics problem. This enables highly accurate solution of the scattering response up to the midfrequency regime. Use of fully three-dimensional elasticity in modeling the structure requires accurate geometric representation of the stiffened shell. In this effort, we used cubic ($p = 3$) basis functions, which require accurate representation of mesh geometry. Both of these requirements were met by using the DoD HPCMP-CREATE(TM) Capstone platform for geometry and mesh generation, also developed by a team based at NRL. We have used a feature-based scripting approach to fully automate the generation of parametric structural geometry and mesh.

Results: We computed the scattering response for the structure in both monostatic and bistatic configurations for frequencies in the range [1kHz, 50kHz]. The computed scattering response, shown in Fig. 1, was compared and validated against experimental data.

DoD Impact/Significance: Parametric models like the one developed in this effort help improve the understanding of structure-acoustic response of complex elastic structure and its sensitivity to various design parameters. This is critical to the development of better undersea-warfare technologies.

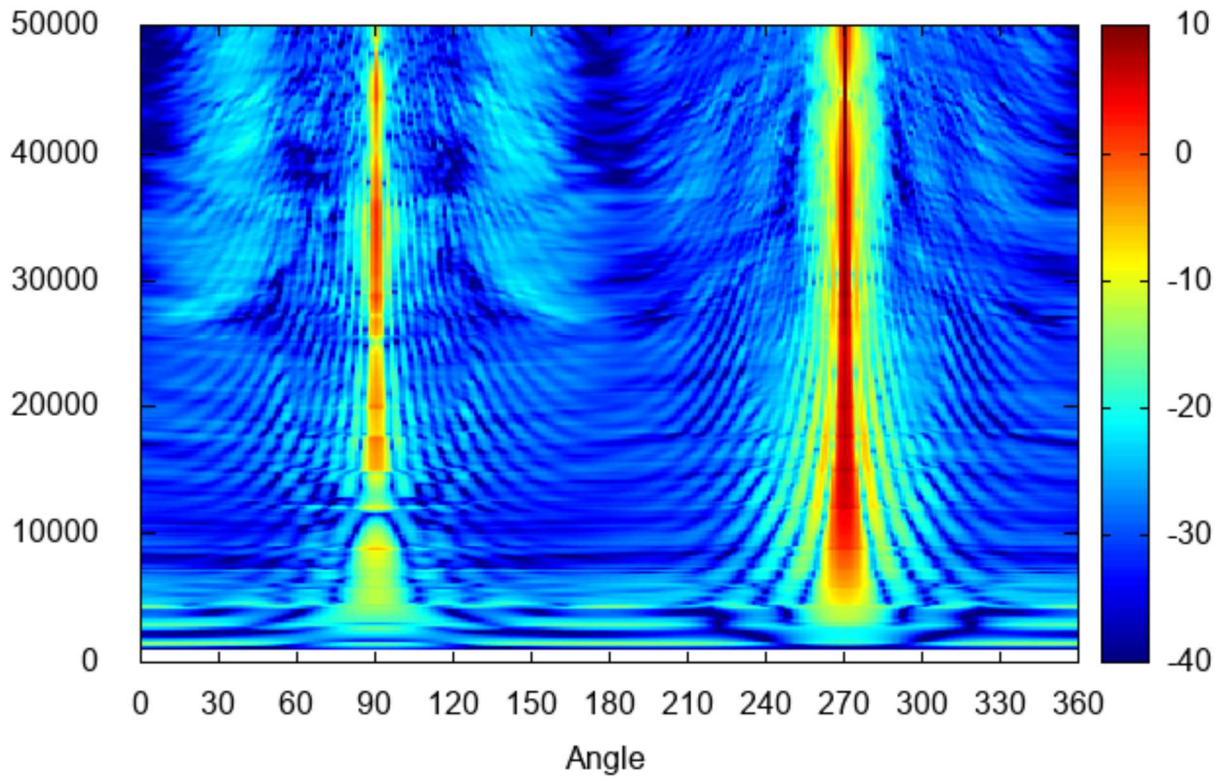


Figure 1. Bistatic scattering response for 90 degree incidence with respect to the axis of the structure.

Title: Acoustic Parameter Variability over an Ocean Reanalysis (AVORA)

Author(s): J.P. Fabre

Affiliation(s): Naval Research Laboratory, Stennis Space Center, MS

CTA: CEA

Computer Resources: Cray XC40 [NAVY, MS]

Research Objectives: Long-time reanalyses of the ocean are becoming available (e.g. NRL 7300) and are potentially extremely useful for understanding the variability of environmental parameters that impact acoustic sensor performance. The objective of this effort is to investigate such potential, to provide recommendations for future Navy products to support operations, and to develop prototype products for test and evaluation.

Methodology: Investigate the NRL 20+-year Ocean Reanalysis in conjunction with the necessary atmospheric reanalysis (e.g. NOAAs CFSR) to quantify and understand the variability over various time frames. Investigate the sensitivity of acoustic propagation and proxy parameters to the environmental variability. Investigate and assess appropriate averaging windows for a number of environments. Develop prototype products and make recommendations based on the results for products that could be derived from the described reanalyses. Such products will facilitate improved understanding of acoustic parameter variability in areas of propagation and ambient noise. Develop prototype products and test various ways of storing and accessing large data sets. NRL has been working extensively in the areas of big data and machine learning. We will include such technologies as part of our analysis, testing and recommendations and will incorporate lessons learned into existing products. If successful, these products could become the Navy standard.

Results: Many hours this year were used to run some of the ocean reanalysis (Metzger), which should be complete in FY20. Delays in running the ocean reanalysis shifted our focus to developing and refining scripts and developing software to be ready for when the ocean reanalysis is complete. We refined some previously developed display types and algorithms and have provided recommendations for out-year analyses. A few prototype algorithms were developed and tested using machine learning and clustering. Fleet users have shown an interest in these algorithms and we have begun to work out plans for finalizing and delivering. An example prototype plot is shown in the Fig. 1.

DoD Impact/Significance: “In *Joint Vision 2020*, the Department of Defense’s strategic plan to ensure battlespace dominance in the 21st century, a key element is information superiority enabled by emerging technologies ...” “An important aspect of information superiority is situational awareness. This implies knowing where you are, where allied and coalition forces are and where enemy forces are. It means understanding the environment, from the sea floor to the top of the atmosphere.” [Heart of ForceNet: Sensor Grid, Advanced Command and Control By RADM STEVEN J. TOMASZESKI]. Our efforts will directly inform environmental variability as it applies to acoustics.

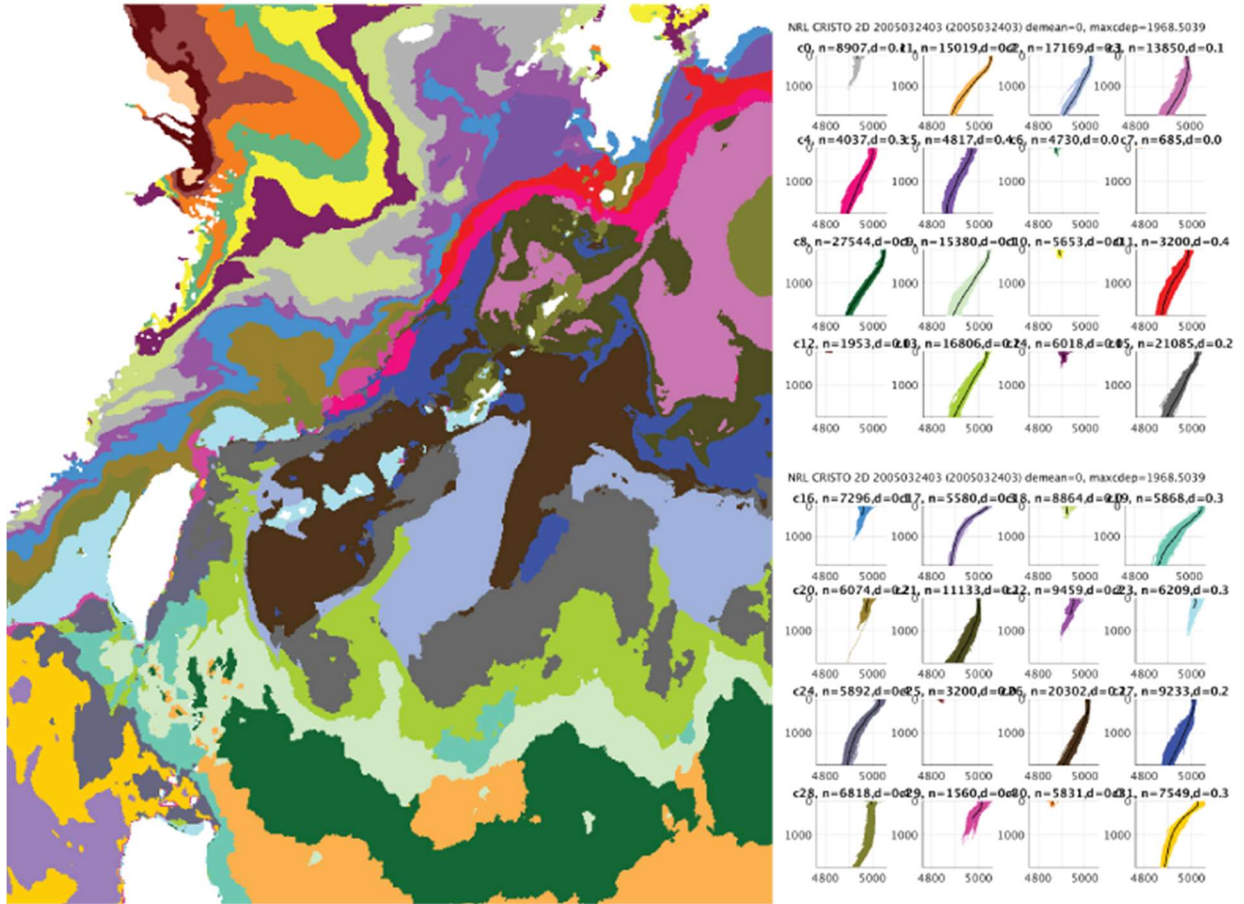


Figure 1. Prototype capability for which sound speeds were clustered into 32 clusters. Cluster numbers are plotted geographically (left) and sound speeds in each cluster plotted as same color (right). This product gives a quick estimate of the type of sound-speed profile to be expected in various parts of the ocean as well as a rough estimate of ocean water masses.

Title: Computer-Aided Design of Vacuum Electronic Devices

Author(s): G. Stantchev¹, S. Cooke¹, J. Petillo², A. Jensen², S. Ovtchinnikov²

Affiliation(s): ¹Naval Research Laboratory, Washington DC; ²Leidos, Billerica, MA

CTA: CEA

Computer Resources: SGI ICE X [AFRL, OH]; Cray XC40 [ARL, MD]; SGI ICE X [ERDC, MS]

Research Objectives: 1. Modify, enhance, and refactor the MICHELLE charged-particle beam-optics code and user environment to take advantage of DOD HPC hardware and software architectures in order to enable significantly larger simulations, optimizations, and sensitivity studies, to reduce simulation times, and to amplify user productivity in the design and development of vacuum electronic components and systems of interest to the DOD. 2. Employ the new capabilities in the design of new vacuum electronic components with optimized performance characteristics.

Methodology: MICHELLE has been extended to a flexible heterogeneous computing framework that can be deployed on distributed memory HPC clusters, and that can use computational accelerators such as multicore CPUs and Graphics Processing Units (GPUs). In addition, we have developed interfaces with existing DOD HPC mesh generation, visualization, simulation environments, and productivity tools, which includes the AFRL Galaxy Simulation Builder (GSB). Including GSB allows us to incorporate design codes in addition to MICHELLE into the pipeline of HPC-based optimizations. MICHELLE is a two-dimensional (2D) and three-dimensional (3D) finite-element, conformal mesh, Electrostatic (ES) Particle-in-Cell (PIC) code, written primarily in C++, that provides both steady-state (“gun-code”) and time-domain initial-value algorithms to predict with high accuracy the formation and transport of high-current charged-particle beams in complex electric and magnetic field geometries. In order to address the challenges necessary to bridge the software gap, we have the following two broad objectives for software improvements:

1. **Exploitation of Heterogeneous Computing Architectures:** Leveraging existing and emerging DOD HPC including multicore CPU and GPU accelerators.
2. **Integration of MICHELLE into existing DOD HPC ecosystem for Mesh Generation, Visualization, Productivity and Optimization:** Bring together the DOD CAPSTONE CAD/Mesh generation software (CREATE-MG), HPC tools such as AFRLs GSB and Kitware’s ParaView visualization software, available and supported through the Data Analysis Assessment Center (DAAC). Figure 1 illustrates the integration of the MICHELLE code under GSB along with CAPSTONE invoking Sandia’s DAKOTA optimization library.

Results: FY19 focus has been on continuing the integration of the HPC version of MICHELLE and other NRL physics codes as well as the integration with the productivity tools. Figure 2 shows the Compass user environment, which is a new productivity tool for rapidly generating geometries, mesh and optimization for GSB. Figure 3 shows an optimization cycle for RF circuits that aims to avoid instability. Figure 4 shows hybrid meshing capability, and Fig. 5 shows results from a numerical study predicting cathode emission and the associated Miram curve, based on material, emission and surface properties. In this project, DOD HPC resources have been used in support of DARPA INVEST and HAVOC programs, researching the latest trends in emission surface physics. Extensive parameter scans have been performed on HPC systems.

DoD Impact/Significance: This development has impacted three DARPA and four NRL programs in Vacuum Electronics by providing the ability to perform rapid analysis and optimization of mission-critical Vacuum Electron devices, previously deemed intractable via state-of-the-art methods.

DoD High Performance Computing (HPC) for Vacuum Electronics Using Galaxy Simulation Builder (GSB) and Compass

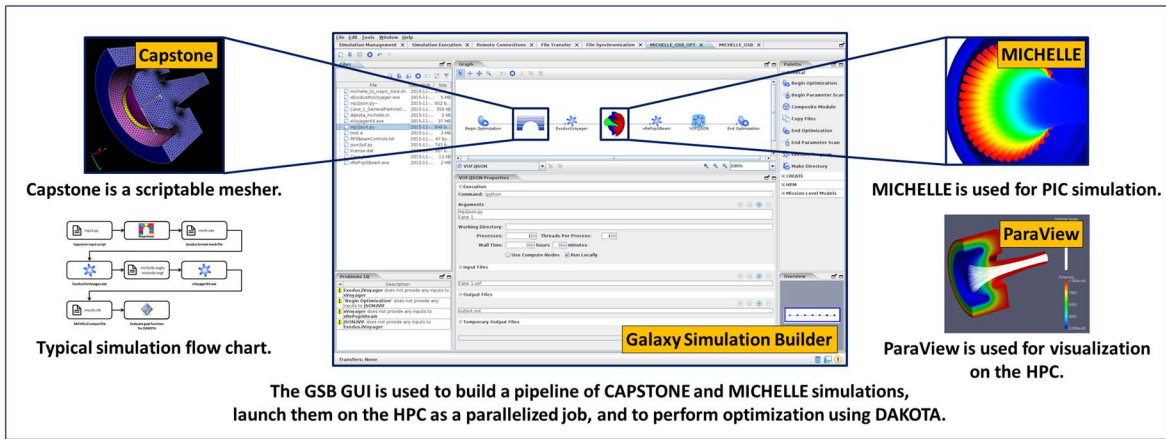


Figure 1

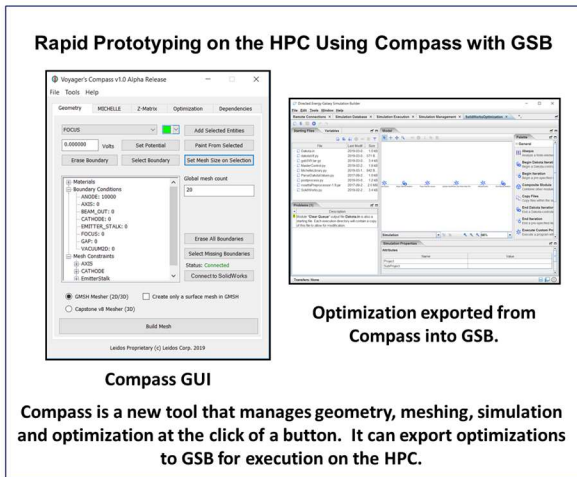


Figure 2

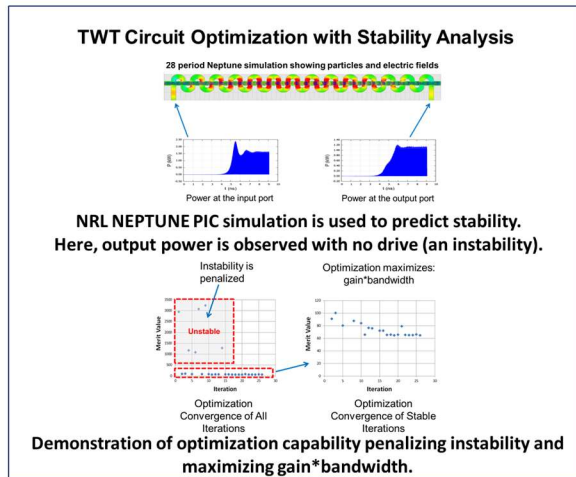


Figure 3

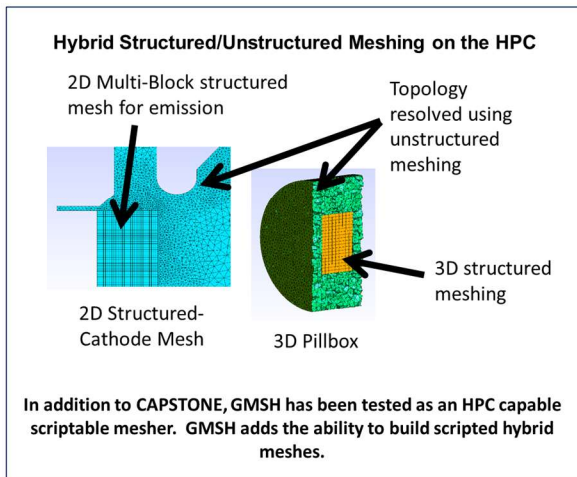


Figure 4

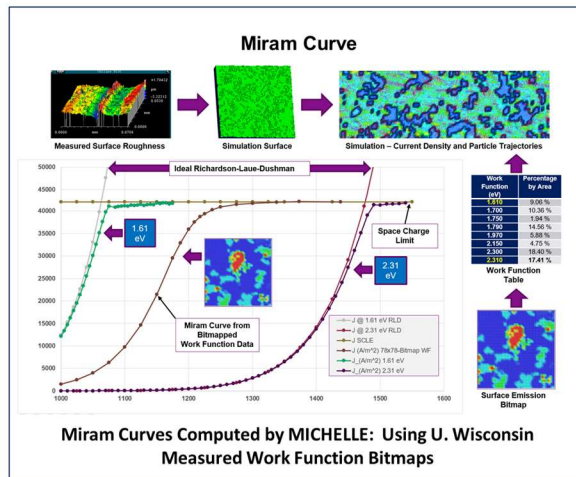


Figure 5

Title: Multidimensional Particle-in-Cell Modeling of Ultrashort Pulse Laser with Solid Targets

Author(s): G.M. Petrov

Affiliation(s): Naval Research Laboratory, Washington, DC

CTA: CEA

Computer Resources: SGI ICE X [ERDC, MS]

Research Objectives: Multidimensional particle-in-cell (PIC) modeling and simulations of the interaction of short-pulse laser with nanomaterials for better understanding of the dynamics of particle acceleration and generation of X-ray and gamma radiation.

Methodology: Intense lasers interact with matter in a wide range of time scales. For processes occurring on the picosecond time scale, multidimensional PIC models provide proper description. Such models are the primary computational tool for laser-produced plasmas because they provide a self-consistent description of the electromagnetic fields and response of the material. Nowadays, PIC models are used extensively for modeling laser-matter interaction on micro- and nano-scale. We use a two-dimensional relativistic PIC code for laser-matter interaction that was developed in-house at the Plasma Physics Division at NRL.

Results: The PIC code was used extensively to study particle acceleration and X-ray/gamma-ray generation from thin (sub-micron) foils covered with nanomaterial irradiated by ultrashort (30 fs) relativistic intensity ($>10^{21}$ W/cm²) laser pulses. The code provided valuable insight into the physical processes occurring during the interaction and was employed to analyze experiments and to gain understanding of the target performance. We did a systematic study by varying laser parameters (intensity, duration and focal spot size) and target parameters (material, thickness, surface coverage) in order to optimize targets and to guide experiments, which are very expensive and time consuming. Such experiments were conducted on the Hercules laser at the University of Michigan and the Texas Petawatt Laser in Austin, Texas. The target layout is shown in Fig. 1. One of the primary objectives was to characterize the laser pulse, itself, and in particular, how pre-pulses will affect the condition of the target when the main pulse arrives and the consequences for the generated proton beam. Simulation results for Au foil irradiated by an ultrashort pulse laser (peak intensity 1.5×10^{21} W/cm², duration 32 femtoseconds, wavelength 0.8 μ m, spot size 1.5 μ m and energy 1.5 Joules) are shown in Fig. 2 at the peak of the laser pulse. On the left are results for a perfectly clean pulse, while on the right are results when a pre-pulse is present. The proton spectra and maximum proton energy are indeed strongly affected by the pre-pulse (bottom, right). The poor performance of the target hit by the pre-pulse is due to a drastic change of its parameters: dense plasma fills the void between the nanowires, which impedes the laser propagation (top, right). The study motivated the upgrade of the Hercules laser, which achieved extremely high contrast with respect to the main pulse, on the order of 10^{-14} .

DoD Impact/Significance: This modeling and the results are of significant interest to the Navy and DoD as it is directly related to problems such as generation of X-rays and gamma rays, as well as directed particle beams (neutrons, protons, radioactive ion beams), all of which can be used for both fundamental research and practical applications such as detection of nuclear materials and improvised explosive devices. The research is also of great interest to the scientific community dealing with high-energy-density plasmas, laser nuclear physics and laser-matter interactions. The simulations have been used to guide experiments related to laser-matter interaction. The payoff of the computational efforts is that long, arduous and expensive experiments have been modeled and guided using “virtual experiments” on computers, saving time and resources.

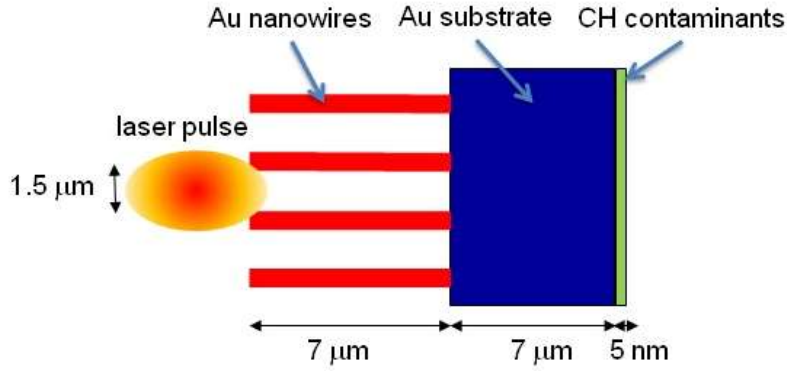


Figure 1. Interaction of short-pulse laser with targets covered with nanowires.

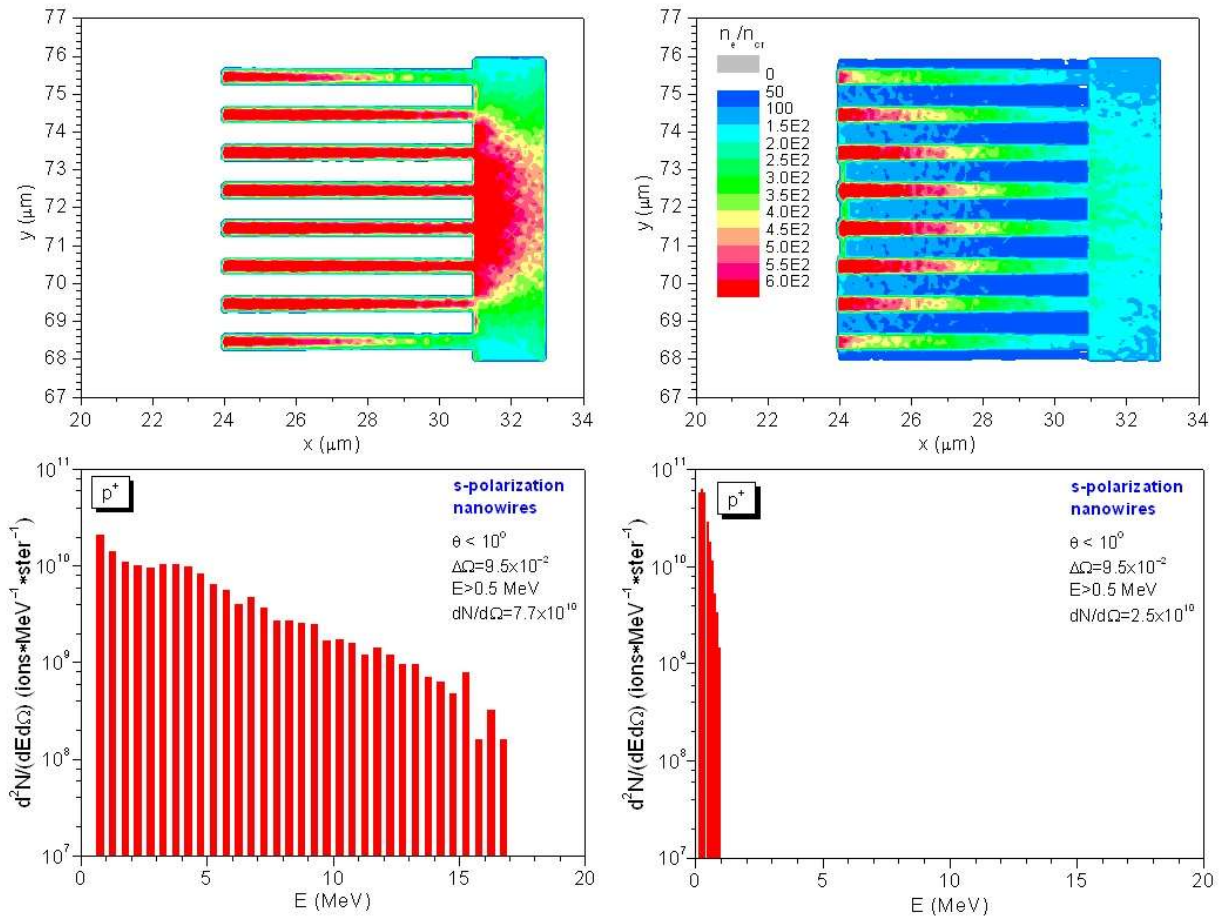


Figure 2. PIC simulations for targets with different numbers of nanowires per focal spot N . Left panels: electron density and proton spectra in forward direction for a "clean" laser pulse. Right panels: electron density and proton spectra in forward direction for a laser pulse having a pre-pulse. Laser parameters: peak intensity $I_0 = 1.5 \times 10^{21}$ W/cm 2 , wavelength $\lambda_0 = 0.8$ μm , spot size $D = 1.5$ μm , pulse duration $\tau = 32$ fs, and energy $E = 1.5$ J.

THIS PAGE INTENTIONALLY LEFT BLANK



Climate Weather Ocean Modeling

CWO focuses on the accurate numerical simulation of the Earth's atmosphere and oceans on those space and time scales important for both scientific understanding and DoD operational use. This CTA includes the simulation and forecast of atmospheric variability (e.g., temperature, winds, pressure, relative humidity, cloud cover, precipitation, storms, aerosols and trace chemicals, surface fluxes, etc.) and oceanic variability (e.g., temperature, salinity, currents, tides, waves, ice motion and concentration, sediment transport, optical clarity, etc.). Numerical simulations and real-time forecasts are performed from the very top of the atmosphere to the very bottom of the ocean. CWO also includes the development of numerical algorithms and techniques for the assimilation of in-situ and remotely sensed observations into numerical prediction systems. CWO has DoD applications on a daily basis for specific warfare areas, mission planning, and execution (air, ground, sea, and space), as well as for flight and sea safety, search and rescue, optimal aircraft and ship routing, and weapon system design. This CTA provides DoD with: (1) real-time, high-resolution weather and oceanographic forecasts leading to incisive decision making and enhanced operational capability in adverse weather and ocean conditions, and (2) realistic simulations of the dynamic oceanic and atmospheric environment to permit effective mission planning, rehearsal and training, and materiel acquisition.

Title: Coastal Mesoscale Modeling - COAMPS-TC Intensity Prediction

Author(s): J.D. Doyle

Affiliation(s): Naval Research Laboratory, Monterey, CA

CTA: CWO

Computer Resources: Cray XC40/50 [ERDC, MS]; HPE SGI 8600 [NAVY, MS]

Research Objectives: Tropical cyclone (TC) track forecasts have improved in a steady manner during the past several decades, but intensity forecasting has shown much slower increase in skill during the same time period. This is due, in part, to our limited ability to properly model physical processes controlling tropical cyclone structure and intensity, but also to the inherent sensitivity that tropical cyclone forecasts exhibit to initial conditions. Our objective is to further advance and demonstrate COAMPS-TC, a state-of-the-science numerical weather prediction (NWP) system designed for the simulation of tropical cyclones in support of Navy and DoD operations, and for civilian applications. The COAMPS-TC system is operational at Fleet Numerical Meteorology and Oceanography Center (FNMOC) and has undergone yearly upgrades since 2013. The overall goal is to improve the COAMPS-TC tropical cyclone intensity predictions through improved vortex initialization and representation of physical processes.

Methodology: There are two types of COAMPS-TC simulations and forecasts. The first type is used to facilitate rapid development and testing of COAMPS-TC. The prototype testing for COAMPS-TC needs to be rigorous and involves running approximately 500 or more individual cases in order to assess in a statistically meaningful manner. Each incremental change in the development process needs to be tested through this procedure. This rapid-testing process is needed to develop and evaluate the new version of COAMPS-TC that will be run operationally at FNMOC. A second type of COAMPS-TC application involves the real-time execution of a more advanced experimental version of COAMPS-TC, which contains more advanced capabilities than the FNMOC version, on the DSRC. The testing of the experimental COAMPS-TC system is performed for many tropical cyclones in all basins worldwide.

Results: Several configurations of COAMPS-TC were tested rigorously over a suite of storms in the Atlantic and Pacific Ocean basins based on several previous TC seasons. A new version with significant improvements was transitioned to operations at FNMOC in May 2019. These improvements included the use of high horizontal resolution (4 km), along with upgrades to the physical parameterizations and vortex initialization. Figure 1 shows a series of five-day forecast tracks for Hurricane Dorian for the time period 1200 UTC August 28 to 1800 UTC September 1, 2019. Hurricane Dorian was the most intense tropical cyclone on record to strike the Bahamas and recurved just to the east of Florida before impacting the North Carolina coast. As illustrated in Fig. 1, the operational Navy's COAMPS-TC more accurately predicted the recurvature of Hurricane Dorian relative to other hurricane models shown in Fig. 1. COAMPS-TC also was the top-performing hurricane-forecast model for Dorian's intensity. COAMPS-TC continues to be one of the top-performing tropical cyclone-prediction models in the world in 2019. This new, advanced version of COAMPS-TC developed at the DSRCs continues to show considerable promise in both research and operational applications.

DoD Impact/Significance: Tropical cyclones remain the most disruptive and devastating environmental threat that impact U.S. Navy operations. We anticipate that an increase in accuracy of tropical cyclone forecasts will result in significant cost benefit to the Navy through better sortie decisions and avoidance of hazardous winds and seas. Real-time testing and development of the system at HPC DSRCs have led to significant improvements in the data assimilation and predictive skill of COAMPS-TC and more rapid transitions to operations at FNMOC. These improvements will inform future directions of tropical cyclone and mesoscale model and data-assimilation development, particularly as computational power increases, allowing for higher resolution capabilities.

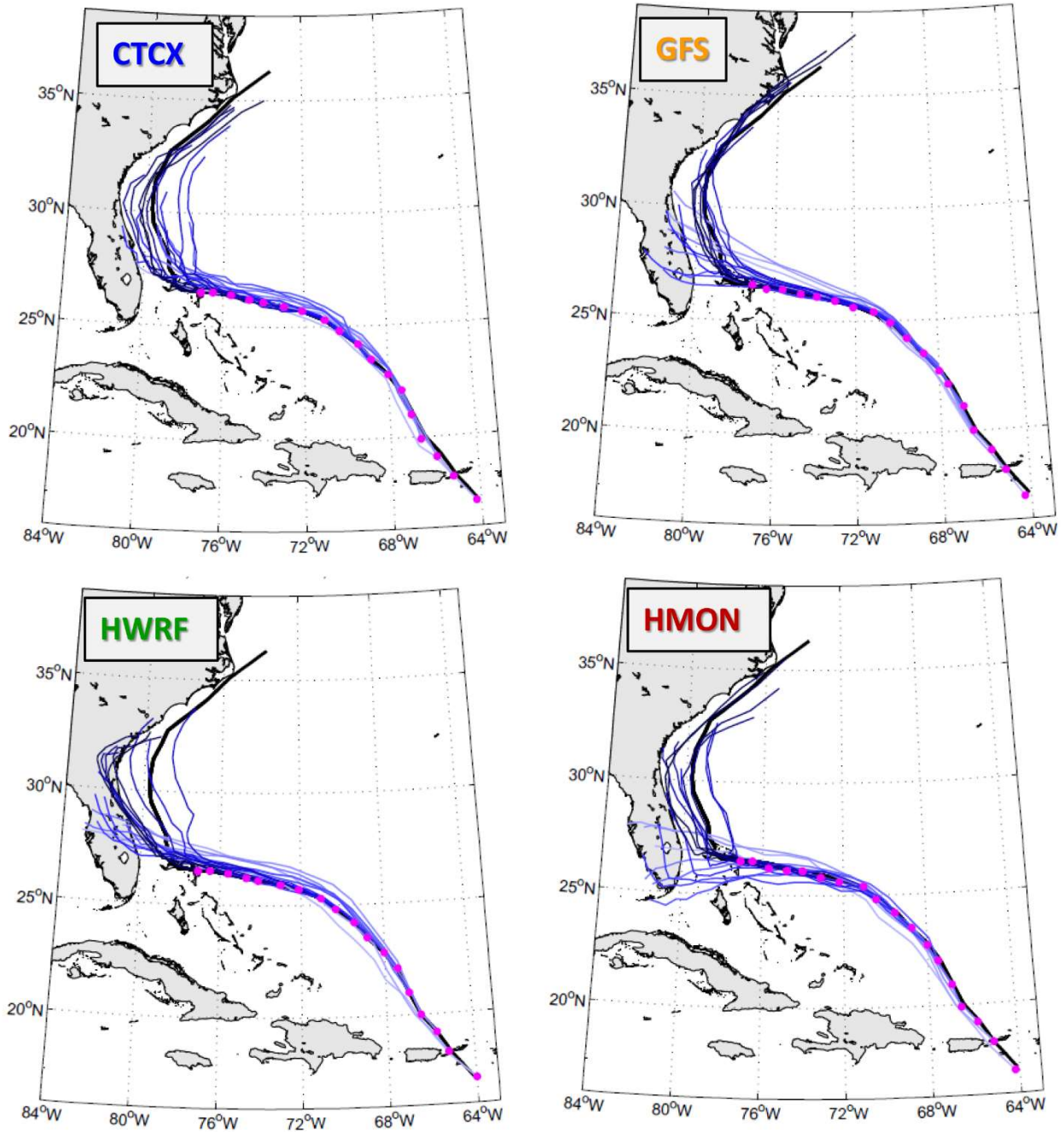


Figure 1. Five-day forecast tracks for Hurricane Dorian tracks (blue) and observed tracks (black) for forecasts initialized every 6 hours beginning with 1200 UTC August 28, 2019 through 1800 UTC September 1, 2019. Forecasts from the operational Navy’s COAMPS-TC (upper left), NOAA Global Forecast System (GFS) (upper right), NOAA HWRF (lower left), and NOAA HMON (lower right) are shown for this key period of Hurricane Dorian. The magenta dot shows the initial position for each forecast every 6 hours.

Title: Coastal Mesoscale Modeling
Author(s): P.A. Reinecke
Affiliation(s): Naval Research Laboratory, Monterey, CA
CTA: CWO

Computer Resources: SGI ICE X [AFRL, OH]; SGI ICE X [ARL, MD]; Cray XC40/50 [ERDC, MS]; Cray XC40, HPE SGI 8600 [NAVY, MS]

Research Objectives: Our objective is to develop and validate a fully coupled coastal/littoral prediction system that can be used to provide high-resolution (<5 km) data assimilation (DA) and short-term (0-48 h) forecast guidance for tactical sized areas of the world. This system also can be used for basic and applied research leading to an improvement in our understanding of atmospheric and oceanic processes. Improvements to the mesoscale prediction and DA systems will result from this research.

Methodology: The Coupled Ocean/Atmosphere Mesoscale Prediction System (COAMPS^{®1}) is being developed further for independent and coupled simulations of the atmosphere and ocean for the mesoscale. The atmospheric component of COAMPS is made up of a DA system; an initialization procedure; and a multi-nested, nonhydrostatic numerical model. This model includes parameterizations for moist processes, surface and boundary-layer effects, and radiation processes. The NRL Coastal Ocean Model (NCOM) is currently being used for the simulation of the mesoscale ocean circulation response to the COAMPS forcing in one-way and two-way interactive modes. Ocean coupling is being developed using the Earth System Modeling Framework (ESMF). A new tropical cyclone capability has been developed for COAMPS, referred to as COAMPS-TC.^{®2} Development and testing of the Navy's next generation prediction system, NEPTUNE (Navy's Environmental Prediction System Using the NUMA Engine) is underway. This system uses a spectral element based approximation to the atmosphere and can scale to more than 1,000,000 cores.

Results: In FY18, COAMPS was demonstrated to be an accurate DA and forecast system capable of predictions and simulations on a variety of horizontal scales of less than 1 km for land-sea effects, topographically driven flows, and tropical cyclones. Numerous studies were performed to explore the impact of the ocean and the sea-state on the atmospheric boundary layer. The development of NEPTUNE continued in 2019 with systematic testing of real-data initial condition forecasts using full physics parameterizations. Figure 1 shows the results of one such study examining the ability of NEPTUNE to capture the merger and genesis of intense Arctic cyclones. The figure shows the analyzed mean sea-level pressure (top row) and a NEPTUNE forecast initialized 12 UTC 05 June 2018 and valid at each of the analysis times (bottom row). The model forecast is able to capture the vortex formation and intensification, but is slightly slower and weaker than the analysis position of the vortex. We will continue to develop the NEPTUNE system in future years and improve the model physics, dynamics, and coupling processes.

DoD Impact/Significance: COAMPS continues to play a significant role in providing atmospheric forecasts in support of Navy missions involving the deployment of weapons systems, strike warfare, radar propagation, and search and rescue. Research and development performed at HPC DSRCs have led to significant improvements in the predictive skill of COAMPS that will greatly benefit the operational performance of COAMPS. HPC resources will be used in FY2019 and beyond for the development of the fully coupled COAMPS system, including the emerging tropical cyclone and ensemble capabilities for COAMPS as well as NEPTUNE, the next-generation global and mesoscale modeling system.

¹ COAMPS[®] is a registered trademark of the Naval Research Laboratory.

² COAMPS-TC[®] is a registered trademark of the Naval Research Laboratory.

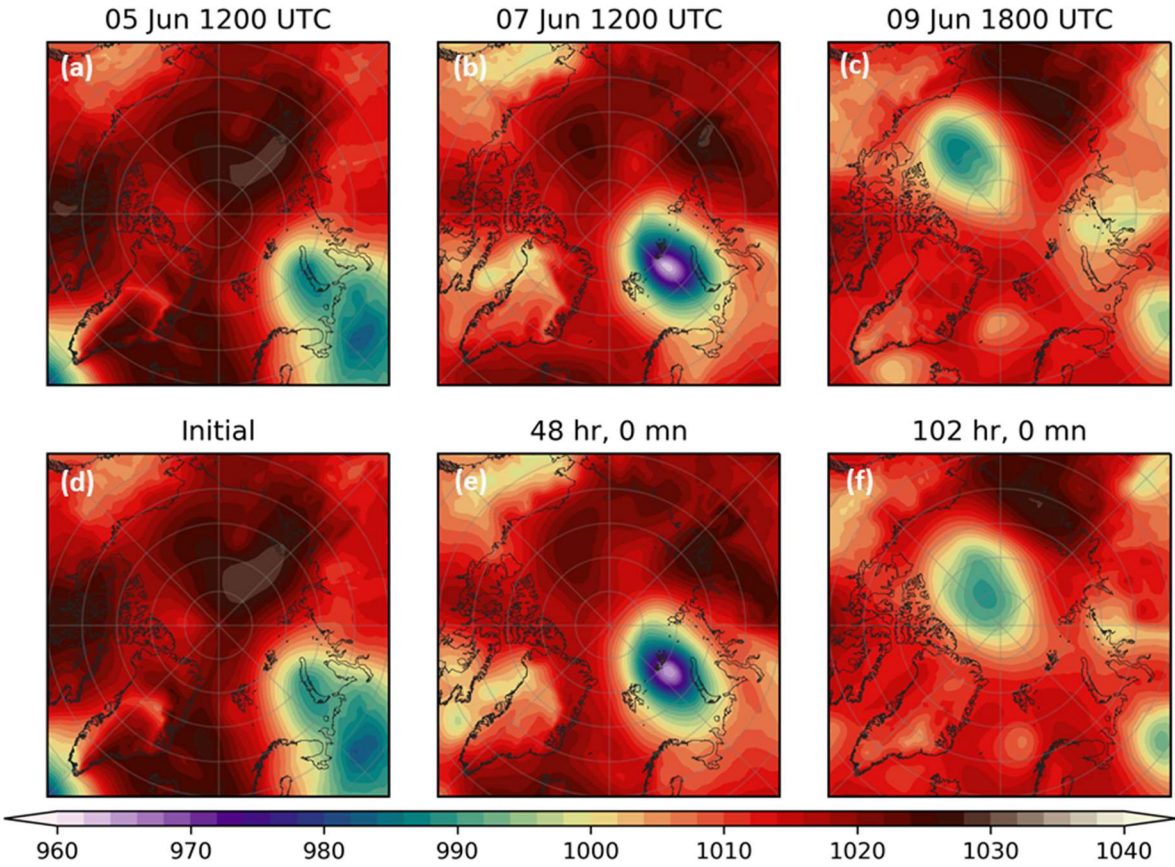


Figure 1. Comparison of analyzed mean sea-level pressure (mslp) (top row) and NEPTUNE forecast of mean sea-level pressure for a forecast of an intense Arctic cyclone from June 2018. The NEPTUNE forecast was initialized 12 UTC 5 June 2018 and was integrated forward for 120 hours. The NEPTUNE forecast is a global numerical weather-prediction simulation with approximate horizontal resolution of 26 km.

Title: Data Assimilation Studies Project
Authors: W.F. Campbell and B. Ruston
Affiliation: Naval Research Laboratory, Monterey, CA
CTA: CWO

Computer Resources: Cray XC40, HPE SGI 8600 [NAVY, MS]

Research Objectives: Data assimilation corrects model analyses of the atmosphere, ocean or surface using non-homogenous observations. This project develops, tests, and improves: 1) our 4D-Var assimilation system, which is coupled to the atmospheric global model NAVGEM (Navy Global Environmental Model), 2) fully ensemble-based data assimilation, 3) hybrid ensemble/4D-Var data assimilation, 4) 4D-Var data assimilation for COAMPS^{®1}, 5) adjoint, tangent linear, and forecast sensitivity to observations, 6) coupled DA (atmosphere and ocean together), and 7) prepares for and test assimilation of new data types, both satellite and conventional. Our goal is to assimilate traditional data (generally in-situ, i.e. weather balloons, ship or buoy reports) as well as data from a variety of new sources (often spaceborne) efficiently and effectively, to provide the best atmospheric analysis, and ultimately to improve numerical weather forecast performance.

Methodology: A variety of experimental setups are used to develop and test our global and regional models and data-assimilation systems, as well as large datasets of in-situ and satellite-based observations for several summer and winter months.

Results: A broad spectrum of research takes place under this project using the Navy's latest global (NAVGEM 2.0, and Middle Atmospheric NAVGEM (HA-NAVGEM)) and mesoscale (COAMPS) models, along with our global (NAVDAS-AR, hybrid NAVDAS-AR, and coupled hybrid NAVDAS-AR) and mesoscale (COAMPS-AR) data-assimilation systems. Results from FY19 research include: 1) Development of an EnKF data assimilation system to assimilate all-sky IR radiance observations into COAMPS-TC^{®2}, which showed substantial positive impacts on tropical cyclone track and intensity, 2) Rapid prototyping and first-in-the-world assimilation of three different GNSS-RO receivers, 3) development and first publication using background fit to observations verification package for satellite radiances and scatterometers, 4) COAMPS-4Dvar experiments evaluating the impact of nontraditional observations, 5) Improved ozone assimilation that increased forecast skill in the troposphere and stratosphere, 6) continued development of the Ensemble-Based Tangent Linear Model, a novel alternative to existing TLM and ADJ atmospheric models, 7) continued testing of Holm transform for the moisture control variable in hybrid NAVGEM, 8) continued development of new Bias Drift Mitigation Technique for NAVGEM radiance data, and 9) testing of the coupled ocean-atmosphere system with the addition of surface-sensitive infrared radiance data.

DoD Impact/Significance: HPCMP computing platforms provide a common environment for collaboration and the rapid development of NRL's data-assimilation systems. Large, common datasets can be stored there and accessed by many researchers. Collaboration between NRL scientists at different locations (Monterey, Stennis, and DC) and among other scientists is greatly facilitated. The advancements of NAVDAS-AR, NAVGEM (including hybrid NAVGEM and HA-NAVGEM), and COAMPS-AR systems have been accelerated by the HPCMP systems, e.g., one researcher was able to effectively use the serial and transfer queue capabilities to accelerate his research. The core and future of Navy data-assimilation capabilities are being mostly, and in many cases solely, developed using the resources provided by HPCMP.

¹ COAMPS[®] is a registered trademark of the Naval Research Laboratory.

² COAMPS-TC[®] is a registered trademark of the Naval Research Laboratory.

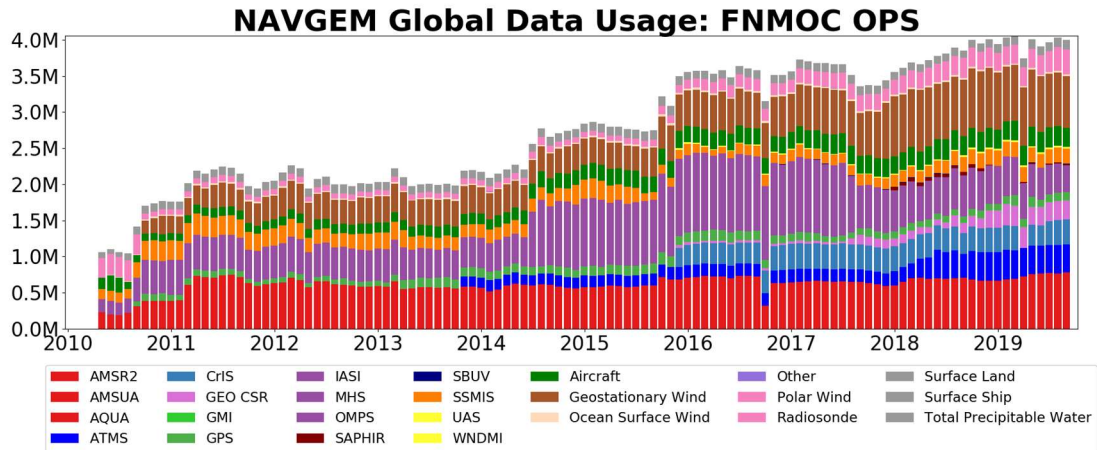


Figure 1. Data types and daily counts (in millions of observations assimilated) for the NAVGEM global model during the past decade.

Title: Coupled Ocean-Wave-Air-Ice Prediction System

Author(s): R. Allard¹, T. Campbell¹, J. Crout², E. Douglass¹, D. Hebert¹, T. Jensen¹, and T. Smith¹

Affiliation(s): ¹Naval Research Laboratory, Stennis Space Center, MS; ²Perspecta, Stennis Space Center, MS

CTA: CWO

Computer Resources: Cray XC40 [NAVY, MS]

Research Objectives: Perform research studies with the Coupled Ocean Atmosphere Mesoscale Prediction System (COAMPS^{®1}) which is six-way-coupled with the Navy Coastal Ocean Model (NCOM), WaveWatch-III (WW3) and SWAN wave models and the COAMPS atmospheric model. Perform modeling studies with the Community Ice Code (CICE v6), which includes a landfast ice parameterization.

Methodology: Numerous tests were performed using CICE (v6) to support the CICE Consortium. A test suite has been developed utilizing cray, intel, gnu, and pgi compilers. We set up a 1 km regional CICE v6 to support the McMurdo Resupply in the Ross Sea for the period of December 15, 2018 – February 15, 2019. Test cases have been developed for the Beaufort Sea and the Fram Strait region to perform validation studies for the COAMPS-CICE system.

Results: NRL received a request from the National Ice Center (NIC) on December 10, 2018, to support Operation Deep Freeze by running a 1 km regional CICE for the transit of the USCG Polar Star from Sydney, Australia, to McMurdo, Antarctica, in the Ross Sea for this annual resupply mission. Due to a short time constraint to set up the regional model, we used NAVGEM to force the new release of CICE v6 in this effort. The system was run daily, producing 96-hour forecasts for the period of December 20, 2018 – February 15, 2019. Upon arrival in McMurdo Sound, Antarctica, the Polar Star broke through 1.5 nautical miles of ice in order to open a channel to the pier at McMurdo Station. Figures 1a through 1d depict examples of the forecast products. Figure 1e shows the location of McMurdo Station in the Ross Sea. Figure 1f depicts an ice-edge error comparison between the Global Ocean Forecasting System (GOFS 3.1) and the 1 km CICE at tau 24 for the period of December 16, 2018 – February 15, 2019. The 1 km CICE consistently shows a reduced ice-edge error throughout the period. CICE v6 was configured for the GOFS 3.1 grid, in which several landfast simulations for the periods of Sept 2011 – July 2012 and Sept 2014 – July 2015 were performed using CFSRv2 atmospheric forcing and existing HYCOM fields. We performed a control run with the landfast ice parametrization turned off, and performed simulations using the grounding (K_1 , K_2) and tensile strength (K_T) parameter settings recommended by Lemieux et al. (2015, 2016). Ice is classified as landfast when the ice velocities are less than $5.0E^{-4}$ m/s for a minimum of two consecutive weeks. Comparisons against ice charts from the Canadian Ice Service showed a reasonable amount of landfast ice in the East Siberian and Laptev seas using the default parameters and the subcycling timestep set to 900. We added a Japanese 55-year Reanalysis (JRA-55) atmospheric forcing option to the gx1 test suite as part of the CICE Consortium testing. JRA-55 forcing for the years 2005-2009 were tested successfully and will be added to the next release of CICE v6.

DoD Impact/Significance: The development of a coupled air-ocean-wave prediction system can have a pronounced effect on Navy forecasting by improving ASW performance, tropical cyclone prediction, and search-and-rescue and mission planning. The relocatable COAMPS-CICE system will provide high-resolution Arctic forecasting of ice thickness, ice drift, and concentration to support navigation. Inclusion of landfast ice in the Navy's global ice-prediction systems will yield a more realistic representation of pan-Arctic sea ice.

¹ COAMPS[®] is a registered trademark of the Naval Research Laboratory.

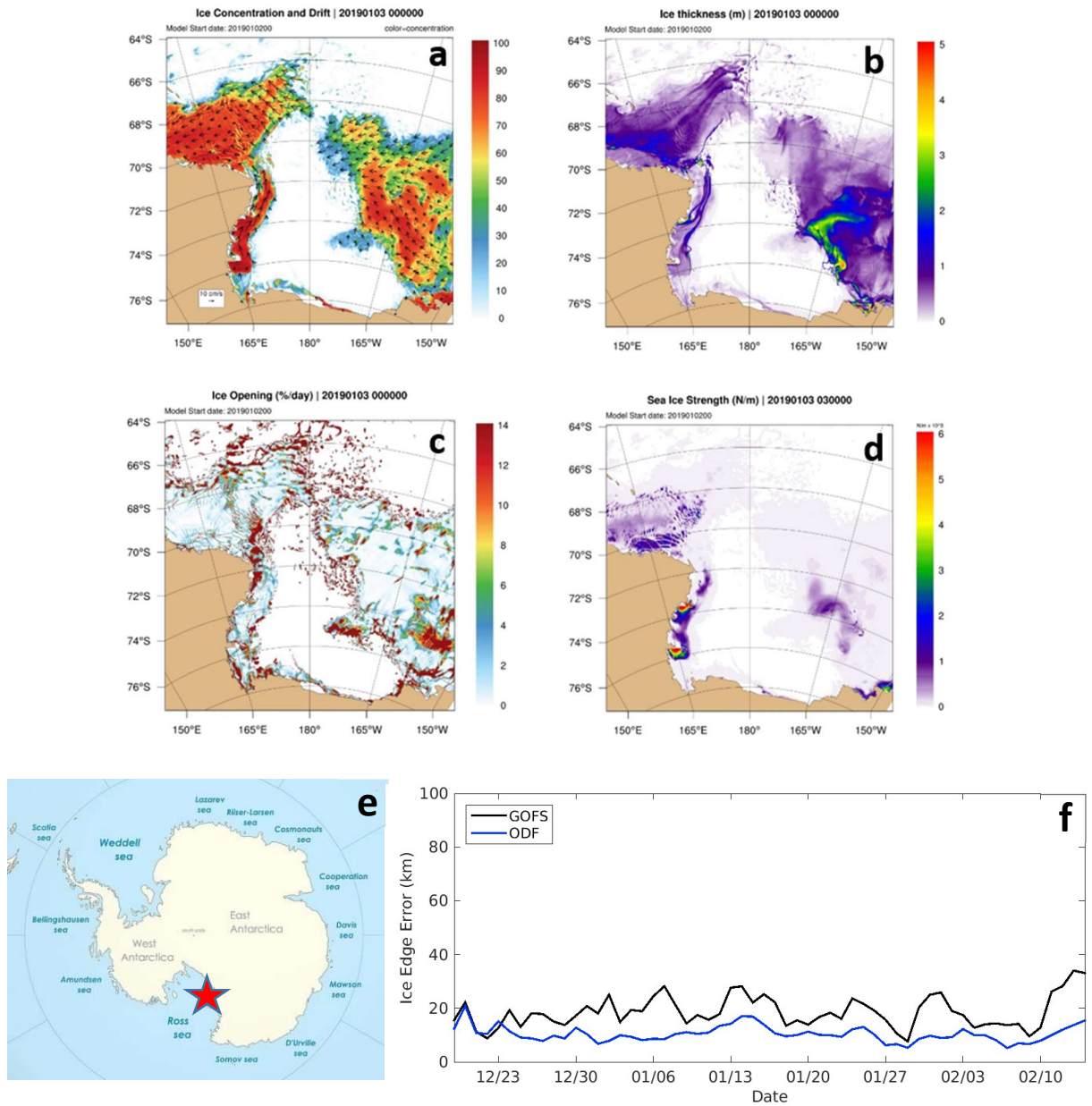


Figure 1. 1 km CICE support for Operation Deep Freeze: Example graphical products for a) ice concentration and drift, b) ice thickness (m), c) ice opening rate (%/day), and d) sea ice strength (N/m). e) location of Ross Sea shown by red star, f) comparison of ice edge error at tau 24 between GOFS 3.1 (black line) and regional CICE (blue line).

Title: Variational Data Assimilation

Author(s): S. Smith¹, C. Amerault², C. Barron¹, S. Boggs³, T. Campbell¹, M. Carrier¹, N. Cheshire³, J. D'Addezio^{1,4}, J. Dastugue¹, C. DeHaan⁵, S. deRada¹, E. Douglass¹, D. Fertitta³, D. Hebert¹, R. Helber¹, P. Martin¹, J. May¹, H. Ngodock¹, J. Osborne^{1,3}, C. Rowley¹, J. Shriver¹, T. Smith¹, I. Souopgui⁶, P. Spence⁵, and M. Yaremchuk¹

Affiliation(s): ¹Naval Research Laboratory, Stennis Space Center, MS; ²Naval Research Laboratory, Monterey, CA; ³American Society for Engineering Education, Stennis Space Center, MS; ⁴University of Southern Mississippi, Stennis Space Center, MS; ⁵QinetiQ North America, Stennis Space Center, MS; ⁶University of New Orleans, Stennis Space Center, MS

CTA: CWO

Computer Resources: Cray XC40, HPE SGI 8600 [NAVY, MS]

Research Objectives: The scope of this project is to advance the analysis and prediction capability of the Navy's environmental modeling and forecasting systems through the improvement of the Navy Coupled Ocean Data Assimilation (NCODA) software. There were seven funded NRL projects that focused on either adding or improving capabilities of NCODA in FY19, and the experiments performed under this HPC project went towards satisfying these efforts. A few of these efforts include: 1) further validating the 4DVAR, 2) developing and testing a multiscale capability to better resolve small-scale features, and 3) implementing and testing the capability to assimilate velocity observations.

Methodology: This HPC project helped advance the NCODA system in FY19 through the following seven funded NRL projects: (1) The 6.4 4DVAR project successfully implemented the 4DVAR within the operational COAMPS5^{®1} system and performed validation experiments in a nonlinear Western Pacific regime. (2) The 6.4 RTP Coupled Ocean-Atmosphere Variational Assimilation and Prediction System project merged 4DVAR capabilities between the atmospheric and oceanic components. (3) The 6.4 RTP Coupled Ocean-Acoustic Assimilative Model project performed a number of validation experiments coupling 4DVAR-NCOM and 4DVAR-RAM systems. (4) The 6.2 Smart Glider Teams for Rapid Update of Local Analysis project tested the multiscale 4DVAR for accurately assimilating coordinated teams of gliders. (5) The 6.1 Propagation and Dissipation of Internal Tides on Coastal Shelves project continued the internal tide study of the NCOM-4DVAR on the Northwest Australia Shelf. (6) The 6.2 Submesoscale Prediction of Eddies through Altimeter Retrieval (SPEAR) project developed a multiscale capability and performed high-resolution (1 km) 3DVAR and 4DVAR experiments assimilating SSH observation from the upcoming Surface Water and Ocean Topography (SWOT) satellite (see figure). (7) 6.4 Velocity Assimilation: The capability to assimilate velocity observations was added to both 3DVAR and 4DVAR and was tested within the operational COAMPS5 system for multiple domains.

Results: Numerous 3DVAR and 4DVAR experiments were performed using NCODA under this FY19 HPC project with the overall result of improving the analysis accuracy, prediction skill, portability and robustness of the system. A few of the specific advancements made include: assimilating at very high resolution, coupling assimilation systems, multiscale, and assimilating velocities, SWOT, and SSS.

DoD Impact/Significance: The assimilation experiments tested under this project went towards improving the Navy's capability of forecasting the ocean environment. Various validation studies for the 4DVAR were performed and showed more accurate analyses and model forecast fields than its predecessor, 3DVAR. Additionally, the work on coupling the assimilation systems for the ocean, atmosphere, and acoustic models made significant progress this fiscal year and these coupled systems ultimately will improve further the forecast skill of all three environments.

¹ COAMPS[®] is a registered trademark of the Naval Research Laboratory.

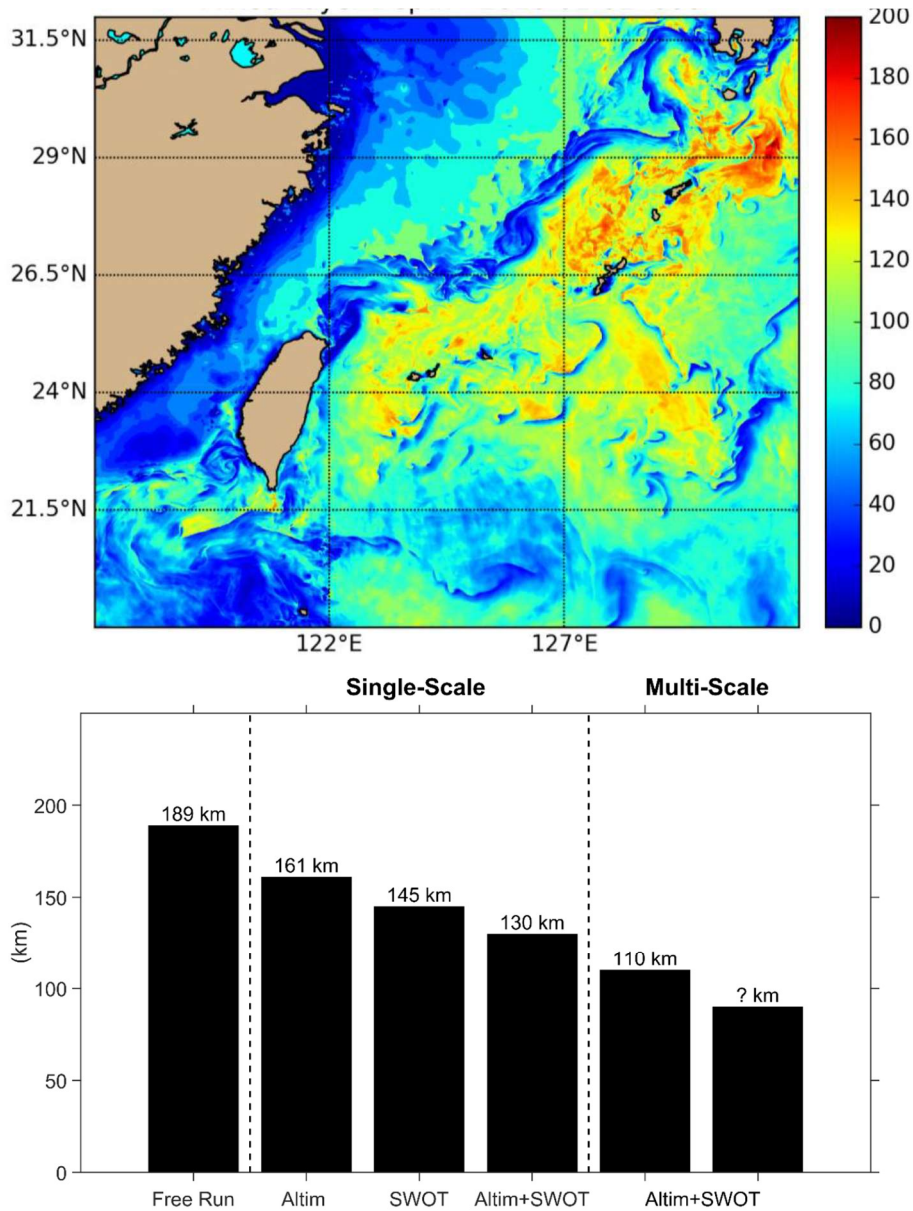


Figure 1. A set of observing-system simulation experiments (OSSEs) were performed in the Western Pacific (Panel A) to test whether a new Multi-Scale NCODA-3DVAR system assimilating sea surface height (SSH) observations from the forthcoming Surface Water and Ocean Topography (SWOT) satellite will be able to resolve submesoscale features. Panel B shows the overall minimum constrained wavelength from each OSSE, and that SWOT data will improve the resolution of small scale features. It is hypothesized that once the submesoscale covariances are implemented, we should be close to resolving submesoscale features with data assimilation (D’Addezio et al., 2019)

Title: Rogue Wave Probability Estimator for WAVEWATCH III

Author(s): M. Orzech¹, J. Simeonov¹, and M. Manolidis²

Affiliation(s): ¹Naval Research Laboratory, Stennis Space Center, MS; ²National Research Council Postdoctoral Research Associate, Stennis Space Center, MS

CTA: CWO

Computer Resources: Cray XC40 [ARL, MD]; Cray XC40 [NAVY, MS]

Research Objectives: The overall objective is to develop a post-processing utility for WAVEWATCH III to forecast the relative threat of rogue waves around the world. The Rogue Threat Index (RTI) system operates in a broad range of deep-water wave environments, using scalar and conditional metrics to estimate rogue threats due to environmental causal factors. Computations are based on established theory and extensive analysis of representative sea states. FY19 objectives include: (1) Analyzing and quantifying the effects of wave direction and crossing seas on rogue wave formation with the model HOS-ocean. (2) Using the continuum mechanics model OpenFOAM to investigate how strong winds (either codirectional or opposing) can dampen or augment the development of rogue waves.

Methodology: For objective (1), run a series of 3D, phase-resolved, higher-order spectral (HOS) simulations initialized by directionally spread JONSWAP spectra, configured either with a single spectral peak or with two peaks in different primary directions. In the single-peak cases, vary the directional spread of the peak from very narrow to very broad. In the bimodal cases, vary the angle between the two peaks from zero (completely overlapping) to 170°. For each test, track the distribution of wave heights, significant wave height (H_s), and maximum kurtosis. Identify and count rogue waves as those with crest height $\eta_{rogue} > 1.25 \cdot H_s$. For objective (2), configure multiple high-resolution simulations in which highly nonlinear, random waves generated from very narrow frequency spectra travel in a 2D numerical wave tank, very close to a rogue wave state. In each simulation, accompany the waves with a different wind state, ranging from no wind to hurricane-force wind in the wave direction. Also test moderate opposing winds. Track the relative intensity of rogue development in simulations by monitoring the wave kurtosis, as it is directly related to spectral nonlinearity.

Results: (1) For HOS tests using single-peak spectra, our simulations validated results from Onorato et al. (2009; see their Fig. 4) and others, indicating that the frequency of extreme waves declines as directional spread of the wave spectrum increases (Fig. 1, left panel). For two-peak spectra (crossing seas), our results were similar to earlier published work (Cavaleri et al., 2012; Gramstad et al., 2018) in showing that something “*different*” occurs when two narrow-banded wave fronts cross at angles of roughly 20° - 50° (Fig. 1, right panels). The primary finding in this case was that rogue wave occurrence and related factors like kurtosis are consistently *reduced* for bimodal spectra relative to single-peak spectra of similar energy. (2) For simulations investigating wind effects, rogue waves appeared after approximately 100 seconds in each test, as evidenced by elevated kurtosis values (Fig. 2). The severity of their development varied with wind speed and direction. Peak kurtosis values in the window 80 sec < t < 120 sec consistently declined as wind speed increased in the direction of the waves, consistent with results of Galchenko et al. (2012). One additional test with a moderate *opposing* wind achieved the highest overall kurtosis, suggesting that wind opposing a developing rogue wave may allow the modulation to persist and produce even larger crests. These results have been incorporated into the RTI utility software for WAVEWATCH III, which will be transitioned to FNMOC upon allocation of funding.

DoD Impact/Significance: Accurate prediction of environmental hazards is important to tactical and strategic operations in the world’s oceans. The results obtained from these simulations will form the core of the configurable WAVEWATCH III rogue threat utility, which will enhance the safety of Naval missions and will reduce the potential for damage or loss of Navy assets in rogue wave events.

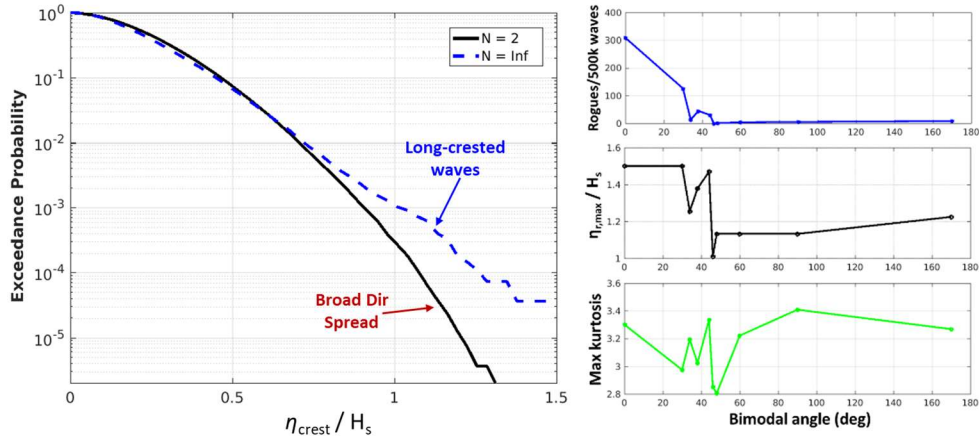
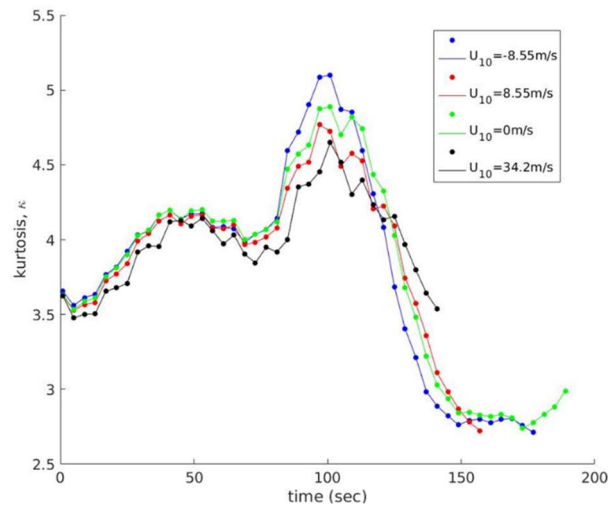


Figure 1. *Left*: Exceedance probability of wave crest height for waves with broad (*black solid*) and narrow (*blue dashed*) directional spread. *Right*: Wave test results for bimodal wave spectra with crossing angles ranging from 0° to 170° : number of rogues per 500,000 waves (*top*); maximum rogue crest height relative to H_s (*middle*); and maximum measured kurtosis (*bottom*).

Figure 2. Kurtosis values in highly nonlinear waves propagating with or without wind, plotted against propagation time for four different configurations: moderate wind directly opposes wave motion (*blue*); moderate wind in same direction as waves (*red*); waves-only simulation without wind (*green*); and hurricane-force wind in same direction as waves (*black*). Results are from 2D simulations with OpenFOAM. Wave group velocity is $c_g = 8.55\text{m/s}$.



Title: Multi-scale Characterization and Prediction of the Global Atmosphere from the Ground to the Edge of Space using Next-Generation Navy Modeling Systems

Author(s): J.P. McCormack¹, S.D. Eckermann¹, C.A. Barton^{1,4}, F. Sassi¹ M.A. Herrera^{1,3}, K.W. Hoppel¹, D.D. Kuhl¹, D.R. Allen¹, J. Ma², and J. Tate²

Affiliation(s): ¹Naval Research Laboratory, Washington, DC; ²Computational Physics Inc., Springfield, VA; ³National Research Council Postdoctoral Research Fellow; ⁴Karles Fellow

CTA: CWO

Computer Resources: Cray XC40, SGI ICE X [ARL, MD]; Cray XC40/50 [ERDC, MS]; Cray XC40, HPE SGI 8600, HPE SGI 8600 (C) [NAVY, MS]

Research Objectives: To develop and test new, seamless, atmospheric specification and prediction capabilities from 0-500 km altitude for a future Navy Earth System Prediction Capability (ESPC) and Space Environment Prediction with High Resolution (SEPHIR) system, linking prediction of the ocean, the atmosphere, and space over time scales from hours to decades.

Methodology: This project develops and tests key components of state-of-the-art systems required for the improved modeling, prediction and analysis of the extended operational environment for Navy applications, focusing on the atmosphere, the near space and the geospace.

Results: Major results include: (a) successful testing and transition of NAVGEM-HA code to operations at Fleet Numerical Oceanography and Meteorology Center through the Navy ESPC program; (b) first demonstration of NAVGEM-HA seasonal forecast skill out to 50 days showing a positive impact on week 4 outlooks of surface weather patterns; (c) first successful tests of the NEPTUNE model extending from the surface to 300 km altitude using numerical algorithms that enable the nonhydrostatic dynamical core to operate at altitudes where conventional assumptions of fluid dynamics or standard algorithms no longer apply; (d) continued development of the non-orographic gravity wave (GW) source retrieval using ensembles of NAVGEM-HA 24-hour and 120-hour forecasts; (e) use of NAVGEM-HA analyses in an external community climate model to show how surface weather can impact neutral atmospheric forcing of the ionosphere (f) COAMPS simulations coupled to new Fourier-ray and multilayer gravity-wave models and an ionospheric model for end-to-end physics-based prediction of traveling ionospheric disturbances seeded by waves generated in the lower atmosphere.

DoD Impact/Significance: This research develops and tests new high-altitude atmospheric specification and prediction capabilities that together will constitute bridge technology to a future Navy ESPC by 2020. The direct benefit this project provides to the Navy is logistical support to install an accurate high-altitude specification and forecast capability in next-generation Navy NWP systems, which ultimately can provide improved near-space specification and prediction capabilities to the warfighter over both tactical and strategic time frames. HPC resources for this project also provide critical support for the development of a new ground-to-thermosphere prediction capability fully coupled to ionospheric models and data assimilation to address key space-environment prediction goals of the Defense Advanced Research Projects Agency's Space Environment Exploitation (DARPA SEE) program.

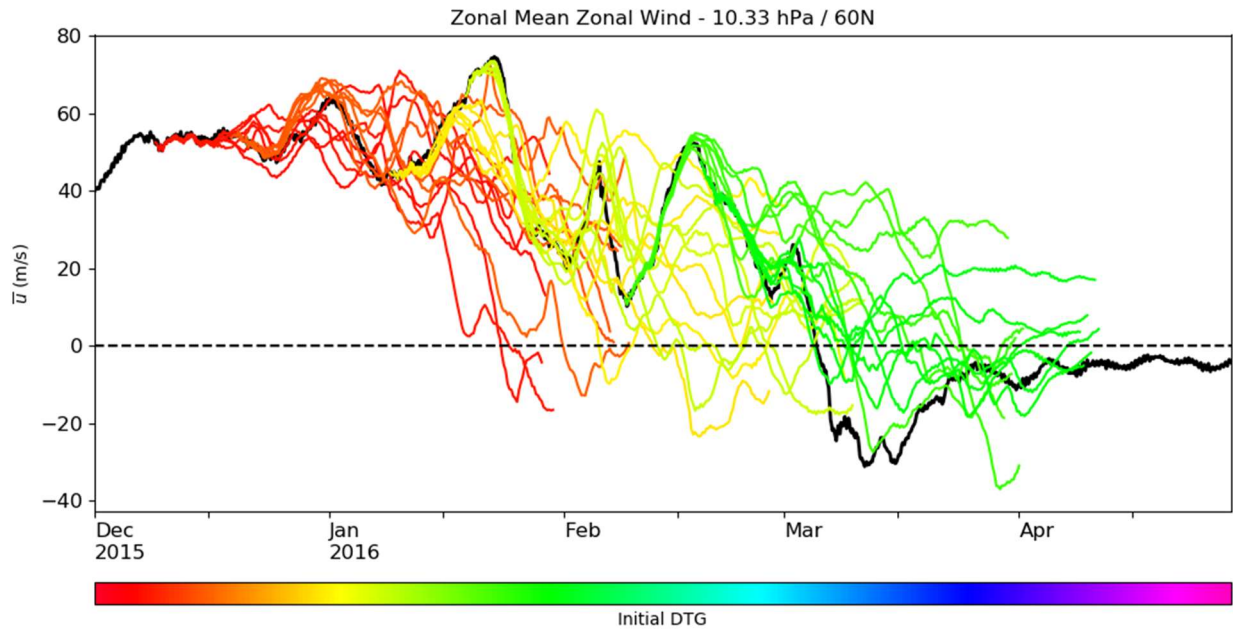


Figure 1. 50-day forecast ensembles of the stratospheric polar jet, a dominant east-west wind pattern of the Northern Hemisphere winter stratosphere that impacts predictability of surface weather patterns on subseasonal and seasonal time scales (10-50 days). Black curve indicates the observed winds during the period from 1 December 2015 to 30 April 2016. Colored curves are individual forecast members with initialization date time group (DTG) grouped by color. Observed and forecast winds were generated using the high-altitude version of the Navy Global Environmental Model (NAVGEM-HA).

Title: Dynamics of Coupled Models

Author(s): I. Shulman, B. Penta, S. Cayula, and C. Rowley

Affiliation(s): Naval Research Laboratory, Stennis Space Center, MS

CTA: CWO

Computer Resources: Cray XC40 [NAVY, MS]

Research Objective: Improve our understanding of coupled bio-optical and physical processes in the coastal zone and the variability and predictability of the coastal ocean's optical properties on time scales of 1-5 days. Investigate the coupled dynamics of ocean bio-optical, physical and atmospheric models. Provide a foundation for the development of scientifically valid, dynamically coupled atmosphere-ocean models.

Methodology: The approach is based on using nested, coupled physical-bio-optical models of the coastal region together with bio-optical and physical in-situ and remotely sensed observations (Fig. 1). Data assimilation techniques for both physical and bio-optical fields are being used to examine project research issues and objectives. Approach is also based on joint studies of the bioluminescence (BL) potential and inherent optical properties (IOPs) over relevant time and space scales. Dynamical, biochemical, physical and BL potential models are combined into a methodology for estimating BL potential and nighttime water-leaving radiance (BLw).

Results: We conducted forward and adjoint simulations to evaluate how much of the observed high BL potential signal in the Arctic during the Polar Night can be explained by the advection of plankton by the North Atlantic water, and by its interaction with the Arctic water. Published two referred papers on issues related to modeling BL potential, as well as on identifying the sources of BL potential based on BL potential and other bio-optical observations.

We conducted the first known study of bioluminescence (BL) potential dynamics at the shelf and shelf-slope break areas of the Delaware Bay. Demonstrated the transition from an autotrophic bioluminescent community to a heterotrophic bioluminescent community during upwelling favorable winds and elevated Delaware Bay river discharges.

We investigated the impact of atmospheric forcing and tidal mixing on fine-scale dynamics in a shallow, coastal area during the field program in the Gulf of Mexico. We demonstrated that combination of the cold front passage through the area, wind reversal and tidal mixing resulted in drastic changes in the model stratification: from a well-defined two layer system in salinity to the well-mixed or very weakly stratified water column.

DoD Impact/Significance: Emerging Navy electro-optical (EO) systems under development and special operations missions require an improved understanding of the ocean optical environment. This is critical for operations and weapon deployment, especially in the coastal and littoral zones. Improved basin scale to mesoscale forecast skill is critical to both military and civilian use of the oceans, particularly on the continental margins.

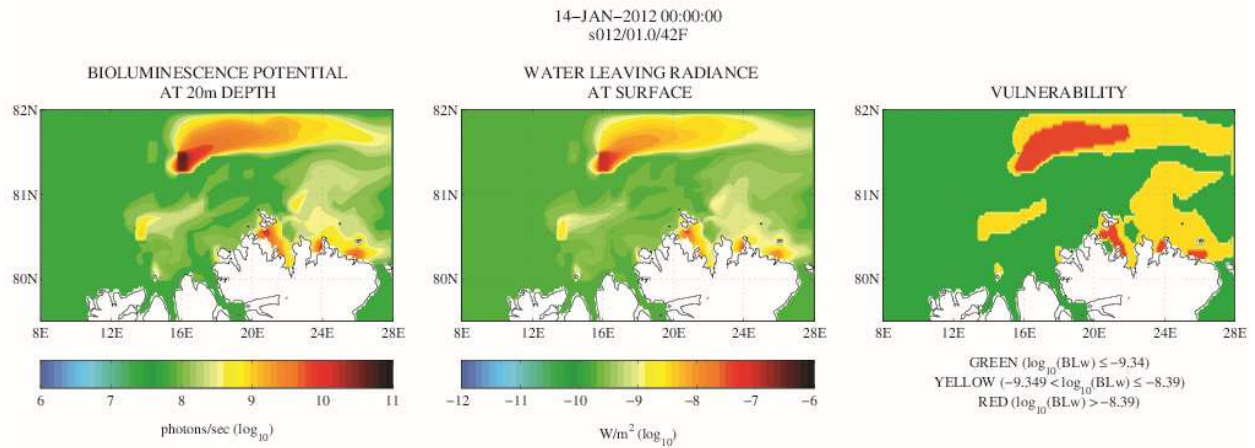


Figure 1. (Left) Prediction of BL potential at 20 m depth to the north of Svalbard, Norway; (Middle) Prediction of water-leaving radiance at surface if we stimulate BL potential at 20 m depth; (Right) Prediction of Vulnerability Risk if we stimulate BL potential at 20 m depth (based on the minimum intensity of light that could be detected by a dark-adapted eye).

Title: Probabilistic Prediction to Support Ocean Modeling Projects

Author(s): C.D. Rowley¹, L.F. Smedstad¹, C.N. Barron¹, R.S. Linzell², P.L. Spence², T.L. Townsend¹, Z.W. Lamb¹, M. Yaremchuk¹, J.C. May¹, J.M. Dastugue¹, T.A. Smith¹, J.J. Osborne V¹, G.G. Penteleev¹, B.P. Bartels², B.R. Maloy¹

Affiliation(s): ¹Naval Research Laboratory, Stennis Space Center, MS; ²Perspecta, Stennis Space Center, MS;

CTA: CWO

Computer Resources: Cray XC40/50 [ERDC, MS]; Cray XC40, HPE SGI 8600 [NAVY, MS]

Research Objectives: Develop ocean and coupled-ensemble data-assimilation (DA) and probabilistic-prediction capabilities using the Coupled Ocean Atmosphere Mesoscale Prediction System (COAMPS^{®1}), the Navy Coastal Ocean Model (NCOM), and the Hybrid Coordinate Ocean Model (HYCOM). Extend ocean data-assimilation capabilities and implement new sources of ocean and ocean-surface observations.

Methodology: Current capability for regional ocean ensemble forecasts is being extended to global ocean and regional and global coupled air-ocean-ice-wave extended-range forecast systems. Work consisted of global coupled-system ensemble initialization and metrics development, support for NRL modeling and data handling, testing of systems for operational use with new types of input data, NCOM/NCODA system development to support NAVOCEANO operational modeling, assimilation tests comparing adjoint-free and standard 4dVar, and a series of assimilation runs to test the full implementation of ice Gaussianization in NCODA (static covariance formulation). Testing and simulations of the Global Heterogenous Observation Systems (GHOST) system were performed to utilize the GHOST system for support of new platforms.

Results: We continue to support operational NCOM/NCODA systems at FNMOC using the allocation in this project. Preliminary results from NCODA with Gaussianization of ice concentration are comparable in the large scale to that from standard NCODA. Multiscale four-dimensional variational data assimilation methods for teams of autonomous ocean-observing platforms were tested. High-resolution COAMPS modeling was performed for the ICoBOD project with 1,000-point nests run at both 125 m and 50 m resolution. Satellite sea surface temperature (SST) work supported evaluations of assimilative forecasts using new SST data streams from JPSS-1/NOAA-20 VIIRS and Sentiental-3A, -33B SLSTR. A significant result of evaluating JPSS-1 VIIRS found that the prior retrieval methodology did not extend north of 80°N, assuming polar regions would remain ice-covered in all seasons, but climate change has allowed ice-free regions to emerge north of 80°N during periods of minimum ice coverage in late Arctic summer. A new version replaces the prior climatology with an up-to-date background based on Global Ocean Forecasting System (GOFS) and overlap error checks using the convergence of near-nadir swaths visible from polar-orbiting satellites. An example of the new retrieval is shown in Fig. 1.

DoD Impact/Significance: Development of extended-range forecasts depends on coupled ensemble forecasting due to the limitations of deterministic predictability and coupled DA to improve initial conditions. High resolutions and large ensembles are needed to ensure forecast reliability and accurate risk assessment in antisubmarine warfare; nuclear, chemical, and biological hazard prediction and monitoring; and search-and-rescue. Operational systems are being embedded with new data types from autonomous systems and controlling larger amounts of autonomous systems requires more complex algorithms and interface from outside of the DSRC environment, which has led to complicated system development.

¹ COAMPS[®] is a registered trademark of the Naval Research Laboratory.

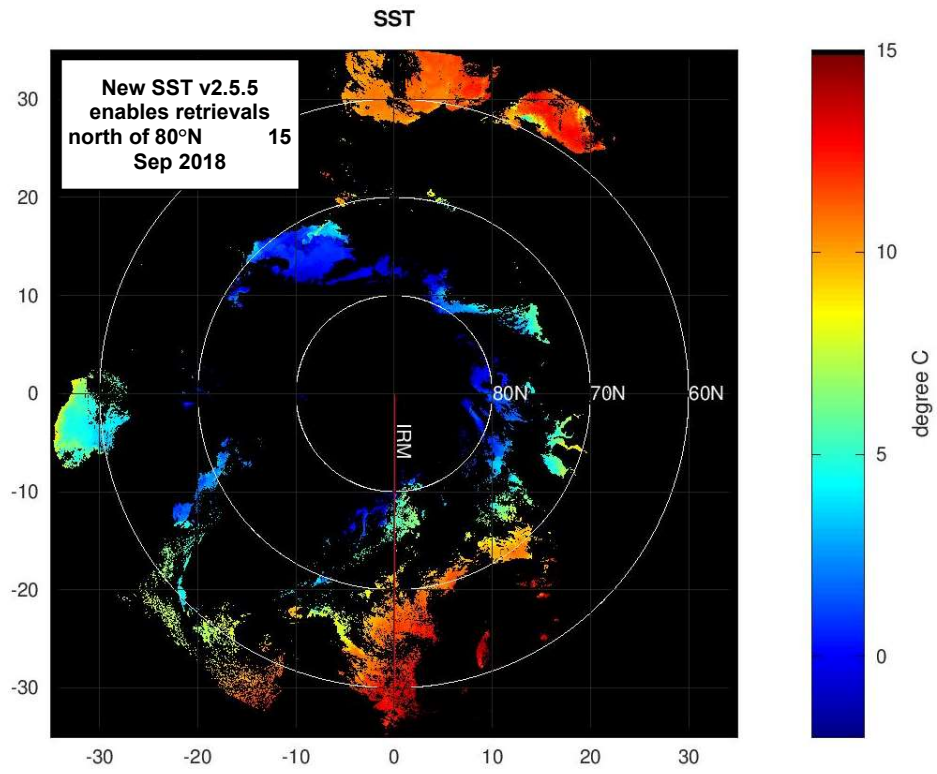


Figure 1. New retrieval.

Title: Guidance for Heterogeneous Observation Systems (GHOST)

Author(s): L.F. Smedstad¹, C.N. Barron¹, G.A. Jacobs¹, P.L. Spence², J.M. D'Addezio¹, B.P. Bartels², C.D. Rowley¹, Z.W. Lamb¹

Affiliation(s): ¹Naval Research Laboratory, Stennis Space Center, MS; ²Perspecta, Stennis Space Center, MS

CTA: CWO

Computer Resources: Cray XC40/50 [ERDC, MS]; Cray XC40, HPE SGI 8600 [NAVY, MS]

Research Objectives: GHOST determines water-sampling plans for a suite of unmanned observation systems under active Navy control. We intend to extend and verify observation-assimilation capabilities of ocean numerical models to ensure accurate use of new types/platforms of ocean and air/ocean surface observations. Researching the optimal balance of available data gives the background needed to use autonomous vehicles further improving battlespace environment forecasts.

Methodology: Observation space-time resolution limits the scales at which ocean forecast systems provide skillful information. The ocean processes of concern are mesoscale instabilities for which an ocean forecast system requires regular corrections of initial conditions to maintain skillful forecasts, and the observations considered are the regular satellite and in situ. Predominantly, the satellite altimeter constellation is the main observing system for this problem. We define constrained scales as those in which the forecast system has skill. The constrained scales are determined by successively filtering small-scale variability from 1 km resolution assimilative model experiments to reach a minimum error relative to ground-truth data. Independent observations are from the LAgrangian Submesoscale ExpeRiment (LASER) consisting of more than 1,000 surface drifters persisting for three months in the Gulf of Mexico. The decorrelation scale of the assimilation system is varied to determine the decorrelation scale that produces the smallest forecast trajectory errors. Several experiments were performed to determine appropriate influence scales of incoming platform observations. A symbiotic relationship exists between the platforms and models, and the best use of platform data must be determined. The regular corrections made to the initial condition through the data assimilation have a prescribed decorrelation length scale, which does vary spatially, and this scale must be consistent with the constrained scales. A series of ocean forecast experiments are set up with a range of decorrelation scales that average from 9 km to 140 km (Fig. 1). The scales constrained in the model experiments are not the same as the decorrelation scale of the assimilation process.

Results: In present ocean-forecast systems using regular observations, the constrained scales are larger than defined by a Gaussian filter with e-folding scale of 58 km or $\frac{1}{4}$ power point of 220 km. The decorrelation scale of 36 km used in the assimilation second-order autoregressive correlation function provides lowest trajectory errors (Fig. 2). Filtering unconstrained variability from the model solutions reduces trajectory errors by 20%.

DoD Impact/Significance: Ocean forecasts are critically reliant on regular corrections of initial conditions on a daily basis via use of environmental observations. We must optimize the parameters controlling the influence scales of observations to produce accurate forecasts. This influences the accuracy of battlespace environment forecasts for the operational Navy operations. These include Anti-Submarine Warfare (ASW) operations, for which sound speed is critical, and currents that affect Naval Special Warfare (NSW) and Mine Warfare (MIW). Search-and-rescue (SAR) operations are also dependent on accurate ocean forecasts. HPC resources support research and development efforts on data assimilation and forecasting.

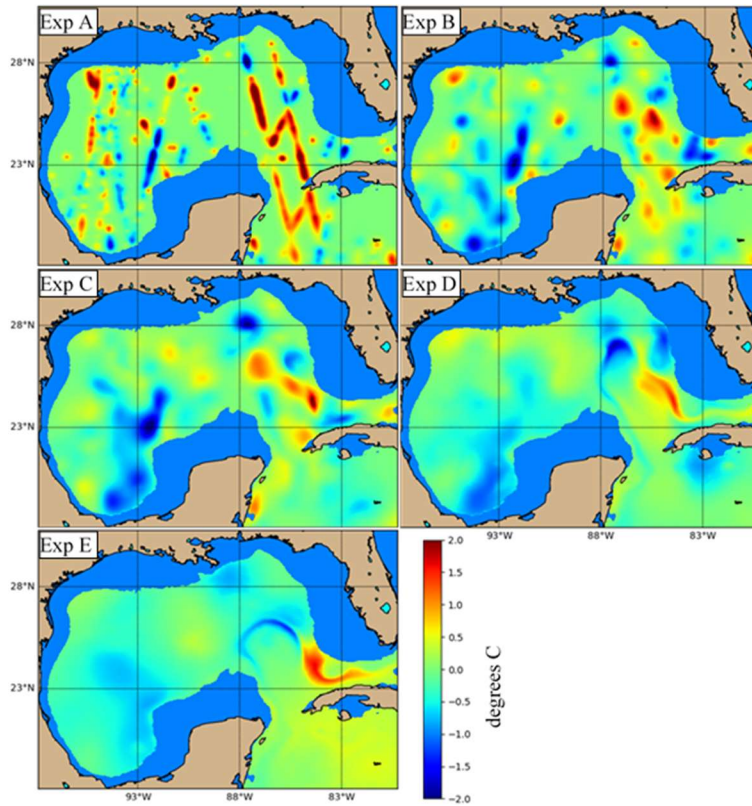


Figure 1. The temperature adjustment to the model at 200 m on March 15, 2016, provides an example of the decorrelation scale effects across the five experiments. The satellite tracks are apparent in experiment A with very localized increments. The flow dependent correlation influence is apparent in experiments D and E around the edge of the Loop Current.

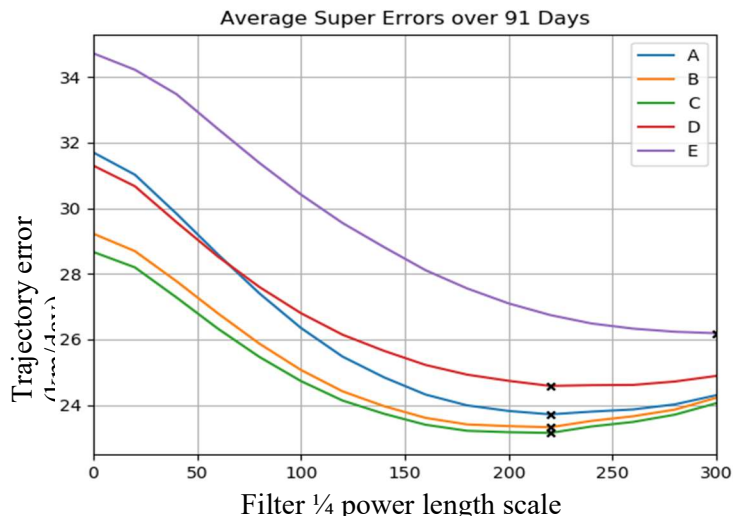


Figure 2. RMS trajectory errors for each of the five experiments as a function of the Gaussian filter $\frac{1}{4}$ power scale. Experiment C provides the lowest errors, and most experiments (A through D) consistently have error minima at the 220 km $\frac{1}{4}$ power point of the Gaussian filter aligning with a 36 km decorrelation length scale of the assimilation process.

Title: High Resolution Global Ocean Reanalysis

Author(s): P.J. Hogan

Affiliation(s): Naval Research Laboratory, Stennis Space Center, MS

CTA: CWO

Computer Resources: Cray XC40, HPE SGI 8600 [NAVY, MS]

Research Objectives: Perform a 25-year high-resolution ocean reanalysis. These reanalyses are useful for several purposes, including for use as boundary conditions for regional models run in hindcast mode (i.e. covering previous time periods), initial conditions for global and regional reforecasting, construction of climatologies for ocean, sea ice, and acoustic variables, for use as a verifying analysis for reforecasting, and for comparison against other global ocean reanalyses, including the Navy's Earth System Prediction Capability (fully coupled) atmosphere-ocean-sea ice reanalysis (but which only covers a few select individual years).

Methodology: A reanalysis is a rerunning of a data-assimilative ocean or sea-ice model using archived observations. It may or may not use observations from the "future" (i.e. a symmetric DA time window), but it definitely will use the same model setup throughout, which makes it more consistent over time than real-time operational products that are otherwise similar. For the ocean, satellite altimeter observations are the most prolific source of large-scale (global) observations, allowing us to start in 1993. The proposed reanalysis will use the Navy Coupled Ocean Data Assimilation (NCODA) system, which also includes advanced data QC (quality control), with 3-dimensional Variational Analysis (3DVar). The primary data types are sea surface height anomaly (SSHA) from satellite altimetry, sea surface temperature (SST) and subsurface T & S profiles. Synthetic T & S profiles are used for downward projection of SSHA and SST. The ocean/sea-ice system is driven by atmospheric products from the National Centers for Environmental Prediction (NCEP) Climate Forecast System Reanalysis (CFSR), which is itself an atmospheric reanalysis, thus ensuring consistent wind and heat flux forcing over the reanalysis time period.

Results: During FY19, the pathfinder award allowed ~6.5 reanalysis years to be completed, including the post-processing. The post-processing consists of calculating various model diagnostics, statistics, plots, and error estimates. Furthermore, the model temperature and salinity profiles are used as input to the APARMS code which calculates acoustic parameters such as sound speed, sonic layer depth, below-layer gradient, etc. In total, ~9 years of the reanalysis was completed, augmented by other HPC accounts (primarily the Eddy-Resolving Global/Basin-Scale Ocean Modeling project (covering years 2009-2016).

DoD Impact/Significance: The Fleet Numerical Meteorology and Oceanography Center (FNMOC) and the Naval Oceanographic Office (NAVOCEANO) have requirements to maintain up-to-date ocean climatologies and databases to provide the Navy with impactful information globally. Thus, this proposed reanalysis will be used to address this Navy requirement. Specifically, the reanalysis will allow for updating the existing Navy model-based global ocean climatologies at higher vertical and horizontal resolutions than are currently available providing safety of navigation information in areas that are currently under resolved. The reanalysis also will be used to provide global monthly and inter-annual statistics of oceanographic parameters that are significant to the Fleet and shall include Navy-relevant statistics for ocean currents, temperature, salinity, elevation, and sound speed. These parameters and statistics are instrumental to the Navy's planning cycle to help maximize the effectiveness and safety of personnel and equipment deployed worldwide.

Tem. vs. depth error analysis GOFS 3.1-73.X July

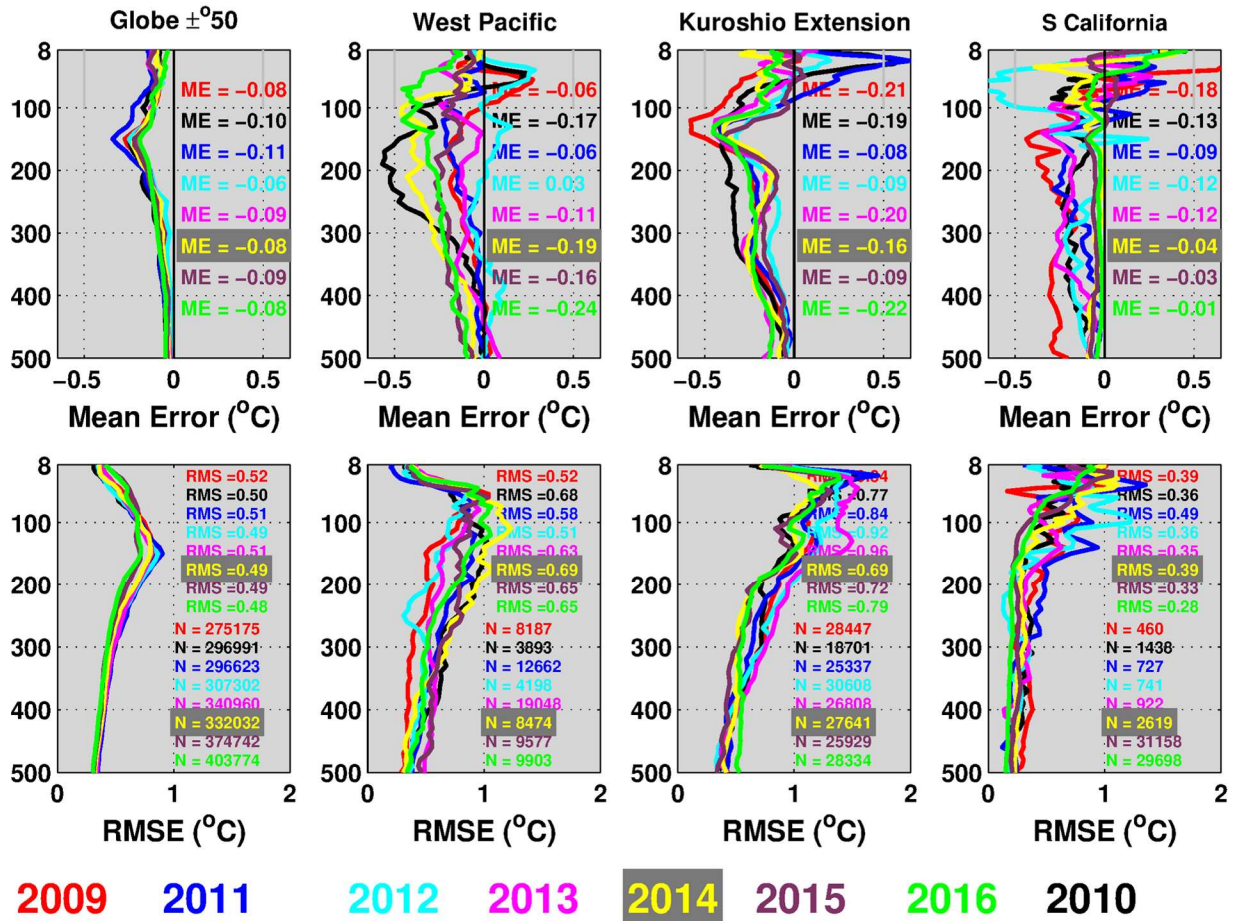


Figure 1. Mean Error (ME) (top) and Root Mean Square (RMS) Error (bottom) for temperature as a function of depth for the globe (+/- 50°) and selected regions, for July from years 2009-2016 from the reanalysis. The analysis is against independent observations for the 24-hour forecast each day of July. The depth averaged values are listed in each panel and N= indicates the number of observations used in the calculations.

Title: Bio-Optical Modeling and Forecasting

Author(s): J.K. Jolliff, S. Ladner, T. Smith, and C. Wood

Affiliation(s): Naval Research Laboratory, Stennis Space Center, MS

CTA: CWO

Computer Resources: Cray XC40 [NAVY, MS]

Research Objectives: The research objectives for FY19 consist of 2 components: (1) to develop and validate three-dimensional, coastal optical prediction systems that leverage results from the Coupled Ocean Atmosphere Mesoscale Prediction System (COAMPS^{®1}) and the Navy Coastal Ocean Model (NCOM); and (2) to begin an operational data flow of satellite-estimated surface ocean optical properties into operational numerical ocean models. The second objective supports the task of improving ocean model representation of in-water radiative transfer. This is also the main task of the 6.4 “Visible Band Satellite Data to Improve Ocean Model Radiative Transfer” program. Most of the allocated HPC hours were devoted to this task, and so this will be the main focus of this brief report.

Methodology: Numerical ocean models must have a designated numerical representation of the attenuation of solar shortwave radiation into the surface ocean. This attenuation calculation determines the potential ocean heating rate and thermal balance for each time step, and thus it broadly impacts thermal- and density-state-variable spaces. The default calculation for the present class of operational numerical ocean models is based upon the *Jerlov* water types [Paulson and Simpson, 1977]. This is the case for NCOM, the ocean numerical model component of COAMPS. Since these tabular attenuation functions do not recognize real-time optical data from the oceans, they are invariably in error. In COAMPS sensitivity experiments, correction of this well-known source of error may result in substantial differences in simulated ocean temperature, mixed-layer depth, density, air temperature, relative humidity, and the computation of turbulent thermal-energy fluxes within the simulated air-sea systems [Jolliff et al., 2012; Jolliff and Smith, 2014]. Since the COAMPS-simulated heat fluxes are particularly sensitive to shortwave attenuation differences in the ocean model (Fig. 1), examples of large discrepancies in EM duct heights and occurrences have been identified in these COAMPS sensitivity experiments.

Results: FY19 saw the completion of work to build the very first ocean-optics branch of the Navy-coupled Ocean Data Assimilation (NCODA) Quality Control (QC) system. Global, monthly, seasonal, and annual optical product climatology files have been developed that will be used as a part of the NCODA variational analysis. Similar to the variational analysis performed on sea surface temperature (SST), the quality control and analysis will ensure that an appropriate (and complete) analysis field of optical attenuation is provided for the ocean models. HPC resources are vital to this effort, as the NCODA QC and analysis codes are being developed/tested on HPC systems using operational build scripts. This will ease transition of the operational systems. We also have developed an NCODA-COAMPS testing domain along the Louisiana coast that will be used as our initial demonstration/validation work for the end-to-end data flow from satellite to NCODA to modeling systems.

DoD Impact/Significance: This research falls directly within the Naval S&T Strategic Plan Focus Area “Assure Access to the Maritime Battlespace” under the “Match Environmental Predictive Capabilities to Tactical Planning Requirements” objective. The ability to forecast the coastal ocean environment is dependent upon high-resolution COAMPS output fidelity to real-world physical dynamics. Improvement of operational ocean models when given realistic solar shortwave attenuation data has been demonstrated, and moving this work to the operational level is of paramount importance.

¹ COAMPS[®] is a registered trademark of the Naval Research Laboratory.

PERCENT CHANGE MEAN LAHFLX+SEHFLX (PLUME001 - PLUME002)/PLUME002
02-JUN-2015 00:00:00 - 12-JUN-2015 00:00:00

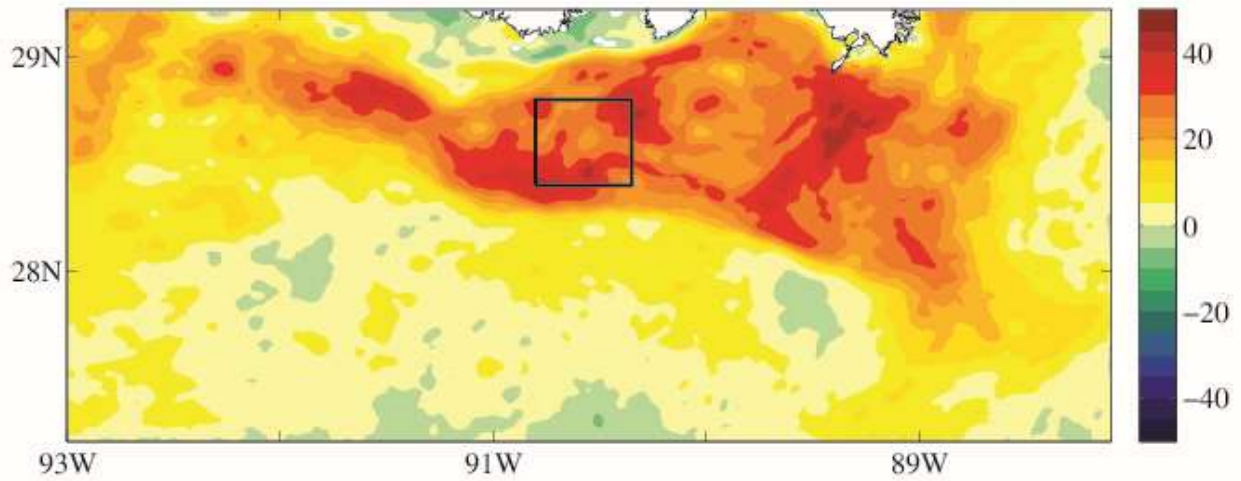


Figure 1. Difference (as percent) between the default (operational) COAMPS model and the prototype with correct optical attenuation of solar shortwave. The positive difference indicates increased fluxes from the ocean to the atmosphere for the prototype (feedback) COAMPS simulation. This is the coastal Louisiana test bed location for COAMPS development.

Title: Atmospheric Process Studies

Author(s): N. Barton¹, T. Whitcomb¹, J. Ridout¹, K. Viner¹, J. McLay¹, W. Crawford², M. Liu¹, and C. Reynolds¹

Affiliation(s): ¹Naval Research Laboratory, Monterey CA; ²American Society for Engineering Education, Washington, DC

CTA: CWO

Computer Resources: Cray XC40 [ARL, MD]; Cray XC40/50 [ERDC, MS]; Cray XC40, HPE SGI 8600 [NAVY, MS]

Research Objectives: The research objectives of this project are to improve our understanding of the fundamental dynamical and physical processes that operate in the atmosphere and to develop and test a state-of-the-art global atmosphere prediction system that includes data assimilation and ensembles.

Methodology: Our work focuses on improving the accuracy and efficiency of the Navy Global Environmental Model (NAVGEM). NAVGEM is the Navy's current global atmosphere operational numerical weather-prediction model, and is used for basic and applied atmospheric research within this project. NAVGEM is developed in conjunction with its data-assimilation capability, NAVDAS-AR, as initial conditions are very important to numerical systems. In addition, seamless prediction across multiple temporal scales and earth-system components is the next frontier of numerical prediction. NAVGEM is being developed and tested when tightly coupled with the HYbrid Coordinate Ocean Model (HYCOM) and the Los Alamos Community sea Ice Code (CICE) using the Earth System Modeling Framework (ESMF) tools under the Earth System Prediction Capability (ESPC) national program.

Results: This year's advances largely fall into the categories of (1) NAVGEM 2.0 testing for transition to FNMOG, (2) coupled physics updates for NAVGEM 2.0, and (3) ensemble forecasting with NAVGEM stand-alone and the coupled model. (1) The test runs for the NAVGEM v2.0 validation test report (VTR) were performed several times in FY19 because of capabilities added throughout the testing. Figure 1 shows the scorecard for NAVGEM v2.0 over the northern hemisphere winter period; the score is a +11 with statistically significant improvements over NAVGEM v1.4.3 when examining 500 hPa geopotential height anomaly correlations (+3), rms errors (+3) in both hemispheres, and 1,000 hPa geopotential height anomaly correlation in both hemispheres (+2). (2) We implemented physics routines designed for subseasonal forecasting with the coupled model into the stand-alone NAVGEM 2.0. This work is preparing the way for testing NAVGEM 2.0 within the coupled model. (3) For the ensemble forecasting system (EFS), we completed a validation test report for a new NAVGEM 2.0 multi-physics deep-convection ensemble including a comprehensive scorecard validation covering both the summer and winter seasons and encompassing the extended forecast range (0-21 days). In addition, we developed a new stochastically perturbed physical tendency (SPPT) capability for the NAVGEM v2.0 EFS to help account for model error in probabilistic forecasts, and extended the NAVGEM v1.4.4 EFS SST variation capability to the NAVGEM v2.0 EFS. For the coupled model, two new capabilities have been tested this FY: (a) a method to account for model error during the ensemble forecast, and (b) a method to relax the perturbations developed in the data assimilation schemes to increase spread in the initial conditions. The modifications have proved beneficial to the EPS in the stand-alone and coupled systems.

DoD Impact/Significance: The continued development of our global forecast system is making significant positive impacts on the skill of our weather forecasts and DoD predictions dependent on weather forecasting (i.e., ocean modeling, wave modeling, ship routing). Developments in coupled modeling and extended-range probabilistic forecasting increase the utility of the forecast and potential number of users. This development serves to provide an improved modeling system for studying the dynamical and physical processes in the atmospheric system.

TOTAL SCORE: 11

Show 100 entries Filter:

| Reference | Level | Region | Lead time | Variable | Level type | Metric | Weight | Score |
|---------------|--------|---------------------|-----------|---------------------|------------|---------------------|--------|-------|
| Fixed Buoy | None | Northern Hemisphere | 96 | Wind Speed | surface | Mean Error | 2 | +2 |
| Fixed Buoy | None | Tropics | 96 | Wind Speed | surface | Mean Error | 2 | 0 |
| Radiosondes | 100.0 | Global | 96 | Geopotential Height | pressure | RMS Error | 1 | +1 |
| Radiosondes | 250.0 | Global | 96 | Air Temperature | pressure | RMS Error | 1 | 0 |
| Radiosondes | 250.0 | Global | 96 | Wind | pressure | Vector RMS Error | 1 | 0 |
| Radiosondes | 500.0 | Global | 96 | Geopotential Height | pressure | RMS Error | 1 | 0 |
| Radiosondes | 850.0 | Global | 96 | Air Temperature | pressure | RMS Error | 1 | 0 |
| Radiosondes | 850.0 | Global | 96 | Wind | pressure | Vector RMS Error | 1 | 0 |
| Self Analysis | 200.0 | Northern Hemisphere | 96 | Wind | pressure | Vector RMS Error | 1 | 0 |
| Self Analysis | 200.0 | Southern Hemisphere | 96 | Wind | pressure | Vector RMS Error | 1 | 0 |
| Self Analysis | 200.0 | Tropics | 96 | Wind | pressure | Vector RMS Error | 1 | 0 |
| Self Analysis | 500.0 | Northern Hemisphere | 120 | Geopotential Height | pressure | Anomaly Correlation | 2 | +2 |
| Self Analysis | 500.0 | Southern Hemisphere | 120 | Geopotential Height | pressure | Anomaly Correlation | 1 | +1 |
| Self Analysis | 500.0 | Northern Hemisphere | 120 | Geopotential Height | pressure | RMS Error | 2 | +2 |
| Self Analysis | 500.0 | Southern Hemisphere | 120 | Geopotential Height | pressure | RMS Error | 1 | +1 |
| Self Analysis | 850.0 | Northern Hemisphere | 96 | Wind | pressure | Vector RMS Error | 1 | 0 |
| Self Analysis | 850.0 | Southern Hemisphere | 96 | Wind | pressure | Vector RMS Error | 1 | 0 |
| Self Analysis | 850.0 | Tropics | 96 | Wind | pressure | Vector RMS Error | 2 | 0 |
| Self Analysis | 1000.0 | Northern Hemisphere | 120 | Geopotential Height | pressure | Anomaly Correlation | 1 | +1 |
| Self Analysis | 1000.0 | Southern Hemisphere | 120 | Geopotential Height | pressure | Anomaly Correlation | 1 | +1 |

Showing 1 to 20 of 20 entries

Figure 1. The NAVGEM scorecard for evaluation of the NAVGEM 2.0 system versus the NAVGEM 1.4.3 system for the period January 1, 2014 – May 1, 2014. The score for each item is given in the final column.

Title: Eddy-Resolving Global/Basin-Scale Ocean Modeling
Author(s): E.J. Metzger and J.F. Shriver
Affiliation(s): Naval Research Laboratory, Stennis Space Center, MS
CTA: CWO

Computer Resources: Cray XC40/50 [ERDC, MS]; Cray XC40, HPE SGI 8600 [NAVY, MS]

Research Objectives: Modeling component of a coordinated 6.1-6.4 effort on the problem of eddy-resolving global and basin-scale ocean modeling and prediction. This includes increased understanding of ocean dynamics, model development, model validation, naval applications, oceanic data assimilation, ocean-predictability studies, observing-system simulation studies, and nested models.

Methodology: The appropriate choice of vertical coordinate is a key factor in ocean model design. Traditional ocean models use a single coordinate type to represent the vertical, but no single approach is optimal for the global ocean. Isopycnal (density tracking) layers are best in the deep stratified ocean, Z-levels (constant depths) provide high vertical resolution in the mixed layer, and terrain-following levels are often the best choice in coastal regions. The HYbrid Coordinate Ocean Model (HYCOM) has a completely general vertical coordinate (isopycnal, terrain-following, and Z-level) via the layered continuity equation that allows for an accurate transition from the deep to shallow water.

Results: 9 refereed articles, 3 non-refereed articles published or in press in FY19.

Global modeling: Validation and verification work for the Global Ocean Forecast System (GOFS) 3.5 (1/25° HYCOM with tides/CICE) was completed. This culminated in a validation test report being submitted to the validation test panel in mid-September. Ocean metrics indicated improved temperature and salinity structure in GOFS 3.5 compared with GOFS 3.1. An updated sea ice model (CICE version 5.1.2 vs. 4.0) led to improved Arctic sea ice edge error statistics in GOFS 3.5 over the entire 7-day forecast length. Significant hours also have been used to keep GOFS 3.5 in near real-time.

Sea ice modeling: Twin 5-month seasonal forecasts were integrated to predict the September 2018 mean and minimum ice extent using the fully coupled Navy Earth System Prediction Capability (ESPC). In the control run, ensemble forecasts were initialized from operational GOFS 3.1 but did not assimilate sea ice thickness data. Another set of forecasts were initialized from the same GOFS 3.1 fields but with sea ice thickness derived from CryoSat-2 (CS2). The Navy ESPC ensemble mean September 2018 minimum sea ice extent initialized with GOFS 3.1 ice thickness was overpredicted by 0.68 M km² (5.27 M km²) versus the ensemble forecasts initialized with CS2 ice thickness that had an error of 0.40 M km² (4.99 M km²), a 56% reduction in error.

Sea ice assimilation: Added sea ice thickness as a new observation type in NCODA and added the ability to assimilate CryoSat2 sea ice thickness that has been tested in a regional domain. Testing that assimilated NAVOCEANO derived swath AMSR2 sea ice concentration data and applied IMS ice mask inside NCODA. This reduced ice edge errors by 19% in the Arctic and 11% in the Antarctic.

DoD Impact/Significance: Data-assimilative eddy-resolving models are important components of global ocean and sea ice-prediction systems. Ocean forecasts are valuable for tactical planning, optimum-track ship routing, search-and-rescue operations, and the location of high current-shear zones. The sea ice environment has become increasingly important for strategic and economic reasons given the diminishing trend in sea ice extent and thickness and the potential summertime opening of the Northwest Passage and Siberian sea routes. Fractures, leads and polynya forecasts are also valuable to the naval submarine community.

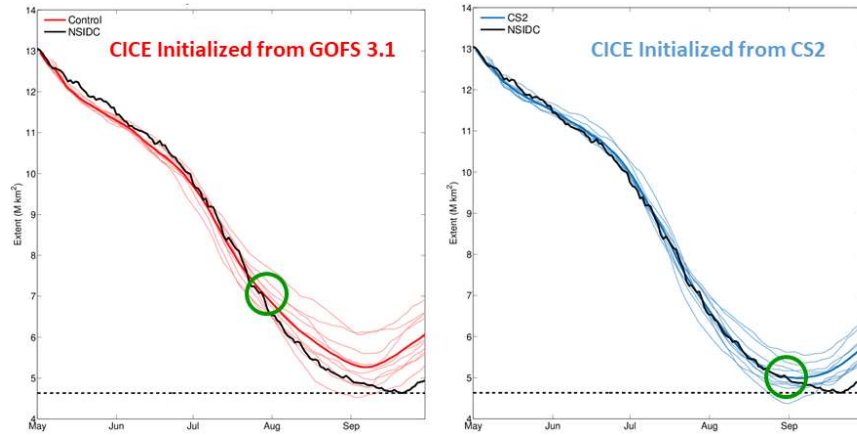


Figure 1. Forecast sea ice extent (M km^2) for the period of May 1 – September 2018 for control run (left, red) and forecasts initialized with CS2 sea ice thickness (right, blue). Open circles denote date when ensemble means begin to separate from NSIDC (black curve) observed ice extent. Using CS2 data, the forecast skill is extended by 33 days. The thick, colored lines are the ensemble mean and the thin, colored lines are the individual ensemble members.

Title: Coastal Mesoscale Modeling – COAMPS-TC
Author(s): W.A. Komaromi and P.A. Reinecke
Affiliation(s): Naval Research Laboratory, Monterey CA
CTA: CWO

Computer Resources: Cray XC40 [NAVY, MS]

Research Objectives: Tropical cyclones (TCs) are a significant threat to DoD assets around the world. The objective of this project is to develop improved TC forecast guidance for the DoD and the Navy. In 2019, we have focused on two specific goals: (1) to test and implement a cycled ocean data-assimilation system for our real-time TC forecasting model, which will make more accurate intensity forecasts possible; and (2) to produce more reliable probabilistic forecasts via our ensemble forecasting system, as explained below.

Methodology: COAMPS-TC^{®1} is a special variant of the Coupled Ocean/Atmosphere Mesoscale Prediction System (COAMPS^{®2}) developed at NRL to predict TC track, intensity and structure around the globe. In previous projects, the Navy Coupled Ocean Data Assimilation (NCODA) system has been demonstrated to improve the initial ocean analysis, which has positive impacts on both atmospheric and oceanic forecasts. The state of the ocean is critically important for TC forecasts, as warm sea-surface temperatures are their primary source of energy. For the current HPC project, we are currently testing and demonstrating the feasibility of real-time COAMPS-TC forecasts using NCODA. While COAMPS-TC produces highly skillful deterministic TC forecasts, weather prediction tends to be probabilistic in nature. Uncertainty in the initial state of the atmosphere due to insufficient observations, errors in our measurements, and approximations in our model equations, all contribute to errors in the model forecast, which grow with time. For this reason, we also have developed the COAMPS-TC Ensemble, which is a collection of forecasts made using the same model at the same initial time, but with slightly different assumptions about the initial state of the atmosphere and/or slightly different model physics.

Results: In 2019, COAMPS-TC and the Ensemble had amongst the best track forecasts for Hurricane Dorian of all available guidance, keeping the storm offshore while most guidance incorrectly insisted upon a Florida landfall (Fig. 1, left). For Typhoon Faxai, COAMPS-TC correctly predicted a path directly over Tokyo Bay three days in advance. The NCODA system is found to produce a more realistic cold wake, associated with wind-induced upwelling, than the existing system. The realism of the cold wake is particularly important for correctly predicting the intensity of slow-moving, intense cyclones such as Hurricane Dorian. Additionally, it was found that increasing the number of members in the COAMPS-TC Ensemble from 11 to 21 produces smoother, more reliable probability distributions for both track (not shown) and intensity (Fig. 1, right). Upgrades to the COAMPS-TC core model for 2019 have resulted in improved skill. As such, the environmental perturbations have been tuned (reduced) to produce a superior spread-skill score versus previous variants, which were slightly over-dispersive for track.

DoD Impact/Significance: Forecasters at the DoD's Joint Typhoon Warning Center (JTWC), as well as Fleet Weather Centers San Diego and Norfolk rely upon real-time TC forecasts from COAMPS-TC and the COAMPS-TC Ensemble, along with corresponding wind and wave guidance for various decision aids. Improved confidence and increased forecast lead time also increase the lead time for sortie decision making, as well as general fleet routing and awareness. The HPC DSRC provides a unique environment to test and improve the COAMPS-TC probabilistic forecast system prior to transition for operation use at FNMOC. These improvements will inform future decisions regarding the design of probabilistic TC prediction systems.

¹ COAMPS-TC[®] is a registered trademark of the Naval Research Laboratory.

² COAMPS[®] is a registered trademark of the Naval Research Laboratory.

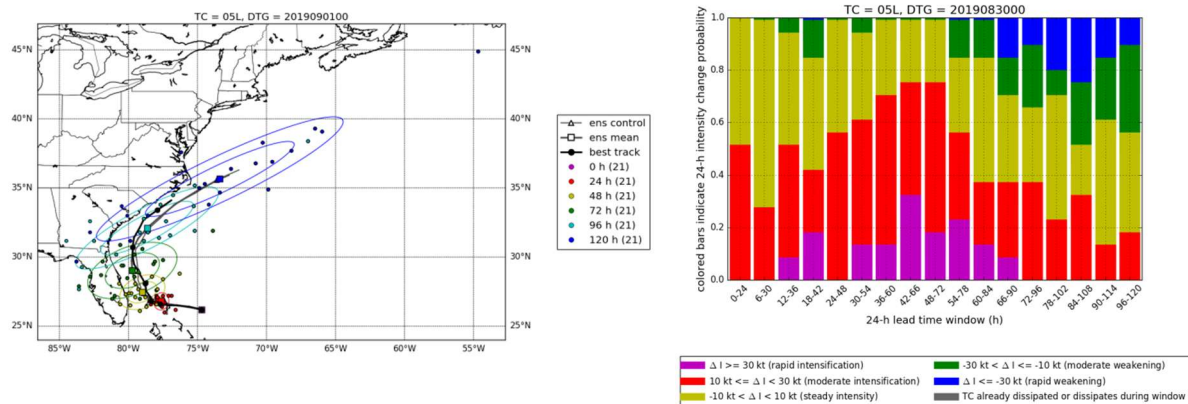


Figure 1. (Left) COAMPS-TC Ensemble 120-h track forecasts for Hurricane Dorian from forecasts initialized 00 UTC 1 September 2019. The unperturbed control member (grey with triangles), ensemble mean (grey with squares), and the verifying “best track” (black with circles) are shown. Colors indicate forecast lead time (hours). Ellipses encapsulate $\frac{1}{3}$ and $\frac{2}{3}$ of the forecast distribution at each lead time. (Right) 24-h intensity change probabilities (out to 120 h) for Hurricane Dorian from the COAMPS-TC Ensemble forecast initialized 00 UTC 30 August 2019. The red and magenta shading indicate the predicted probabilities of moderate and rapid intensification, respectively.

Title: The Effect of Langmuir Turbulence in Upper Ocean Mixing
Author(s): Y. Fan
Affiliation: Naval Research Laboratory, Stennis Space Center, MS
CTA: CWO

Computer Resources: Cray XC40 [NAVY, MS]

Research Objectives: The goal of this project is to understand the effect of Langmuir turbulence (LT) in upper-ocean mixing within a broad parameter space and during complex oceanic conditions through extensive ocean, wave, and Large Eddy Simulation (LES) modeling studies. The results from this project will provide a greater understanding of the generation, growth and decay of the LT, how it is affected by the mesoscale and submesoscale structures and its impact on vertical and horizontal momentum and heat fluxes within the ocean on larger scales.

Methodology: The NCAR Large Eddy Simulation (LES) model is used to determine the effect of LT in real, complex ocean and atmospheric settings. A suite of LES experiments is conducted for the CASPER-East field experiment with constant variation of wind forcing, strong local variability in temperature and salinity, and cooling events. A suite of idealized experiments also is conducted to determine the effect of large wind-wave misalignments. These idealized experiments are also used to support the development of a more physically based Langmuir turbulence parameterization.

Results: The Casper East field experiments are conducted in the Gulf Stream region with strong fluctuations of river inflow, which brings fresh and cold water and significantly alters the temperature and salinity in the research region both spatially and temporally. At the same time, large wind variations and strong cooling events occur constantly during the research period. Through the LES experiments conducted at this site, we found that while LT enhances the turbulence in the water column and deepens the mixed layer during most of the simulation period, being consistent with previous studies, significant reduction in turbulent intensity is observed in the simulation with Stokes drift, compared with that without Stokes drift, during a one-day period, in contradiction of previous findings. Two main reasons are found to contribute to reducing the turbulence: the large misalignment between the wind and surface gravity waves and the interaction of LT with deep convection. The large wind-wave misalignment not only reduces the turbulence in the water column and traps it in a shallower surface layer, but also traps the momentum in shallower surface layer, thus producing large surface-mean currents and consequently leads to further reduction of the turbulent intensity. During the cooling event, strong upwelling induced by LT at the base of the mixed layer counteracts on the downwelling associated with the deep convection and reduces the total turbulence level in the water column. This study also demonstrated that even if the model relaxes its temperature and salinity towards observations, the turbulence in the water column is still very different with and without the presence of surface gravity waves. Since available ocean observations are very limited both spatially and temporally, good representation of the turbulence in the water column is still critical for ocean models, especially for the transfer of heat, momentum, and gas within the oceanic boundary layer.

DoD Impact/Significance: This study can help improve Battlespace Environment forecasting accuracy for both ocean and atmosphere (HYCOM, NCOM and COAMPS^{®1}). Better understanding of the mechanism, growth and dissipation of LT will help improve the air-sea interaction process in our coupled models (i.e. COAMPS and ESPC), which will lead to more accurate vertical thermal profile simulations in the ocean models and better predication of acoustic and optic properties in the upper ocean.

¹ COAMPS[®] is a registered trademark of the Naval Research Laboratory.

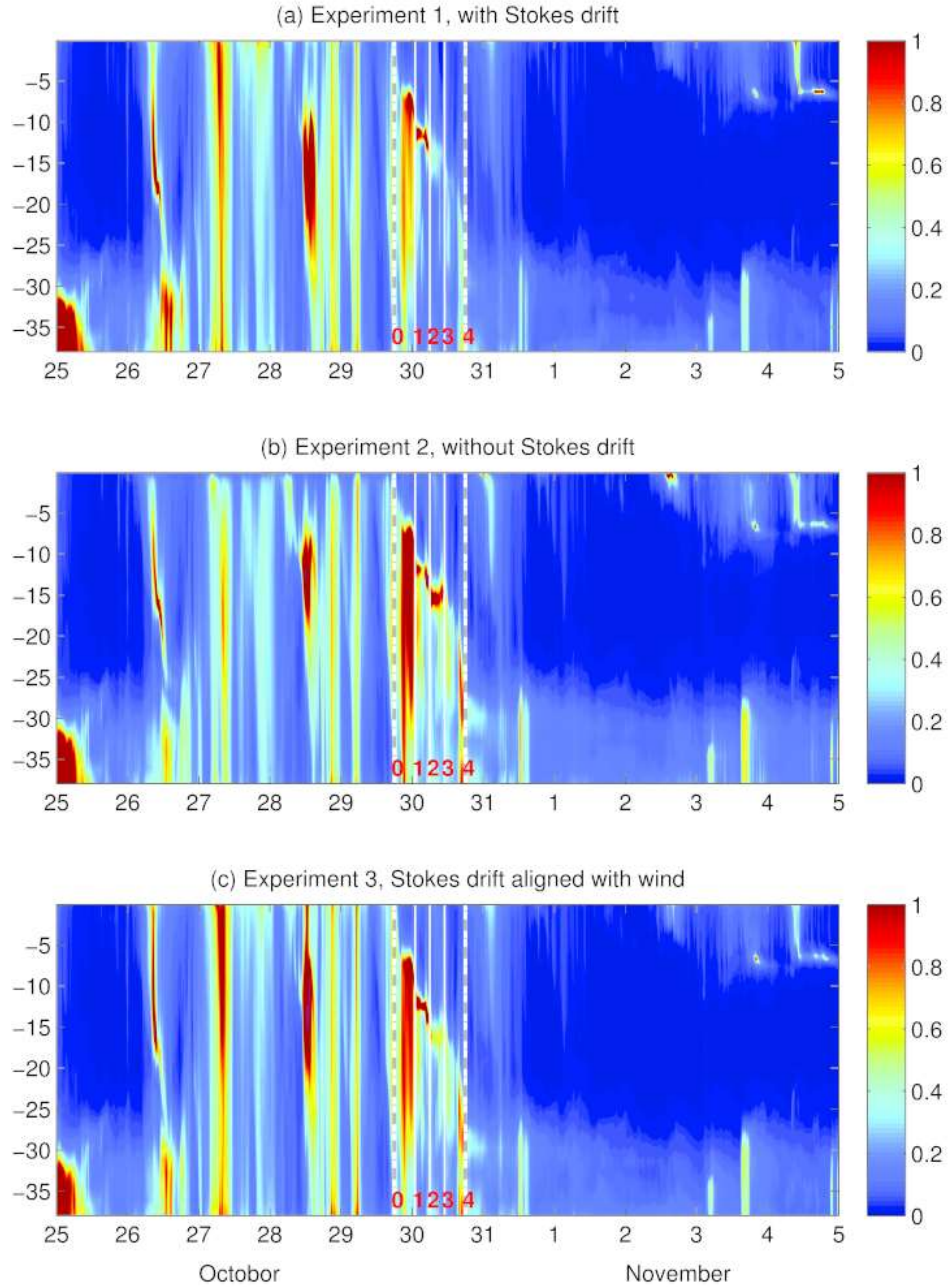


Figure 1. LES-simulated turbulent intensity defined as the magnitude of the turbulent velocity divided by the magnitude of resolved mean current

$$(I = \sqrt{\frac{u'^2 + v'^2 + w'^2}{3}} / \sqrt{u^2 + v^2 + w^2})$$

for (a) experiment 1 with the Stokes drift, (b) experiment 2 without the Stokes drift, and (c) experiment 3 with artificially aligned Stokes drift along the wind direction. The gray dash-dotted vertical lines highlighted the period with reduced turbulence with the inclusion of Stokes drift, and the thin, white lines indicate identified short research periods.

THIS PAGE INTENTIONALLY LEFT BLANK



Signal Image Processing

SIP covers the extraction of useful information from sensor outputs in real time. DoD applications include surveillance, reconnaissance, intelligence, communications, avionics, smart munitions, and electronic warfare. Sensor types include sonar, radar, visible and infrared images, and signal intelligence (SIGINT) and navigation assets. Typical signal-processing functions include detecting, tracking, classifying, and recognizing targets in the midst of noise and jamming. Image-processing functions include the generation of high-resolution low-noise imagery, and the compression of imagery for communications and storage. The CTA emphasizes research, evaluation, and testing of the latest signal-processing concepts directed toward these embedded systems. Usually, such processors are aboard deployable military systems and hence require hefty packaging, minimum size, weight, and power. System affordability is expected to improve an order of magnitude through the development of scalable codes running on flexible HPC systems. This will enable the traditional, expensive, military-unique 'black boxes' required to implement high-speed signal/image processing to be replaced by COTS HPC-based equipment.

Title: Reducing the Burden of Massive Training Data for Deep Learning

Author(s): L.N. Smith, E.A. Gilmour, S.N. Blisard, and K.M. Sullivan

Affiliation(s): Naval Research Laboratory, Washington, DC

CTA: SIP

Computer Resources: Cray XC40/50 [ERDC, MS]

Research Objectives: The successes of deep learning in the past several years rely on three pillars: faster computer hardware, lots of labeled training data, and new algorithms. In this basic research project, we design, develop, and evaluate novel deep-learning algorithms for training deep neural networks that significantly reduce the training time and eliminate the current requirement for massive labeled training datasets in order to allow application of deep networks in situations in which labeled data is scarce or expensive.

Methodology: Our methodology is primarily based on the following process: Based on our understanding, we develop hypotheses, which often requires experimenting with many variations of neural networks and hyperparameters to determine which of those hypotheses are beneficial and when they are beneficial, and to develop a new understanding as to why they work. The majority of the work done was in the most popular deep-learning frameworks: TensorFlow, Caffe, Torch, and PyTorch. Hence, it is valuable that the HPC staff installs and maintains these frameworks. Typically, our experiments build on previous work, so the first step is to download code from github.com, to replicate previous results, and then to test our own hypotheses.

Results: In FY19, the majority of the work on this project attempted to combine our primary objective of reducing the amount of labeled data needed to train a neural network with other high-priority goals. One such effort was to develop new approaches for novelty detection in image classification so that an object that was not one of the training classes can be identified and used to train a second network. Of course, we needed methods that would be effective in training this second network with only one example of the class. Figure 1 provides a diagram of our architecture, in which Net_{base} detects the base classes plus any novel object that does not belong to any of the original classes. Then, Net_{novel} is trained to recognize all of the novel classes.

DoD Impact/Significance: Our work on reducing the amount of labeled training data needed, new approaches to novelty detection, and improving the adversarial robustness of networks are fundamental achievements focused on the three pillars of deep learning and are having far-reaching impacts in the field and future applications. In addition, the understanding gained by the experiments on the HPC GPU servers builds on all the previous understandings gained from previous experiments, and this understanding is crucial for our future progress in the field.

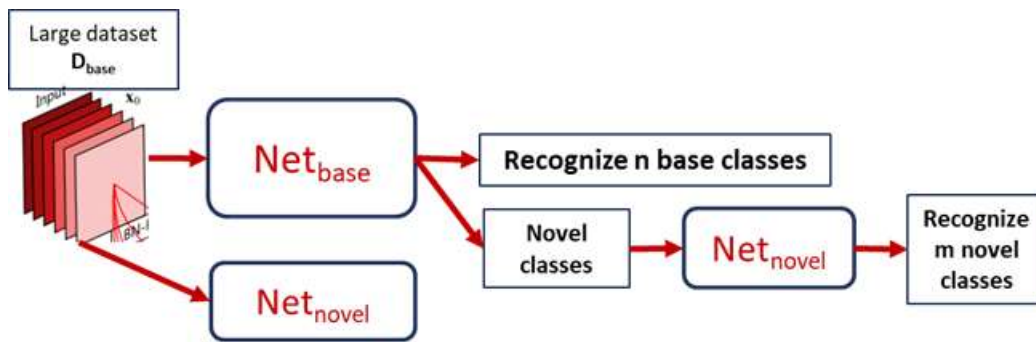


Figure 1. Diagram of the architecture to detect object of novel classes and to train a second network to recognize them.

THIS PAGE INTENTIONALLY LEFT BLANK



Space and Astrophysical Science

Space and Astrophysical Sciences (SAS) research and development advances understanding, specification and prediction of the Earth's atmospheric and space domains to exploit the extended operational environment for military advantage and to minimize environmental impacts on military operations. The SAS Computational Technology Area (CTA) embodies the use of mathematics, computational science, and engineering in the analysis, design, identification, modeling, and simulation of the space and near-space environment, and of all objects therein, whether artificial or natural. The SAS CTA encompasses foundational-discovery research to study the atmospheres of the Sun and the Earth, including solar activity and its effects on the Earth's atmosphere, ionosphere, and near-Earth space, and the unique physics and properties of celestial sources. SAS employs an extensive array of physical and empirical models and analysis tools to integrate observations and theoretical understanding, for ever-improving DoD enterprises within, and exploitation of, the extended operational environment. The CTA melds the strengths of a broad range of physical sciences — atomic and molecular physics, materials science, plasma physics, applied optics, radiation survivability, electronic warfare, directed-energy technology, astronautics and space propulsion, orbital mechanics, space situational awareness, and remote sensing — into a structure that helps the DoD multiply force-combat effectiveness.

Title: Meteorology and Climatology of the Thermosphere
Author(s): D.P. Drob, M. Jones, and M. Dhadly
Affiliation(s): Naval Research Laboratory, Washington, DC
CTA: SAS

Computer Resources: HPE SGI 8600, SGI ICE X [AFRL, OH]; Cray XC40/50, SGI ICE X [ERDC, MS]; Cray XC40 [NAVY, MS]

Research Objectives: This effort seeks to understand and specify the physics and meteorology of the Thermosphere and Ionosphere for High Frequency (HF) radio wave applications. Real-time Ionospheric specification and forecasting involves a detailed accounting of the mass, momentum, and energy budgets of the thermosphere and ionospheric plasma as perturbed from below by meteorological waves and small-scale fluctuations, as well as from above by in-situ solar extreme ultraviolet (EUV) flux and solar wind-driven geomagnetic storm perturbations. Global time-dependent codes that solve the fully coupled multispecies neutral gas and plasma transport equations, together with the resulting global electrostatic potential fields, are required.

Methodology: The National Center for Atmospheric Research (NCAR), Thermosphere Ionosphere Mesosphere Electrodynamics General Circulation Model (TIME-GCM) and related Thermosphere Ionosphere Electrodynamics General Circulation Model (TIE-GCM) are utilized to provide meteorological drivers of the ionosphere from below, and to develop a better understanding of the physical processes involved. The resulting time-dependent neutral atmospheric winds, temperatures, and composition from these GCMs are then utilized to drive the plasma-transport processes computed by the NRL SAMI3 model (Sami3 is A Model of the Ionosphere) to represent the hour-to-hour and day-to-day variability of the ionosphere. The resulting high-fidelity global ionospheric specifications then are used by the NRL MoJo HF electromagnetic propagation code to understand how ionospheric conditions effect long-range HF radio wave propagation characteristics that ultimately influence the performance of various DoD HF systems.

Results: This year, advances were made in scientific understanding and the ability to predict the transport of long-lived ionospheric metallic ion species in the Earth's ionosphere with the SAMI3 model. Day-night variations in the thermospheric wind patterns driven by periodic solar heating of lower, middle, and upper atmosphere (known as the solar migrating diurnal and semidiurnal tides) result in phenomena known as descending tidal metal ion layers. These tidal metal ion layers have a significant impact on HF radio wave propagation in the 3-to-15-MHz frequency band. Example results are shown in Fig 1. Descending tidal layers, primarily comprising Mg⁺ and Fe⁺ from micrometeorite ablation, form after sunset about 200 km altitude and descend to below 100 km just before sunrise. A second descending layer also forms during the daytime hours (12-hours apart), but is generally not significant compared with the daytime electron density of O₂⁺ and NO⁺ generated by direct solar EUV photoionization in the same altitude region. Advances also were made in specifying how these ionospheric conditions affect long-range HF radio wave propagation characteristics. Improvements were made to the NRL MoJo HF ray-tracing code, which accounts for the Earth's spherical geometry, full 3D ionospheric gradients, electron-neutral and electron-ion collision frequency attenuation losses, and the polarization effects of the Earth's 3D magnetic field. Example results are shown in Fig 2.

DoD Impact/Significance: The coupled physical-based Thermosphere-Ionosphere model validation studies performed here address the DoD/Navy long-term need of the environmental prediction of space weather effects for tactical planning purposes, as well as the maximization of DoD HF and Space systems performance through adaption to the variable environment (ref: SECNAVINST 2400.2A).

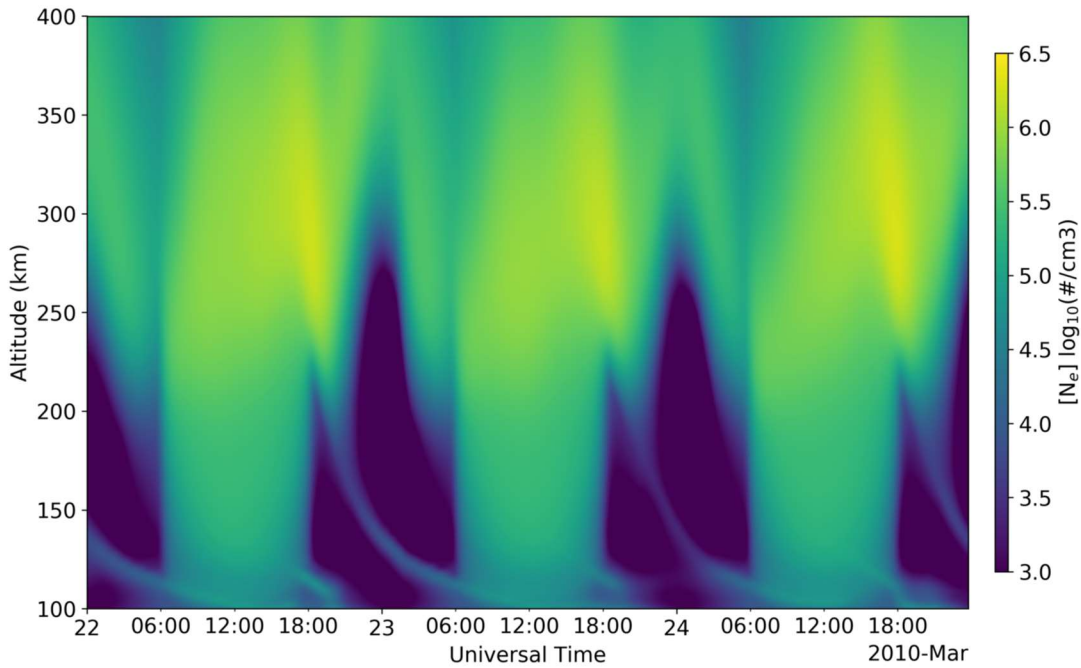


Figure 1. A SAMI3-E_s 72-hour electron density profile forecast for 0°E, 20°N.

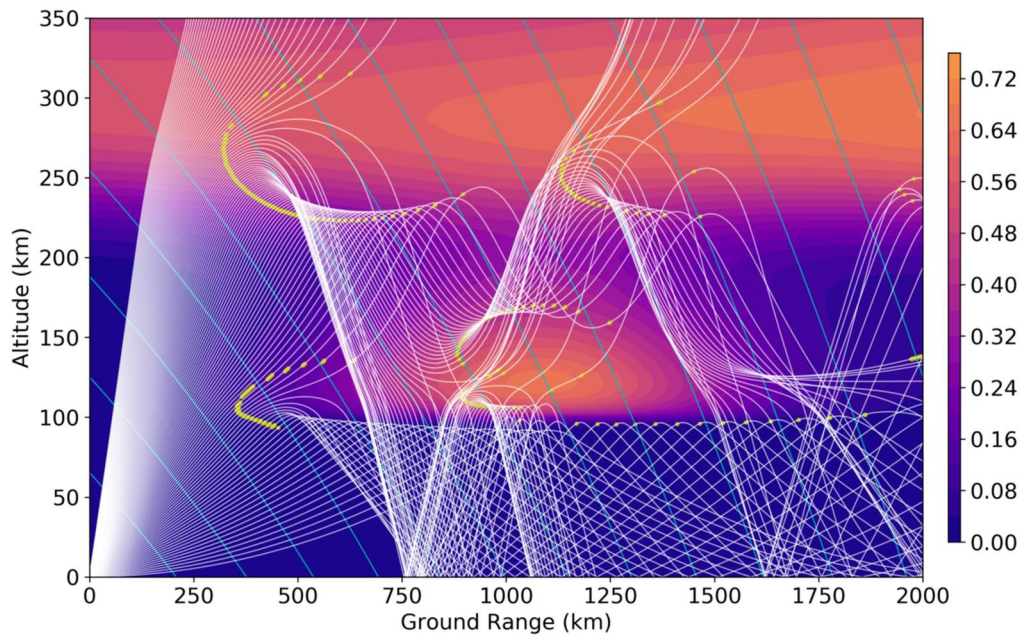


Figure 2. MoJo HF ray-trace calculations through a simulated high-latitude aurora E-region electron density enhancement. The color contours represent the index of refraction for 4.8 MHz radio waves, which is proportional to the square root of the background electron density. The yellow points along the ray paths indicate the locations where the radio wave vector is perpendicular the Earth's magnetic field (aqua) and strong backscatter can occur.

Title: Radiative Signatures and Dynamical Interactions of AGN Jets

Author(s): M.T. Wolff¹, and J.H. Beall²

Affiliation(s): ¹Naval Research Laboratory, Washington, DC; ²St. John's College, Annapolis, MD

CTA: SAS

Computer Resources: SGI Altix ICE [NRL, DC]

Research Objectives: The scientific goal of this research is to investigate the physical processes that occur as an astrophysical jet interacts with the ambient medium through which it propagates. During FY19, we completed a series of large-scale, three-dimensional, relativistic, magneto-hydrodynamic (RMHD) jet simulations in order to explore the jet parameter space so we can better establish the stability of the code, and to understand the various modes of jet-ambient-medium interaction. With our colleagues at University of the Free State (UFS), Bloemfontain, South Africa, we have also succeeded in using the relativistic hydrodynamic (RHD) version of the Pluto.4.2 code to show estimates of synchrotron emission from the RHD jet with an estimated magnetic field in equipartition with the gas pressure of the jet-ambient medium structures. These efforts enable NRL to engage in state-of-the-art three-dimensional relativistic hydrodynamic and magneto-hydrodynamic modeling.

Methodology: For these recent, long-term, large-scale numerical simulations, we use the PLUTO code, which has the capability of simulating hydrodynamic (HD), magneto-hydrodynamic MHD, RHD, and RMHD processes. The PLUTO code has proven itself to be a robust tool for simulating astrophysical jets. We are continuing to explore the long-term jet evolution in the RMHD regimes. We are planning to use our RMHD simulations in conjunction with the UFS post-processing algorithms as noted above. We also plan to incorporate “microscopic” plasma processes, including the two-stream instability, the parametric instability, and the ion-acoustic instability, into these simulations. These processes remove energy from the jet during its interaction with the ambient medium and enhance the transfer of momentum and kinetic energy from the jet to the ambient medium. Their inclusion provides for a more realistic simulation of the jet-ambient-medium interaction. The resulting plasma simulations then can provide a self-consistent estimation of the expected radiation from the jet structures in the form of both thermal radiation and synchrotron emission.

Results: The largest 3D simulations thus far (10243) using the PLUTO code have been for both RHD and RMHD applications. Jet velocities of $0.5c$ to $0.998c$, where c is the velocity of light, have been simulated extensively using the PLUTO code. During our latest runs, we have moved to 512^3 with PPM and Runge-Kutta solvers and have tested the stability of these solutions extensively. As noted earlier, we have also used post-processing algorithms to estimate the 10 GHz radio emission of these jets. Figure 1 shows the long-term simulation of the RMHD jet for a 512^3 simulation for density only at 65 kpc on a side for a fully 3D, relativistic hydrodynamic simulation of an astrophysical jet. The density structure is shown as an x-z slice across the jet length. Note the well-developed Rayleigh-Taylor instabilities at the jet-ambient medium boundary and the Kelvin-Helmholtz instabilities in the jet column. The simulation size is ~ 65 kpc lengthwise and ~ 65 kpc on a side. We show the structure after $\sim 10^8$ time steps. In this simulation, the jet-to-ambient medium density ratio is 0.01 and the ratio of jet input pressure to ambient medium pressure is 5×10^{-3} .

DoD Impact/Significance: Many U.S. government agencies, in addition to the DoD, have an interest in developing a robust capability to hydrodynamically model plasma and fluid systems in a highly anisotropic medium. A related and closely following interest is in developing the ability to model radiative transfer in such a multidimensional plasma and fluid environment. These calculations will advance the science of modeling astrophysical and near-earth space plasma environments.

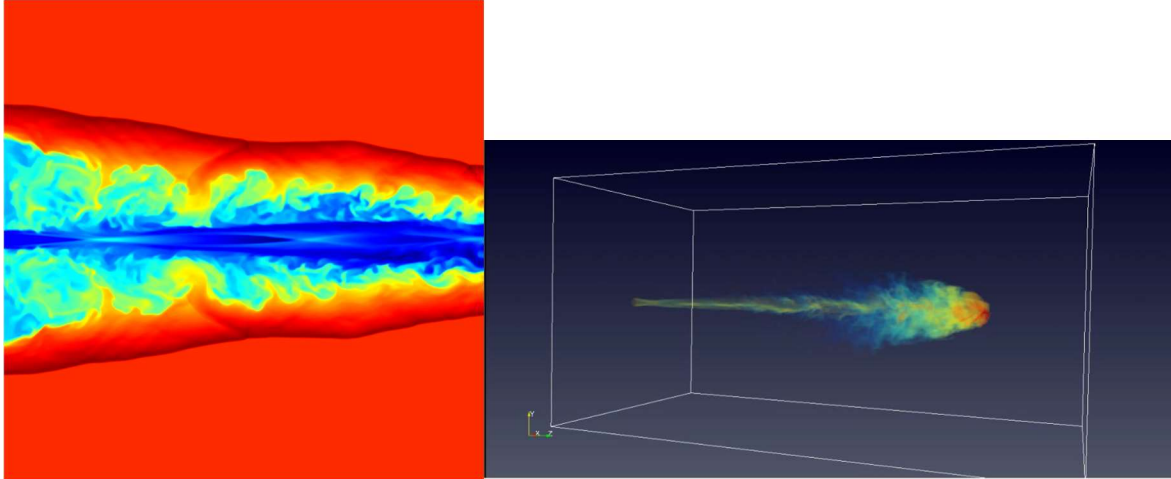


Figure 1. The left panel shows the fully 3D, relativistic, magneto-hydrodynamic simulation of an astrophysical jet density profile at a time of 4×10^7 years, with a jet bulk velocity of $v=0.995c$. This image shows $512 \times 512 \times 512$ grid cells in an x-z cut of the simulation. Note the well-developed Rayleigh-Taylor instabilities at the jet-ambient medium boundary and the internal shocks in the jet's column. The simulation size has a scale of ~ 65 kpc on a side. We show the structure after $\sim 10^8$ time steps. In this simulation, the jet-to-ambient medium density ratio is 0.01 and the ratio of jet input pressure to ambient medium pressure is 5×10^{-3} . The right panel shows the post-processed simulation of 10 GHz radio emission in a volumetric rendering for an RHD simulation with a velocity of $v = 0.5c$ from an earlier simulation, as noted in the text above. The Kelvin-Helmholtz instabilities in the jet column are clearly visible, as are the Rayleigh-Taylor instabilities at the jet-ambient medium boundary near the head of the jet. We expect the emission from the post-processing of the RMHD simulation to yield a similar pattern to that shown in the figure.

This research is supported by NASA Fermi Mission under DPR S-15633-Y.

Title: Development of a Weather Model of the Ionosphere

Author(s): S.E. McDonald¹, F. Sassi¹, C.A. Metzler¹, D.P. Drob¹, J.L. Tate², and M.S. Dhadly³

Affiliation(s): ¹Naval Research Laboratory, Washington, DC; ²Computational Physics, Inc., Springfield, VA; ³George Mason University, Fairfax, VA

CTA: SAS

Computer Resources: Cray XC40 [ARL, MD]; Cray XC40 [NAVY, MS]

Research Objectives: The scientific goal of the proposed research is to characterize and simulate the physical processes that are important for improving numerical forecasting of high-frequency (HF) radio wave propagation through the Earth's atmosphere and ionosphere across the range of conditions relevant to DoD operations. To achieve the objectives of this project, we have developed a fully coupled atmosphere-ionosphere model. In FY19, the main objectives were to complete the development of the fully coupled model, to perform validation studies, and to investigate lower atmospheric effects on the ionosphere.

Methodology: We have developed the Navy Highly Integrated Thermosphere and Ionosphere Demonstration System (Navy-HITIDES), which consists of SAMI3, a state-of-the-art NRL model of the ionosphere, along with couplers that use the Earth System Modeling Framework (ESMF) for interpolation between the atmosphere and ionosphere grids. Navy-HITIDES has been integrated with the Whole Atmosphere Community Climate Model eXtended (WACCM-X); it also is being designed to work with any NUOPC (National Unified Operational Prediction Capability) and ESMF-compliant whole-atmosphere model that includes a thermosphere.

Results: We carried out WACCM-X simulations to tune eddy diffusion in the lower thermosphere to reproduce the interseasonal variability in thermospheric density represented in the empirical model NRLMSISE-00. The goal was to assess whether the thermospheric physics can, or must, be tuned to improve the ionospheric state, and its interseasonal variations. In a separate study, we carried out paired forecast simulations for January 2013 in which the Navy-HITIDES/WACCM-X coupled model was nudged toward atmospheric analysis, and toward atmospheric forecast from the Navy Global Environmental Model - High Altitude (NAVGEN-HA). The goal of this study was to determine how the quality of atmospheric specifications without observations impacts ionospheric predictions. We found that that ionospheric prediction using forecasted atmospheric parameters degraded after one to two days as compared with the ionosphere prediction that was nudged toward atmospheric analysis. The forecast errors (Figure 1) were larger on days during a stratospheric sudden-warming event, in which thermospheric tides are modulated by processes in the stratosphere and impact ionospheric electron densities. This study highlights the importance of lower atmosphere on the ionosphere and its relevance to improving the forecast skill of ionospheric models. We also continued to perform validation simulations of Navy-HITIDES/WACCM-X for specific periods of interest, including January – April 2014.

DoD Impact/Significance: This effort will lead to a better understanding of the physics, dynamics, and chemistry of the bottomside ionosphere, with direct implications on future capabilities for nowcasting and forecasting of the environment relevant to DoD/Naval systems.

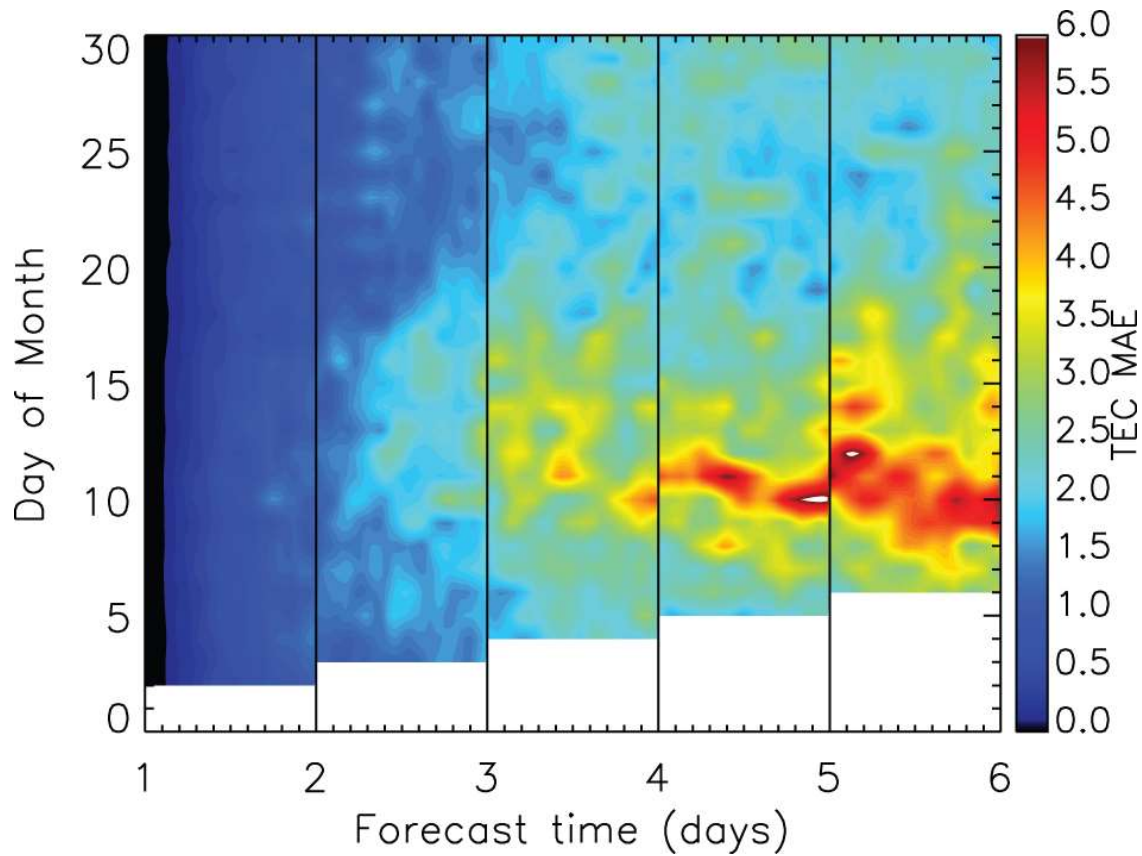


Figure 1. We performed simulations of the ionosphere/thermosphere for January 2013 with Navy-HITIDES/WACCM-X that includes the effects of the lower atmosphere by nudging the model toward the NAVGEM-HA atmospheric specification (baseline) and forecast products (1 – 5 day forecasts). The figure depicts the mean absolute error (MAE) of the ionospheric total electron content (TEC) of the 1- to 5-day forecast simulations with respect to the baseline simulation. Forecast errors begin to increase in the 2-day forecast. The 3-day through 5-day forecasts show significantly larger errors on the days in January 2013 in which the ionosphere was impacted by a sudden stratospheric warming (SSW) event.

Title: Navy Ionosphere Model for Operations

Author(s): S.E. McDonald¹, C.A. Metzler¹, J.L. Tate², R.K. Schaefer³, P.B. Dandenault³, A.T. Chartier³, G. Romeo³, G.S. Bust³, and R. Calfas⁴

Affiliation(s): ¹Naval Research Laboratory, Washington, DC; ²Computational Physics, Inc., Springfield, VA; ³The Johns Hopkins Applied Physics Laboratory, Laurel, MD; ⁴The University of Texas at Austin Applied Research Laboratories, Austin, TX

CTA: SAS

Computer Resources: Cray XC40 [ARL, MD]; Cray XC40, HPE SGI 8600 [NAVY, MS]

Research Objectives: The objective of this effort is to develop a physics-based ionosphere model coupled to an ionospheric data-assimilation system that provides global and regional electron density specifications and short-term forecasts (0 – 24 hours). This capability will form the basis of a future Navy operational ionospheric forecasting system, running at multiple resolutions and fully coupled to operational atmospheric forecast models. In FY19, the main objectives were to couple the data-assimilation system with a physics-based 3D ionosphere model, to add high-resolution capability to the ionosphere model, and to continue verification & validation studies.

Methodology: The Navy Ionosphere Model for Operations (NIMO) is a physics-based model, the Navy Highly Integrated Thermosphere and Ionosphere Demonstration System (Navy-HITIDES), and a 3DVAR ionospheric data assimilation system (IDA4D) that can ingest a wide variety of ionospheric datasets. Navy-HITIDES consists of SAMI3, a state-of-the-art NRL model of the ionosphere, along with couplers that use the Earth System Modeling Framework (ESMF) for interpolation the ionosphere and data assimilation grids. IDA4D currently uses an empirical ionosphere, the International Reference Ionosphere (IRI), as its background model and thus far has been used only for ionospheric specification. For NIMO, IRI is being replaced with Navy-HITIDES, which will enable improved specifications and short-term forecasts. The MPI-enabled Earth System Modeling Framework (ESMF) interpolation routines are used to interpolate between the unstructured IDA4D grid and the geomagnetic field-aligned SAMI3 grid.

Results: We have fully coupled IDA4D to Navy-HITIDES using ESMF to interpolate between the unstructured grid in IDA4D to the geomagnetic field-aligned grid in SAMI3. The cycling between the background model and the data-assimilation system occurs at a five-minute cadence. This two-way coupled model is superior to either model alone. The standalone SAMI3 produces a physics-based forecast tuned to reproducing the average climatology, but it does not capture the rich structure of the actual ionosphere, especially during big geomagnetic storms. These storms can drive the ionosphere into a highly dynamic state both spatially and temporally. We have run NIMO for the storm period of 19-21 November 2003. This was an intense storm and the Wide Area Augmentation System that tracks flights over the United States had severe problems with GPS single-frequency geolocation during this storm. Results are shown in Fig. 1, where we show the prestorm difference between SAMI3 alone and NIMO followed by a another comparison at the height of the storm. To further improve the performance of NIMO, we are developing an estimation of the SAMI3 model error covariances. We are using two free-running, yearlong SAMI3 simulations (2010 and 2014), which reflect solar minimum and maximum conditions, to estimate the covariance matrix using time lagged forecasts. Currently, NIMO is running on a low-resolution global grid. To move toward a high-resolution regional capability, SAMI3 has been modified to run with an embedded high-resolution region.

DoD Impact/Significance: The development of an operational ionospheric forecast model will aid in the numerical forecasting of high-frequency (HF) radio wave propagation through the Earth's atmosphere and ionosphere across the range of conditions relevant to DoD/Navy operations.

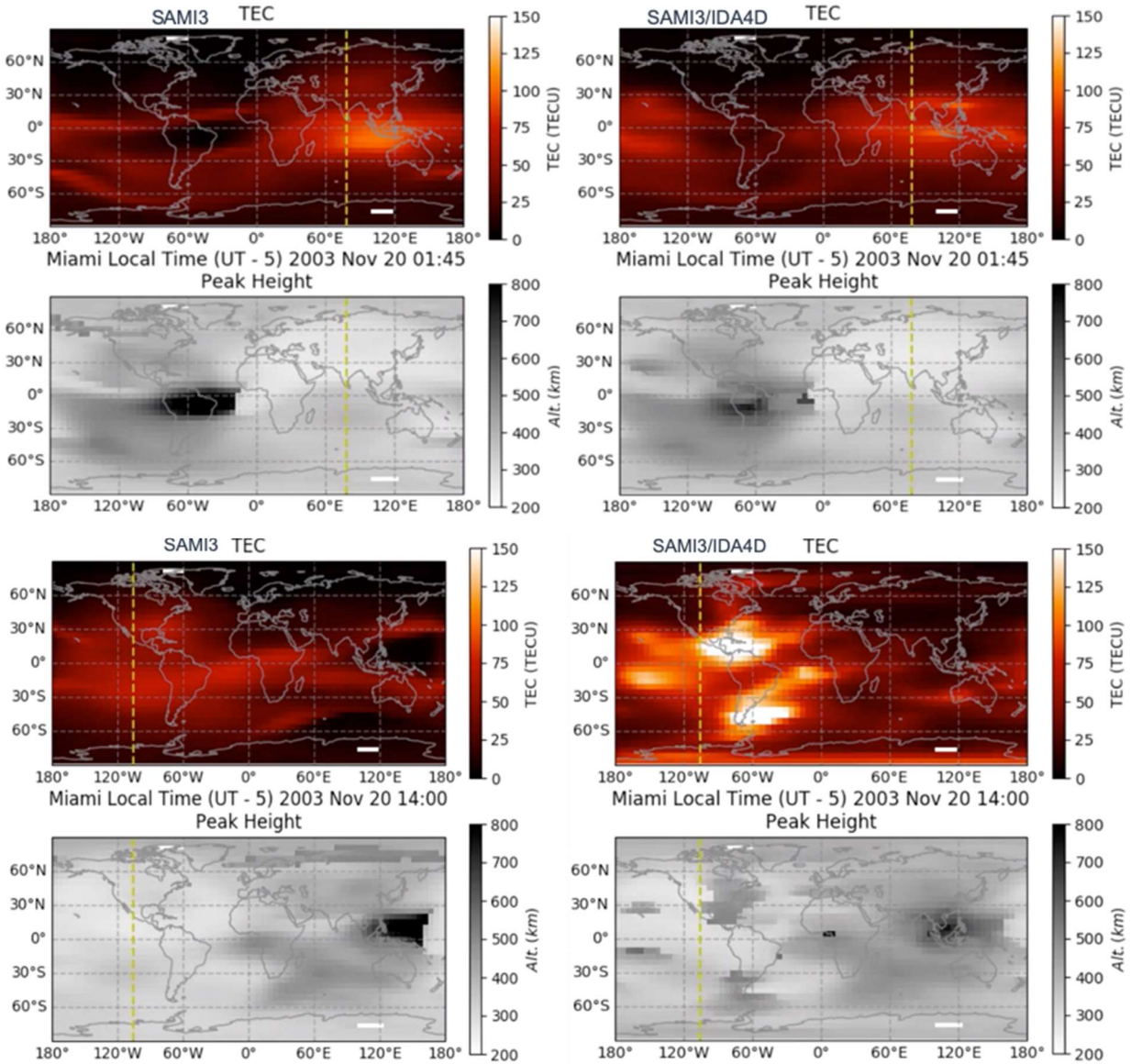


Figure 1. SAMI3 vs. NIMO (coupled IDA4D/SAMI2) during a run of storm-time conditions on Nov 20, 2003. The panels on the left are runs with SAMI3 alone, which is driven by solar geophysical indices. The panels on the right are the coupled IDA4D/SAMI3 run, assimilating data from 1,400 GPS receivers (processed by Haystack). Each panel contains two plots, a TEC heat map and the height of the maximum electron density. The top panels are pre-storm conditions, while the bottom two panels are during the peak of the storm effects on the ionosphere. The use of data assimilation captures the highly variable state of the ionosphere during this disturbed time.

Title: Electromagnetic Pulses from Hypervelocity Impacts on Spacecraft

Author(s): A. Fletcher

Affiliation(s): Naval Research Laboratory, Washington, DC

CTA: SAS

Computer Resources: GI ICE X [ARL, MD]

Research Objectives: The objective of this project is to use large-scale simulations to understand electromagnetic pulses (EMPs) that are associated with hypervelocity impacts (HVIs) on spacecraft and to develop mitigation strategies.

Methodology: The problem can be split into two regimes (impact and EMP) for which we will run separate codes. ALEGRA, a hydrocode from Sandia National Laboratories, will be used to simulate the impact and plasma generation. JABBERWOCK, a particle-in-cell code from Naval Research Laboratory, will be used to simulate the plasma expansion and generation of the EMP. We first will run a series of simulations to verify the predictive capability of the simulation pipeline by validating against ground-based Van de Graaff impact experiments. We then will run a series of simulations in order to build a model that describes the EMP properties as a function of impact parameters.

Results: We have performed a battery of simulations using ALEGRA to study the total plasma content (as well as the profiles in plasma density, temperature, and expansion velocity) for various impact speeds and angles. There is not general agreement (in simulation or experiment) on the total charge generated by hypervelocity impacts and we aim to use this series of simulations to settle this question, and also 1) to determine the possible effect of non-collisional ionization on the eventual state of the plasma plume, and 2) to determine critical velocities at which the plasma plume changes from unionized to weakly ionized to strongly ionized.

We also have upgraded Jabberwock to be able to directly use the results of the ALEGRA simulations. This requires implementation of a charge-conserving current-collection algorithm and full domain decomposition of the PIC particles. We used a new feature of the PETSc library to implement the particle decomposition. Jabberwock simulations have been used independently of ALEGRA to test the original EMP mechanism and to determine a mode conversion efficiency of $\sim 1\%$, which would lead to EMPs that could threaten satellites for impactors with high enough speed.

DoD Impact/Significance: Protection of critical DoD space assets from this threat is necessary to assure uninterrupted C4ISR capability, which is critical for operational success as envisioned in the Navy's S&T strategic plan for information dominance. Countermeasures against hypervelocity impacts of micro-projectiles on DoD space assets depend on the knowledge of the electromagnetic power and frequency spectrum of the impact-associated EMPs.

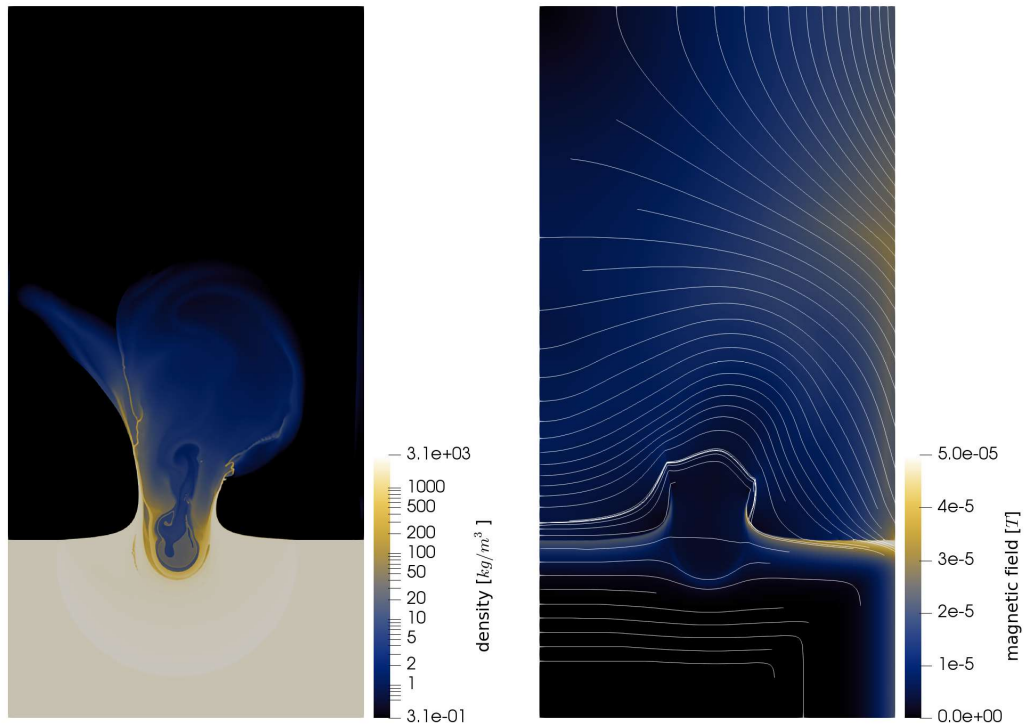


Figure 1. Mass density (left) and magnetic field (right) from a 72 km/s hypervelocity impact on aluminum. The shock in the target, crater the near the impact site, and ejecta can be seen clearly in the density. On the right, the deformation in Earth's magnetic field due to the expanding plasma is evident, including the formation of the predicted diamagnetic cavity.

Title: Global Kinetic Simulations of Space Plasma Waves and Turbulence

Author(s): A. Fletcher

Affiliation(s): Naval Research Laboratory, Washington, DC

CTA: SAS

Computer Resources: SGI ICE X [ARL, MD]

Research Objectives: The objectives of this project are 1) to support an NRL and DARPA sounding rocket experiment program, SMART (space measurement of a rocket-released turbulence), by helping to choose mission parameters and understanding the data from the experiment, and 2) to develop the capability to simulate near-Earth space plasmas on both a global scale while including kinetic effects.

Methodology: We will use a combination of two codes. The first is JABBERWOCK, a particle-in-cell (PIC) code, and the second is WICKED, a wave-in-cell (WIC) code. Both have been developed at NRL and both simulate kinetic plasma phenomena. We will determine the density and optical/radar signature of the barium cloud, the amplitude and spectrum of the electrostatic and electromagnetic waves, and the rate of particle precipitation from the radiation belts. WIC, which could simulate the entire process, will need validation via comparable PIC runs. WIC then will be used to simulate as much of the cascade as possible within one simulation.

Results: Numerous simulation results have been used to help design the SMART experiment, including choosing the altitude, instruments on the payload, and optimal launch conditions. Furthermore, kinetic simulation results have been used as validation for newly developed linear, quasilinear, and nonlinear theoretical models of the plasma physics cascade in SMART. We also have begun implementation of the first parallel version of the continuous WICKED code.

Using a modified version of our PIC code, JABBERWOCK, we have performed large-scale direct simulation Monte Carlo (DSMC) simulations of the neutral beam injection, which is the first stage of the SMART experiment. From this, we have discovered that our previous model of ideal ion ring distributions is not entirely accurate. Instead, a helical ion velocity distribution forms that becomes tighter and tighter as one moves farther from the release point. Critically, near the release point where the instrument payload will fly, the distribution will be strongly non-gyrotropic. We also discovered a higher-density slow barium component in addition to the fast beam, which changes the expected character of the electrostatic (and electromagnetic) waves that are produced.

Using this new understanding of the helical distribution functions, we performed electrostatic PIC simulations of the lower-hybrid wave-generation from non-gyrotropic partial ring distributions. These simulations show that the amplitude of the waves, as well as the energy conversion from the beam, increases significantly compared with our original ideal model. This result increases the odds of success for the SMART mission, specifically the odds of measuring the resulting whistler waves in the magnetosphere with a satellite of opportunity.

DoD Impact/Significance: The SMART experiment and associated simulations ultimately will demonstrate a method for precipitating energetic particles from the radiation belts. These particles cause malfunctions in and disable sensors on DoD/Navy spacecraft. Given the DoD/Navy reliance on spaceborne assets, their protection is critical to assure uninterrupted C4ISR capability and to maintain information dominance.

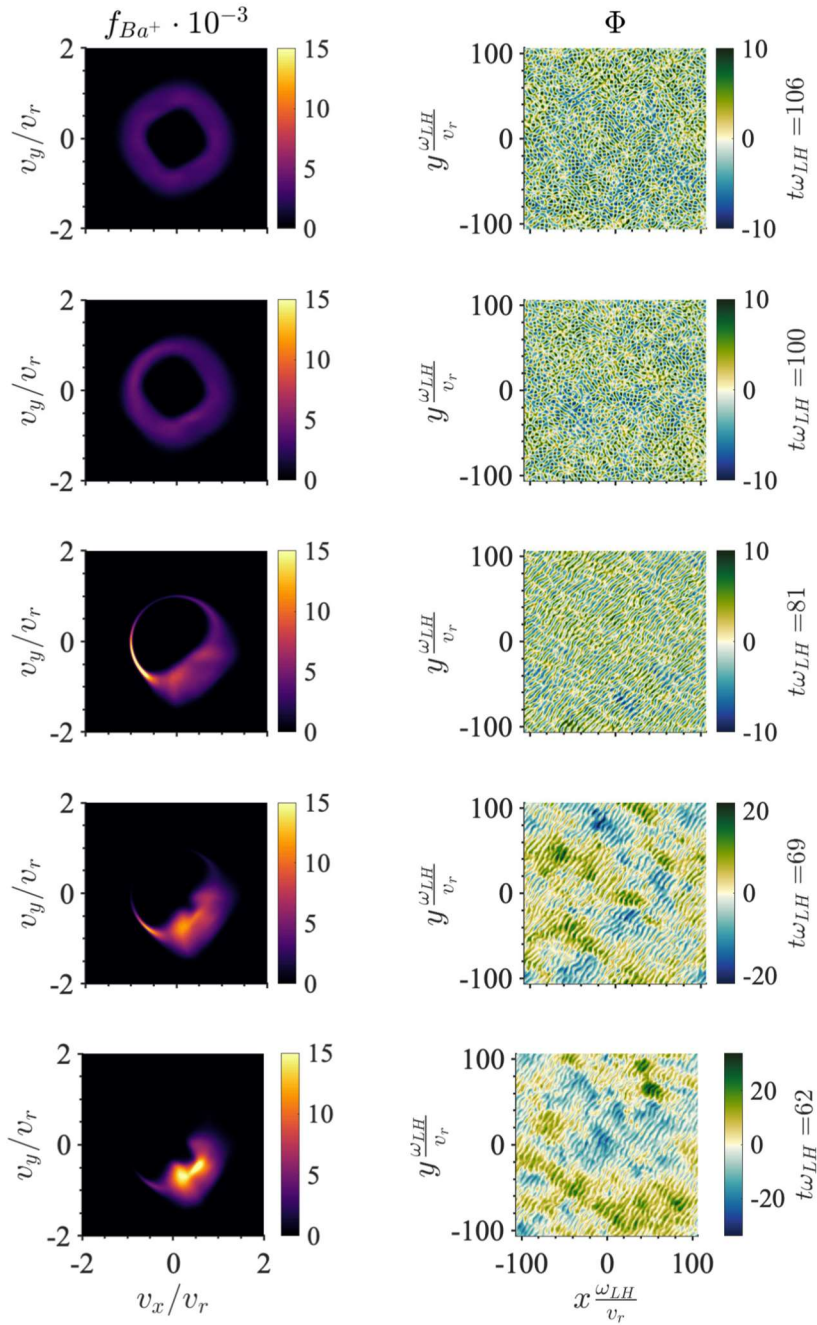


Figure 1. Velocity distribution function (left) and electrostatic potential (right) for the non-gyrotropic partial ring distributions that will be generated in the NRL/DARPA SMART experiment. As the ion rings on the right become more and more non-gyrotropic, the wave amplitude is seen to increase and symmetry of the wave vector is broken. The first row shows an ideal ring distribution with isotropic waves, while the subsequent rows contain a third of a ring, a sixth of a ring, a ninth of a ring, and a twelfth of a ring.

Title: Dynamic Phenomena in the Solar Atmosphere
Author(s): M.G. Linton
Affiliation(s): Naval Research Laboratory, Washington, DC
CTA: SAS

Computer Resources: SGI ICE X [AFRL, OH]; Cray XC40, SGI ICE X [ARL, MD]; Cray XC40/50, Cray XE6m [ERDC, MS]; Cray XC40 [NAVY, MS]

Research Objectives: The goal of this HPC program is to investigate the solar drivers of the space weather that disrupts DoD and civilian communications and navigation systems. The program is focused on understanding, and ultimately predicting, the initiation processes of the two key solar drivers: coronal mass ejections (CMEs) and solar flares. The fundamental questions that we are investigating are how the emergence of magnetic fields through the photosphere into the corona drives CMEs and flares, and how the reconnection that releases energy in these events occurs in both coronal and chromospheric conditions.

Methodology: Our work focuses on explorations of the emergence of magnetic fields from the convection zone into the solar corona, with the goal of determining how solar activity is generated. This year, we investigated how the buoyant rise and expansion of twisted flux ropes in the convection zone change their properties so that they become unstable to the kink instability. This then writhes them up into a configuration that produces flaring, active regions known as delta-spots. In parallel, we studied how the propagation of magnetohydrodynamic (MHD) waves from the photosphere up into the corona generates current sheets and heating along the coronal magnetic fields. Our third focus was on implementing and testing our new wave-characteristics-based boundary conditions, with the goal of driving the simulated coronal evolution with observed photospheric magnetic field information. For these studies, we used our MHD code LAREXD for two dimensional (2D) and three dimensional (3D) simulations.

Results: We have simulated the propagation and dissipation of magnetohydrodynamic waves through a magnetized and stratified solar atmosphere. We have found that a portion of these waves refract to null points in the coronal magnetic field, collapsing them into current sheets. The reconnection and dissipation generated at this null and the fieldlines leading to it causes these fieldlines to be heated. This work helps us understand one of the proposed contributions to the anomalously high temperature of the solar corona.

We have worked this year to study how twisted flux ropes rise from deep in the convection zone, expand due to the lower-pressure environment, and kink to form distorted activity complexes. We also have worked to study the rise to the surface of the more common counterpart of these flux ropes, namely, the very weakly twisted flux ropes that form most active regions. Both of these efforts are revealing important aspects of how the convection zone affects the rise and eventual emergence of magnetic fields.

We have implemented our newly developed MHD wave-characteristic boundary-driving methods into our three-dimensional LARE code. These now have tested successfully for classical non-reflecting characteristic boundary conditions for 1D MHD waves and for 3D hydrodynamic waves. We are now testing this implementation for 3D MHD waves, and then will progress to the implementation and testing of full data-driving characteristic boundary conditions. The ultimate goal is to drive our LARE simulations with observed photospheric vector magnetic fields as well as inferred photospheric vector velocity fields.

DoD Impact/Significance: These numerical simulations are providing new insight into how solar flares and coronal mass ejections are driven by photospheric flux emergence, and how wave driving energizes and heats the chromosphere and the corona. Furthering understanding of how solar activity is generated is a critical step toward building space weather-prediction models, and toward mitigating dangers of space weather.

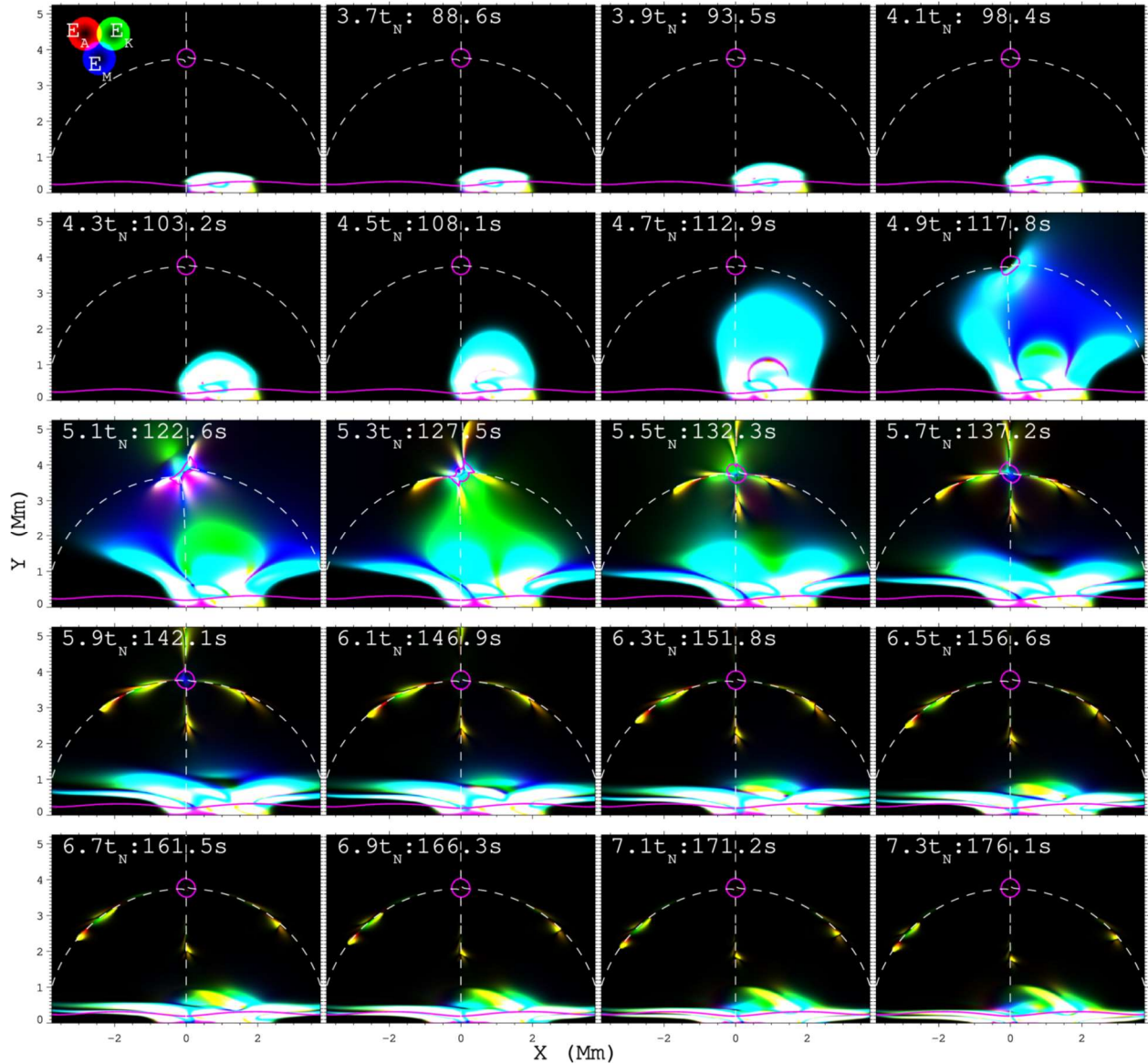


Figure 1. This figure illustrates the propagation and dissipation of magnetohydrodynamic waves in a simulation of the magnetized, gravitationally stratified solar atmosphere. The intensity of the acoustic (red), kinetic (green), and magnetic (blue) wave energies are indicated by the colors. The dashed lines show the four magnetic fieldlines which lead to or away from the coronal null. As time progresses from the upper left panel to the lower right panel, this figure shows the wave as it propagates up into the corona from the photosphere, as it is refracted toward the null ($4.9t_N$), as new wave modes are then created (yellow, which indicates an equipartition between kinetic and acoustic wave energies, $5.3t_N$), and as these modes then propagate down along the dashed fieldlines, heating them up as they go.

Title: Modeling Propagation of Ionospheric Disturbances Initiated by Magnetospheric Substorms
Author(s): J. Haiducek and J. Helmboldt
Affiliation(s): Naval Research Laboratory, Washington, DC
CTA: SAS

Computer Resources: Cray XC40 [NAVY, MS]

Research Objectives: A traveling ionospheric disturbance (TID) consists of a wavelike density perturbation that moves through the ionosphere. Our primary objective is to improve understanding of TIDs, their spatial structure, and the physical processes that drive them. Our main focus will be on TIDs that are observed by the Very Large Array (VLA) Low-Band Ionosphere and Transient Experiment (VLITE), an observational capability developed jointly by the Naval Research Laboratory and the National Radio Astronomy Observatory. VLITE provides the capability to measure total electron content (TEC) in the ionosphere with a very high precision and spatial resolution, but with a limited field of view. Our computational efforts aim to model TIDs observed by VLITE in order to understand better how the area observed by VLITE interacts with the surrounding environment. A secondary objective is to explore the processes by which TIDs are generated in the auroral zone by magnetospheric substorms. A magnetospheric substorm is an explosive release of energy from the night-side magnetosphere. Some of the energy of the substorm is deposited in the auroral ionosphere, and can result in the production of TIDs that propagate to the middle and lower latitudes, where they can be observed by VLITE. We aim to better understand this process by using a combination of VLITE observations and numerical simulations.

Methodology: We are modeling TID propagation using the SAMI3 (SAMI is Another Model of the Ionosphere 3D) simulation code. In order to better simulate the ionospheric density perturbations associated with TIDs, we are developing a data-assimilation system that uses TEC observations collected by VLITE and GPS receivers to update the SAMI3 simulation state. The data assimilation will be performed using an ensemble Kalman filter to update an ensemble of SAMI3 simulations. SAMI3 will be used to simulate TID events that are observed by VLITE, with a focus on TIDs that occur following magnetospheric substorms. The SAMI3 output will provide context for the VLITE and GPS observations. By analyzing the output from SAMI3 and the parameters required to reproduce observed TIDs in a computational simulation, we hope to gain insights into the physical processes governing TIDs that are observed by VLITE.

Results: We have conducted initial simulations of TIDs using SAMI3, and have developed data-assimilation code that updates an ensemble of model states using an ensemble Kalman filter. The data-assimilation code has been tested using a one-dimensional advection solver. Work is now in progress to integrate the data assimilation code with SAMI3. We also have compiled a list of substorm events that occurred during the time period for which VLITE observations are available, and analyzed VLITE observations for corresponding TID activity.

DoD Impact/Significance: The density perturbations associated with TIDs can introduce errors in global navigation satellite systems (GNSS) positioning solutions, with particular impacts on applications requiring centimeter-level-or-better precision. TID activity also can impact radio communications. The assimilative-modeling capabilities developed by this program will lead to predictive capabilities that can be used to provide advance notice of TID-related impacts on navigation and communications.

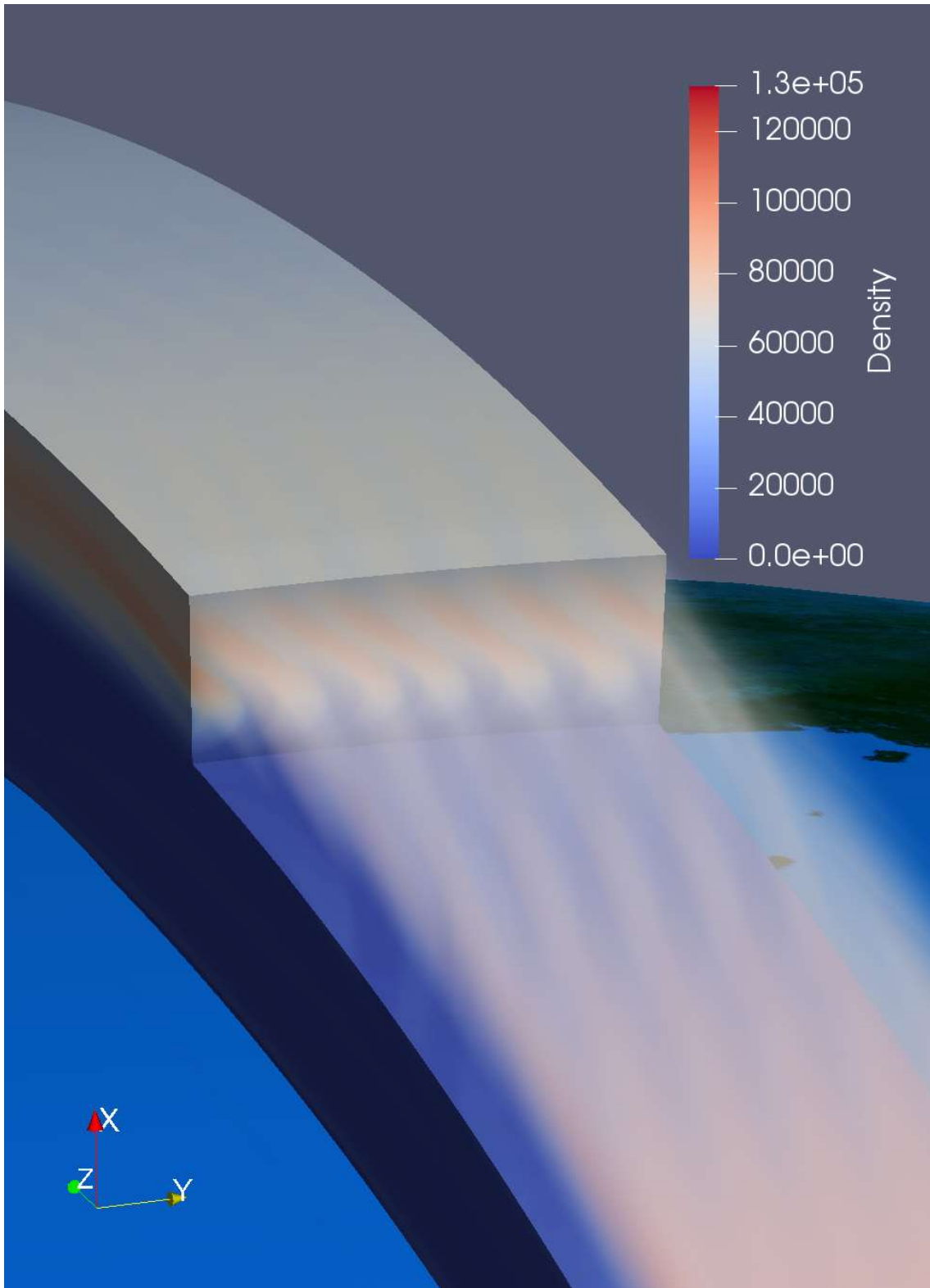


Figure 1. Ionospheric electron density from a SAMI3 simulation, showing a traveling ionospheric disturbance.

Title: Radio and Gamma-Ray Searches for Millisecond Pulsars and Radio Transients*

Author(s): P.S. Ray and J. Deneva

Affiliation(s): Naval Research Laboratory, Washington, DC

CTA: SAS

Computer Resources: SGI Altix ICE [NRL, DC]

Research Objectives: The purpose of this project is to search for millisecond pulsars in gamma-ray data from NASA's *Fermi* Large Area Telescope as well as pulsars and radio transients in ground-based data from the Robert C. Byrd Green Bank Telescope in West Virginia and the Arecibo telescope in Puerto Rico. These searches require high-performance computing resources because of the massive parameter spaces that must be searched.

Methodology: We use custom codes to search for pulsations in our radio and gamma-ray data sets. These correct for frequency-dependent delays caused by interstellar dispersion and variable Doppler shifts caused by orbital acceleration in a binary system, then search over a broad range of candidate frequencies using very large Fourier transforms and harmonic summing. *We split up the trials over a set of nodes on the cluster.

Results: During FY19, we searched 350 hours of data from the 327 MHz Arecibo drift pulsar survey (AO327). This survey began in 2010 and aims to cover the part of the sky accessible to the Arecibo telescope. It is currently the largest conducted with the Arecibo telescope, both in terms of sky coverage and observing-time allocation. NRL was one of three processing sites this year, in addition to West Virginia University and the University of New Mexico. Our code for automatically selecting radio transient candidates based on their likelihood of originating from an astrophysical source discovered six new objects: two pulsars and four rotating radio transients. We also searched 18 hours of Green Bank Telescope data at 2 GHz from a search for pulsations in 11 steep-spectrum radio sources in the Galactic Center. A population of millisecond pulsars in the Galactic Center is one of two competing explanations for the excess of gamma-ray emission detected in that region by the *Fermi* spacecraft. This project is ongoing and will have more observations scheduled in FY20. Although there are no new pulsar discoveries so far from this project, a pulsation search is a necessary step towards determining the type of compact radio sources in the Galactic Center whose spectra are similar to those of known pulsars.

DoD Impact/Significance: The main goal of AO327 is to find millisecond pulsars that are very stable rotators and therefore useful for detecting gravitational waves with a PTA. Among the ~2800 known pulsars, only 35 fit this criterion, and any addition to this set is a significant contribution to the nanohertz gravitational wave detection effort, as it improves the sensitivity of the PTA. The PTA approach to gravitational wave detection is complementary to LIGO and sensitive to a different range of gravitational wave frequencies. To date, AO327 has contributed two such discoveries to the PTA. Another major goal of the survey is to catalog the local pulsar population at 327 MHz, which would contribute to improved models of the pulsar population and evolution in the galaxy as a whole. Our searches are part of a worldwide campaign to understand the nature of the large population of unidentified gamma-ray sources being uncovered by *Fermi*. The large population of millisecond pulsars in short-period interacting binaries (the black widows and redbacks) has been a real surprise. This work is an important contribution to the science return of the major NASA mission and will help us understand the physics and astrophysics of neutron stars, one of the most extreme environments anywhere in the universe.

*This work was supported by NASA.

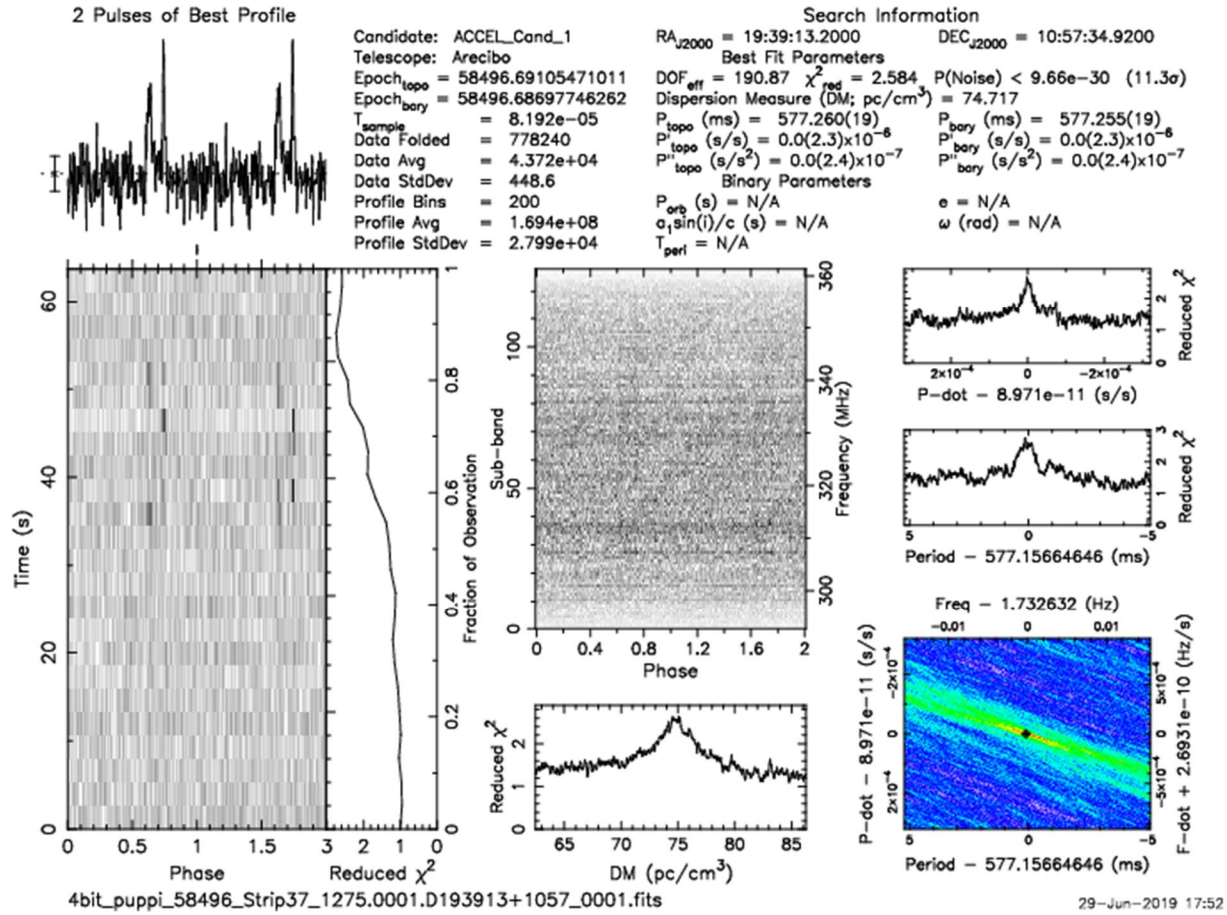


Figure 1. Discovery of the rotating radio transient J1939+10 in the AO327 survey. This object was identified by our code for automatically classifying radio pulses based on their likelihood for being of astrophysical origin. This radio transient has a rotation period of 577 ms and is an example of one type of object that conventional periodicity searches cannot detect due to the very few emitted pulses.

THIS PAGE INTENTIONALLY LEFT BLANK

OTH

Other

Work that is not easily categorized as one of the other computational technology areas.

Title: Simulation of High-Energy Radiation Environments
Author(s): J. Finke and A. Hutcheson
Affiliation: Naval Research Laboratory, Washington, DC
CTA: OTH

Computer Resources: Cray XC40 [ARL, MD]; Cray XC40/50 [ERDC, MS]; SGI Altix ICE [NRL, DC]

Research Objectives: Apply 3-D Monte Carlo methods to simulate the transport of high-energy particles for use in space applications and for modeling detection systems, radiation environments, and the operational concepts relevant to the detection of special nuclear materials and other radiological/nuclear materials in maritime and urban scenarios of interest to DoD and other civilian agencies.

Methodology: Our studies involve using three industry-standard ionizing radiation transport codes: two 3D Monte Carlo packages, Geant4 (CERN) and MCNP (Los Alamos National Lab), and one discrete ordinates package, Denovo (Oak Ridge National Lab). We use an NRL-developed front-end package called SoftWare for Optimization of Radiation Detectors (SWORD) to prototype geometries and radiation environments quickly for running our simulations. For many of the situations we simulate, very large numbers of particles must be tracked, and is a compute-intensive process. HPCMP resources make this possible in a reasonable time frame.

Results: Many of the simulations conducted were in direct support of Defense Threat Reduction Agency (DTRA) and the Department of Homeland Security's Countering Weapons of Mass Destruction office (DHS/CWMD) operational scenarios and/or exercises and were classified FOUO or higher. In addition, we have continued support of the Data Mining, Analysis and Modeling Cell (DMAMC) program at DHS/CWMD. As part of our effort to supply measured radiation background spectra to DMAMC, we have performed simulations to understand instrument response to various background configurations. Along with supporting these agencies, two additional simulations are discussed here. First, in support of investigations at the National Institute of Standards and Technology (NIST) research reactor, we performed modeling and simulations of both thermal and cosmogenic neutrons in an experiment "cave" to help determine residual backgrounds. Second, we conducted research into using the gamma-ray spectra of active galactic nuclei to measure the extragalactic background light (EBL) and the cosmic star formation rate (SFR) as a function of redshift. We used Markov Chain Monte Carlo (MCMC) fits to the gamma-ray opacity measurements with a model that allows a parameterized SFR to vary. A result can be seen in Fig. 1. The squares represent a variety of SFR data from ultraviolet (UV) and Lyman break galaxy (LBG) surveys. The shaded blue and green regions represents the 68% confidence interval SFR from MCMC fits to the gamma-ray data with two different methods. This is the first point-source-independent measurement of the SFR; it has been published by the journal *Science*. Future work continues, combining gamma-ray spectra and results of galaxy surveys to provide a tighter constraint on the SFR.

DoD Impact/Significance: The ability to produce accurate predictions of radiation-detection instrument effectiveness reduces risk and cost in development. Similarly, simulation of radiation detection concepts of operation allows assessment of their effectiveness in realistic environments. The ability to provide timely answers to the questions posed by DHS/CWMD, DTRA, NASA and other government sponsors is also important for the continued success in supporting the DoD mission. In addition, the science addressed by ionizing-radiation simulations such as the studies described above is often impractical or not cost effective to study in any manner other than simulation. The results of these studies directly address our understanding of the high-energy-radiation environment in which we live and operate.

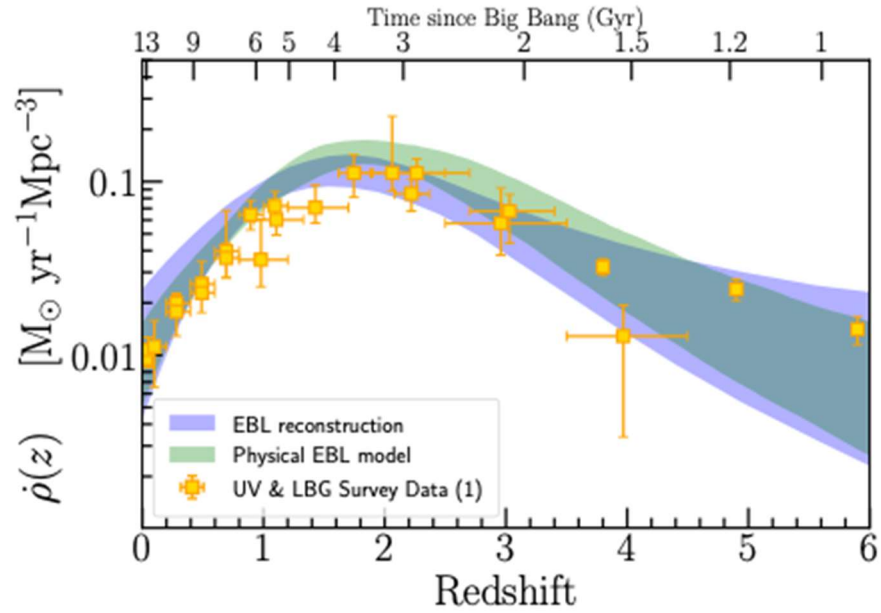


Figure 1. The Star Formation Rate (SFR) as a function of redshift, or equivalently, the time since the Big Bang. The yellow squares are the SFR measured from UV and LBG surveys. The green and blue shaded regions represent the 68% confidence intervals from MCMC fits to the gamma-ray data with two different methods. Published as Abdollahi et al. (2018), *Science*, vol. 362, pp. 1031-1034.

THIS PAGE INTENTIONALLY LEFT BLANK

Author Index

| | |
|----------------------------------|-----------------------------|
| Adamson, P.E.-----46 | Douglass, E. ----- 108, 110 |
| Alatishe, J. -----84 | Doyle, J.D. ----- 102 |
| Allard, R. ----- 108 | Drob, D.P.----- 140, 144 |
| Allen, D.R. ----- 114 | |
| Amerault, C. ----- 110 | Eckermann, S.D. ----- 114 |
| Ananth, R.-----18 | Edwards, K.-----24 |
| Anderson, R.M. -----64 | |
| Arcari, A.----- 2 | Fabre, J.P. -----94 |
| Aubry, R.M. -----92 | Fan, Y.----- 132 |
| | Fertitta, D. ----- 110 |
| Bartels, B.P.----- 118, 120 | Finke, J. ----- 160 |
| Barron, C.N. ----- 110, 118, 120 | Fletcher, A. ----- 148, 150 |
| Barton, C.A. ----- 114 | |
| Barton, N.P.----- 126 | Gamezo, V.N. ----- 14 |
| Bateman, S.P.-----22 | Giles, I.D. -----58 |
| Bates, J.W. -----12 | Gilmour, E.A. ----- 136 |
| Beall, J.H. ----- 142 | Glasbrenner, J. -----68 |
| Bermudez, V.M.-----56 | Goodwin, G. -----42 |
| Bernstein, N. -----72 | Gordon, D.F.----- 88 |
| Blisard, S.N. ----- 136 | |
| Boggs, S. ----- 110 | Hafizi, B.-----88 |
| Bust, G.S. ----- 146 | Haiducek, J.----- 154 |
| | Hangarter, C.M. -----64 |
| Calantoni, J.-----22 | Hasler, D.J. -----2 |
| Calfas, R. ----- 146 | Harrison, S. ----- 24 |
| Campbell, T. ----- 108, 110 | Hebert, D. ----- 108, 110 |
| Campbell, W.F.----- 106 | Helber, R. ----- 110 |
| Carrier, M. ----- 110 | Hellberg, C.S. -----66 |
| Cayula, S. ----- 116 | Helmboldt, J. ----- 154 |
| Chartier, A.T. ----- 146 | Herrera, M.A.----- 114 |
| Cheshire, N.----- 110 | Hervey, W.J.----- 60, 62 |
| Chong, Y.K. -----48 | Hogan, P.J.----- 122 |
| Cooke, S. -----96 | Holman, T.D.----- 16 |
| Corrigan, A.----- 26, 36 | Hoppel, K.W.----- 114 |
| Crawford, W. ----- 126 | Hou, W. ----- 32 |
| Crout, J.----- 108 | Huba, J.D.-----44 |
| | Hutcheson, A. ----- 160 |
| D'Addezio, J. ----- 110, 120 | Hyde, E.W. ----- 20 |
| Dandenault, P.B. ----- 146 | |
| Dastugue, J.M.----- 110, 118 | Imler, G.H.----- 58 |
| Davidson, A. -----88 | Isaacs, J. -----88 |
| DeHaan, C.----- 110 | |
| Deneva, J. ----- 156 | Jacobs, G.A. ----- 120 |
| deRada, S. ----- 110 | Jensen, A. -----96 |
| Dey, S.----- 82, 92 | Jensen, T. ----- 108 |
| Dhadly, M.S.----- 140, 144 | Johannes, M.----- 70 |

Author Index

| | |
|--------------------------------|---------------------------------------|
| Johnson, L. ----- 88 | Ouellette, J.D. ----- 90 |
| Johnson, R.F. ----- 26, 28, 36 | Ovtchinnikov, S. ----- 96 |
| Jolliff, J.K. ----- 124 | |
| Jones, M. ----- 140 | |
| | Palmsten, M. ----- 24 |
| Kaganovich, D. ----- 88 | Patnaik, G. ----- 10 |
| Kercher, A.D. ----- 26 | Penano, J. ----- 88 |
| Kessler, D.A. ----- 26 | Penko, A. ----- 22, 24 |
| Kim, Y. ----- 76 | Penta, B. ----- 116 |
| Komaromi, W.A. ----- 130 | Penteleev, G.G. ----- 118 |
| Krall, J. ----- 44 | Perez, A. ----- 32 |
| Kuhl, D.D. ----- 114 | Petillo, J. ----- 96 |
| | Petrov, G.M. ----- 98 |
| Ladner, S. ----- 124 | Photiadis, D. ----- 86 |
| Lamb, Z.W. ----- 118, 120 | Policastro, S.A. ----- 64 |
| Lambrakos, S. ----- 76 | Poludnenko, A.Y. ----- 14 |
| Lee, W. ----- 24 | |
| Linton, M.G. ----- 152 | Ramamurti, R. ----- 30, 36, 40 |
| Linzell, R.S. ----- 118 | Ray, P.S. ----- 156 |
| Liu, J. ----- 36, 38 | Reinecke, P.A. ----- 104, 130 |
| Liu, M. ----- 126 | Reinecke, T.L. ----- 78 |
| Lyons, J.L. ----- 74 | Reynolds, C. ----- 126 |
| | Richardson, A.S. ----- 46 |
| Ma, J. ----- 114 | Ridout, J. ----- 126 |
| Maloy, B.R. ----- 118 | Rogers, R.E. ----- 20 |
| Manolidis, M. ----- 112 | Romano, A.J. ----- 82 |
| Martin, P. ----- 110 | Romeo, G. ----- 146 |
| Matt, S. ----- 32 | Rowley, C.D. ----- 110, 116, 118, 120 |
| May, J.C. ----- 110, 118 | Ruston, B. ----- 106 |
| Maxwell, J.R. ----- 20 | |
| Mazin, I. ----- 68 | Sassi, F. ----- 114, 144 |
| McCormack, J.P. ----- 114 | Saunders, R.N. ----- 2, 4, 6 |
| McDonald, S.E. ----- 144, 146 | Schaefer, R.K. ----- 146 |
| McLay, J. ----- 126 | Schmitt, A.J. ----- 12 |
| Mestreau, E.L. ----- 92 | Schweigert, I.V. ----- 52, 54 |
| Metzger, E.J. ----- 128 | Schwer, D.A. ----- 34 |
| Metzler, C.A. ----- 144, 146 | Shabaev, A. ----- 76 |
| Michopoulos, J.G. ----- 2 | Shriver, J.F. ----- 110, 128 |
| Mott, D.R. ----- 26 | Shulman, I. ----- 116 |
| Mukhopadhyay, S. ----- 78 | Simeonov, J.A. ----- 22, 112 |
| | Sletten, M.A. ----- 90 |
| Ngodock, H. ----- 110 | Smedstad, L.F. ----- 118, 120 |
| | Smith, L.N. ----- 136 |
| Obenschain, K. ----- 10, 12 | Smith, S. ----- 110 |
| Orzech, M. ----- 112 | Smith, T.A. ----- 108, 110, 118, 124 |
| Osborne, J.J. ----- 110, 118 | Souopgui, I. ----- 110 |
| | Spence, P.L. ----- 110, 118, 120 |

Author Index

| | |
|------------------------|---------------|
| Stantchev, G. ----- | 96 |
| Sullivan, K.M. ----- | 136 |
| Swanekamp, S.B. ----- | 46 |
| Szymczak, W.G. ----- | 82 |
| | |
| Tan, X.G. ----- | 4 |
| Tate, J.L. ----- | 114, 144, 146 |
| Teferra, K. ----- | 6 |
| Toporkov, J.V. ----- | 90 |
| Townsend, T.L. ----- | 118 |
| Trimble, S. ----- | 24 |
| | |
| Valdivia, N. ----- | 86 |
| Veeramony, J. ----- | 24 |
| Viner, K. ----- | 126 |
| Viswanath, K. ----- | 40 |
| Vora, G.J. ----- | 60, 62 |
| | |
| Whitcomb, T. ----- | 126 |
| Williams, D. ----- | 92 |
| Williamschen, M. ----- | 92 |
| Wimmer, S.A. ----- | 2 |
| Wolff, M.T. ----- | 142 |
| Wood, C. ----- | 124 |
| | |
| Yaremchuk, M. ----- | 110, 118 |
| | |
| Zhuang, X. ----- | 18 |

Division/Branch Index

Systems Directorate (Code 5000)

Radar Division (Code 5300)

Surveillance Technology (Code 5340) 84

Information Technology Division (Code 5500)

Navy Center for Applied Research in Artificial Intelligence (Code 5510) 136

Materials Science and Component Technology Directorate (Code 6000)

Laboratory for Computational Physics and Fluid Dynamics
(Code 6040) 10, 12, 14, 26, 28, 30, 34, 36, 38, 40

Chemistry Division (Code 6100)

Center for Corrosion Science and Engineering (Code 6130) 2, 64
Navy Technology Center for Safety and Survivability (Code 6180) 18, 52, 54

Materials Science and Technology Division (Code 6300)

Multifunctional Materials (Code 6350) 2, 4, 6
Materials and Sensors (Code 6360) 76
Center for Computational Materials Science (Code 6390)..... 2, 66, 68, 70, 72, 74, 76

Plasma Physics Division (Code 6700)

Radiation Hydrodynamics (Code 6720) 48
Laser Plasma (Code 6730) 12
Charge Particle Physics (Code 6750) 44, 148, 150
Pulsed Power Physics (Code 6770) 46
Beam Physics (Code 6790)..... 88, 98

Electronics Science and Technology Division (Code 6800)

Microwave Technology (Code 6850) 96
Electronic Materials (Code 6870)..... 56, 78

Center for Bimolecular Science and Engineering (Code 6900)

Laboratory for Biosensors and Biomaterials (Code 6910) 58, 60, 62
Laboratory for Biomaterials and Systems (Code 6920) 76
Laboratory for Molecular Interfaces (Code 6930)..... 58

Ocean and Atmospheric Science and Technology Directorate (Code 7000)

Acoustics Division (Code 7100)

Physical Acoustics (Code 7130)..... 82, 86, 92
Acoustics Signal Processing and Systems (Code 7160)..... 82
Acoustics Simulation, Measurements and Tactics (Code 7180) 94

Remote Sensing Division (Code 7200)

Radio/Infrared/Optical Sensors (Code 7210)..... 154
Remote Sensing Physics (Code 7220) 90, 114
Image Science and Applications (Code 7260)..... 90

Oceanography Division (Code 7300)

Information Technology Office (Code 7309)..... 118
Ocean Dynamics and Prediction (Code 7320).... 24, 108, 110, 112, 116, 118, 120, 124, 128, 132
Ocean Sciences (Code 7330) 32, 110, 116, 124
Seafloor Sciences (Code 7350)..... 22, 24, 122

Marine Meteorology Division (Code 7500)

Probabilistic Prediction (Code 7504)..... 126
Atmospheric Dynamics and Prediction (Code 7530) 102, 104, 106, 110, 126, 130

Space Science Division (Code 7600)

Geospace Science and Technology (Code 7630)..... 114, 140, 144, 146
High-Energy Space Environment (Code 7650) 142, 145, 160
Solar and Heliospheric Physics (Code 7680)..... 152

Naval Center for Space Technology Directorate (Code 8000)

Spacecraft Engineering (Code 8200)

Space Mechanical Systems Development (Code 8220) 16, 20, 42

Site Index

DSRCs

AFRL 2, 4, 6, 10, 12, 14, 18, 22, 26, 32, 34, 36, 44, 46, 48, 52, 54, 56, 60, 62, 66, 68, 70, 72, 74, 78, 82, 86, 88, 96, 104, 140, 152

ARL 4, 12, 16, 20, 22, 24, 26, 28, 30, 32, 34, 36, 38, 40, 42, 46, 48, 52, 54, 58, 60, 62, 66, 72, 74, 84, 88, 90, 92, 96, 104, 112, 114, 126, 144, 146, 148, 150, 152, 160

ERDC 4, 12, 14, 22, 28, 36, 40, 44, 48, 54, 60, 62, 66, 68, 70, 76, 78, 82, 88, 90, 92, 96, 98, 102, 104, 114, 118, 120, 126, 128, 136, 140, 152, 160

NAVY 6, 20, 36, 64, 94, 102, 104, 106, 108, 110, 112, 114, 116, 118, 120, 122, 124, 126, 128, 130, 132, 140, 144, 146, 152, 154

ARCs

NRL 4, 46, 56, 142, 156, 160